PhD Thesis

School of Chemistry

Cardiff University

The *in situ* generation of H_2O_2 from H_2 and O_2 for use in oxidation reactions

Thesis submitted in accordance with the requirements of the University of Cardiff for the degree of doctor in philosophy by:

Ricci Underhill

2017

Summary

This thesis concerns the direct synthesis of H_2O_2 from H_2 and O_2 which is then utilised in oxidation reactions. The direct synthesis of H_2O_2 provides a potentially more environmentally-friendly approach than the widely employed anthraqunione process. This work aims to design catalysts that are capable of producing H_2O_2 via the direct synthesis route, then utilising the produced H_2O_2 in oxidation reactions.

The first part of this thesis concerns the oxidation of phenol using H_2O_2 generated *in situ* from H_2 and O_2 in a one-pot process. Phenol was chosen as the model compound to represent organic contamination in wastewater. H_2O_2 is a desirable oxidant for application in wastewater treatment owing to its high active oxygen content and the fact that it produces only water as a by-product of its decomposition. A palladium and iron containing catalyst was found to be an effective catalyst for completing this reaction. Additionally, the occurrence and cause of leaching was extensively studied.

The second part of this thesis concerns the oxidation of glycerol using H_2O_2 generated *in situ* from H_2 and O_2 in a one-pot process. Glycerol is a highly-functionalised material that can be used as a platform molecule for a variety of value-added products. Glycerol is currently produced as a by-product of biodiesel production, therefore there is considerable interest into its transformation into higher value products. Palladium and iron containing catalysts were found to also be effective for completing this reaction. The effectiveness of *in situ* formed H_2O_2 and the bulk addition of commercial H_2O_2 was compared and highlighted the benefit of performing the reaction using *in situ* generated H_2O_2.

Acknowledgements

Firstly, I would like to express my gratitude to Professor Graham Hutchings for providing me with the opportunity, support and guidance that enabled me to complete this work.

I would also like to thank my supervisory team of Dr Jennifer Edwards, Dr Peter Miedziak, Dr Ouardia Akdim and Dr Simon Freakley for their support and direction throughout my research project. I would also like to especially thank Dr Peter Miedziak and Dr Richard Lewis for their invaluable help and support throughout the process of writing this thesis. I would also like to extend my gratitude towards Dr David Morgan and Dr Andrea Folli for their contributions to the XPS and EPR sections of this work. I would also like to thank all the staff at Cardiff University for their help and technical support and to Robert Jenkins for his help in teaching me about the various analytical methods.

I also wish to acknowledge Selden and especially Peter Woodhead for their sponsorship and support of my PhD project. Additionally, I would like to extend my thanks to all the people in the Cardiff Catalysis Institute for their help, support and for making my time there so enjoyable and memorable. Finally, I would like to thank my family and friends for putting up with me over the last 3 years. Without them this wouldn't have been possible.

Table of contents

1 Introduction

1.1 General

1.1.1 Aims of this review

This thesis concerns the design and testing of catalysts for the oxidation of various compounds using H_2O_2 generated *in situ* from H_2 and O_2. The development of these catalysts could lead to applications in the treatment of wastewater effluents and provide alternative routes for the transformation of materials into higher value products. Therefore, the purpose of this introduction is to provide a background to catalysis, its application and an overview of the current state-of-the-art research into the direct synthesis of H_2O_2 from H_2 and O_2. The applications of H_2O_2 in wastewater treatment and glycerol oxidation will also be covered.

1.1.2 Green chemistry

Over recent years there has been increasing attention paid to increasing the sustainability and 'greenness' of various industrial processes ranging from the generation of energy to the manufacture of materials. Within chemistry, there has been widespread research interest in the development of more environmentally-friendly processes, termed 'green chemistry'. The guiding principles of green chemistry were developed by Paul Anastas and John Warner in 1998.[1] The principles were defined as follows:

1. **Prevention**: It is better to prevent waste than to treat or clean up waste after it is formed.
2. **Atom Economy**: Synthetic methods should be designed to maximise the incorporation of all materials used in the process into the final product

3. **Less Hazardous Chemical Synthesis**: Whenever practicable, synthetic methodologies should be designed to use and generate substances that pose little to no toxicity to human health and the environment.
4. **Designing Safer Chemicals**: Chemical products should be designed to preserve efficacy of the function while reducing toxicity.
5. **Safer solvents and Auxiliaries**: The use of auxiliary substances (e.g. solvents) should be made unnecessary whenever possible and, when used, innocuous.
6. **Design for Energy Efficiency**: Energy requirements of chemical processes should be recognised for their environmental and economic impacts and should be minimised. If possible, synthetic methods should be conducted at ambient temperature and pressure.
7. **Use of Renewable Feedstocks**: A raw material or feedstock should be renewable rather than depleting whenever technically and economically practicable.
8. **Reduce Derivatives**: Unnecessary derivatisation (use of blocking groups, protection/deprotection, temporary modification of physical/chemical processes) should be minimised or avoided if possible, because such steps require additional reagents and can generate waste.
9. **Catalysis**: Catalytic reagents (as selective as possible) are superior to stoichiometric reagents.
10. **Design for degradation**: Chemical products should be designed so that at the end of their function they break down into innocuous degradation products and do not persist in the environment.
11. **Real-Time Analysis for Pollution Prevention**: Analytical methodologies need to be further developed to allow for real-time, in-process monitoring and control prior to the formation of hazardous substances.
12. **Inherently Safer Chemistry for Accident Prevention**: Substances and the form of a substance used in a chemical process should be chosen to minimize the potential for chemical accidents, including releases, explosions, and fires.

These 12 principles of green chemistry provide a framework through which chemical researchers can develop more environmentally-benign processes. One of these principles highlighted the use of catalysis to achieve 'greener' processes.

1.1.3 Catalysis

Catalysis can be defined as increasing the rate of a chemical reaction using a catalyst. The catalyst is not consumed within the reaction. The term catalysis was first coined by Berzelius in 1835[2] when he proposed the existence of a new force called 'catalytic force' and wrote:

"It is, then, proved that several simple or compound bodies, soluble and insoluble, have the property of exercising on other bodies an action very different from chemical affinity. By means of this action they produce, in these bodies, decompositions of their elements and different recombinations of these same elements to which they remain indifferent."

One of the earliest examples of catalysis was observed by Humphry Davy during the development of the safety lamp for miners. He found that when a hot platinum wire was introduced into a mixture of coal gas an air, it immediately became incandescent. The same effect was also observed with other combustible vapours mixed with air. It was later discovered when using finely divided platinum, these reactions could occur even at room temperature.

Catalysts are widely employed for industrial chemicals production. In 1999 it was estimated that without the catalysed Haber-Bosch process for the production of ammonia fertiliser, food production would not be able to sustain half the world's population.[3] Typically, catalysts can be subdivided into two classifications, homogeneous and heterogeneous. Homogeneous catalysis employs the catalytic material in the same phase as the reactants whereas heterogeneous catalysis employs the catalytic material in a different phase to the reactants (typically a solid catalyst alongside liquid/gaseous reactants). The utilisation of heterogeneous catalysts leads to far easier separation of the catalytic material after reaction. Within this thesis, the focus will be on the design and development of heterogeneous catalysts.

1.1.4 Heterogeneous catalysis

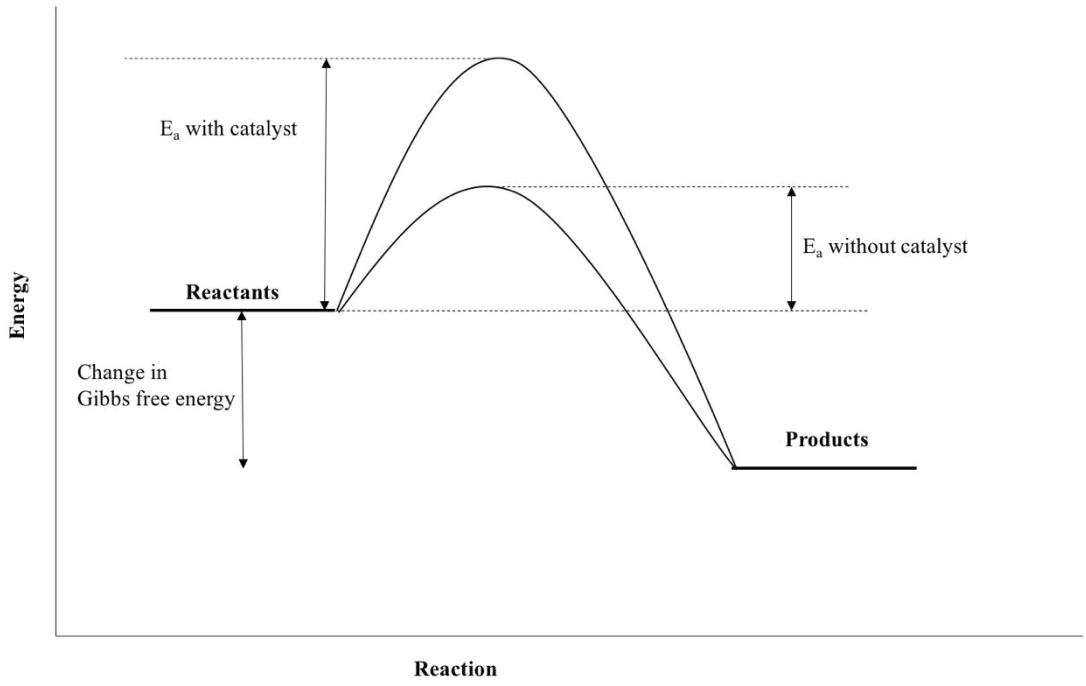

Figure 1: Energy level diagram for both catalysed and uncatalysed reactions

The employment of a heterogeneous catalyst can significantly increase the rate of a chemical reaction. Many reactions will only proceed at a very low rate due to a high-energy barrier associated with a reaction intermediate or transition state, called the activation energy. The use of a catalyst can provide an alternative pathway with a lower activation energy through which the reaction can proceed, thereby increasing the rate of reaction as shown in Figure 1. In heterogeneous catalysis, this is typically achieved by the adsorption of the reactant on the surface of the catalyst which involves the breaking of bonds and creation of new bonds with the surface.[4] A good example of this is the dissociation of hydrogen. Due to its high dissociation energy, very high temperatures are required for its dissociation in the absence of a catalyst. However, in the presence of an active metal such as platinum, it is readily dissociated into two atoms due to the formation of a bond between each hydrogen and the platinum surface. Therefore, the use of a catalyst can overcome what is typically the hardest step for hydrogenation reactions, the dissociation of hydrogen.

Overall, there are three elementary steps which typically comprise a heterogeneously catalysed reaction. The first step involves the adsorption of the reactants on the surface of the catalyst, which involves the breaking or weakening of bonds in the reactants. The next step involves the reaction between surface-bound reactants on the surface of the catalyst to give a product. The final step involves the desorption of the product from the surface of the catalyst, leaving the catalyst remaining unchanged from the start of this process.

These steps occur on what is termed the 'active site' of the catalyst. In many cases the 'active sites' of these catalysts comprise of expensive metals such as palladium, gold or platinum. Since these catalytic processes occur only on the surface exposed metal sites, it is essential to maximise the available surface area of the active metal. To achieve this, the catalytically active metals are typically dispersed over supports with a high surface area (such as a metal oxide or activated carbon).

1.1.5 Preparation of supported metal catalysts

Supported catalysts can be prepared in a wide-variety of ways. However, some of the most common preparation methods are as follows[5]:

'Incipient-wetness' impregnation: In this method, a solution containing the appropriate metal salts is added to the support material in a volume equal to the pore volume of the support. The catalyst is then dried and heat treated under an oxidative or reductive atmosphere to provide the desired metal oxide or metal particles. This method can be limited by the solubility of the metal salt precursor

'Wet' impregnation: This method is much the same as 'incipient-wetness' impregnation. However, in this case the volume of metal salt precursor solution volume is in excess with respect to the pore volume of the support material. In this case, the mixture is often heated under stirring to remove the excess solvent. The

catalyst is usually then dried and heat treated in the same way as for 'incipient-wetness' impregnation procedures.

Co-precipitation: This method involves the mixture of solutions containing metal salts and the support precursor salts. A base is then added to precipitate the salts as hydroxides or carbonates. These can then be converted to the appropriate oxides by performing an oxidative heat treatment.

Deposition-precipitation: This method is very much like co-precipitation and involves the precipitation of metal salt onto the surface of a pre-formed support material using a base. In this case, care must be taken to ensure that the precipitation occurs on the inside of the pores and not only in the external bulk solution, which would lead to large particles which are only on the surface. This can be achieved by ensuring thorough mixing and slow addition of the base.

While these procedures appear very simple, it is essential that all parameters are carefully controlled. For example, the temperature and length of heat treatments employed can have a significant effect on the size of the nanoparticle performed. If the heat-treatment is conducted at too high a temperature or for too long a period, severe sintering of the particles can occur which may lead to a detrimental effect upon catalyst activity due to lower surface metal concentration. However, if the heat-treatment is conducted at too low a temperature or for too short a period, the catalysts formed may not be sufficiently stable for reuse.

These catalyst preparation methods are often also modified to provide catalyst materials that are better suited to the target application. An example is the 'modified impregnation' method developed by Sankar *et al*.[6] This method utilises an excess of Cl^- (*via* addition of HCl to the precursor salt solution) for supported Au-Pd catalysts which was reported to result in a tighter particle size distribution and greater mixing of the Au and Pd leading to a homogeneous alloy composition. The improved activity of this catalyst, compared to conventional impregnation, was reported for the direct synthesis of H_2O_2 and benzyl alcohol oxidation.

1.2 The direct synthesis of hydrogen peroxide

1.2.1 Current manufacture of H_2O_2

Hydrogen peroxide (H_2O_2) is an oxidant that was first isolated by L J Thenard in 1881.[7] He achieved this by reacting barium peroxide with nitric acid to produce low concentrations of H_2O_2. This was later improved by using hydrochloric acid *via* the following route:

$BaO_2 + 2HCl \rightarrow BaCl_2 + H_2O_2$

$BaCl_2 + H_2SO_4 \rightarrow BaSO_4 + 2HCl$

$BaO_2 + H_2SO_4 \rightarrow BaSO_4 + H_2O_2$

In modern times, most of the commercial H_2O_2 production has been achieved using what is known as the anthraquinone auto-oxidation process (Riedl Pfleiderer process). For this process, a 2-alkylanthraquinone is dissolved in a suitable solvent and then hydrogenated to the corresponding 2-alkylanthrahydroquinone using a hydrogenation catalyst. The solution is then separated from the hydrogenation catalyst and exposed to oxygen which results in the reformation of the 2-alkylanthraquinone and the production of H_2O_2. This process is shown in Figure 2.

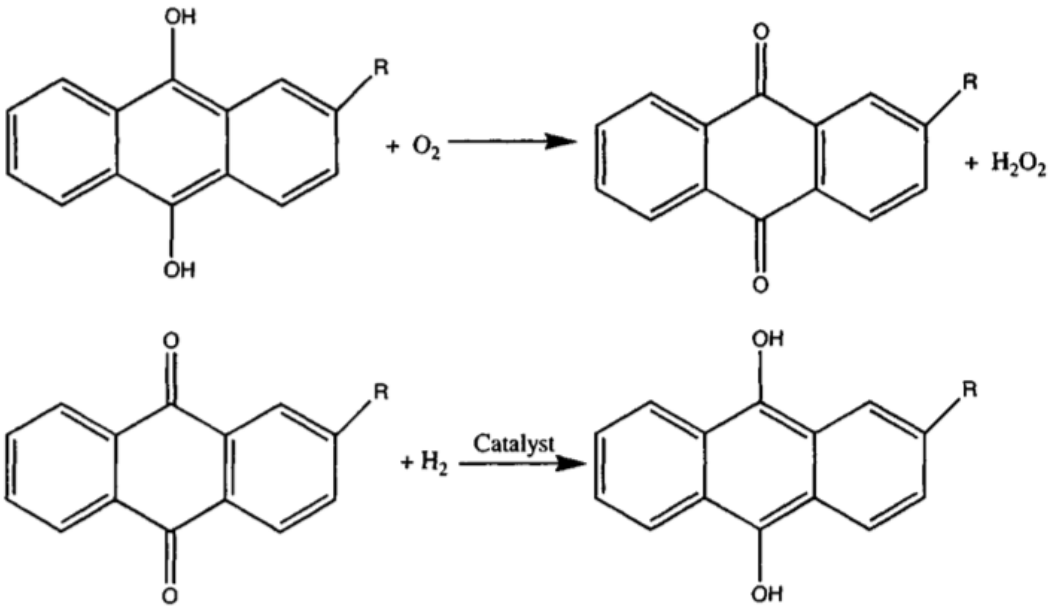

Figure 2: Anthraquinone auto oxidation process.[7]

This process can produce large quantities of concentrated H_2O_2 for commercial use. It also avoids the mixture of H_2 and O_2 in the explosive region. However, there are some downsides to this approach such as the catalytic reduction of the 2-alkylanthrahydroquinone which can lead to a lot of waste and a reduction in the atom efficiency of the reaction. In addition to this, the production of H_2O_2 using this method tends to only be performed on a large scale. This results in the requirement to store and transport large quantities of H_2O_2 which can prove hazardous. It is also a very expensive and energy-intensive process to separate and concentrate the produced H_2O_2 so it is suitable for use. Therefore, there has been significant research interest into the production of H_2O_2 using the direct synthesis route.

1.2.2 Introduction to the direct synthesis route

The direct synthesis route for H_2O_2 involves the reaction of H_2 and O_2 using a catalyst. This reaction is desirable as it is 100% atom efficient and avoids the use of additional reagents. If the direct synthesis reaction were to be performed in water, it would also be possible to avoid the costly extraction of H_2O_2. However, there are some significant

challenges associated with the direct synthesis route. Despite its deceptively simple reaction scheme, there are other reaction pathways that must be considered.

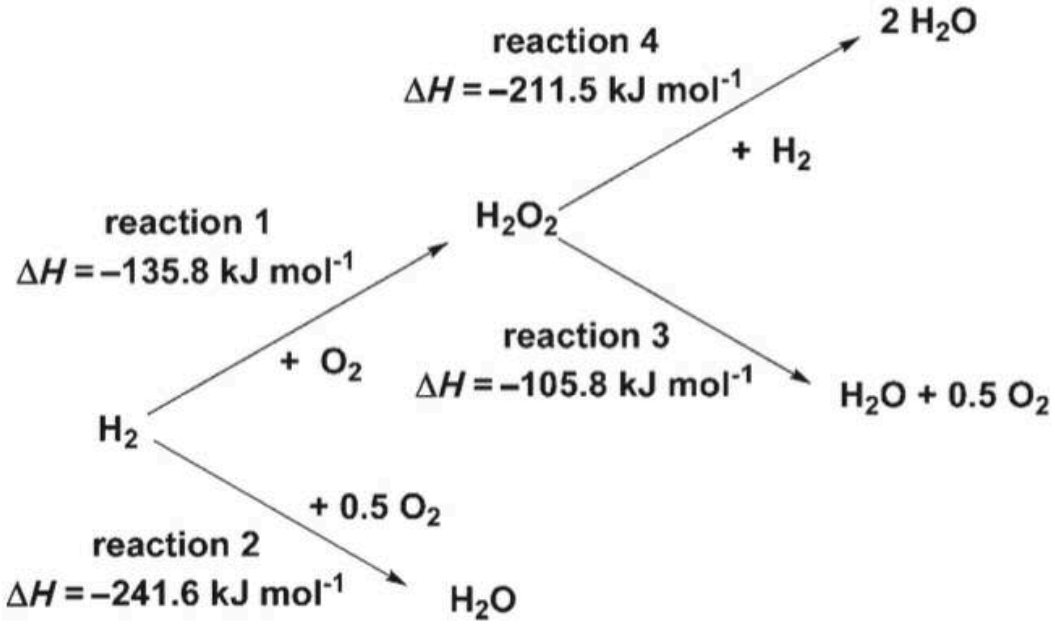

Scheme 1: Reactions involved in direct synthesis of H_2O_2.[8]

Scheme 1 illustrates the additional reactions that must be considered when designing catalysts for the direct synthesis of H_2O_2. While it is desirable to complete reaction 1, reactions 2-4 are all undesirable water-forming side reactions. In addition to this, the combustion of H_2 (reaction 2) and the hydrogenation of H_2O_2 (reaction 4) are more thermodynamically favourable than the direct synthesis reaction. The principle challenge associated with the design of catalysts for this reaction is to avoid these undesirable reactions which lead to a waste of H_2. Another challenge involves the mixture of H_2 and O_2. To avoid explosive mixtures of H_2 and O_2, reactions are typically performed using diluents such as N_2 or CO_2 (H_2 is typically diluted to 5% or lower).

1.2.3 Palladium catalysts for the direct synthesis of H_2O_2

It has long been known that Pd is active for the direct synthesis reaction. However, despite its high activity, it is generally unfavourable due to its high activity towards the subsequent water forming hydrogenation step from H_2O_2. To limit this, multiple approaches have been employed. The addition of acid/halide promotors into the reaction medium have been employed to increase selectivity towards H_2O_2. Choudhary *et al*.[9] investigated the effect of acid/halide addition upon H_2O_2 decomposition in water using a Pd/C catalyst. They found that upon addition of acids into the reaction medium, H_2O_2 decomposition was suppressed. They observed that the halide-containing acids tended to suppress H_2O_2 decomposition more significantly than the others. When the concentrations of H_2SO_4 and H_3PO_4 were increased, a corresponding suppression of H_2O_2 decomposition was observed. They also observed that the nature of the halide anion was important with the halides showing the follow H_2O_2 decomposition suppression activity: $Br^- > I^- > Cl^- >> F^-$. This effect was thought to be likely due to selective poisoning of sites responsible for H_2O_2 decomposition. When catalysts were prepared with halides incorporated into the active phase, H_2O_2 decomposition was also suppressed, except upon incorporation of fluorine which had a deleterious effect. In additional studies[10,11] they observed that upon addition of Br-, both decomposition/hydrogenation pathways of H_2O_2 could be suppressed. This was thought to be due to an inhibition of O-O bond cleavage. It is important to note that addition of acids such as HCl can lead to dissolution of Pd into the reaction medium, which can catalyse the direct synthesis reaction.[12] Park *et al*. have reported a variety of Pd catalysts which are active for H_2O_2 synthesis. Supports used include TiO_2-ZrO_2[13], SO_3 functionalised SBA-15[14], H-ZSM 5[15] and mesoporous silica supported heteropolyacids[16,17]. All these catalysts systems utilised NaBr as a halide additive. While the addition of acid/halide promoters has been shown to greatly increase the selectivity of H_2O_2 synthesis (in some cases reaching nearly 100%[18]), it would be preferable to design a catalyst that does not require these additional promoters for optimum selectivity.

1.2.4 Gold-Palladium catalysts for the direct synthesis of H_2O_2

Another method that can be employed to increase the selectivity of palladium catalysts without addition of acid/halide promoters is the addition of a secondary metal. Landon *et al*.[19] observed that addition of Au to a Pd catalyst led to a substantial increase in H_2O_2 production. Au-Pd catalysts have been prepared and tested for the H_2O_2 synthesis reaction on a variety of supports[20,21,22,23] including Al_2O_3, Fe_2O_3, TiO_2, SiO_2, MgO, carbon and zeolites. Generally, carbon supported Au-Pd catalysts were shown to have the lowest rates of H_2O_2 hydrogenation/decomposition activity. Additionally, acidic supports tended to be preferable to basic supports, likely due to base catalysed decomposition of H_2O_2. In all cases, it was observed that to obtain a stable and reusable catalyst required the use of a heat treatment (calcination) step prior to catalyst testing. While the non-calcined catalysts were highly active, a significant decrease in catalyst activity was observed upon reuse, likely due to leaching of active metal into the reaction medium. Although essential for catalyst stability, this calcination step has been shown to lead to particle sintering and decreased H_2O_2 synthesis activity.[24] Depending on the support, the calcination step can lead to changes in particle morphology such as the formation of core-shell particles with Pd-rich surfaces on supports such as TiO_2 and Al_2O_3 or homogeneous alloy compositions on supports such as carbon.[25] Interestingly, the addition of promotors such as NaBr and H_3PO_4 when using the Au-Pd catalysts lead to a decrease in H_2O_2 synthesis activity[26], whereas it has been observed to have the opposite effect when using monometallic Pd catalysts. In a subsequent investigation they found that, depending on the support used, a promotional effect on H_2O_2 selectivity could be observed upon acid/halide addition at lower concentrations than that used for monometallic Pd catalysts. It is important to note that the H_2O_2 synthesis reactions discussed employed CO_2 as a diluent for the H_2 and O_2 reactant gases. This CO_2 can form carbonic acid in water which acts as an *in situ* acid promoter. Therefore, an acid promotor is still employed for H_2O_2 synthesis using Au-Pd catalysts, although the separation is far easier.

The incorporation of a third metal into Au-Pd catalysts has also been reported. Addition of Ru to an Au-Pd/TiO_2 catalyst has been shown[27] to lead to improved production of H_2O_2, although catalyst stability was problematic at certain ratios. It was also observed that addition of very small amounts of Pt to an Au-Pd catalyst led

to greater production of H_2O_2 and suppression of the unfavourable decomposition/hydrogenation reactions.[28] Sterchele *et al*.[29] also observed an increase in H_2O_2 yields upon addition of Pt to a Pd catalyst.

In 2009, Edwards *et al*.[30] observed that by pre-treating an activated carbon support with 2%HNO_3 you could prepare an Au-Pd catalyst that did not catalyse the hydrogenation of H_2O_2. The effect was partly thought to be due to a modification in the surface ratios of Pd^{2+}/Pd^0.[31] This finding represented a large step forward in the design of catalysts for the direct synthesis reaction as it provided a means to achieve extremely high H_2O_2 selectivities in the absence of acid/halide promoters (excluding the carbonic acid from CO_2 diluent). This effect was also retained upon catalyst re-use testing. Performing this treatment on TiO_2[32] and SiO_2[33] supports also resulted in an Au-Pd catalyst with greatly enhanced H_2O_2 selectivity. However, the hydrogenation of H_2O_2 was not switched off completely when using these acid pre-treated supports.

1.2.5 Mechanistic insight into the direct synthesis reaction

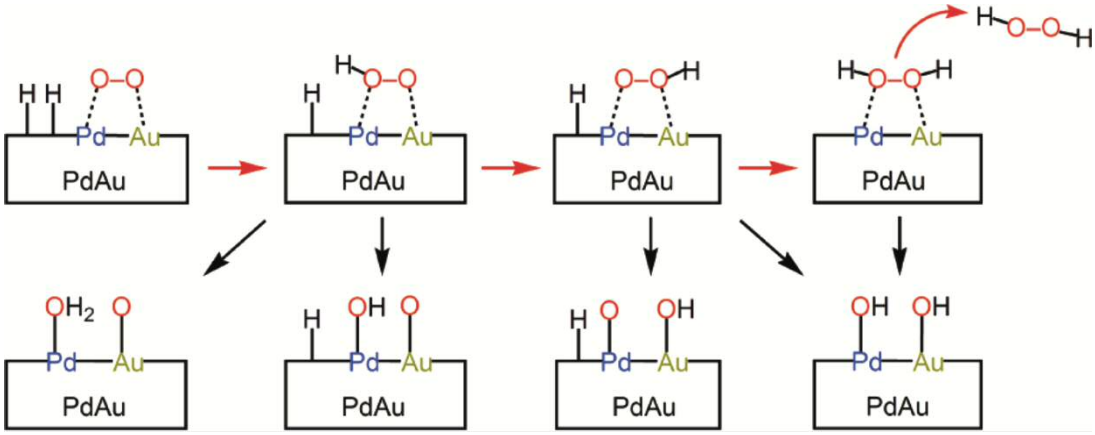

Figure 3: Proposed reaction mechanism for H_2O_2 synthesis and degradation from computational study.[34]

Multiple computational studies have been performed to gain greater insight into the nature of the mechanism for H_2O_2 synthesis over Au-Pd, Pd and Au nanoparticles. Computational investigations[35,34] propose a Langmuir-Hinshelwood type mechanism

whereby the H_2 and O_2 molecules chemisorb to the surface of the metal, the chemisorbed H then reacts with a neighbouring chemisorbed O-O to form a chemisorbed OOH species. Finally, the chemisorbed OOH can react with another neighbouring chemisorbed H to form H_2O_2 which desorbs from the metal surface. The presence of Au on the Pd surface is shown to suppress cleavage of the O-O bonds which leads to the unfavourable water-forming side reactions. Their proposed mechanism is shown in Figure 3.

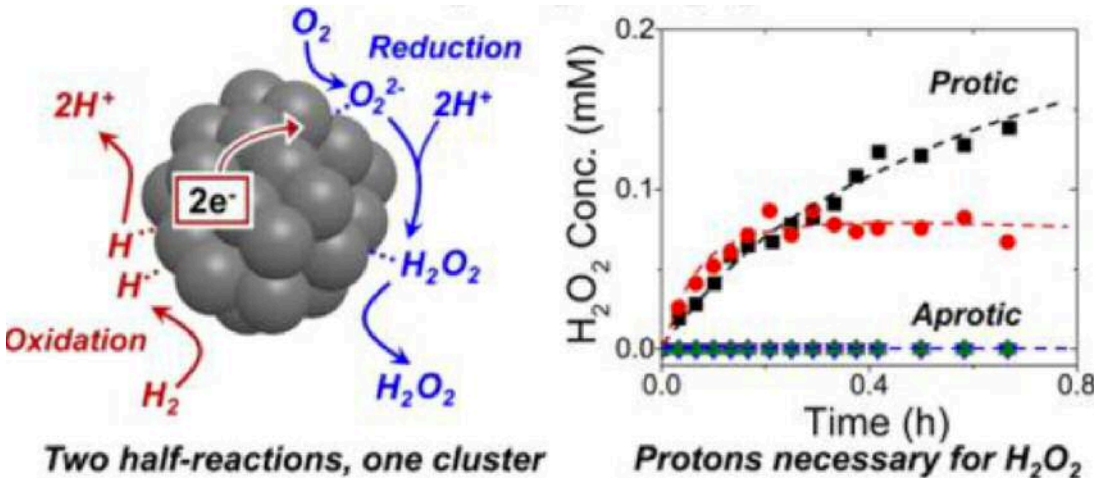

Figure 4: Alternative proposed mechanism for H_2O_2 synthesis.[36]

Wilson *et al*.[36] proposed an alternative mechanism through which the direct synthesis of H_2O_2 proceeded on Pd clusters. They proposed that H_2O_2 was formed by a proton-electron transfer to surface-bound O_2 and OOH intermediates, as shown in Figure 4. They found that the rate of H_2O_2 production was significantly decreased when an aprotic solvent was used rather than a protic solvent. This mechanism would explain the beneficial effect upon the addition of acid promoters. Although, another explanation could be the stabilising effect of acids upon H_2O_2.

1.2.6 Beyond Gold-Palladium for the direct synthesis of H_2O_2

Despite the substantial benefits of employing gold within catalysts for H_2O_2 synthesis, gold is still an expensive and relatively scarce commodity. Therefore, it is desirable to aim for the design of gold-free catalysts while maintaining catalyst performance

and the improvements gained in H_2O_2 selectivity. Freakley *et al*.[37] reported Pd-Sn catalysts that were highly active for the H_2O_2 synthesis reaction but with no activity towards the unfavourable H_2O_2 decomposition/hydrogenation pathways under the conditions used. This selectivity was made possible by the employment of a sequential oxidation-reduction-oxidation heat treatment. Using this treatment, it was possible to synthesis Pd-Ni, Pd-Zn, Pd-Ga, Pd-In and Pd-Co catalysts that were all active for H_2O_2 synthesis with 100 % selectivity. There are currently very few examples in the literature on Pd-free catalysts that are active for the direct synthesis of H_2O_2. Monometallic Au catalysts have been shown[19] to be active in the absence of Pd, but this activity is far inferior to that obtained by Pd-containing catalysts. The lack of Pd-free catalysts for the direct synthesis of H_2O_2 can likely be attributed to the need for the catalyst to perform a low temperature hydrogenation. It is not viable to conduct the direct synthesis of H_2O_2 at elevated temperatures due to decreased H_2 solubility and the decomposition of H_2O_2 at higher temperatures.

1.2.7 Direct synthesis of H_2O_2 in water

Most catalyst testing for the direct synthesis of H_2O_2 in the literature has been conducted in solvent systems comprising of methanol, ethanol, or a mixture of either with water. However, examples of H_2O_2 synthesis in fully aqueous solvent systems in the literature is currently sparse (apart from some examples of biological enzymes). One of the primary reasons is due to the poor solubility of H_2 in water. Additionally, reactions are typically performed at lower than ambient temperatures to increase the solubility of H_2 and limit the decomposition of H_2O_2. Although lower temperatures when conducting H_2O_2 synthesis reactions in water are unfeasible due to the freezing of the solvent. Crole *et al*.[38] observed a significant decrease in H_2O_2 yield upon changing from a water/methanol solvent to a solely water solvent. In addition to this, H_2O_2 yield was also observed to decrease when conducting the synthesis reaction at ambient temperatures. This was rationalised in terms of higher H_2O_2 degradation under these conditions alongside the decreased solubility of H_2. Other studies[39] have highlighted the importance of reaction conditions upon the direct synthesis reaction. Ntainjua *et al*.[40] reported the direct synthesis of H_2O_2 on Au, Pd and Au-Pd exchanged

and supported heteropolyacids using water as the solvent. Also, Freakley *et al*.[41] reported additional Au-Pd exchanged and supported heteropolyacids that were active for H_2O_2 synthesis using water. However, it is clear that more work is required in designing catalysts that are highly effective for the direct synthesis of H_2O_2 when using water as the solvent.

1.3 Applications of hydrogen peroxide for wastewater treatment

1.3.1 Why use hydrogen peroxide as an oxidant?

With the drive to create more environmentally-benign processes, H_2O_2 has gained increasing attention as a 'greener' alternative to more polluting chromate and chlorine based oxidants. It is a highly attractive oxidant owing to its high active oxygen content and the fact that it produces only water as a by-product. This compares favourably to other common oxidants as shown in Table 1.

Table 1: Various common oxidants.[42]

Oxidant	**% Active oxygen**	**By-product**
H_2O_2	47.0	H_2O
O_3	33.3	O_2
t-BuOOH	17.8	t-BuOH
NaClO	21.6	NaCl
NaBrO	13.4	NaBr
HNO_3	25.4	NO_x
$KHSO_5$	10.5	$KHSO_4$
$NaIO_4$	7.2	$NaIO_3$
PhIO	7.3	PhI

While H_2O_2 is a relatively weak oxidant it can be activated in a variety of ways to produce highly oxidising species as shown in Figure 5. The •OH radical, which can be produced from H_2O_2 using a catalyst, is one of the most powerful oxidants known.

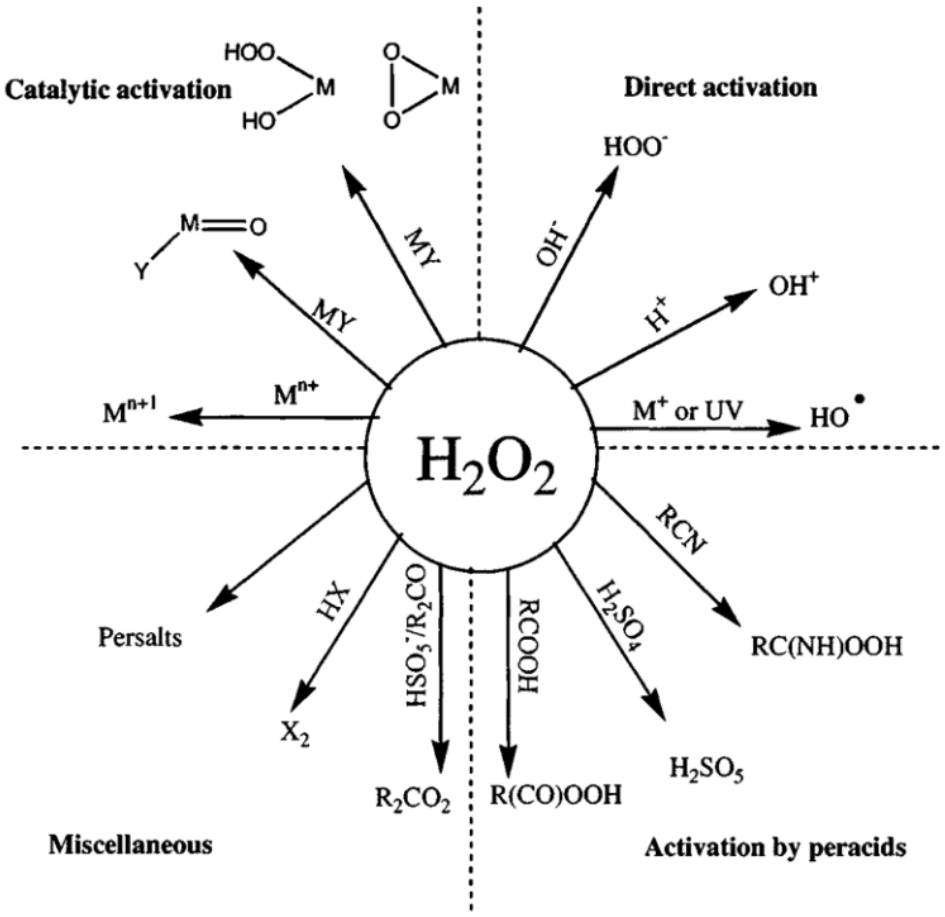

Figure 1: Activation of hydrogen peroxide.[7]

1.3.2 Hydrogen peroxide in wastewater treatment

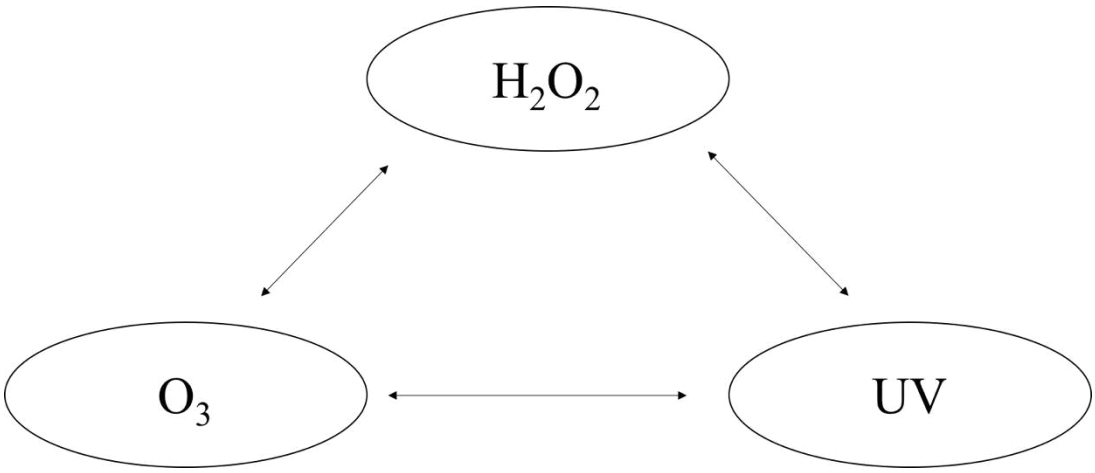

Figure 6: Advanced oxidation processes.

Due to the environmentally-benign nature of H_2O_2 (when compared to other common oxidants) it is the preferred oxidant for use in the treatment of wastewater. Advanced oxidation processes[43] utilise a combination of H_2O_2, UV irradiation and O_3 to generate radicals that can be used to totally oxidise organic molecules in wastewater effluents. These treatments are highly effective for the treatment of wastewaters containing moderate organic loadings. The organic loadings of wastewaters are typically described in terms of chemical oxygen demand. Chemical oxygen demand is the amount of oxygen which is required to achieve the total oxidation of the organic contaminants in a given wastewater effluent, typically described as mg/L O_2. It is often calculated using the following method[44]:

- Refluxing a known volume of wastewater in a solution containing $K_2Cr_2O_7$ in 50 % H_2SO_4 for 2 hours at 150 °C using Ag_2SO_4 as a catalyst.
- $HgSO_4$ is added to suppress interference from Cl^- anions.
- It is assumed that all organics in wastewater will be oxidised under these conditions.
- The $K_2Cr_2O_7$ consumed is then measured *via* titration with $(NH_3)_2Fe(SO_4)_2.6H_2O$.
- From this measurement, the chemical oxygen demand can be determined.

This method for testing the chemical oxygen demand of wastewaters is obviously not very environmentally friendly, but it remains the standard method that is employed worldwide.

Advanced oxidation processes have been applied for the removal of a variety of organic compounds from wastewater effluents such as pharmaceuticals[45], dyes[46] and chlorophenols[47].

1.3.3 Classic Fenton's oxidation

Another type of advanced oxidation process that is widely employed in the treatment of wastewater is the Fenton process.[48] Discovered in 1894[49], the Fenton process utilises H_2O_2 alongside a homogenous Fe^{2+} catalyst for the generation of highly oxidising •OH species which can totally oxidise wastewater contaminants. In a comparison of various advanced oxidation techniques for phenol degradation by Esplugas *et al*.[50], Fenton's oxidation was found to achieve the highest rate of phenol degradation. However, there are numerous drawbacks to the Fenton process such as waste of H_2O_2 oxidant due to quenching of •OH radicals by excess H_2O_2 (H_2O_2 + •OH → •OOH + H_2O), the requirement of an acidic reaction medium to prevent Fe precipitation and removal of Fe after treatment. Therefore, there has been considerable research interest into the heterogenisation of the Fenton process to allow for easier separation of the catalyst post-treatment.

1.3.4 Heterogeneous Fenton's oxidation

A wide variety of heterogeneous Fenton-like processes have been reported for the oxidation of multiple wastewater substituents using catalysts such as transition metal (typically Fe or Cu) containing zeolites[51,52,53,54,55], clays[56,57,58,59,60,61,62,63,64] and various iron oxides[65,66,67,68,69,70,71,72,73,74,75,76]. In addition to these, several supported nanoparticle catalysts have been reported in the literature. These catalysts include zero valent Fe supported on NaY[77], polymer supported Fe_3O_4[78], Fe supported on SBA-15[79] and Mn_3O_4 supported on SBA-15,[80]

However, with these heterogeneous Fenton catalysts, the leaching of active metal during the Fenton reaction was mostly problematic, especially under acidic conditions. A promising aspect of these catalysts is that many are active over a greater pH range than classic Fenton's reagent. This is vitally important as a major downside to Fenton's oxidation is the need to acidify the effluent for treatment which later requires re-neutralisation. As discussed previously, bulk concentrations of H_2O_2 can lead quenching of the hydroxyl radicals by reaction with excess H_2O_2. Therefore, it would be desirable to be able to generate a continuous low concentration of H_2O_2 for utilisation by the Fenton catalyst. However, to date there have been very few reports in the literature on the application of *in situ* generated H_2O_2 for use in the Fenton reaction.

Yalfani *et al*. reported the use of a Pd catalyst[81] which was able to oxidise low concentrations of phenol (100 ppm) using H_2O_2 generated *in situ* from formic acid and O_2. They reported that the catalyst was reusable. They also reported an Al_2O_3 supported Pd-Fe[82,83] catalyst capable of oxidising low concentrations of phenol (100 ppm) using H_2O_2 generated *in situ* from formic acid and O_2. Although, low concentrations of Fe were detected in the post-reaction effluent. This system was also tested for the degradation of chlorophenols.[84,85] Additionally, they tested other hydrogen substitutes such as hydrazine and hydroxylamine.[86] Luo *et al*.[87] reported an electro-Fenton process using Pd supported on magnetic Fe_3O_4 using H_2O_2 generated *in situ* from H_2 and O_2 (produced from water electrolysis), although this system utilises homogeneous Fe^{2+}. It is clear from these promising examples that further investigation into Fenton's oxidation using *in situ* generated H_2O_2 is required. It is also important to gain a greater understanding into the occurrence of metal leaching to design fully heterogeneous Fenton-like catalysts.

1.3.5 Other oxidation reactions using in situ generated H_2O_2

There have been numerous reports in the literature of other oxidation processes that have utilised *in situ* generated H_2O_2. These processes have been highlighted in a review by Puertolas *et al.*[88] Processes that have been investigated using *in situ* generated H_2O_2 include propylene epoxidation to propylene oxide, benzene

hydroxylation to form phenol and the oxidation of methane to oxygenates such as methanol and formic acid. Other applications of *in situ* generated H_2O_2 include oxidative desulphurisation, the oxidation of sulphides to sulphones, the oxidation of cyclohexane to cyclohexanol[89] and the oxidation of benzyl alcohol[90]. These examples show the diversity of oxidation processes that can be achieved using *in situ* generated H_2O_2. Although, further research is required to improve these processes to the point that they can be applied commercially.

1.4 Glycerol oxidation

1.4.1 Introduction to glycerol

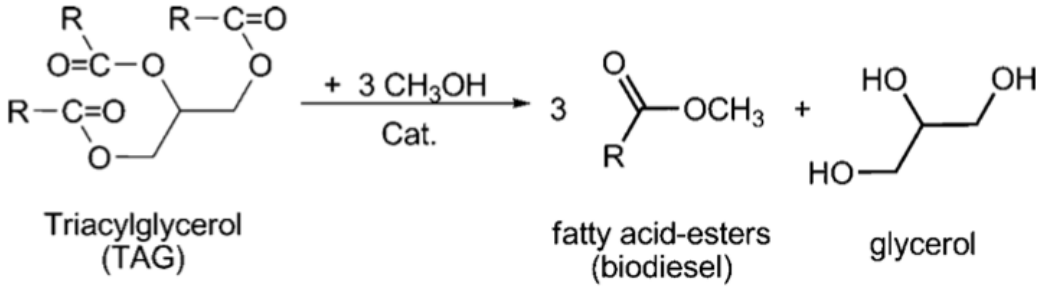

Scheme 2: Transesterification of fats to produce biodiesel and glycerol.[91]

Glycerol is colourless, odourless, viscous liquid that is non-toxic and highly functionalised. There is currently a large surplus of glycerol formed as a by-product during the manufacture of biodiesel.[92,91] The production of biodiesel involves the transesterification of vegetable or animal fats. The reaction, involving the use of methanol and promoted by acid or basic catalysts, cleaves the fatty acids from the glycerol backbone and transforms them into methyl esters. This reaction is described in Scheme 2. Therefore, this abundant source of crude glycerol has led researchers to find multiple innovative ways to make use of it. Due the functionality of this molecule, one potential use for glycerol is for the manufacture of higher value products. With the aid of a catalyst, it is possible to convert glycerol into a wide range of valuable products. Many of the potential products from glycerol oxidation are described in Scheme 3. To produce the products with the highest practical usage (such as dihydroxyacetone which is used in the cosmetics industry), it is necessary to develop highly selective catalysts.

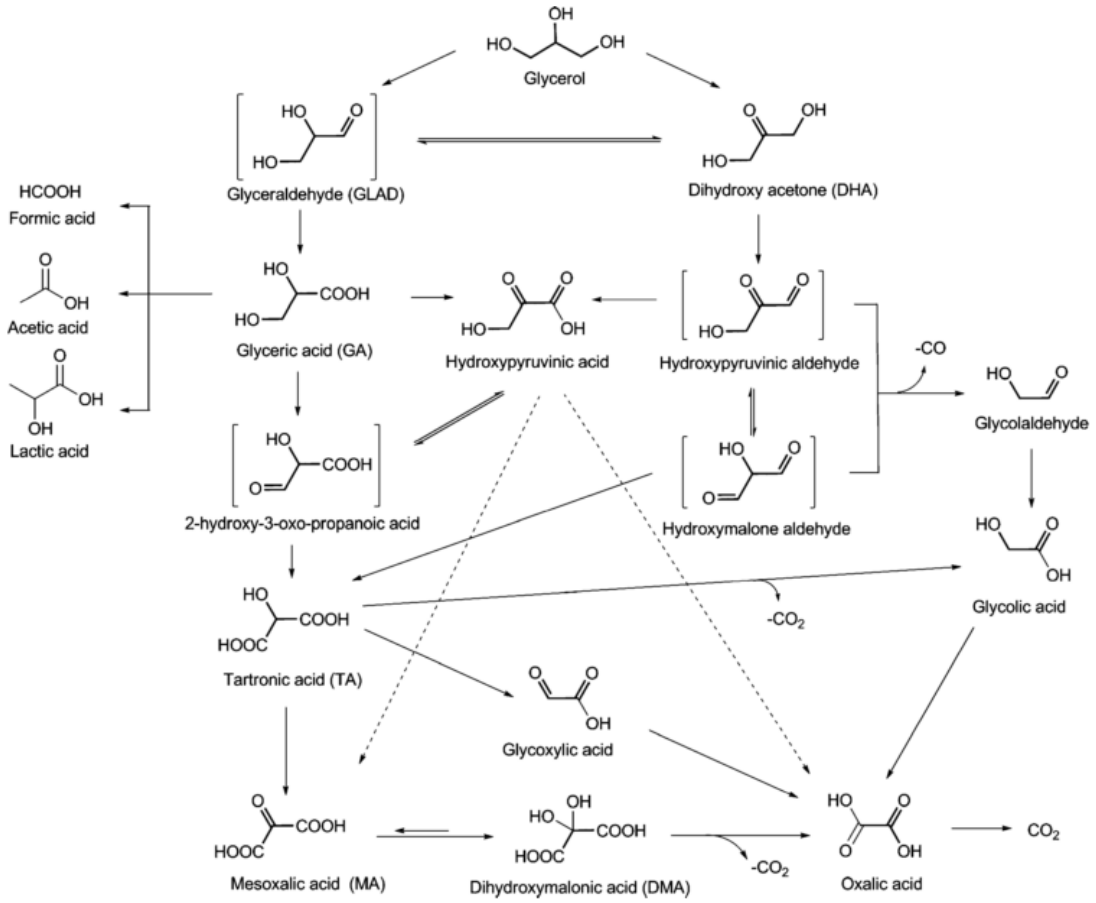

Scheme 3: Products obtained from the oxidation of glycerol.[91]

1.4.2 Selective oxidation of glycerol using gold catalysts

Many papers have been published covering the selective oxidation of glycerol using gold catalysts, these have been covered in a review by Villa *et al.*[93] Monometallic Au catalysts have been reported to achieve high selectivities towards glyceric acid during glycerol oxidation in the presence of O_2 and NaOH. It was initially thought that the presence of base was required to perform the initial H abstraction. However, work by Zope *et al.*[94] using labelling experiments showed that the oxygen incorporated into the products is derived from hydroxide ions rather than from the O_2. It was also demonstrated that the addition of a secondary metal (either Pd or Pt) could lead to greater conversion and selectivities (with Pd enhancing selectivity towards glyceric acid and Pt towards glycolic acid). It has been suggested that the formation of H_2O_2 during the glycerol oxidation reaction is responsible for the occurrence of C-C

cleavage and a decrease in selectivity towards C_3 products. Despite the high activities observed when performing the oxidation of glycerol under basic conditions, it is undesirable as it results in the formation of salts of the acid products rather than the free acid. Several examples have been reported in the literature of Au (with either Pd, Pt or both) catalysts that are active for glycerol oxidation in the absence of added NaOH. Under base-free conditions, the reactions were typically performed for longer periods at higher temperatures to achieve substantial glycerol conversion (catalyst activity tended to decrease significantly under base-free conditions). High activity and C_3 selectivity was reported when using basic supports such as MgO. However, the role played by potential dissolution of the basic supports during reaction is currently unclear. Therefore, further investigation is required into the oxidation of glycerol under base-free conditions.

1.4.3 Oxidation of glycerol using H_2O_2

Rather than using the O_2 under basic conditions, the reaction can also be performed using H_2O_2 as the oxidant. While the use of O_2 is desirable to perform oxidation reactions, the addition of a more powerful oxidising agent such as H_2O_2 may prove to be more effective when performing the reaction under base-free conditions.

McMorn *et al*.[95] investigated a series of metal containing silicate (containing Ti, V or Fe) and aluminophosphate (containing Cr, V, Mn or Co) catalysts for the oxidation of glycerol using H_2O_2. However, formic acid was found to be the dominant product. Very low concentrations of the desired partial oxidation products were observed. Additionally, a series of transition metal complexes have been supported on layered-double hydroxides and tested for the oxidation of glycerol.[96,97,98] The LDH supported Cr(III) complex was found to achieve high conversions (85.5 %) and reasonable selectivity towards dihydroxyacetone (59.3 %).

Sankar *et al*.[99] reported the oxidation of glycerol using a supported Au-Pd catalyst to glycolic acid with H_2O_2 as the oxidant. However, it is important to note that these experiments were performed in a basic medium (with addition of NaOH). Therefore, in the presence of base, it can be difficult to distinguish the contribution from H_2O_2, and O_2 generated via H_2O_2 decomposition.

Laurie *et al*.[100] investigated the effect of the Fenton reaction (Fe^{2+}/H_2O_2) upon glycerol as part of a study into wine aging. They identified glyceraldehyde and dihydroxyacetone as major products. However, other known products from glycerol oxidation were not discussed.

Crotti *et al*.[101] reported the oxidation of glycerol to formic acid and dihydroxyacetone using Fe complexes with H_2O_2 as the oxidant under mild conditions. Interestingly, they found that by modifying conditions such as the H_2O_2/glycerol ratio, 100 % selectivity to dihydroxyacetone could be achieved. This testing was performed in a water/acetonitrile mixture. They also observed that glycerol could be oxidised selectively to formic acid using $FeCl_2$ or $FeCl_3$ in aqueous solutions with H_2O_2 as the oxidant.[102]

Therefore it is clear that Fe based catalysts show a lot of potential for the oxidation of glycerol when using H_2O_2 as the oxidant. To the best of this authors knowledge, there are currently no examples in the literature of glycerol oxidation utilising H_2O_2 generated *in situ* from H_2 and O_2.

1.5 Aims of this thesis

The aims of this thesis are as follows:

- Design and test catalysts for H_2O_2 synthesis from H_2 and O_2 with the ability to then utilise the H_2O_2 for wastewater treatment applications.
- Conduct experiments at ambient temperature, which would be more applicable to real world application.
- Use a solution containing phenol as a model wastewater sample.
- Investigate the occurrence of leaching and determine the cause of this leaching.
- Attempt to produce catalysts that are stable against leaching.
- Investigate the oxidation of glycerol using H_2O_2 generated *in situ* from H_2 and O_2.

1.6 References

1 P. T. Anastas and J. C. Warner, *Green Chemistry: Theory and Practice*, Oxford University Press, 1998.

2 A. J. B. Robertson, *Platin. Met. Rev.*, 1975, **19**, 64–69.

3 V. Smil, *Nature*, 1999, **400**, 415–415.

4 G. C. Bond, C. Louis and D. T. Thompson, *Catalysis by Gold*, Imperial College Press, 2006.

5 F. Pinna, *Catal. Today*, 1998, **41**, 129–137.

6 M. Sankar, Q. He, M. Morad, J. Pritchard, S. J. Freakley, J. K. Edwards, S. H. Taylor, D. J. Morgan, A. F. Carley, D. W. Knight, C. J. Kiely and G. J. Hutchings, *ACS Nano*, 2012, **6**, 6600–6613.

7 C. W. Jones, *Applications of Hydrogen Peroxide and Derivatives*, The Royal Society of Chemistry, 1999.

8 J. M. Campos-Martin, G. Blanco-Brieva and J. L. G. Fierro, *Angew. Chemie - Int. Ed.*, 2006, **45**, 6962–6984.

9 V. R. Choudhary, C. Samanta and T. V. Choudhary, *J. Mol. Catal. A Chem.*, 2006, **260**, 115–120.

10 C. Samanta and V. R. Choudhary, *Catal. Commun.*, 2007, **8**, 2222–2228.

11 V. R. Choudhary, C. Samanta and P. Jana, 2007, 3237–3242.

12 D. P. Dissanayake and J. H. Lunsford, *J. Catal.*, 2003, **214**, 113–120.

13 S. Y. Park, J. G. Seo, J. C. Jung, S.-H. Baeck, T. J. Kim, Y.-M. Chung, S.-H. Oh and I. K. Song, *Catal. Commun.*, 2009, **10**, 1762–1765.

14 S. Park, T. J. Kim, Y.-M. Chung, S.-H. Oh and I. K. Song, *Catal. Letters*, 2009, **130**, 296–300.

15 S. Park, J. Lee, J. H. Song, T. J. Kim, Y. M. Chung, S. H. Oh and I. K. Song, *J. Mol. Catal. A Chem.*, 2012, **363**–**364**, 230–236.

16 S. Park, D. R. Park, J. H. Choi, T. J. Kim, Y. M. Chung, S. H. Oh and I. K. Song, *J. Mol. Catal. A Chem.*, 2010, **332**, 76–83.

17 S. Park, D. R. Park, J. H. Choi, T. J. Kim, Y. M. Chung, S. H. Oh and I. K. Song, *J. Mol. Catal. A Chem.*, 2011, **336**, 78–86.

18 Q. Liu, J. C. Bauer, R. E. Schaak and J. H. Lunsford, *Angew. Chemie - Int. Ed.*, 2008, **47**, 6221–6224.

19 P. Landon, P. J. Collier, A. J. Papworth, J. Kiely and J. Graham, *Chem. Commun.*, 2002, 2058–2059.

20 G. Li, J. Edwards, A. F. Carley and G. J. Hutchings, *Catal. Today*, 2007, **122**, 361–364.

21 J. K. Edwards, A. Thomas, B. E. Solsona, P. Landon, A. F. Carley and G. J. Hutchings, *Catal. Today*, 2007, **122**, 397–402.

22 B. E. Solsona, J. K. Edwards, P. Landon, A. F. Carley, A. Herzing, C. J. Kiely and G. J. Hutchings, *Chem. Mater.*, 2006, **18**, 2689–2695.

23 E. Ntainjua N., J. K. Edwards, A. F. Carley, J. A. Lopez-Sanchez, J. A. Moulijn, A. a. Herzing, C. J. Kiely and G. J. Hutchings, *Green Chem.*, 2008, **10**, 1162.

24 A. A. Herzing, A. F. Carley, J. K. Edwards, G. J. Hutchings and C. J. Kiely, *Chem. Mater.*, 2008, **20**, 1492–1501.

25 J. K. Edwards, A. F. Carley, A. A. Herzing, C. J. Kiely and G. J. Hutchings, *Faraday Discuss.*, 2008, **138**, 225–239.

26 J. K. Edwards, A. Thomas, A. F. Carley, A. a. Herzing, C. J. Kiely and G. J. Hutchings, *Green Chem.*, 2008, **10**, 388.

27 E. N. Ntainjua, S. J. Freakley and G. J. Hutchings, *Top. Catal.*, 2012, **55**, 718–722.

28 J. K. Edwards, J. Pritchard, L. Lu, M. Piccinini, G. Shaw, A. F. Carley, D. J. Morgan, C. J. Kiely and G. J. Hutchings, *Angew. Chemie - Int. Ed.*, 2014, **53**, 2381–2384.

29 S. Sterchele, P. Biasi, P. Centomo, P. Canton, S. Campestrini, T. Salmi and

M. Zecca, *Appl. Catal. A Gen.*, 2013, **468**, 160–174.

30 J. K. Edwards, B. Solsona, E. N. N, A. F. Carley, A. a Herzing, C. J. Kiely and G. J. Hutchings, *Science (80-.).*, 2009, **323**, 1037–1041.

31 J. K. Edwards, J. Pritchard, M. Piccinini, G. Shaw, Q. He, A. F. Carley, C. J. Kiely and G. J. Hutchings, *J. Catal.*, 2012, **292**, 227–238.

32 J. K. Edwards, N. N. Edwin, A. F. Carley, A. A. Herzing, C. J. Kiely and G. J. Hutchings, *Angew. Chemie - Int. Ed.*, 2009, **48**, 8512–8515.

33 J. K. Edwards, S. F. Parker, J. Pritchard, M. Piccinini, S. J. Freakley, Q. He, A. F. Carley, C. J. Kiely and G. J. Hutchings, *Catal. Sci. Technol.*, 2013, **3**, 812–818.

34 J. Li, T. Ishihara and K. Yoshizawa, *J. Phys. Chem. C*, 2011, **115**, 25359–25367.

35 A. Staykov, T. Kamachi, T. Ishihara and K. Yoshizawa, *J. Phys. Chem. C*, 2008, **112**, 19501–19505.

36 N. M. Wilson and D. W. Flaherty, *J. Am. Chem. Soc.*, 2016, **138**, 574–586.

37 S. J. Freakley, Q. He, J. H. Harrhy, L. Lu, D. A. Crole, D. J. Morgan, E. N. Ntainjua, J. K. Edwards, A. F. Carley, A. Y. Borisevich, C. J. Kiely and G. J. Hutchings, *Science*, 2015, **351**, 279–296.

38 D. A. Crole, S. J. Freakley, J. K. Edwards and G. J. Hutchings, *Proc. R. Soc. A Math. Phys. Eng. Sci.*, 2016, **472**, 20160156.

39 S. J. Freakley, M. Piccinini, J. K. Edwards, E. N. Ntainjua, J. A. Moulijn and G. J. Hutchings, *ACS Catal.*, 2013, **3**, 487–501.

40 E. N. Ntainjua, M. Piccinini, S. J. Freakley, J. C. Pritchard, J. K. Edwards, A. F. Carley and G. J. Hutchings, *Green Chem.*, 2012, **14**, 170–181.

41 S. J. Freakley, R. J. Lewis, D. J. Morgan, J. K. Edwards and G. J. Hutchings, *Catal. Today*, 2015, **248**, 10–17.

42 G. Strukul, *Catalytic Oxidations with Hydrogen Peroxide as Oxidant*, Springer, 1st edn., 1992.

43 R. Andreozzi, V. Caprio, A. Insola and R. Marotta, *Catal. Today*, 1999, **53**, 51–59.

44 E. W. Rice, L. Bridgewater, A. P. H. Association, A. W. W. Association and W. E. Federation, *Standard Methods for the Examination of Water and Wastewater*, American Public Health Association, 2012.

45 M. M. Huber, S. Canonica, G.-Y. Park and U. Von Gunten, *Environ. Sci. Technol.*, 2003, **37**, 1016–1024.

46 S. Atalay and G. Ersöz, *Advanced Oxidation Processes for Removal of Dyes from Aqueous Media*, 2015.

47 M. Pera-Titus, V. Garcia-Molina, M. A. Banos, J. Gimenez and S. Esplugas, *Appl. Catal. B Environ.*, 2004, **47**, 219–256.

48 J. J. Pignatello, E. Oliveros and A. MacKay, *Crit. Rev. Environ. Sci. Technol.*, 2006, **36**, 1–84.

49 H. J. H. Fenton, *J. Chem. Soc. Trans.*, 1894, **65**, 899–910.

50 S. Esplugas, J. Gimenez, S. Contreras, E. Pascual and M. Rodriguez, *Water Res.*, 2002, **36**, 1034–1042.

51 R. Aravindhan, N. N. Fathima, J. R. Rao and B. U. Nair, *J. Hazard. Mater.*, 2006, **138**, 152–159.

52 M. Neamţu, C. Zaharia, C. Catrinescu, A. Yediler, M. Macoveanu and A. Kettrup, *Appl. Catal. B Environ.*, 2004, **48**, 287–294.

53 M. Neamţu, C. Catrinescu and A. Kettrup, *Appl. Catal. B Environ.*, 2004, **51**, 149–157.

54 O. A. Makhotkina, E. V. Kuznetsova and S. V. Preis, *Appl. Catal. B Environ.*, 2006, **68**, 85–91.

55 D. J. Doocey and P. N. Sharratt, *Process Saf. Environ. Prot.*, 2004, **82**, 352–358.

56 S. Caudo, C. Genovese, S. Perathoner and G. Centi, *Microporous Mesoporous Mater.*, 2008, **107**, 46–57.

57 G. Giordano, S. Perathoner, G. Centi, S. De Rosa, T. Granato, A. Katovic, A. Siciliano, A. Tagarelli and F. Tripicchio, *Catal. Today*, 2007, **124**, 240–246.

58 N. Sanabria, A. Álvarez, R. Molina and S. Moreno, *Catal. Today*, 2008, **133**–**135**, 530–533.

59 J. Carriazo, E. Guélou, J. Barrault, J. M. Tatibouët, R. Molina and S. Moreno, *Water Res.*, 2005, **39**, 3891–3899.

60 J. G. Carriazo, E. Guelou, J. Barrault, J. M. Tatibouët and S. Moreno, *Appl. Clay Sci.*, 2003, **22**, 303–308.

61 L. Chirchi and A. Ghorbel, *Appl. Clay Sci.*, 2002, **21**, 271–276.

62 J. Barrault, J.-M. Tatibouët and N. Papayannakos, *Comptes Rendus l'Académie des Sci. - Ser. IIC - Chem.*, 2000, **3**, 777–783.

63 J. Barrault, M. Abdellaoui, C. Bouchoule, A. Majesté, J. M. Tatibouët and A. Louloudi, 2000, **27**, 225–230.

64 J. H. Ramirez, C. A. Costa, L. M. Madeira, G. Mata, M. A. Vicente, M. L. Rojas-Cervantes, A. J. López-Peinado and R. M. Martín-Aranda, *Appl. Catal. B Environ.*, 2007, **71**, 44–56.

65 J. J. Wu, M. Muruganandham, J. S. Yang and S. S. Lin, *Catal. Commun.*, 2006, **7**, 901–906.

66 R. Andreozzi, A. D'Apuzzo and R. Marotta, *Water Res.*, 2002, **36**, 4691–4698.

67 J. C. Barreiro, M. D. Capelato, L. Martin-Neto and H. C. Bruun Hansen, *Water Res.*, 2007, **41**, 55–62.

68 C. K. J. Yeh, C. Y. Hsu, C. H. Chiu and K. L. Huang, *J. Hazard. Mater.*, 2008, **151**, 562–569.

69 S. H. Kong, R. J. Watts and J. H. Choi, *Chemosphere*, 1998, **37**, 1473–1482.

70 R. Andreozzi, V. Caprio and R. Marotta, *Water Res.*, 2002, **36**, 2761–2768.

71 S. Chou and C. Huang, *Chemosphere*, 1999, **38**, 2719–2731.

72 M. C. Lu, J. N. Chen and H. H. Huang, *Chemosphere*, 2002, **46**, 131–136.

73 H. H. Huang, M. C. Lu and J. N. Chen, *Water Res.*, 2001, **35**, 2291–9.

74 M. J. Liou and M. C. Lu, *J. Hazard. Mater.*, 2008, **151**, 540–546.

75 K. Hanna, T. Kone and G. Medjahdi, *Catal. Commun.*, 2008, **9**, 955–959.

76 P. Baldrian, V. Merhautová, J. Gabriel, F. Nerud, P. Stopka, M. Hrubý and M. J. Beneš, *Appl. Catal. B Environ.*, 2006, **66**, 258–264.

77 W. Wang, M. Zhou, Q. Mao, J. Yue and X. Wang, *Catal. Commun.*, 2010, **11**, 937–941.

78 S. Shin, H. Yoon and J. Jang, *Catal. Commun.*, 2008, **10**, 178–182.

79 L. Xiang, S. Royer, H. Zhang, J. M. Tatibouët, J. Barrault and S. Valange, *J. Hazard. Mater.*, 2009, **172**, 1175–1184.

80 Y. F. Han, F. Chen, K. Ramesh, Z. Zhong, E. Widjaja and L. Chen, *Appl. Catal. B Environ.*, 2007, **76**, 227–234.

81 M. S. Yalfani, S. Contreras, F. Medina and J. Sueiras, *Appl. Catal. B Environ.*, 2009, **89**, 519–526.

82 S. Contreras, M. S. Yalfani, F. Medina and J. E. Sueiras, *Water Sci. Technol.*, 2011, 63, 2017–2024.

83 M. S. Yalfani, S. Contreras, J. Llorca, M. Dominguez, J. E. Sueiras and F. Medina, *Phys. Chem. Chem. Phys.*, 2010, **12**, 14673–14676.

84 M. S. Yalfani, A. Georgi, S. Contreras, F. Medina and F. D. Kopinke, *Appl. Catal. B Environ.*, 2011, **104**, 161–168.

85 M. Munoz, Z. M. de Pedro, J. A. Casas and J. J. Rodriguez, *Water Res.*, 2013, **47**, 3070–3080.

86 M. S. Yalfani, S. Contreras, F. Medina and J. E. Sueiras, *J. Hazard. Mater.*, 2011, **192**, 340–346.

87 M. Luo, S. Yuan, M. Tong, P. Liao, W. Xie and X. Xu, *Water Res.*, 2014, **48**, 190–199.

88 B. Puértolas, A. K. Hill, T. García, B. Solsona and L. Torrente-Murciano, *Catal. Today*, 2015, **248**, 115–127.

89 L. I. Kuznetsova, N. I. Kuznetsova and O. S. Koscheeva, *Catal. Commun.*, 2017, **88**, 50–52.

90 I. Moreno, N. F. Dummer, J. K. Edwards, M. Alhumaimess, M. Sankar, R. Sanz, P. Pizarro, D. P. Serrano and G. J. Hutchings, *Catal. Sci. Technol.*, 2013, **3**, 2425.

91 B. Katryniok, H. Kimura, E. Skrzyńska, J.-S. Girardon, P. Fongarland, M. Capron, R. Ducoulombier, N. Mimura, S. Paul and F. Dumeignil, *Green Chem.*, 2011, **13**, 1960.

92 M. Pagliaro, R. Ciriminna, H. Kimura, M. Rossi and C. Della Pina, *Angew. Chemie - Int. Ed.*, 2007, **46**, 4434–4440.

93 A. Villa, N. Dimitratos, C. E. Chan-Thaw, C. Hammond, L. Prati and G. J. Hutchings, *Acc. Chem. Res.*, 2015, **48**, 1403–1412.

94 B. N. Zope, D. D. Hibbitts, M. Neurock and R. J. Davis, *Science (80-.).*, 2010, **330**, 74–78.

95 P. Mcmorn, G. Roberts and G. J. Hutchings, *Catal. Letters*, 1999, **63**, 193–197.

96 X. Wang, C. Shang, G. Wu, X. Liu and H. Liu, *Catalysts*, 2016, **6**, 101.

97 G. Wu, X. Wang, T. Jiang and Q. Lin, *Catalysts*, 2015, **5**, 2039–2051.

98 X. Wang, G. Wu, F. Wang, K. Ding, F. Zhang, X. Liu and Y. Xue, *Catal. Commun.*, 2012, **28**, 73–76.

99 M. Sankar, N. Dimitratos, D. W. Knight, A. F. Carley, R. Tiruvalam, C. J. Kiely, D. Thomas and G. J. Hutchings, *ChemSusChem*, 2009, **2**, 1145–1151.

100 V. F. Laurie and A. L. Waterhouse, *J. Agric. Food Chem.*, 2006, **54**, 4668–4673.

101 C. Crotti and E. Farnetti, *J. Mol. Catal. A Chem.*, 2015, **396**, 353–359.

102 E. Farnetti and C. Crotti, *Catal. Commun.*, 2016, **84**, 1–4.

2 Experimental

2.1 Catalyst preparation

2.1.1 Impregnation

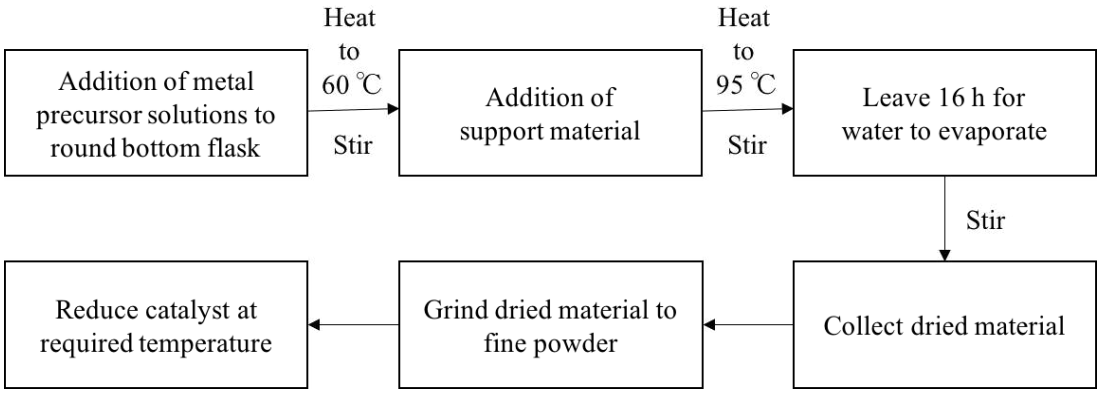

Figure 1: Flow chart schematic for impregnation procedure.

Pd, Fe, Pd-Fe, Pd-Au, Pd-Cu and Pd-Mn bimetallic catalysts were prepared using an impregnation procedure[1] on various supports: titania (TiO_2, P25, Degussa), silica (SiO_2, 35-70 micron, Fisher Scientific), carbon (C, SX1G, Norit), carbon (C, L2S, Ceca), carbon (C, L4S, Ceca), carbon (C, CPL, Ceca), carbon (C, G60, Darco), iron oxide (Fe_2O_3, nanopowder, Sigma Aldrich). Various metal salt precursors were used; palladium (II) chloride ($PdCl_2$, 99.999 %, Sigma Aldrich), iron (III) chloride ($FeCl_3.6H_2O$, > 99 %, Fluka), gold (III) chloride ($HAuCl_4.3H_2O$, > 99.9 %, Sigma Aldrich), manganese (II) nitrate ($Mn(NO_3)_2.xH_2O$, 99.99%, Sigma Aldrich), copper (II) nitrate ($Cu(NO_3)_2.xH_2O$, 99.999 %, Sigma Aldrich), palladium (II) nitrate ($Pd(NO_3)_2.2H_2O$, ~40 % Pd basis, Sigma Aldrich), iron (III) nitrate ($Fe(NO_3)_3.9H_2O$, > 99.999 %, Sigma Aldrich).

In a typical preparation of Pd-Fe/TiO_2, the requisite amount of $PdCl_2$ solution (6 mg / ml Pd, 0.58 M HCl) and $FeCl_3$ solution (6 mg / ml Fe) were added to a 50 ml round bottom flask. Water was then added to achieve a total solution volume of 16 ml. The solution was then heated to 60 °C with 1000 rpm stirring and the required amount of

support (TiO_2) added to produce 2 g of supported metal catalyst. After complete addition of support, the mixture was then heated to 95 °C with stirring (1000 rpm) for 16 h to allow complete evaporation of the water. The dried catalyst was then recovered and ground using a pestle and mortar. The ground catalyst was then treated under flowing 5 % H_2 / Ar at 500 °C for 4 h with a ramp rate of 10 °C / min. The treated catalyst was then allowed to cool to room temperature under flowing 5% H_2 / Ar.

2.1.2 Sol immobilisation

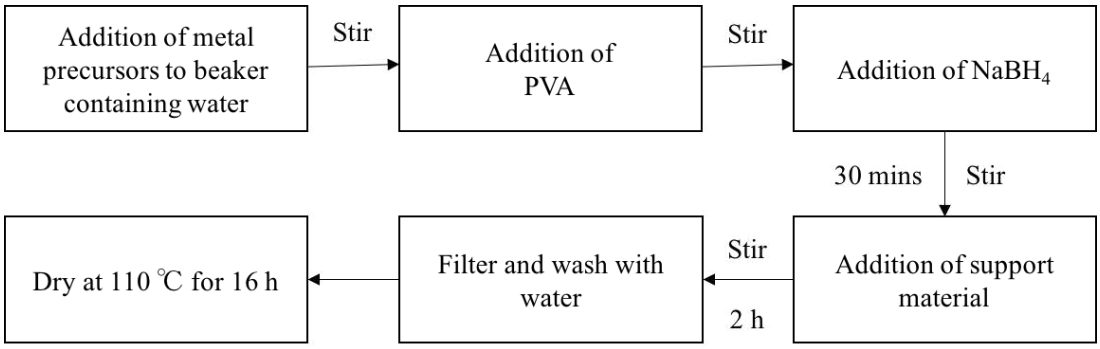

Figure 2: Flow chart schematic for sol immobilisation procedure.

Pd-Fe bimetallic catalysts were prepared using a sol immobilisation procedure described in the literature.[2] Silica (SiO_2, 35-70 micron, Fisher Scientific) was used as the support. Metal salts used included palladium (II) chloride ($PdCl_2$, 99.999 %, Sigma Aldrich) and iron (III) chloride ($FeCl_3.6H_2O$, > 99 %, Fluka). Poly(vinyl alcohol) (PVA, M_w 9000-10000, 80 % hydrolysed, Sigma Aldrich)

In a typical preparation for Pd-Fe/SiO_2, the requisite amount of $PdCl_2$ solution (6 mg / ml Pd, 0.58 M HCl) and $FeCl_3$ solution (6 mg / ml Fe) were added to water (800 ml) under stirring (1000 rpm). To this solution, the requisite concentration of PVA (1 % solution) was added (PVA / (Au + Pd) (w / w) = 1.3). After addition of the PVA, a solution of $NaBH_4$ (0.1 M) was prepared. The requisite amount of $NaBH_4$ solution was then added ($NaBH_4$ / (Au + Pd) (mol / mol) = 5). After 30 mins, the requisite amount of support (SiO_2) was added. After 2 h, the slurry was filtered and then washed

with distilled water (2 L). The obtained material was then dried for 16 h under static air.

2.2 Phenol oxidation

2.2.1 Catalyst testing

2.2.1.1 Phenol oxidation with in situ generated hydrogen peroxide

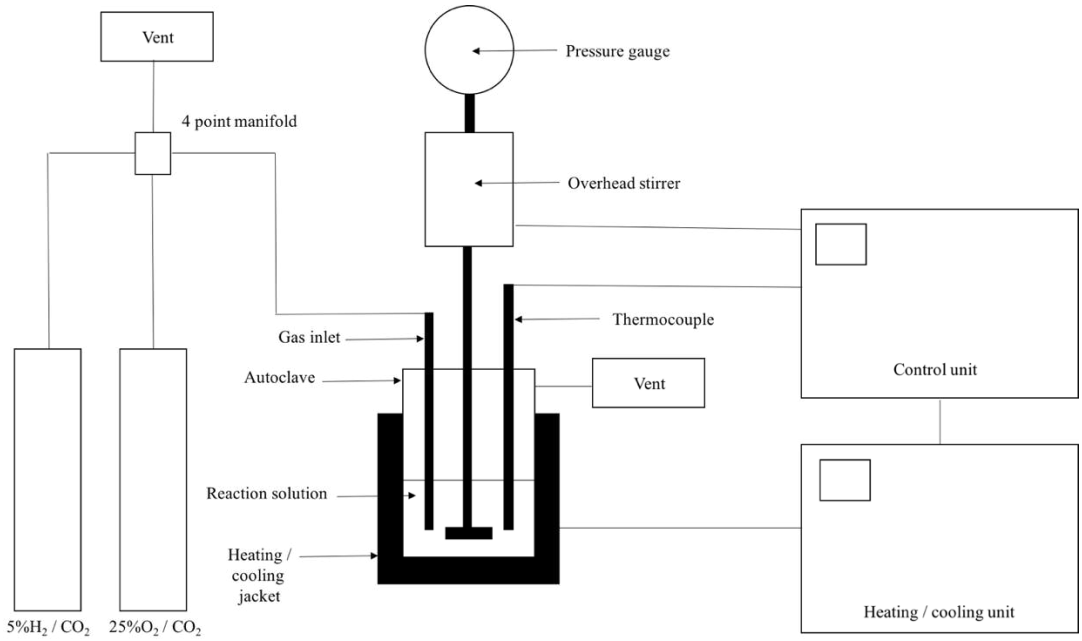

Figure 3: Autoclave reactor schematic.

Phenol oxidation reactions were performed in a Parr stainless steel autoclave fitted with a PTFE reactor liner and a reactor volume of ~ 50 ml (35 ml with liner inserted). In a typical reaction, the PTFE liner was charged with the requisite amount of phenol solution and catalyst. The PTFE liner was then inserted into the reactor and the reactor sealed. The reactor was then purged with dilute hydrogen mixture (5%H_2 / CO_2, 100 psi) 3 times. The reactor was then charged with the requisite amount of dilute hydrogen mixture (5% H_2 / CO_2, 420 psi) and dilute oxygen mixture (25% O_2 / CO_2, 160 psi). The reactor was then heated to 30 °C and stirring commenced immediately

(1200 rpm). After the reaction had run for the requisite amount of time, the gases were vented and the reaction solution collected and filtered. The filtered solution was then analysed using HPLC.

2.2.1.2 Phenol oxidation with addition of *ex situ* H_2O_2

Phenol oxidation reactions were performed in a Parr stainless steel autoclave fitted with a PTFE reactor liner and a reactor volume of ~ 50 ml. In a typical reaction, the PTFE liner was charged with the requisite amount of phenol solution, catalyst and either stabilised hydrogen peroxide (50 wt. % in H_2O stabilised, Fluka) or unstabilised hydrogen peroxide (30 wt. % in H_2O unstabilised, ACROS). The PTFE liner was then inserted into the reactor and the reactor sealed. The reactor was then purged with dilute oxygen mixture (25%O_2 / CO_2, 100 psi) 3 times. The reactor was then charged with the requisite amount of dilute oxygen mixture (25% O_2 / CO_2, 580 psi). The reactor was then heated to 30 °C and stirring commenced (1200 rpm). After the reaction had run for the requisite amount of time, the gas was vented and the reaction solution collected and filtered. The filtered solution was then analysed using HPLC.

2.2.1.3 Testing effect of reaction products on catalyst stability

To determine the effect of reaction products upon catalyst stability, the catalyst was stirred in solutions of the different products and the extent of leaching observed. Reactions were performed in a Parr stainless steel autoclave fitted with a PTFE reactor liner and a reactor volume of ~ 50 ml.

In a typical reaction, the PTFE liner was charged with the requisite amount of product solution and catalyst. The PTFE liner was then inserted into the reactor and the reactor sealed. When testing the effect of the high pressure gases, the reactor was then purged with dilute hydrogen mixture (5%H_2 / CO_2, 100 psi) 3 times. The reactor was then charged with the requisite amount of dilute hydrogen mixture (5% H_2 / CO_2, 420 psi) and dilute oxygen mixture (25% O_2 / CO_2, 160 psi). The reactor was then heated to 30 °C and stirring commenced (1200 rpm). After the reaction had run for the requisite

amount of time, the gas was vented and the reaction solution collected and filtered. The filtered solution was then analysed using MP-AES.

Additionally, the effect of flowing oxalic acid and catechol over the catalyst was measured. To perform the test, the catalyst (50 mg) was loaded into a PVC tube (inner diameter = 5 mm, outer diameter = 8 mm) and held in place using glass wool. The PVC tube was then attached to a burette and solutions of either oxalic acid or catechol (1000 ppm, 40 ml, ~ 1 ml / min) flowed over the catalyst. Aliquots of 5 ml were then collected and analysed using MP-AES to determine concentrations of leached metals. The catalyst was then collected and dried in a desiccator (48 h) for reusability testing.

2.2.1.4 Testing effect of leachate on reaction

For the experiments measuring the effect of catalyst leachate upon the reaction, the leachate was prepared as follows:

The reaction was performed in a Parr stainless steel autoclave fitted with a PTFE reactor liner and a reactor volume of ~ 50 ml. The PTFE liner was charged with the requisite amount of phenol solution (1000 ppm, 10 g) and catalyst (0.5%Pd-0.5%Fe/SiO_2, 50 mg). The PTFE liner was then inserted into the reactor and the reactor sealed. The reactor was then purged with dilute hydrogen mixture (5%H_2 / CO_2, 100 psi) 3 times. The reactor was then charged with the requisite amount of dilute hydrogen mixture (5% H_2 / CO_2, 420 psi) and dilute oxygen mixture (25% O_2 / CO_2, 160 psi). The reactor was then heated to 30 °C and stirring commenced (1200 rpm). After the reaction had run for 2 h, the gases were vented and the reaction solution collected and filtered.

2.2.2 Reaction analysis

2.2.2.1 High-performance liquid chromatography (HPLC)

HPLC is a powerful chromatography technique for the separation of products in a reaction mixture for analysis. The basic principle behind HPLC is that a sample containing multiple compounds is passed through a column packed with a material that the compounds have differing affinities towards (termed stationary phase) with the aid of a solvent (termed mobile phase). Due to the varying affinities of the compounds towards the stationary phase, the compounds pass through the column at different rates, thereby becoming separated. These separated compounds can then be detected and quantified using a variety of detectors. The degree and speed of separation can be altered by appropriate selection of stationary phase, mobile phase, column temperature and the rate at which mobile phase is passed through the column. Common detectors utilised include diode array (DAD) which measures UV absorbance at chosen wavelengths and refractive index (RID) which measures the refractive index of the sample. Multiple detectors are commonly utilised due to limitations associated with the use of individual detectors. For example, the use of DAD is only appropriate for the detection of compounds able to absorb UV light whereas RID is unsuitable for use where the composition of the mobile phase changes over time (which would lead to an unstable baseline).

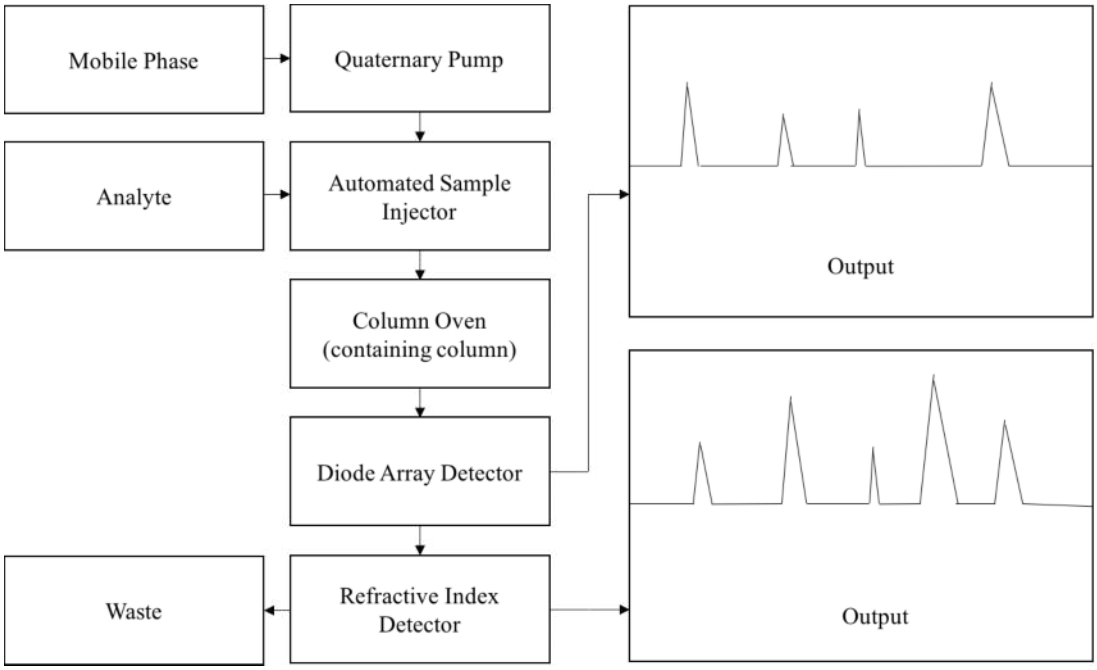

Figure 4: Flow chart schematic of HPLC set up.

Analysis was performed on an Agilent 1260 Infinity series HPLC comprising a quaternary pump, automated sample injector, column oven, diode array detector and refractive index detector. The HPLC was fitted with a MetaCarb 67h column and phosphoric acid (0.1% H_3PO_4) used as the mobile phase. The following conditions were employed for the analysis: flow rate (mobile phase) = 0.25 ml / min, column temperature = 30 °C, Injection volume = 10 µl. Calibrations were performed using known standards.

2.2.2.2 Microwave plasma atomic emission spectroscopy (MP-AES)

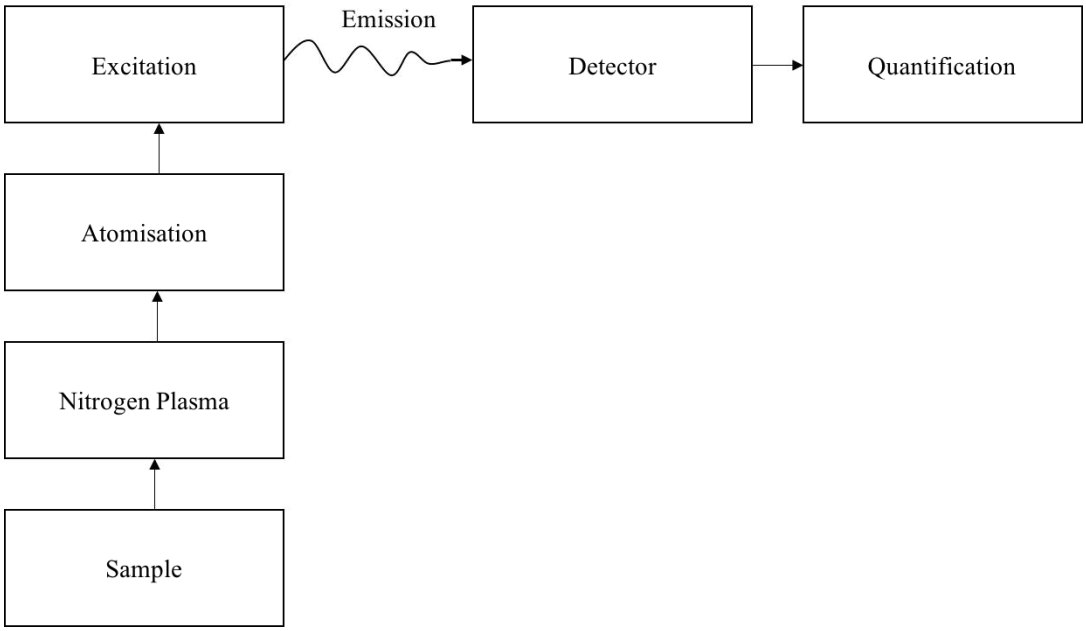

Figure 5: Flow chart schematic showing basic principles of MP-AES.

MP-AES is a technique that enables the identification and quantification of metals in solution. It utilises a plasma heated to ~ 5000 K through which the sample is passed. The basic principle behind MP-AES is that the sample is passed into the plasma, atomisation occurs and the electrons excited. As the electrons relax to lower energy states, a photon is released with a characteristic energy and wavelength. With the use of a monochromator detector and mirror grating, various wavelengths can be measured sequentially to identify the presence/concentration of metals in solution. With the selection of appropriate wavelengths (to avoid interference from other metals in solution), highly accurate information can be obtained about the concentration of metals in solution.

To determine the presence of metal ions in solution, post-reaction solutions were collected and analysed using an Agilent MP-AES 4100. The post reaction solutions were filtered using PTFE syringe filters (0.45 μm) and analysed to determine the presence of Fe, Pd and La (where appropriate). Calibration solutions were prepared via dilution with deionised water over a suitable concentration range using atomic

absorption standards for Fe (1000 mg/L Fe in 1 wt. % HCl, Sigma Aldrich), Pd (1000 mg/L Pd in 5% HCl, Sigma Aldrich) and La (1000 mg/L La in 1 wt.% HNO_3, Sigma Aldrich). For analysis of Fe, wavelengths of 371.993 nm and 259.940 nm were used. For analysis of Pd, wavelengths of 324.270 nm and 351.694 nm were used. For analysis of La, wavelengths of 394.910 nm and 408.672 nm were used. These wavelengths were chosen to limit interference from other metals present in solution.

2.2.2.3 Determination of H_2O_2 concentration

H_2O_2 concentration analysis was performed using a redox titration. Aliquots of the post-reaction solutions were taken and titratred against an acidified $Ce(SO_4)_2$ solution using a ferroin indicator.

2.3 Glycerol oxidation

2.3.1 Catalyst Testing

2.3.1.1 Glycerol oxidation with *in situ* generated hydrogen peroxide H_2O_2

Glycerol oxidation reactions were performed in a Parr stainless steel autoclave fitted with a PTFE reactor liner and a reactor volume of ~ 50 ml. In a typical reaction, the PTFE liner was charged with the requisite amount of glycerol solution (typically 10 g, 0.3 M) and catalyst (typically 50 mg). The PTFE liner was then inserted into the reactor and the reactor sealed. The reactor was then purged with dilute hydrogen mixture (5%H_2 / CO_2, 100 psi) 3 times. The reactor was then charged with the requisite amount of dilute hydrogen mixture (5% H_2 / CO_2, 420 psi) and dilute oxygen mixture (25% O_2 / CO_2, 160 psi). The reactor was then heated to 30 °C and stirring commenced (1200 rpm). After the reaction had run for the requisite amount of time, the gases were vented and the reaction solution collected and filtered. The filtered solution was then analysed using HPLC.

2.3.1.2 Glycerol oxidation with addition of *ex situ* H_2O_2

Glycerol oxidation reactions were performed in a Parr stainless steel autoclave fitted with a PTFE reactor liner and a reactor volume of ~ 50 ml. In a typical reaction, the PTFE liner was charged with the requisite amount of glycerol solution, catalyst and hydrogen peroxide (50 wt. % in H_2O stabilised, Fluka). The PTFE liner was then inserted into the reactor and the reactor sealed. The reactor was then purged with dilute oxygen mixture (25%O_2 / CO_2, 100 psi) 3 times. The reactor was then charged with the requisite amount of dilute oxygen mixture (25% O_2 / CO_2, 580 psi). The reactor was then heated to 30 °C and stirring commenced (1200 rpm). After the reaction had run for the requisite amount of time, the gas was vented and the reaction solution collected and filtered. The filtered solution was then analysed using HPLC.

2.3.1.3 Radical trapping experiments

Glycerol oxidation reactions were performed in a Parr stainless steel autoclave fitted with a PTFE reactor liner and a reactor volume of ~ 50 ml. In a typical reaction, the PTFE liner was charged with the requisite amount of glycerol solution (typically 10 g, 0.3 M) and catalyst (50 mg) and 5,5-dimethyl-1-pyrroline n-oxide (DMPO, 10 μL, Sigma Aldrich). The PTFE liner was then inserted into the reactor and the reactor sealed. The reactor was then purged with dilute hydrogen mixture (5%H_2 / CO_2, 100 psi) 3 times. The reactor was then charged with the requisite amount of dilute hydrogen mixture (5% H_2 / CO_2, 420 psi) and dilute oxygen mixture (25% O_2 / CO_2, 160 psi). The reactor was then heated to 30 °C and stirring commenced (1200 rpm). After the reaction had run for 5 min, the gases were vented and the reaction solution collected and filtered. The filtered solution was then frozen in liquid nitrogen to be analysed by EPR spectroscopy at room temperature. Post-reaction solutions were also analysed by NMR spectroscopy to determine the level of DMPO degradation.

2.3.2 Reaction analysis

2.3.2.1 High-performance liquid chromatography (HPLC)

Analysis was performed on an Agilent 1260 Infinity series HPLC comprising a quaternary pump, automated sample injector, column oven, diode array detector (DAD) and refractive index detector (RID). The HPLC was fitted with a MetaCarb 67h column and phosphoric acid (0.1% H_3PO_4) used as the mobile phase. The following conditions were employed for the analysis: flow rate (mobile phase) = 0.8 ml / min, column temperature = 50 °C, Injection volume = 10 μl. Calibrations were performed using known standards. The following compounds were calibrated as shown in Table 1:

Table 1: Compounds calibrated for HPLC analysis

Compound	Detector	Retention time (s)
Glycerol	RID	7.5
Oxalic Acid	DAD	3.4
Mesoxalic acid	DAD	3.6
Tartronic acid	DAD	4.1
Pyruvic acid	DAD	4.8
Glyoxylic acid	DAD	5.2
Glyceric acid	DAD	5.9
Glyceraldehyde	DAD	6.2
Glycolaldehyde	DAD	6.7
Glycolic acid	DAD	6.7
Lactic acid	DAD	7.0
Dihydroxyacetone	DAD	7.4
Formic acid	DAD	7.5
Acetic Acid	DAD	8.2

Carbon mass balance analysis was also performed by calculating the concentration of carbon at the start of the reaction and then comparing this with the concentration of carbon at the end of reaction, which was calculated from the concentrations of reactant and known products detected by HPLC analysis.

2.3.2.2 Microwave plasma atomic emission spectroscopy (MP-AES)

To determine the presence of metal ions in solution, post-reaction solutions were collected and analysed using an Agilent MP-AES 4100. The post reaction solutions were filtered using PTFE syringe filters (0.45 μm) and analysed to determine the presence of Fe, Pd. Calibration solutions were prepared via dilution with deionised water over a suitable concentration range using atomic absorption standards for Fe (1000 mg/L Fe in 1 wt. % HCl, Sigma Aldrich) and Pd (1000 mg/L Pd in 5% HCl, Sigma Aldrich). For analysis of Fe, wavelengths of 371.993 nm and 259.940 nm were used. For analysis of Pd, wavelengths of 324.270 nm and 351.694 nm were used. These wavelengths were chosen to limit interference from other metals present in solution.

2.3.2.3 Gas chromatography (GC)

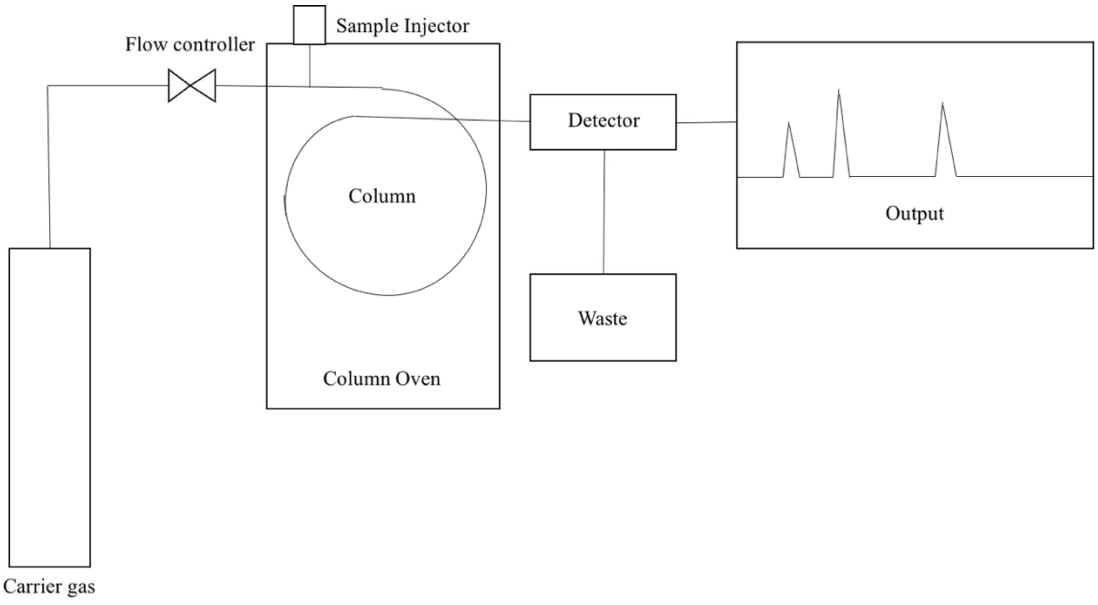

Figure 6: Basic schematic of GC instrument.

In gas chromatography, the gaseous sample is passed through a column with the aid of a ‘mobile phase’ (typically an inert gas such as helium or argon). The column is coated with a ‘stationary phase’ which is a thin layer of liquid or polymer. The gaseous

products injected into the column then interact with the stationary phase as they pass though the column leading to different compounds eluting at different times. After the compounds elute from the column they can be detected by a variety of detectors. Commonly employed detectors include flame ionisation (FID) and thermal conductivity (TCD). TCD works by measuring the thermal conductivity of the effluent. As the compounds eluting from the column tend to have different thermal conductivities to the carrier gas, this difference is measured and a signal is produced. TCD is useful as a universal detector as all compounds possess a thermal conductivity, FID works by the detection of ions formed during the combustion of hydrocarbons in a hydrogen flame. FID is only suitable for the detection of hydrocarbons from the column effluent.

Post reaction gas analysis was performed using GC analysis. GC analysis was performed using a Varian cp3390 equipped with a TCD detector. The GC was fitted with a Poropak Q (80-100 mesh, 2 m) column. The conditions were as follows: carrier gas = Ar, column pressure = 38 psi, column temperature = 30 °C, injection volume = 250 µl and analysis time = 20 min.

2.3.2.4 Electron paramagnetic resonance (EPR) spectroscopy

EPR spectroscopy is a useful analytical technique for determining the presence of radicals in solution during reactions. Electrons have spin, which gives them magnetic properties. Therefore, when an external magnetic field is applied, the unpaired electrons can either orient parallel (lower energy) or anti parallel (higher energy) to the magnetic field. Whilst initially a greater number of electrons orient parallel to the external magnetic field, microwave radiation can be applied to excite some electrons from the lower energy level to the higher energy level. For this excitation to occur, the microwave radiation frequency needs to be equal to the energy level separation between the lower and upper states. Therefore, a fixed frequency of microwave radiation is applied and the external magnetic field is ‘sweeped’ to produce the EPR resonance.

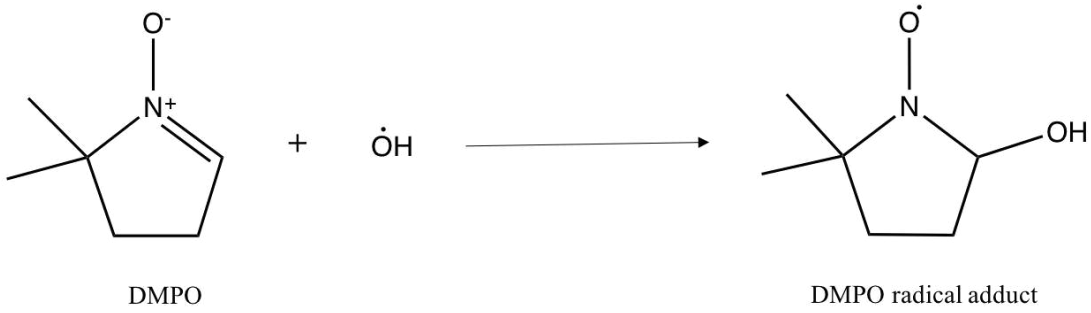

Figure 7: Reaction of DMPO with hydroxyl radical.

Some radicals, such as hydroxyl, are undetectable due to short lifetimes. Therefore, to detect these short-lived species, the reactions are performed in the presence of a radical trap (such as DMPO) which form a more stable radical adduct upon reaction with the shorter lived radicals.

The EPR testing was performed and analysed by Dr Andrea Folli at Cardiff University.

2.3.2.5 Nuclear magnetic resonance (NMR) spectroscopy

^{1}H NMR spectroscopy is widely employed for the analysis of organic compounds. Hydrogen possesses a nuclear spin value (I) of 1/2. This means that when the nucleus is in the presence of a magnetic field it can either align parallel to it (lower energy) or anti parallel to it (higher energy). As energy (in the form of radio waves) is applied, nuclei in the lower energy state can be excited to the higher energy state. This absorption of energy and subsequent release of energy can then be monitored. The modern form of NMR, called the Fourier Transform method, utilises one big pulse of radio waves which excite all nuclei. ^{1}H nuclei also experience the magnetic effect of neighbouring nuclei and electrons, and therefore require differing radio frequencies for excitation. These frequencies can be referenced to a standard (such as TMS). Therefore, you can obtain information about the chemical environments of the ^{1}H nuclei detected. Peaks on NMR spectra are expressed in terms of chemical shift (δ) in ppm (e.g. a chemical shift of 2 means that the nuclei require a radio frequency 2 millionths more than TMS to reach resonance).

^{1}H NMR analysis was performed in conjunction with the radical trapping experiments to determine the extent of degradation of the DMPO radical trap. ^{1}H NMR analysis was performed at ambient temperature on a 500 MHz Bruker Avance III HD spectrometer fitted with a Prodigy Cryoprobe. Due to the strong solvent peak arising from H_2O, H_2O suppression was utilised. To perform the analysis, an NMR tube was filled with filtered reaction solution (0.7 ml) and deuterium oxide (D_2O, 1 ml, Aldrich). Additionally, a glass ampule containing tetramethyl silane (TMS, Aldrich) in deuterated chloroform ($CDCl_3$, Aldrich) was inserted to enable quantification of the analyte.

2.3 Catalyst characterisation

2.3.1 X-ray photoelectron spectroscopy (XPS)

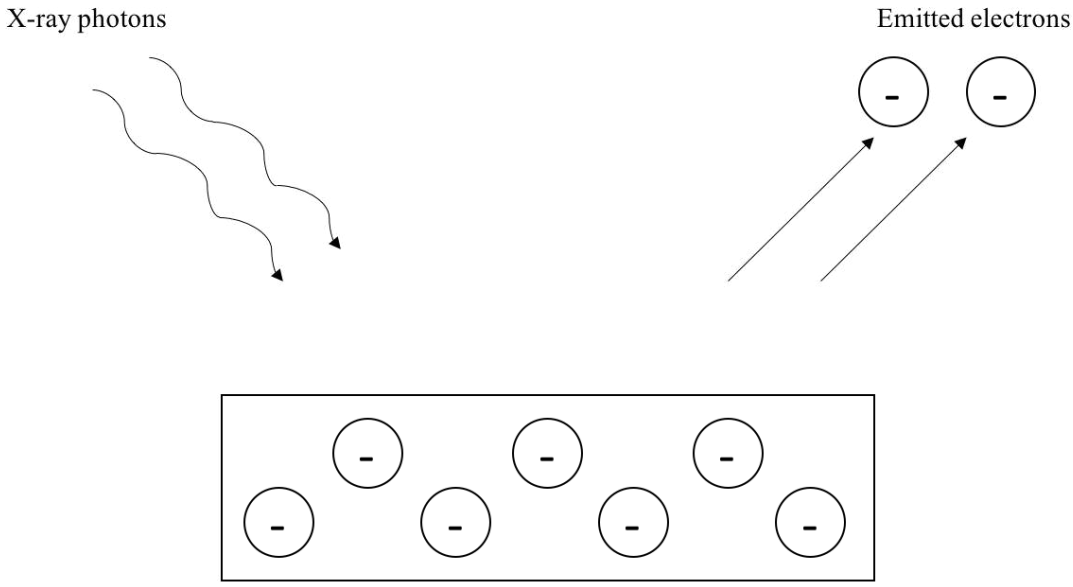

Figure 8: Diagram illustrating the photoelectric effect.

XPS is a technique that enables the user to gain information about atoms on the surface of a catalyst (to a depth of around 10 nm). It is a useful technique for identification of the oxidation state of surface metals on supported metal catalysts and can give an indication of the dispersion of the metals on the surface and the presence of alloying. XPS is based upon the photoelectric effect, whereby when a material is bombarded with photons, electrons are emitted provided the photons are of greater energy than the binding energy of the electron to the nucleus. If the photon is of great enough energy to eject the electron, the kinetic energy of the emitted electron can be related to the binding energy and photon energy using the following equation:

Binding Energy = hν - Kinetic Energy

Therefore, when a monochromatic x-ray source is employed, alongside a detector to determine the kinetic energy of the emitted electrons, the binding energy can be determined. Each element has its own unique characteristic binding energies. Upon measurement of the binding energies of emitted electrons, these binding energies can

be referenced with databases (such as NIST) to identify the chemical environment of the atom from which the electron was emitted.

XPS analysis was performed using a Kratos Axis ultra-DLD instrument with a monochromatic AlK_a x-ray source (120 W) and analyser pass energies of 160 eV (for survey scans) or 40 eV (for detailed scans). The samples were mounted using double sided adhesive tape and analysed under ultra-high vacuum ($<5x10^{-10}$ Torr). Binding energies were referenced to the C (1s) binding energy of adventitious carbon contamination which was taken to be 284.7 eV. The XPS experiments were performed with the help of Dr David Morgan of Cardiff University

2.3.2 Transmission electron spectroscopy (TEM)

Conventional TEM is a valuable technique for determining information about the surface of a supported metal catalyst on the nanometre scale. TEM employs a high-energy beam of electrons which are passed through electromagnetic coils towards the sample. These electromagnetic coils focus the beam into a thin stream of electrons which are then focused onto the area of interest. The electron beam passes straight through the sample, then through a projector lens and onto a fluorescent screen which provides the image of the catalyst surface (in modern usage a digital camera is utilised). Scanning transmission electron microscopy works by focussing the electron beam into a narrow point which is then scanned over the surface in a raster. This, coupled with a high angle annular dark field detector can provide images where contrast is related to the atomic number (Z) of the imaged atoms. This can also be coupled with energy dispersive x-ray spectroscopy to provide elemental analysis of the imaged surface.

HR-TEM (high resolution – transmission electron microscopy) and HAADF-STEM (high angle annular dark field – scanning transmission electron microscopy)) analysis was performed in a JEOL JEM-2100 microscope at 200 kV. Energy Dispersive X-ray (EDX) analysis was performed using Oxford Instruments X-Max^N analyser and Aztec software. Samples were prepared by dispersion in methanol with sonication before supporting on holey carbon film copper grids. TEM experiments were performed with the help of Dr Georgi Lalev of Cardiff University.

2.4 References

1 M. Sankar, Q. He, M. Morad, J. Pritchard, S. J. Freakley, J. K. Edwards, S. H. Taylor, D. J. Morgan, A. F. Carley, D. W. Knight, C. J. Kiely and G. J. Hutchings, *ACS Nano*, 2012, **6**, 6600–6613.

2 M. Sankar, E. Nowicka, R. Tiruvalam, Q. He, S. H. Taylor, C. J. Kiely, D. Bethell, D. W. Knight and G. J. Hutchings, *Chem. - A Eur. J.*, 2011, **17**, 6524–6532.

3 Oxidation of phenol utilising H_2O_2 generated *in situ* from H_2 and O_2

3.1 Introduction

Within this chapter, a range of Pd containing catalysts were tested for oxidation using *in situ* generated H_2O_2 from H_2 and O_2 for application in wastewater treatment. H_2O_2 is a highly desirable oxidant for wastewater treatment owing to its generation of only H_2O and O_2 as a waste product. For this study, phenol has been employed as a model wastewater substrate. There has been significant interest in the direct synthesis of H_2O_2[1,2,3] due to hazards associated with transporting and storing large quantities of H_2O_2. For wastewater treatment applications, the ability to produce the H_2O_2 on-site, preferably from H_2 generated using electrolysis, would be highly advantageous.

A review by Puertolas *et al*.[4] highlighted the variety of research that has been conducted in the literature on oxidations using *in situ* generated H_2O_2. The oxidation reactions investigated include propylene epoxidation to propylene oxide, hydroxylation of benzene to phenol and selective oxidation of methane.

However, literature on the application of in situ generated H_2O_2 from H_2 and O_2 for wastewater treatment applications is currently sparse. Yalfani *et al*.[5] reported the use of *in situ* generated H_2O_2 for applications in the Fenton reaction using formic acid and oxygen as reagents. They also reported the use of hydroxylamine and hydrazine as potential hydrogen substitutes.[6] The oxidation of 100 ppm phenol was reported using a heterogeneous Pd-Fe catalyst when using formic acid as a hydrogen substitute.[7,8] Additionally, Osegueda *et al*.[9] reported the oxidation of phenol with *in situ* generated H_2O_2 using a catalytic membrane reactor. Yuan *et al*.[10] reported the Fenton's oxidation (using Fe^{2+}) of Rhodamine B using H_2O_2 generated *in situ* from H_2 and O_2 produced via electrolysis.

Therefore, the aim of this study is to gain further insight into the oxidation of phenol using H_2O_2 generated from H_2 and O_2 using heterogeneous catalysis. In addition to this, the aim is to identify the best catalyst to perform this reaction efficiently. After

identification of a suitable catalyst, the aim is to investigate the degradation of other model wastewater substituents to determine the wider applicability of this system.

3.2 Results and discussion

3.2.1 Bimetallic Pd-based catalysts for the conversion of phenol using *in situ* generated H_2O_2

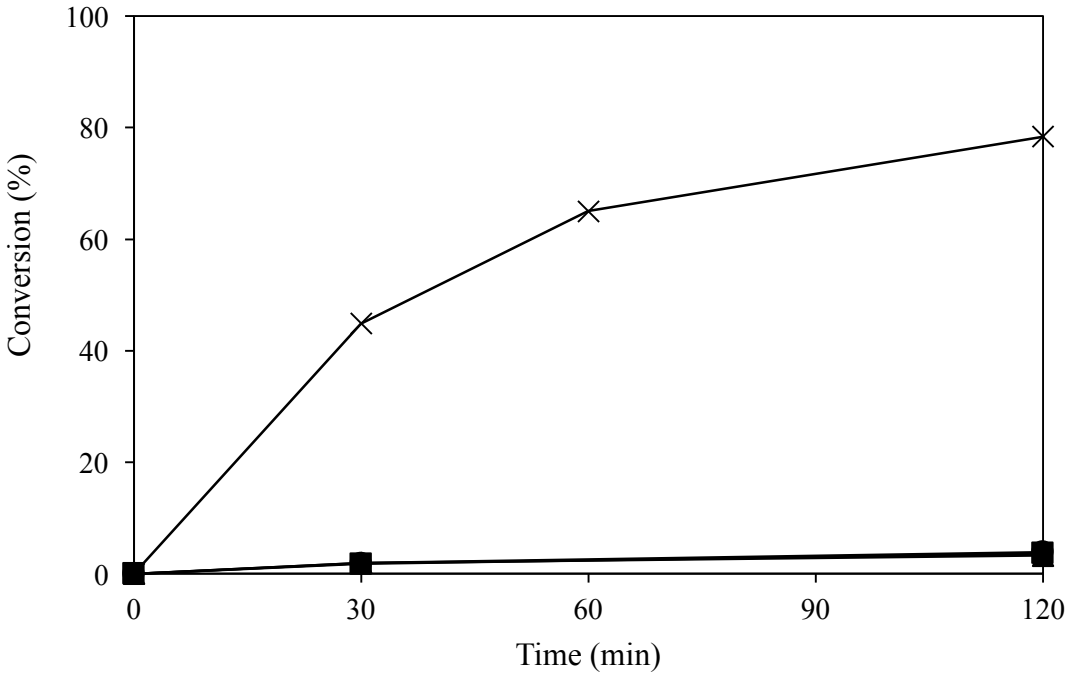

Figure 1: Testing Pd-based bimetallic catalysts for the oxidation of phenol. Conditions: 8.5 g 1000 ppm phenol solution, 420 psi 5%H_2/CO_2, 160 psi 25%O_2/CO_2, 10 mg 5%X/TiO_2, 1200 rpm stirring, 30 °C, reactions performed in Parr stainless steel autoclave. Legend: crosses = Pd-Fe, circles = Pd-Au, squares = Pd-Mn, triangles = Pd-Cu.

2.5%Pd-2.5%Fe/TiO_2, 2.5%Pd-2.5%Au/TiO_2, 2.5%Pd-2.5%Mn/TiO_2 and 2.5%Pd-2.5%Cu/TiO_2 catalysts were tested for the oxidation of phenol using *in situ* generated H_2O_2 at 30 °C as shown in Figure 1. Pd-based catalysts have been widely reported in the literature to be highly effective for the direct synthesis of H_2O_2 from H_2 and O_2.[1] The secondary metals were chosen to assist in the decomposition of H_2O_2 and formation of reactive oxygen species to oxidise the phenol under mild conditions. All catalysts were heat treated at 400 °C for 4 h under flowing 5%H_2/Ar. However, very

little activity was observed for the Pd catalysts containing either Au, Mn or Cu. In the case of the Au containing catalyst this was unsurprising; Au has been demonstrated to be highly effective for enhancing the selectivity towards H_2O_2 in the direct synthesis reaction and supressing the decomposition pathways.[11,12] To determine whether the lack of activity observed for the 2.5%Pd-2.5%Mn/TiO_2 and 2.5%Pd-2.5%Cu/TiO_2 catalysts was due to the reductive heat treatment, the catalysts were also prepared with a heat treatment of 400 °C for 4 h under static air. However, these catalysts were also found to be inactive for the oxidation of phenol utilising *in situ* generated H_2O_2.

In contrast, when the 2.5%Pd-2.5%Fe/TiO_2 catalyst was utilised for the reaction, high activity was observed for the oxidation of phenol under the described conditions. After 120 minutes, 78.4 % phenol was converted during the reaction. Many peaks were observed in the HPLC chromatogram indicating the production of a variety of further oxidation products. It was not possible to calibrate and quantify many of these peaks. However, the retention times of many of these peaks corresponded to what was typically expected for short chain organic acids.

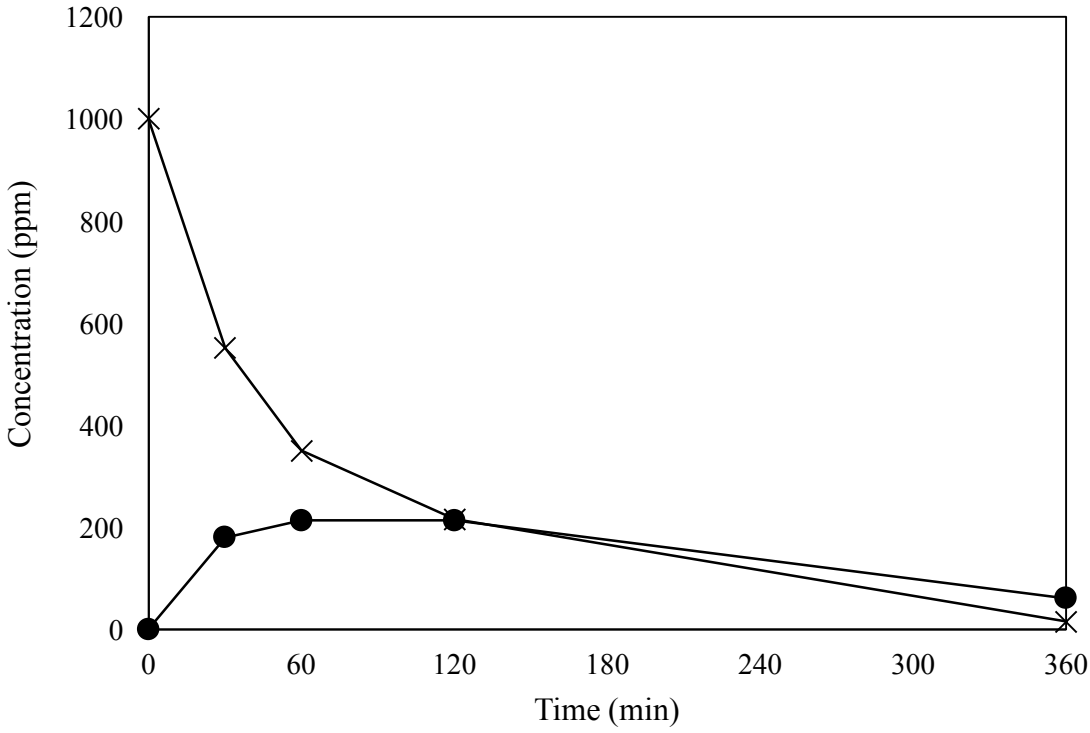

Figure 2: Evolution of intermediates during phenol oxidation reaction. Conditions: 8.5 g 1000 ppm phenol solution, 420 psi 5%H_2/CO_2, 160 psi 25%O_2/CO_2, 10 mg

2.5%Pd-2.5%Fe/TiO_2, 1200 rpm stirring, 30 °C, reactions performed in Parr stainless steel autoclave. Legend: crosses = phenol, circles = catechol.

When the reaction was continued for 6 h, almost complete conversion of the phenol was observed, as shown in Figure 2. The concentration of catechol, the primary aromatic product observed, was also followed using HPLC. The concentration of catechol was found to increase during the initial 60 minutes of reaction. However, the concentration of catechol was observed to decrease after this point, indicating the formation of further oxidation products. Zazo *et al*. has proposed a route for phenol oxidation by Fenton's reagent as shown in Figure 3.[13]

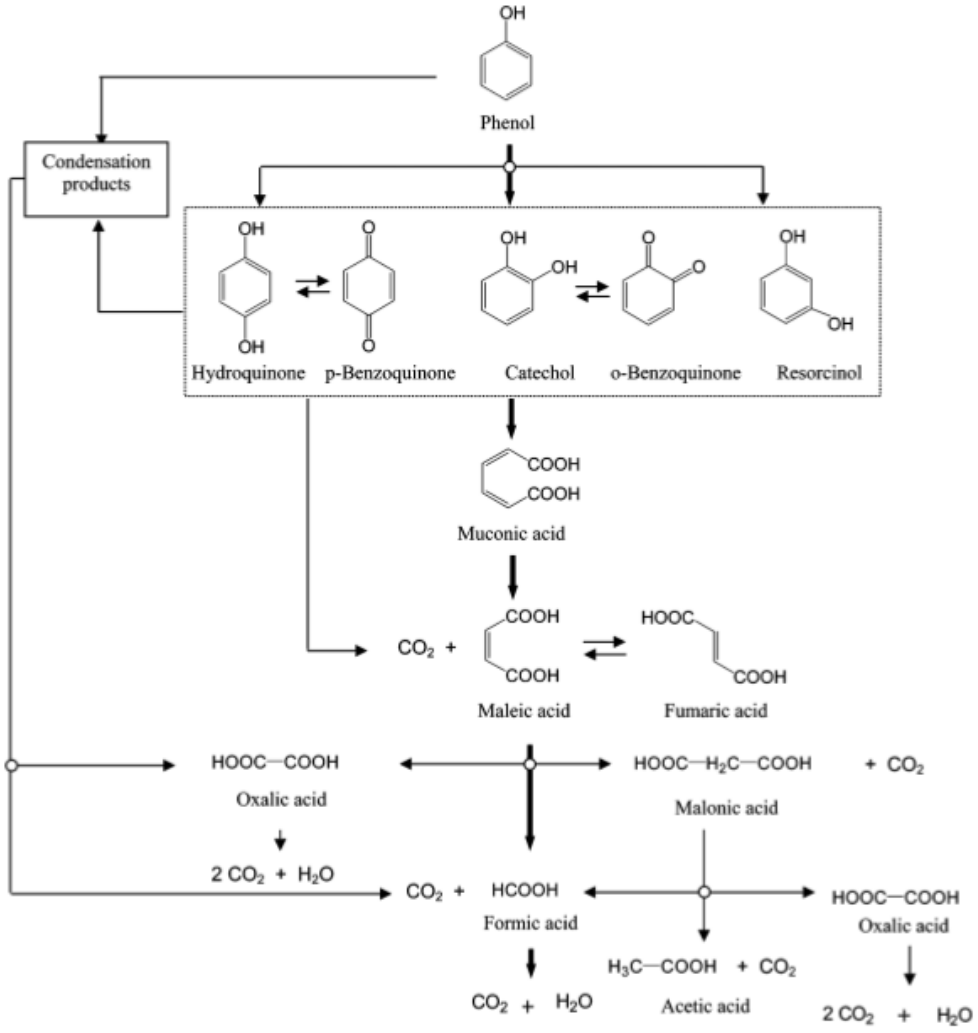

Figure 3: Proposed route for phenol oxidation using Fenton's reagent.[13]

From the proposed route, it appeared that the conversion of catechol led to the formation of organic acids which could then be ultimately converted to CO_2. However, it was not possible to check for the formation of CO_2 during the *in situ* reaction due to the use of CO_2 as a diluent for the H_2 and O_2 reagent gases. The high concentrations of CO_2 present in these gases would mask any potential CO_2 arising from the total oxidation of phenol.

3.2.2 Confirming the role of *in situ* generated H_2O_2

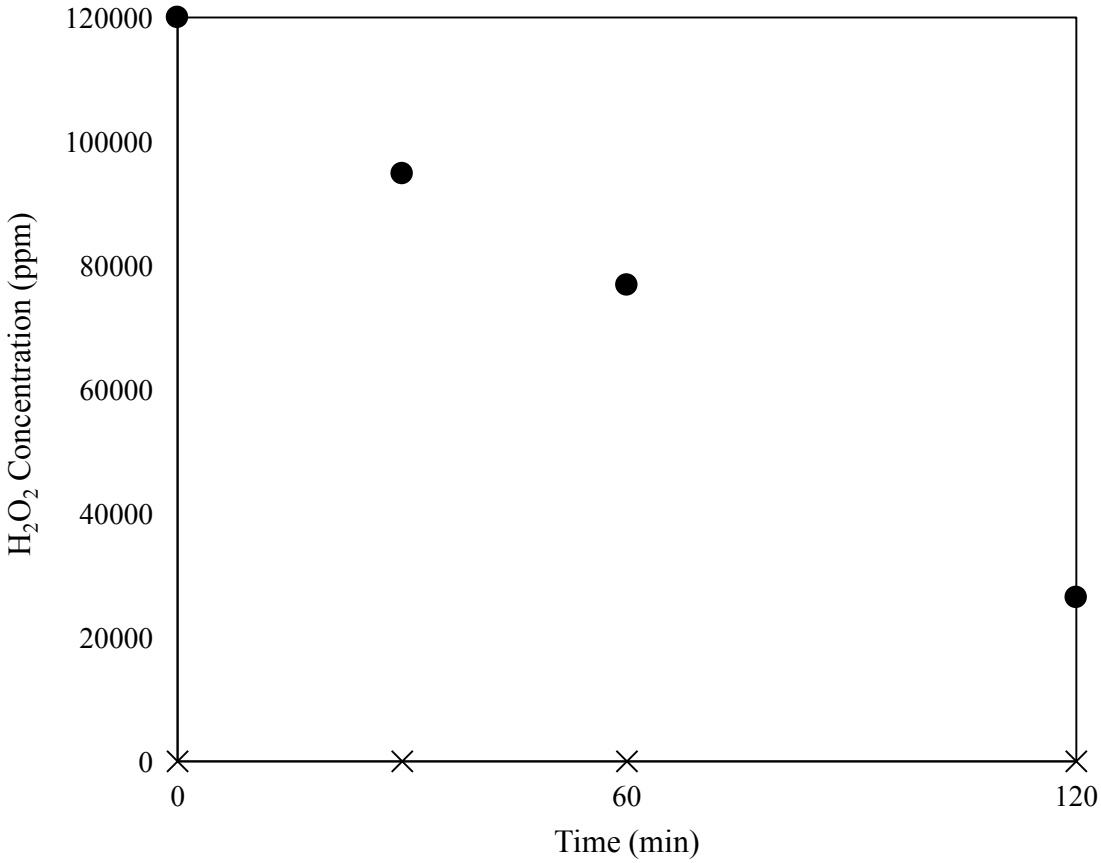

Figure 4: Production and decomposition of H_2O_2. Conditions for H_2O_2 synthesis: 8.5 g water, 420 psi 5%H_2/CO_2, 160 psi 25%O_2/CO_2, 10 mg 2.5%Pd-2.5%Fe/TiO_2, 1200 rpm stirring, 30 °C, reactions performed in Parr stainless steel autoclave. Conditions for H_2O_2 degradation: 8.5 g 120,000 ppm H_2O_2 solution (aq), 580 psi 25%O_2/CO_2, 10 mg 2.5%Pd-2.5%Fe/TiO_2, 1200 rpm stirring, 30 °C, reactions performed in Parr stainless steel autoclave. H_2O_2 concentration analysed using redox titration. Legend: Crosses = H_2O_2 synthesis reaction, circles = H_2O_2 decomposition reaction.

To evaluate whether the phenol oxidation activity could be attributed to *in situ* generated H_2O_2, a series of H_2O_2 synthesis reactions were performed using the active Pd-Fe catalyst, shown in Figure 4. Interestingly, there was no H_2O_2 detected in the post reaction solution for any of the synthesis reactions. However, it was considered that this could likely be attributed to the rate of H_2O_2 decomposition exceeding that of the H_2O_2 synthesis rate. Therefore, a series of H_2O_2 decomposition reactions were performed using a 120,000 ppm H_2O_2 solution, also shown in Figure 4. These

decomposition reactions demonstrated that the catalyst was highly effective at decomposing H_2O_2 which provides a likely explanation for why there was no H_2O_2 detected in the post-reaction solutions for the synthesis reactions.

Table 1: Investigating the role of *in situ* generated H_2O_2. Conditions: 8.5 g 1000 ppm phenol solution, 1200 rpm stirring, 30 °C, 2h, reactions performed in Parr stainless steel autoclave.

Reaction Conditions	**Phenol conversion (%)**
420 psi 5% H_2/CO_2 160 psi 25%O_2/CO_2 10 mg 2.5%Pd-2.5%Fe/TiO_2	78
10 mg 2.5%Pd-2.5%Fe/TiO_2	2
160 psi 25%O_2/CO_2 10 mg 2.5%Pd-2.5%Fe/TiO_2	2
420 psi 5% H_2/CO_2 10 mg 2.5%Pd-2.5%Fe/TiO_2	3
420 psi 5% H_2/CO_2 160 psi 25%O_2/CO_2	2

Therefore, to confirm that the observed phenol conversion was due to oxidation with *in situ* generated H_2O_2, a series of experiments were performed which excluded different components of the system to observe whether the conversion of phenol would still proceed as shown in Table 1. When the catalyst was utilised alongside H_2 and O_2. A phenol conversion of 78 % was observed. However, when the catalyst was used in the absence of H_2 or O_2, only 2 % conversion of phenol was observed. This demonstrated that the observed conversion of phenol was not due to adsorption of phenol on the catalyst surface. When the catalyst was used alongside O_2, only 2 % conversion of phenol was observed. This excluded the possibility that the conversion

of phenol could be attributed to oxidation by O_2. When the catalyst was used alongside H_2, only 3 % conversion of phenol was observed. This excluded the possibility that the conversion of phenol could be attributed to hydrogenation of phenol. The palladium-catalysed hydrogenation of phenol under mild aqueous conditions has been previously reported in the literature.[14] However, it appeared that under the current conditions, very little hydrogenation of phenol was observed. Finally, when a H_2 and O_2 mixture was used in the absence of catalyst, only 2 % conversion of phenol was observed. This confirmed that the presence of the catalyst was required to achieve high conversions of phenol. Therefore, when the series of experiments were considered, it was confirmed that a combination of catalyst, H_2 and O_2 was required to observe significant levels of phenol conversion. This appeared to confirm that the observed conversion of phenol could be attributed to the *in situ* generation of H_2O_2. Another factor to consider is that it is well known that TiO_2 is capable of oxidising organic substrates in the presence of light. However, this was considered not possible as the reaction was performed in an autoclave where there was no source of light.

3.2.3 Effect of bimetallic Pd-Fe catalyst

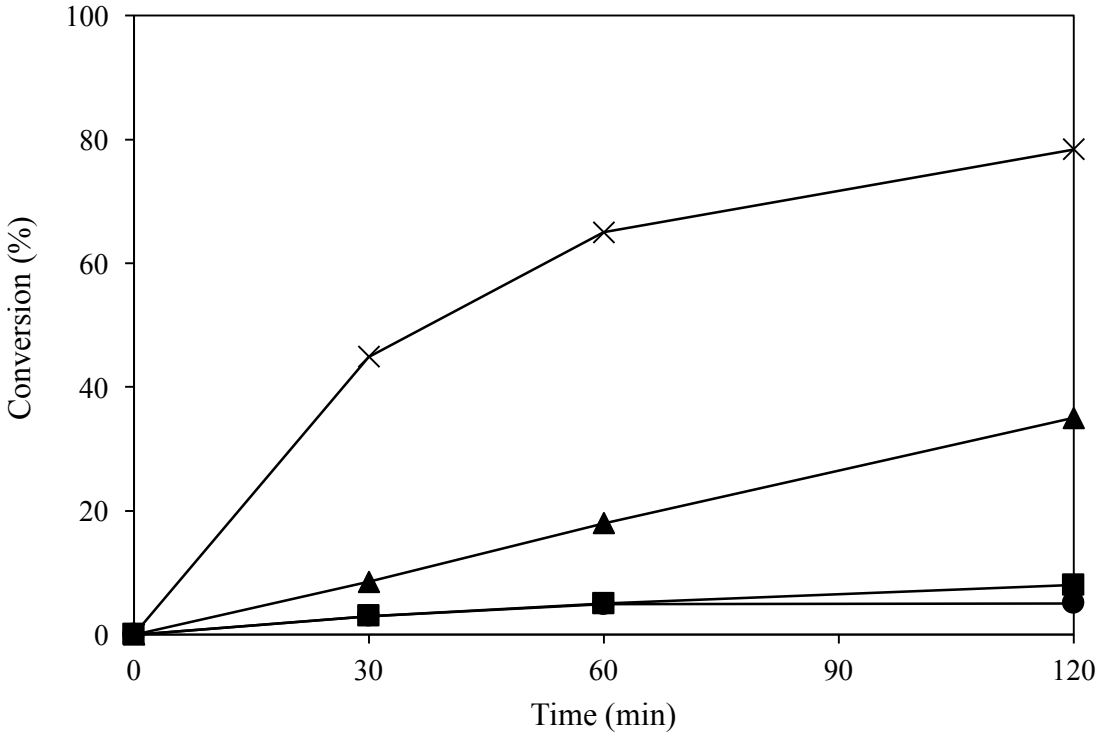

Figure 5: Comparison of bimetallic Pd-Fe catalyst with monometallic Pd and Fe catalysts. Conditions: 8.5 g 1000 ppm phenol solution, 420 psi 5%H_2/CO_2, 160 psi 25%O_2/CO_2, 10 mg 5%X/TiO_2 or 2.5%X/TiO_2 for monometallic catalysts (20 mg for physical mixture), 1200 rpm stirring, 30 °C, reactions performed in Parr stainless steel autoclave. Legend: crosses = Pd-Fe, circles = Pd, squares = Fe, triangles = Pd + Fe.

To determine the role performed by the individual components of the bimetallic 2.5%Pd-2.5%Fe/TiO_2 catalyst, a series of experiments were performed utilizing the monometallic counterparts of the catalyst as shown in Figure 5. It was previously shown that when 2.5%Pd-2.5%Fe/TiO_2 was used for the reaction, a phenol conversion of 78.4% was observed. When a monometallic 2.5%Pd/TiO_2 catalyst was employed for the reaction, only 5% phenol conversion was observed. It is well known that palladium is highly effective for the formation of H_2O_2 from H_2 and O_2. However, one of the problems associated with the use of monometallic Pd catalysts is that they are also effective for catalysing the subsequent decomposition/hydrogenation of the

generated H_2O_2. That is why strategies have been employed such as the addition of a secondary metal to help suppress these unfavourable reactions.[15,16] Therefore, as the palladium is capable of decomposing H_2O_2 it was surprising that higher conversions of phenol was not observed. It appears that the decomposition route of H_2O_2 over Pd is not efficient for the generation of reactive oxygen species capable of oxidising the phenol substrate. Therefore, the addition of iron is required to achieve high conversions of phenol. When a monometallic 2.5%Fe/TiO_2 was employed for the reaction, very low conversions of phenol were also achieved. This was unsurprising as the presence of Pd is typically required to perform the direct synthesis of H_2O_2 under ambient conditions. The only example of a palladium-free catalyst that has been found to be active for the direct synthesis of H_2O_2 under mild conditions is a supported gold catalyst, although the levels of H_2O_2 produced were far lower than for the Pd containing catalysts.[11,17] There has been reports in the literature of model $Al_{13}Fe_4$ surfaces capable of performing low temperature hydrogenations as a low-cost alternative to Pd.[18,19] However, these have yet to be produced on a scale large enough to enable testing under the desired conditions. Therefore, from the previous experiments it appeared that a combination of both Pd and Fe was required to achieve high conversions of phenol. To determine whether there was a synergistic effect of having the two metals on the same support, an experiment was performed utilising a physical mixture of both the 2.5%Pd/TiO_2 and 2.5%Fe/TiO_2 monometallic catalysts as shown in Figure 4. With the physical mixture of catalysts, a substantial phenol conversion of 35% was achieved. However, this was still far lower than the phenol conversion of 78.4% achieved when employing the bimetallic catalyst, indicating a synergistic effect. Therefore, to achieve the greatest conversions of phenol, it appeared to be essential that both Fe and Pd were utilised on the same support. One problem associated with the utilisation of the 2.5%Pd-2.5%Fe/TiO_2 catalyst was the occurrence of Fe leaching from the catalyst during the reaction. When the post reaction solutions were analysed, significant concentrations of Fe were detected using MP-AES. Therefore, a multitude of strategies were employed to attempt to limit the occurrence of Fe leaching.

3.2.4 Effect of catalyst reduction treatment temperature

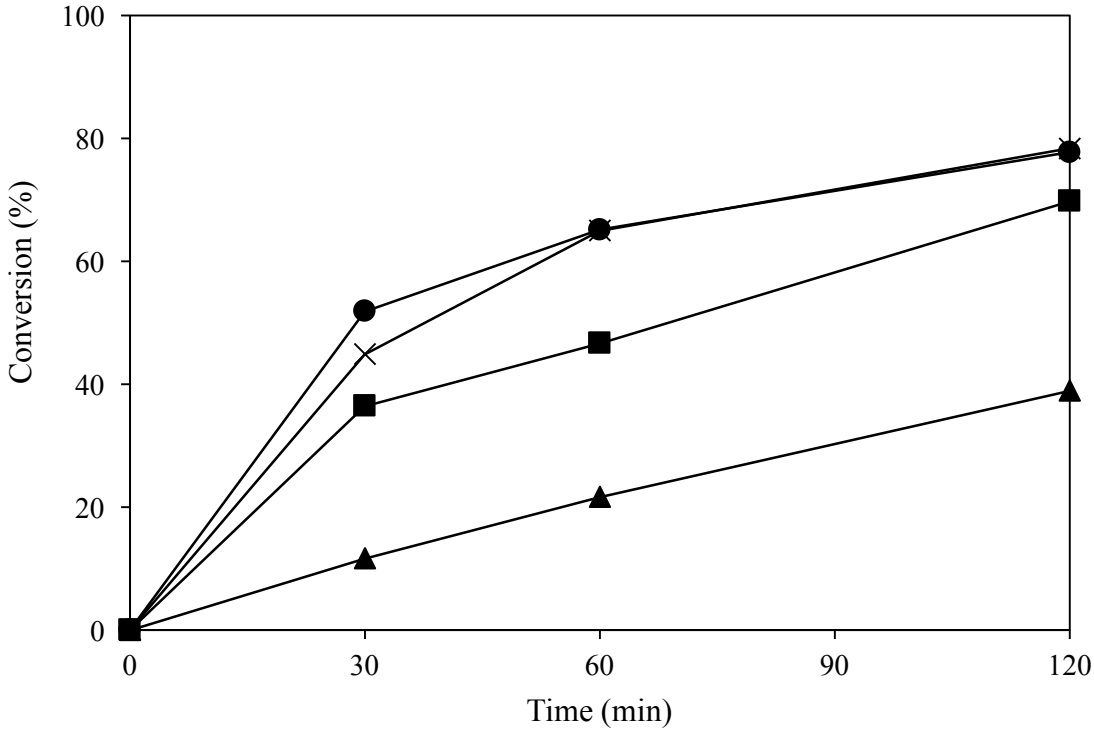

Figure 6: The effect of catalyst reduction treatment temperature upon phenol conversion. Conditions: 8.5 g 1000 ppm phenol solution, 420 psi 5%H_2/CO_2, 160 psi 25%O_2/CO_2, 10 mg 2.5%Pd-2.5%Fe/TiO_2, 1200 rpm stirring, 30 °C, reactions performed in Parr stainless steel autoclave. Catalysts treated at X °C/4 h under flowing 5%H_2/Ar. Legend: crosses = 400, circles = 500, squares = 550, triangles = 600.

Heat treatments have previously been shown to be crucial to enhancing the stability and reusability of metal oxide supported catalysts for the direct synthesis of H_2O_2 from H_2 and O_2.[20,21] To investigate this further, 2.5%Pd-2.5%Fe was prepared and subjected to heat treatments at various temperatures as shown in Figure 6. As shown previously, the catalyst treated at 400 °C was observed to achieve a phenol conversion of 78.4% after 120 minutes. When the heat treatment temperature was increased to 500 °C, a phenol conversion of 77.8% was achieved. Therefore, it appeared that increasing the heat treatment temperature by 100 °C had little effect on the observed catalyst activity. However, when the heat treatment temperature was increased further

to 550 °C and 600 °C, phenol conversion decreased to 69.8% and 39% respectively. This could likely have been attributed to the sintering of nanoparticles on the surface of the catalyst leading to larger particles and therefore lower surface concentrations of active metals. To determine the effect of the heat treatments upon catalyst stability, the post-reaction solutions were collected and then analysed using MP-AES to determine the concentrations of Fe leached from the catalyst surface. The results of this analysis are shown in Figure 7.

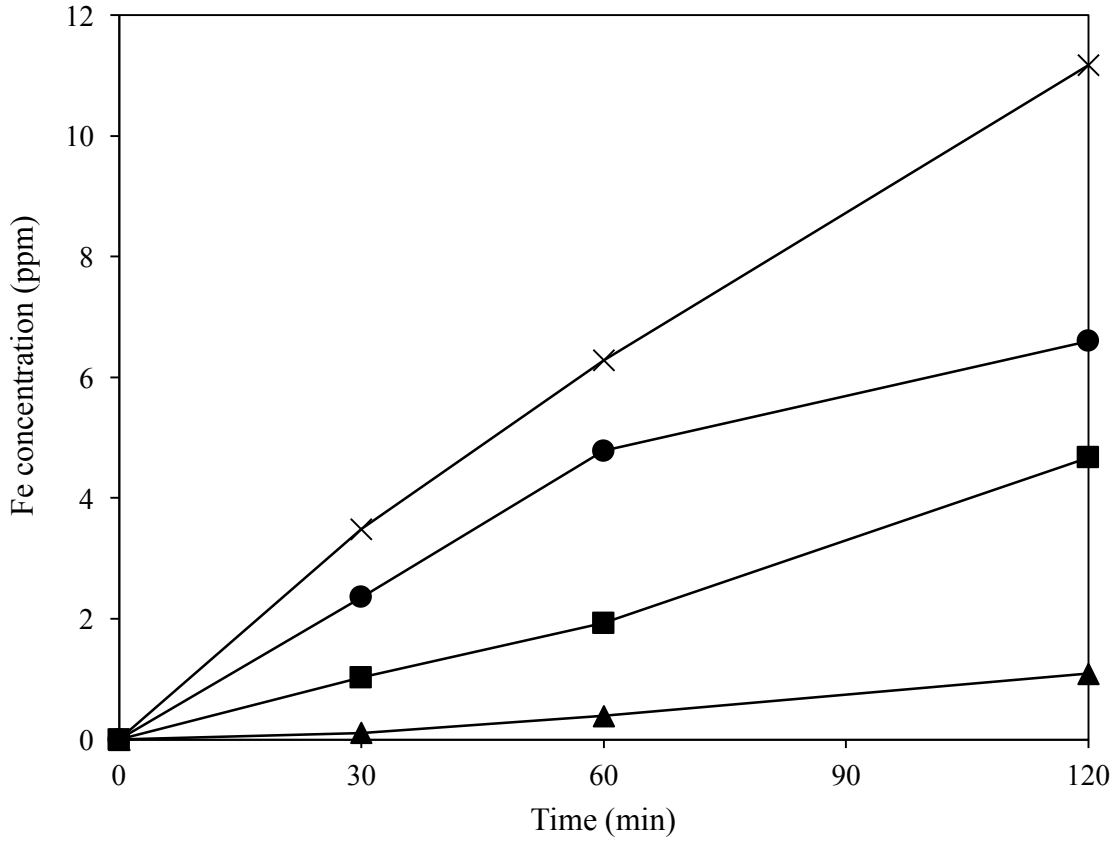

Figure 7: Leaching of Fe during reaction detected via MP-AES analysis. Conditions: 8.5 g 1000 ppm phenol solution, 420 psi 5%H_2/CO_2, 160 psi 25%O_2/CO_2, 10 mg 2.5%Pd-2.5%Fe/TiO_2, 1200 rpm stirring, 30 °C, reactions performed in Parr stainless steel autoclave. Catalysts treated at X °C/4 h under flowing 5%H_2/Ar. Legend: crosses = 400, circles = 500, squares = 550, triangles = 600.

Interestingly, it was observed that the catalyst that was heat treated at 500 °C leached only 6.6 ppm of Fe into solution after 120 minutes, whereas the catalyst that was heat treated at 400 °C leached 11.2 ppm of Fe into solution. However, within the same period, near equal conversions of phenol were observed. This demonstrated the ability of heat treatments for increasing the stability of supported metal catalysts. The catalysts that were heat treated at 550 °C and 600 °C were found to leach 4.7 ppm and 1.1 ppm of Fe into solution respectively. However, while those catalysts were found to be more stable, this stability was accompanied by a corresponding decrease in activity towards phenol oxidation. Therefore, a heat treatment temperature of 500 °C was employed going forward.

3.2.5 Effect of oxidation-reduction-oxidation treatment

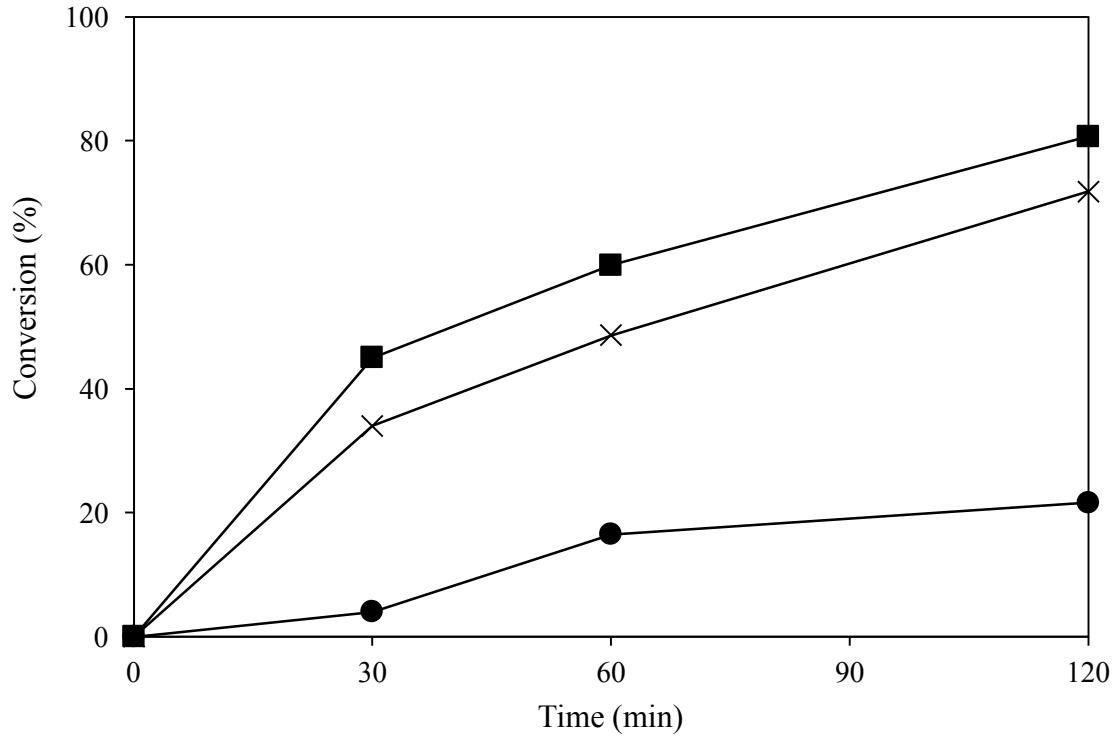

Figure 8: Effect of oxidation-reduction-oxidation catalyst treatment upon phenol oxidation. Conditions: 8.5 g 1000 ppm phenol solution, 420 psi 5%H_2/CO_2, 160 psi 25%O_2/CO_2, 10 mg 2.5%Pd-2.5%Fe/TiO_2, 1200 rpm stirring, 30 °C, reactions performed in Parr stainless steel autoclave. Oxidation treatment = 500 °C/ 3 h under

static air, reduction treatment = 200 °C/ 2 h under flowing 5%H_2/Ar. Legend: crosses = OR, circles = ORO, squares = OROR.

Freakley *et al*.[16] previously demonstrated that an oxidation-reduction-oxidation heat treatment cycle on Pd-base metal catalysts could provide stable, re-usable and selective catalysts for the direct synthesis of H_2O_2 from H_2 and O_2. Therefore, the oxidation-reduction-oxidation heat treatment cycle was employed for the 2.5%Pd-2.5%Fe/TiO_2 catalyst with the aim of increasing stability as shown in Figure 8. However, the phenol conversion was observed to be quite low for the catalyst where the oxidation-reduction-oxidation heat treatment was employed. The catalysts where oxidation-reduction and oxidation-reduction-oxidation-reduction heat treatments were employed achieved far higher conversions of phenol. This appeared to indicate that a heat treatment in a reducing atmosphere was required prior to catalyst testing. Interestingly, when comparing the catalysts that underwent oxidation-reduction and oxidation-reduction-oxidation-reduction heat treatments, very little difference was observed in the observed phenol conversions. This indicated that the increased duration of the heat treatment lead to very little sintering of the metal nanoparticles. Additionally, the occurrence of Fe leaching was determined by MP-AES analysis of the post-reaction solutions as shown in Figure 9.

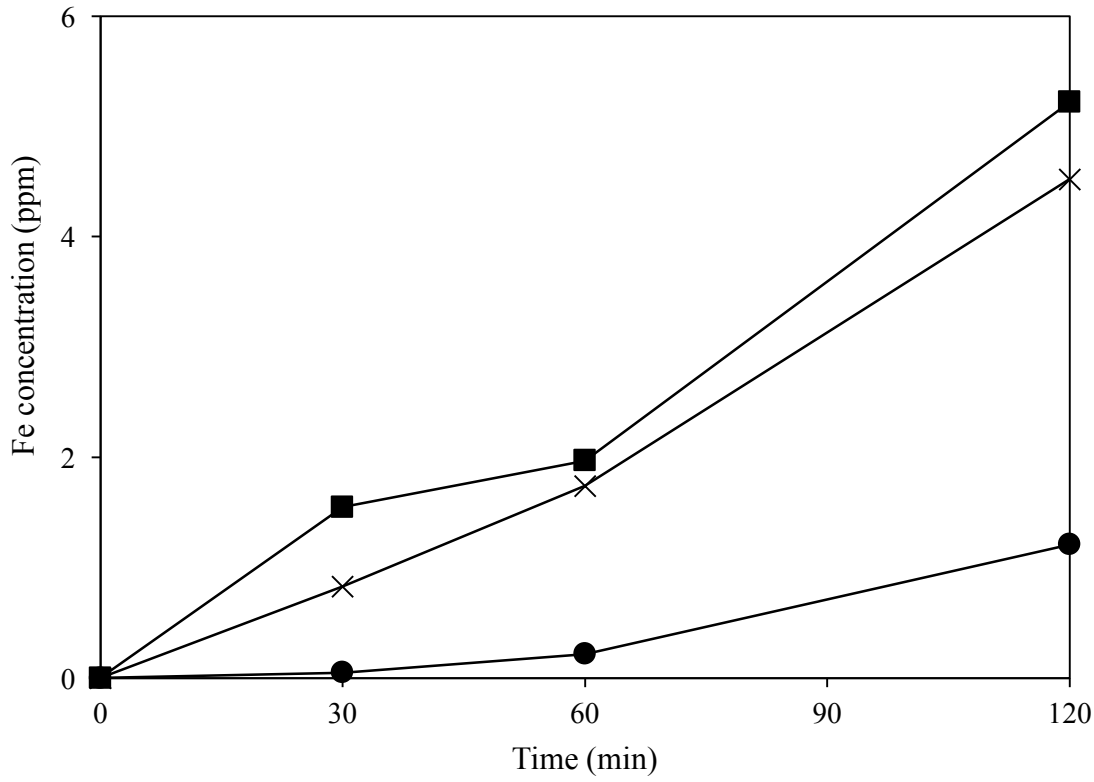

Figure 9: Leaching of Fe during reaction detected via MP-AES analysis. Conditions: 8.5 g 1000 ppm phenol solution, 420 psi 5%H_2/CO_2, 160 psi 25%O_2/CO_2, 10 mg 2.5%Pd-2.5%Fe/TiO_2, 1200 rpm stirring, 30 °C, reactions performed in Parr stainless steel autoclave. Oxidation treatment = 500 °C/ 3 h under static air, reduction treatment = 200 °C/ 2 h under flowing 5%H_2/Ar. Legend: crosses = OR, circles = ORO, squares = ORORO.

From the analysis of the post reaction solutions it was determined that both the oxidised-reduced and oxidised-reduced-oxidised-reduced catalysts showed largely similar amounts of Fe leaching. This showed that the extended heat treatment cycle provided little improvement in the stability of the catalysts towards leaching of Fe. While the oxidised-reduced-oxidised catalyst was observed to leach far less Fe during reaction, this was accompanied by very poor performance in the oxidation of phenol.

3.2.6 Effect of Fe loading

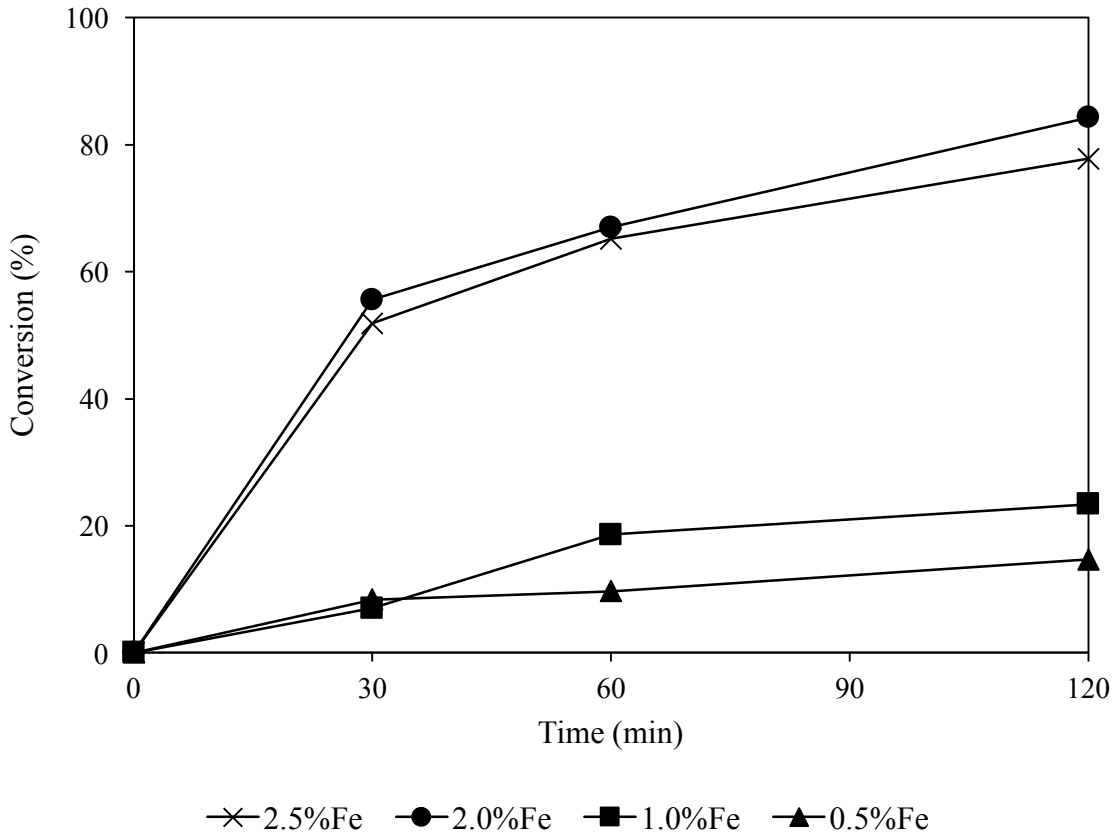

Figure 10: The effect of catalyst Fe loading upon phenol conversion. Conditions: 8.5 g 1000 ppm phenol solution, 420 psi 5%H_2/CO_2, 160 psi 25%O_2/CO_2, 10 mg 2.5%Pd-X/TiO_2, 1200 rpm stirring, 30 °C, reactions performed in Parr stainless steel autoclave. Catalysts treated at 500 °C / 4 h under flowing 5%H_2/Ar. Legend: crosses = 2.5%Fe, circles = 2.0%Fe, squares = 1.0%Fe, triangles = 0.5%Fe.

To determine whether adjusting Fe loading would affect the stability of Fe towards leaching, a series of catalysts were prepared with varying loadings of Fe. The series of catalysts were tested for the phenol oxidation reaction as shown in Figure 10. When 2.5%Pd-2.5%Fe/TiO_2 and 2.5%Pd-2.0%Fe/TiO_2 were compared, they were found to achieve phenol conversions of 77.8% and 84.3% at 120 minutes respectively. Therefore, it was found that decreasing the iron loading from 2.5 wt.% to 2.0 wt.% had only a minor effect on the observed phenol conversion activity. The catalyst with a slightly lower Fe loading showed a slight improvement in phenol oxidation activity.

However, when the Fe loadings were decreased further to 1.0 wt.% and 0.5 wt.%, phenol conversion was observed to decrease to 23.4 % and 14.7% at 120 minutes respectively. It was unclear why catalyst activity improved slightly when decreasing Fe loading from 2.5 wt.% to 2.0 wt.%, but then decreased substantially when Fe loading was decreased further to 1.0 wt.% and 0.5 wt.%. One potential reason for this may have been due to the molar concentrations of Fe with respect to Pd. 2.5%Pd-2.5%Fe/TiO_2 and 2.5%Pd-2.0%Fe/TiO_2 were both Fe-rich with respect to the molar ratio of Fe to Pd. On the other hand, 2.5%Pd-1.0%Fe/TiO_2 and 2.5%Pd-0.5%Fe/TiO_2 were both Pd-rich with respect to the molar ratio of Fe to Pd. The occurrence of Fe leaching was also determined by MP-AES analysis of the post-reaction solutions as shown in Figure 11.

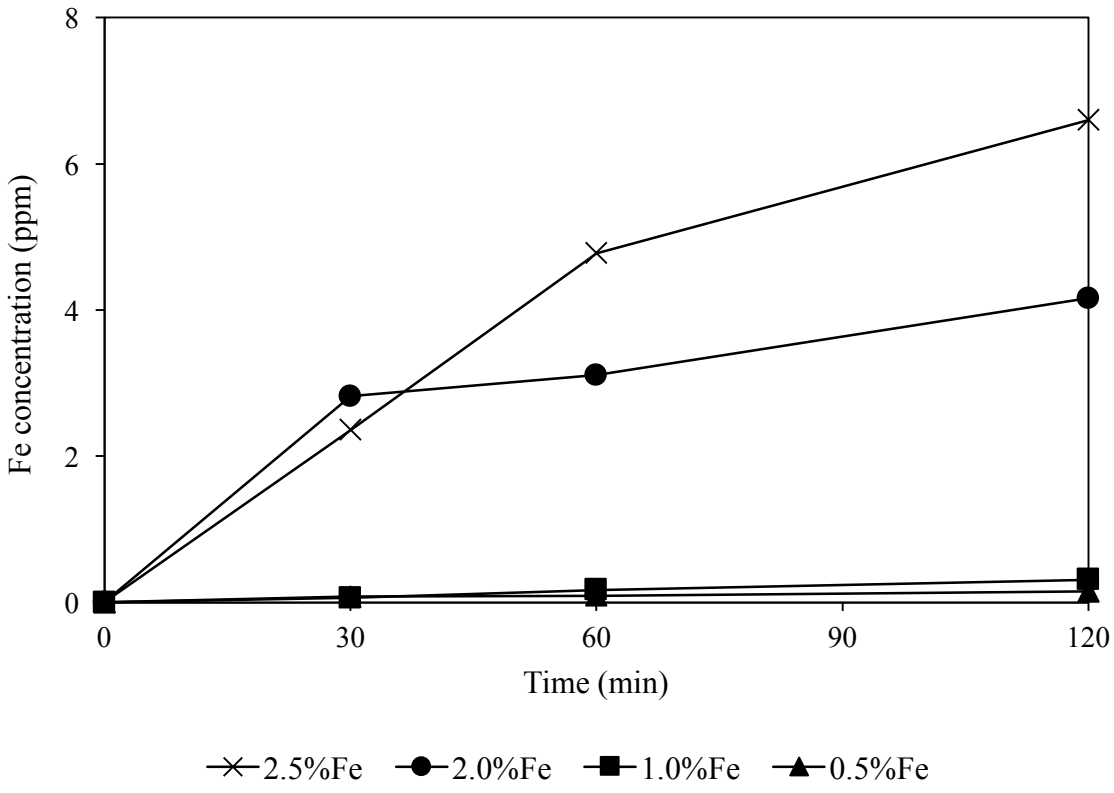

Figure 11: Leaching of Fe during reaction detected via MP-AES analysis. Conditions: 8.5 g 1000 ppm phenol solution, 420 psi 5%H_2/CO_2, 160 psi 25%O_2/CO_2, 10 mg 2.5%Pd-X/TiO_2, 1200 rpm stirring, 30 °C, reactions performed in Parr stainless steel autoclave. Catalysts treated at 500 °C / 4 h under flowing 5%H_2/Ar. Legend: crosses = 2.5%Fe, circles = 2.0%Fe, squares = 1.0%Fe, triangles = 0.5%Fe.

Interestingly, the 2.5%Pd-2.0%Fe/TiO_2 catalyst was found to leach less Fe than the 2.5%Pd-2.5%Fe/TiO_2 catalyst despite achieving slightly higher conversions of phenol. Both the 2.5%Pd-1.0%Fe/TiO_2 and 2.5%Pd-0.5%Fe/TiO_2 leached only very low quantities of Fe into solution. From this investigation, it was observed that modification of Fe loading on the catalyst had the potential to decrease the severity of Fe leaching, although was not suitable for complete elimination of the Fe leaching problem. Therefore, further investigation was performed to help determine the cause behind Fe leaching from the catalyst.

3.2.7 Fe leaching during oxidation reaction

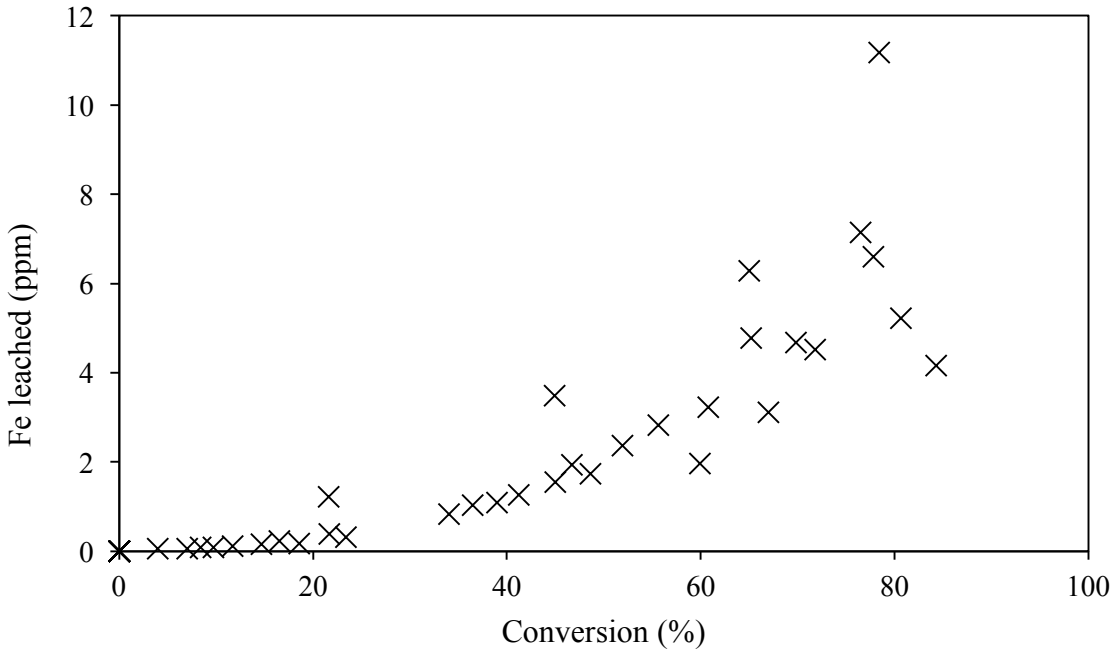

Figure 12: Correlation between Fe leaching and conversion observed.

From the previous experiments, it was noticed that the degree of Fe leaching appeared to be closely related to the conversion of phenol. To further investigate this, a graph was plotted showing the extent of Fe leaching against the observed phenol conversion for the prior reactions, as shown in Figure 12. From this graph, it was clearly observed that the extent of Fe leaching was closely related to the phenol conversion observed.

Interestingly, very little leaching of Fe was observed when phenol conversion was less than 30 %. However, when phenol conversion exceeded around 30 % the extent of Fe leaching increased greatly. This indicated that the generation of further oxidation products could have been responsible for the leaching of Fe from the catalyst. No detectable concentrations of Pd were observed in any of the post-reaction solutions. Additionally, leaching of Fe was observed to increase as the reaction proceeded. This was thought to indicate that the cause of Fe leaching was unlikely to be due to an inherent instability of the Fe due to a poor metal-support interaction. It was thought that, if this was the case, most the leaching would have occurred at the very start of the reaction.

3.2.8 Effect of reaction intermediates on Fe leaching

Table 2: Effect of reaction substrates/products upon catalyst stability. Conditions: 10 mg 2.5%Pd-2.5%Fe/TiO_2 stirred in 8.5 g substrate solution for 30 minutes in Parr stainless steel autoclave.

Substrate	**Fe leaching (ppm)**	**Pd leaching (ppm)**
Water	0	0
Phenol (1000 ppm)	0	0
420 psi 5%H_2/CO_2 160 psi 25%O_2/CO_2	0	0
Catechol (1000 ppm)	2.8	0
Oxalic Acid (1000 ppm)	9.8	4.0
Acetic acid (1000 ppm)	0	0

To further investigate whether the cause of Fe leaching was due to the reaction substrates/products, a series of experiments were performed as described in Table 2. Initially, 2.5%Pd-2.5%Fe/TiO_2 was stirred in water with no leaching of Pd and Fe observed. Ruling out that the leaching observed during testing could be due to poor

metal-support interaction. When 2.5%Pd-2.5%Fe/TiO_2 was stirred in a solution of phenol, no leaching of Pd and Fe was observed. This indicated that the observed leaching of Fe during the reaction was not due to the presence of phenol in the reaction medium. This was unsurprising and fitted with the observation that little/no leaching of Fe was observed during the initial stages of the reaction. The 2.5%Pd-2.5%Fe/TiO_2 catalyst was then stirred in water under 420 psi 5%H_2/CO_2 and 160 psi 25%O_2/CO_2, however no leaching of Pd or Fe was observed in the post-reaction solution. This was thought to rule out that the leaching of Fe was caused by the acidic conditions created by the formation of carbonic acid due to the presence of high pressure CO_2. When the 2.5%Pd-2.5%Fe/TiO_2 catalyst was stirred in a solution of catechol which was one of the primary oxidation products from phenol, 2.8 ppm Fe was detected in the post-reaction solution. In addition to this, when the 2.5%Pd-2.5%Fe/TiO_2 catalyst was stirred in a solution of oxalic acid which is a known oxidation product from phenol, 9.8 ppm Fe and 4.0 ppm Pd was detected in the post-reaction solution. The 2.5%Pd-2.5%Fe/TiO2 catalyst was also stirred in a solution of acetic acid which is also a known oxidation product from phenol. However, no leaching of Fe and Pd was observed in the presence of acetic acid. From the results described it appeared clear that the leaching could have been caused due to the formation of catechol and potentially oxalic acid during the reaction. Catechol and oxalic acid have been reported as chelators of Fe.[22,23] The chelation of Fe during fentons oxidation processes has been reported in the literature as far back as 1928.[24] Further experiments were performed to gain more insight into Fe and Pd leaching from the catalyst due to the presence of oxalic acid and catechol.

3.2.9 Effect of catalyst treatment with catechol and oxalic acid

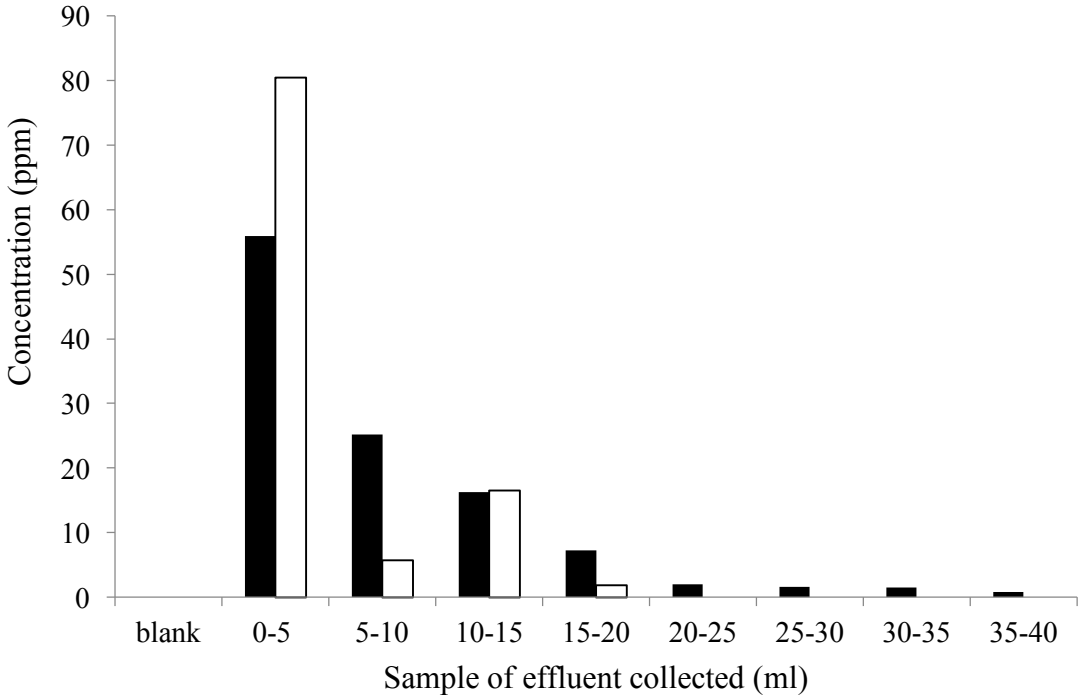

Figure 13: Effect of oxalic acid on the leaching of metals from catalyst. Conditions: 1000 ppm oxalic acid flowed over 50 mg of 0.5%Pd-0.5%Fe/TiO_2 and metal leaching analysed using MP-AES. Legend: filled = Fe concentration (ppm), unfilled = Pd concentration (ppm).

To further investigate the effect of oxalic acid upon the leaching of metal from 2.5%Pd-2.5%Fe/TiO_2, an experiment was performed whereby a solution of oxalic acid was flowed over the catalyst. The effluent was collected in aliquots of 5 ml and the Fe and Pd concentrations were measured using MP-AES as shown in Figure 13. The initial 5 ml aliquot of oxalic acid solution contained 55.9 ppm Fe and 80.4 ppm Pd after being passed over the catalyst at a rate of 1 ml/min. This showed that metals readily leached from the catalyst in the presence of oxalic acid. However, the concentrations of metals leached from the catalyst then decreased in subsequent aliquots until only very small concentrations of metals were leached from the catalyst in later aliquots. This may have been caused by a complete loss of metal from the

surface of the catalysts. Therefore, from the concentrations of metals present in the aliquots, the % metal loss from the catalyst was calculated as shown in Figure 14.

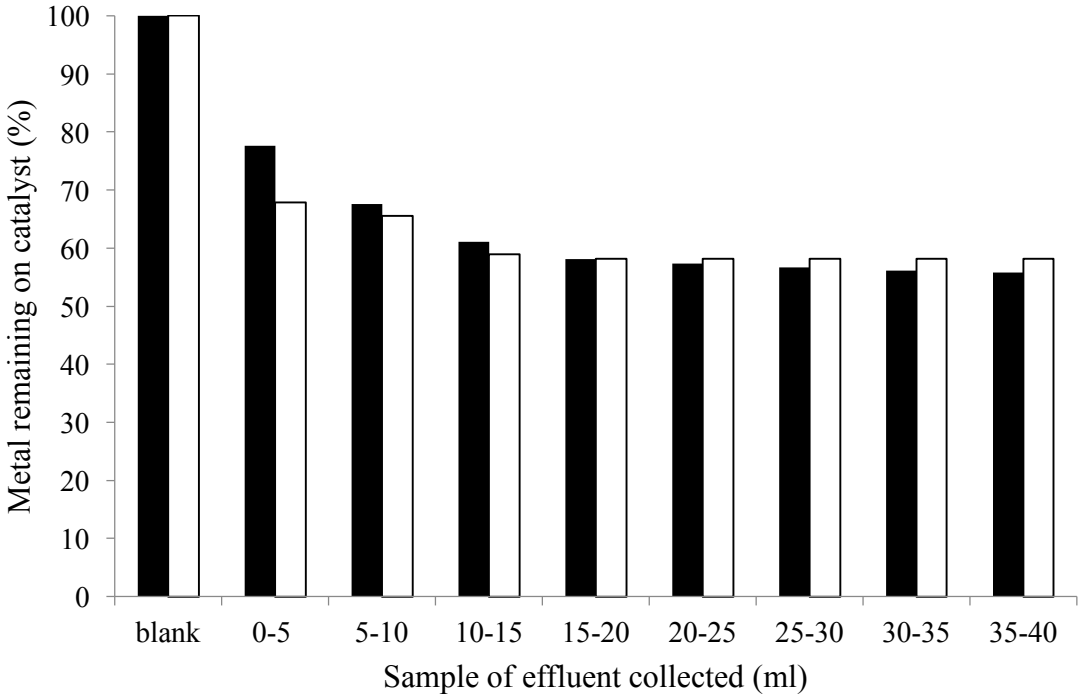

Figure 14: Effect of oxalic acid on the leaching of metals from catalyst. Conditions: 1000 ppm oxalic acid flowed over 50 mg of 0.5%Pd-0.5%Fe/TiO_2 and metal leaching analysed using MP-AES. Legend: filled = Fe remaining (%), unfilled = Pd remaining (%).

From Figure 14, it was observed that that a large percentage of metal was lost from the catalyst as the initial aliquots of oxalic acid solution were passed over the catalyst. However, only a very small percentage of metals was leached as later aliquots of oxalic acid solution were passed over the catalyst. Interestingly, over 50% of both Fe and Pd remained on the catalyst after treatment with flowing oxalic acid. This indicated that not all the metal supported on the catalyst was susceptible to leaching by chelation with oxalic acid. This could have been either due to the metals being deposited on the support in areas less accessible to the oxalic acid or due to the oxidation state of the remaining metals. To determine the reusability of the catalyst after treatment with oxalic acid, the catalyst was collected and then tested for the oxidation of phenol as shown in Table 3.

Table 3: Re-usability of catalyst after treatment of catalyst with flowing oxalic acid. Conditions: 8.5 g 1000 ppm phenol solution, 420 psi 5%H_2/CO_2, 160 psi 25%O_2/CO_2, 10 mg 2.5%Pd-2.5%Fe/TiO_2, 1200 rpm stirring, 30 °C, reactions performed in Parr stainless steel autoclave.

Catalyst	**Conversion (%)**	**Fe leaching (ppm)**
2.5%Pd-2.5%Fe/TiO_2 (before treatment)	78	6.6
2.5%Pd-2.5%Fe/TiO_2 (after treatment)	26	2.55

From the reusability testing described in Table 3, it was observed that the catalyst treated with oxalic acid achieved a phenol conversion of 26% compared to the fresh catalyst that achieved a conversion of 78%. The decrease in catalyst activity observed was thought to potentially be due to the decreased metal loading on the catalyst. Interestingly, leaching of Fe from the catalyst was still observed. This further leaching could have been due to residual Fe-oxalic acid complex that remained on the surface of the catalyst which was then washed off under the vigorous stirring conditions employed during the phenol oxidation reaction. To investigate the effect of catechol upon the catalyst, the same series of experiments were performed employing a solution of catechol in place of a solution of oxalic acid. The results of this experiment are described in Figure 15.

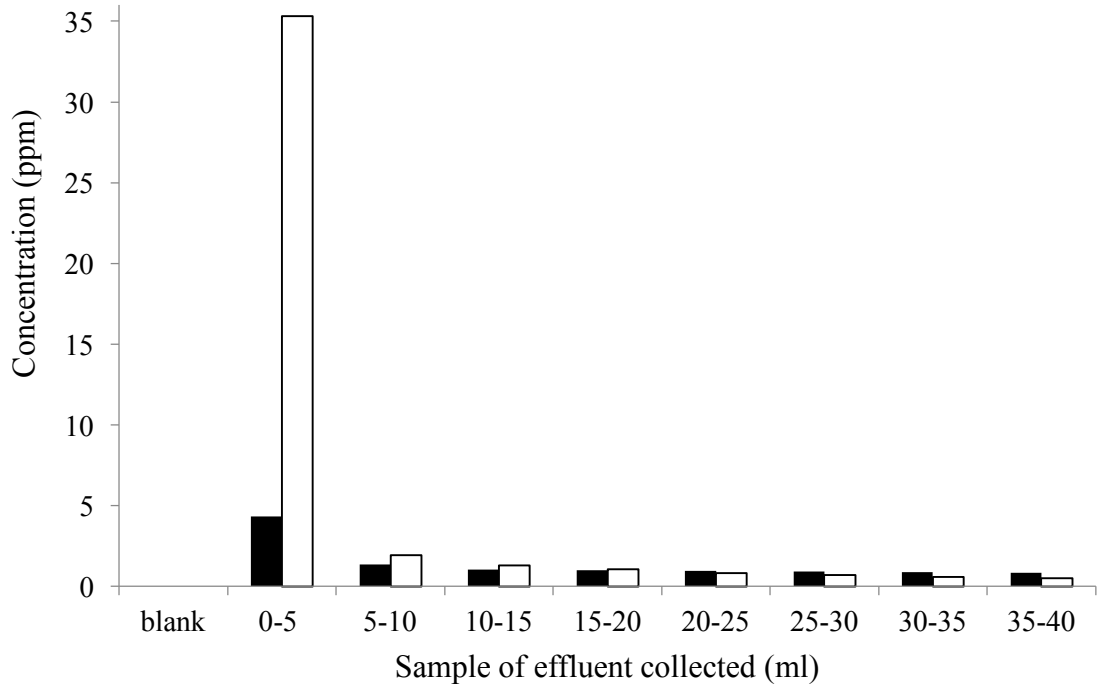

Figure 15: Effect of catechol on leaching of metals from catalyst. Conditions: 1000 ppm catechol flowed over 50 mg of 0.5%Pd-0.5%Fe/TiO_2 and metal leaching analysed using MP-AES. Legend: filled = Fe concentration (ppm), unfilled = Pd concentration (ppm).

To further investigate the effect of catechol upon the leaching of metal from 2.5%Pd-2.5%Fe/TiO_2, an experiment was performed whereby a solution of catechol was flowed over the catalyst. The effluent was collected in aliquots of 5 ml and the Fe and Pd concentrations were measured using MP-AES as shown in Figure 15. The initial 5 ml aliquot of catechol solution contained 4.4 ppm Fe and 35.3 ppm Pd after being passed over the catalyst. Interestingly, flowing catechol over the catalyst resulted in far greater concentrations of Pd being leached when compared to the concentrations of Fe leached. This observation was surprising because when the catalyst was stirred in a solution of catechol in the autoclave, no Pd was detected in the catechol solution afterwards. In addition to this, no Pd has been detected in the post-reaction effluents collected after phenol oxidation. This was thought to potentially be due to the leached Pd 'sticking' to the stainless-steel overhead stirrer utilised with the Parr autoclave reactors. Therefore, it appeared that leaching of Pd was also a problem during the phenol reaction due to complex formation with catechol and/or oxalic acid.

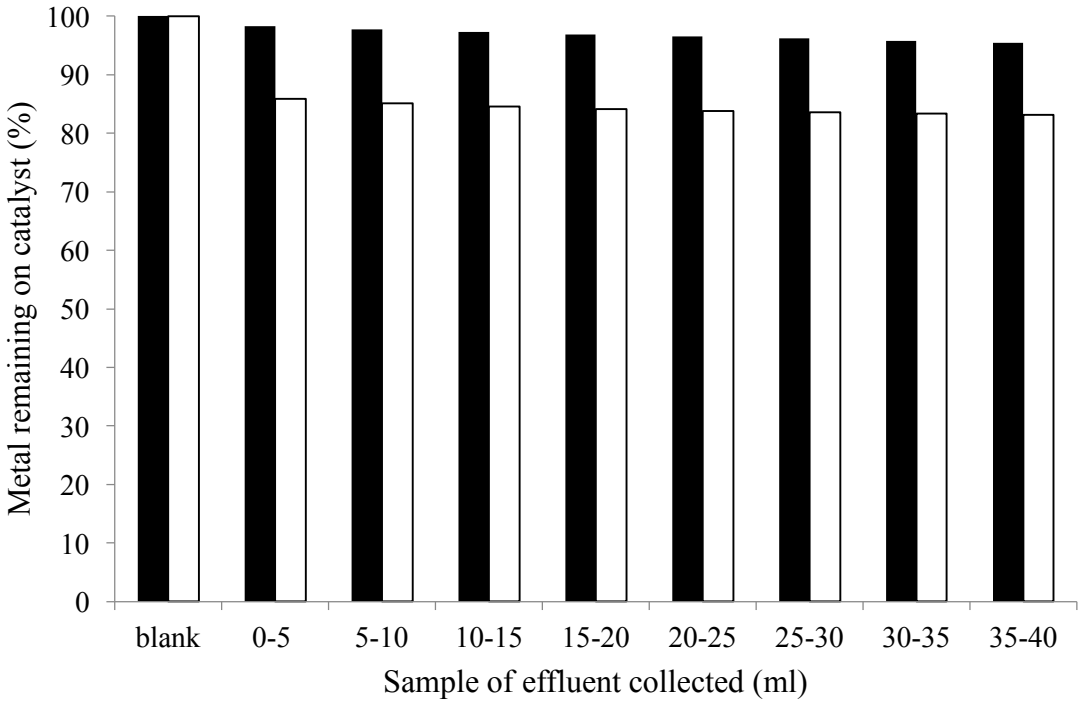

Figure 16: Effect of catechol on leaching of metals from catalyst. 1000 ppm catechol flowed over 50 mg of 0.5%Pd-0.5%Fe/TiO_2 and metal leaching analysed using MP-AES. Legend: filled = Fe remaining (%), unfilled = Pd remaining (%)

When the percentage metal lost from the catalyst was considered, as shown in Figure 16, it appeared that far less Pd and Fe were leached from the catalyst when catechol was used as opposed to oxalic acid. Part of this difference could be related to the difference in molar concentration of oxalic acid with respect to the molar concentration of catechol. While both the concentrations of oxalic acid and catechol were 1000 ppm, this equated to a molar concentration of 0.0111 M and 0.0091 M respectively. However, this did not explain the large difference in the leaching of metals when using catechol and oxalic acid solutions. It therefore appears that oxalic acid had a far more detrimental effect towards catalyst stability when compared with catechol. To determine the reusability of the catalyst after treatment with catechol, the catalyst was collected and then tested for the oxidation of phenol as shown in Table 4.

Table 4: Catalyst re-usability after treatment with flowing catechol. 8.5 g 1000 ppm phenol solution, 420 psi 5%H_2/CO_2, 160 psi 25%O_2/CO_2, 10 mg 2.5%Pd-2.5%Fe/TiO_2, 1200 rpm stirring, 30 °C, reactions performed in Parr stainless steel autoclave.

Catalyst	Conversion (%)	Fe leaching (ppm)
2.5%Pd-2.5%Fe/TiO_2 (before treatment)	78	6.6
2.5%Pd-2.5%Fe/TiO_2 (after treatment)	23	1.35

From the reusability testing described in Table 4, it was observed that the catalyst treated with catechol achieved a phenol conversion of 23% compared to the fresh catalyst that achieved a conversion of 78%. The large decrease in catalyst activity was surprising because a relatively low percentage of the total metal was removed from the catalyst during the treatment of the catalyst with catechol. The decrease in catalyst activity was thought to potentially be due to adsorbed catechol poisoning the surface of the catalyst. As was the case with the oxalic acid treated catalyst, leaching of Fe was also observed during the reuse of the catalyst. This further leaching could have been due to residual Fe-catechol complex that remained on the surface of the catalyst which was then washed off under the vigorous stirring conditions employed during the phenol oxidation reaction. To investigate whether the oxidation state of the supported metals influences their propensity to leach in the presence of oxalic acid and catechol, a series of XPS experiments were performed to determine the oxidation state of the supported metals before and after treatment with oxalic acid and catechol.

3.2.10 XPS Analysis of catalysts post-treatment

Table 5: Surface concentrations of different elements on 2.5%Pd-2.5%Fe/TiO_2 after treatment with flowing catechol or oxalic acid. Analysis performed using XPS.

Name	**Fresh catalyst (At %)**	**Catechol treated (At %)**	**Oxalic acid treated (At %)**
O 1s	30.99	37.56	36.59
C 1s	54.78	48.47	47.70
Ti 2p	9.70	10.79	13.25
Fe 2p	2.66	2.71	1.40
Pd 3d	0.82	0.47	0.17
Cl 2p	1.05	0	0

The surface concentrations of expected elements were determined using XPS, as shown in Table 5. It was observed that for the catechol treated catalyst, the surface concentration of Fe was similar to that of the fresh. However, for the oxalic treated catalyst, there was a decrease from 2.66 At % to 1.40 At %. These results agreed with the leaching of Fe detected using MP-AES. In the case of Pd, there was a large loss in surface concentration for both the catechol and oxalic acid treated catalysts. When catechol was used the surface concentration of Pd decreased from 0.82 At % to 0.47 At %. When oxalic acid was used the surface concentration of Pd decreased from 0.82 At % to 0.17 At %. From the MP-AES analysis it was observed that treatment with oxalic acid led to greater loss of Pd when compared with catechol, which agreed with this XPS analysis.

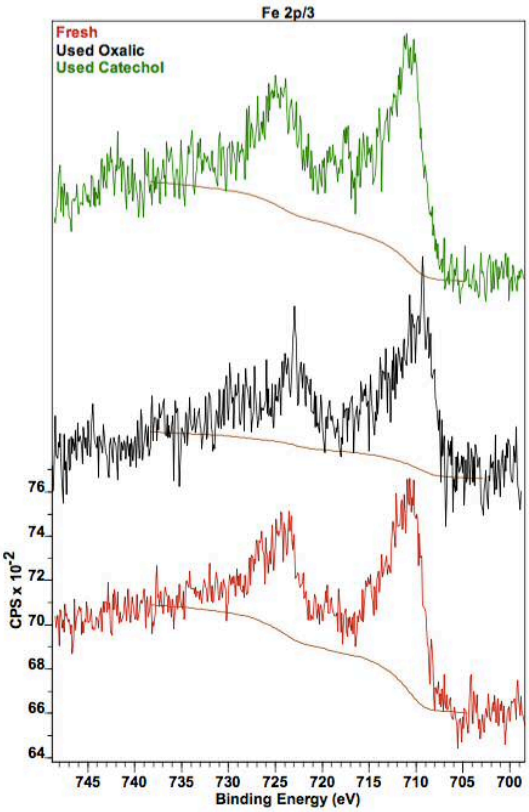

Figure 17: Fe $2p_{3/2}$ spectra of fresh, catechol-treated and oxalic acid-treated 2.5%Pd-2.5%Fe/TiO_2.

From the Fe $2p_{3/2}$ spectra, as shown in Figure 17, it was determined that most of the Fe present was as Fe_2O_3 for the fresh catalyst. The spectra remained mostly the same for the catalyst treated with catechol. However, for the catalyst treated with oxalic acid, a slight shift in the peak to a lower binding energy was observed. This may have been associated with a change in the oxidation state from Fe^{3+} to Fe^{2+} due to this treatment.

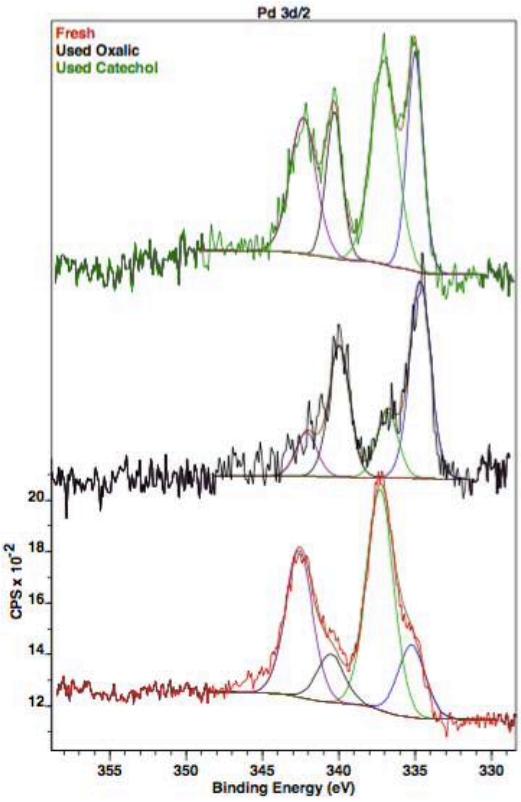

Figure 18: Pd $3d_{5/2}$ spectra of fresh, catechol-treated and oxalic acid-treated 2.5%Pd-2.5%Fe/TiO_2.

From the Pd $3d_{5/2}$ spectra, as shown in Figure 18, it was determined that Pd was present as both Pd^{2+} (at around 337 eV) and (Pd^0 at around 335 eV) in the fresh catalyst. However, Pd^{2+} appeared to be the dominant form of Pd in the fresh catalyst. Upon treatment with catechol, a large decrease in the Pd^{2+} peak was observed, whereas the peak associated with Pd^0 remained largely the same. Upon treatment with oxalic acid, an almost complete loss of the Pd^{2+} peak was observed, whereas the peak associated with Pd^0 remained largely the same. From these observations, it was clear that Pd^{2+} was far more susceptible to leaching under the reaction conditions than Pd^0. Therefore, an attempt should be made to increase the amount of Pd^0 on the catalyst.

3.2.11 Effect of chloride-free catalyst preparation on Fe leaching

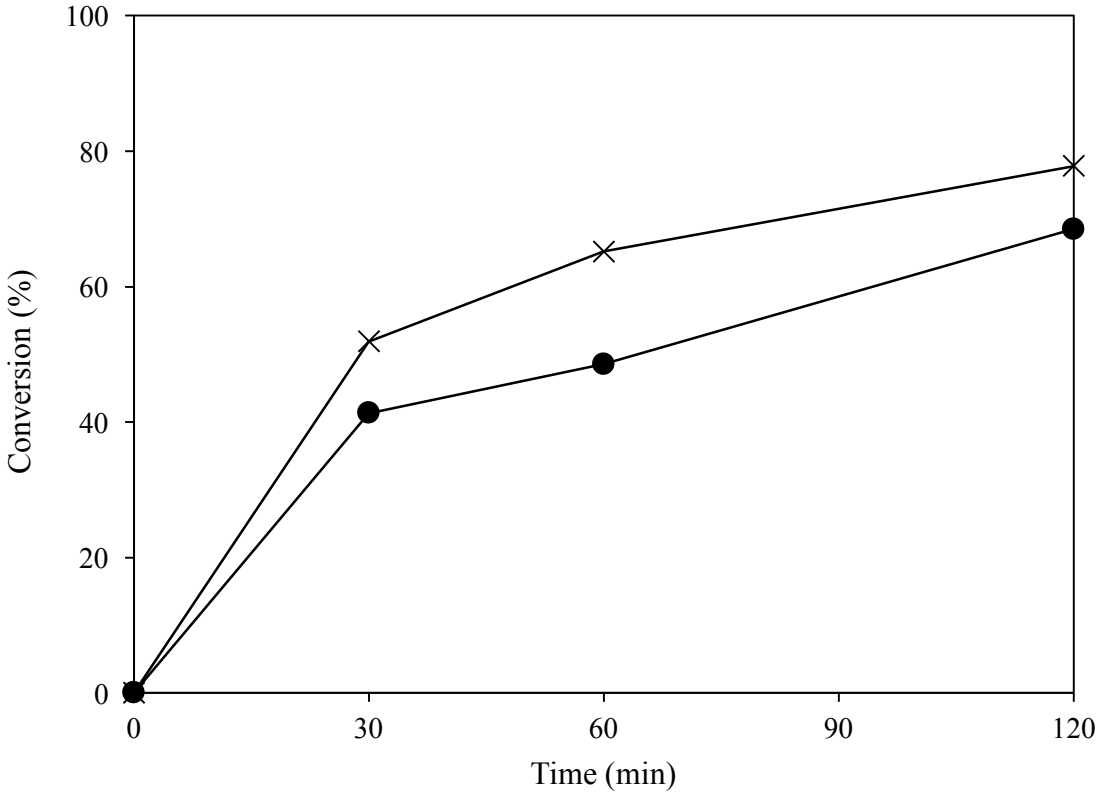

Figure 19: Effect of chloride-free catalyst preparation on the conversion of phenol. Conditions: 8.5 g 1000 ppm phenol solution, 420 psi 5%H_2/CO_2, 160 psi 25%O_2/CO_2, 10 mg 2.5%Pd-2.5%Fe/TiO_2, 1200 rpm stirring, 30 °C, reactions performed in Parr stainless steel autoclave. Legend: crosses = chloride, circles = chloride-free.

An attempt was made to improve the stability of the catalyst by using nitrate precursors as an alternative to the chloride precursors used previously. A nitrate precursor was chosen due to its lower decomposition temperature when compared to the chloride precursor. It was hoped that this would lead to a greater concentration of reduced metal on the surface of the catalyst. The catalyst was prepared and tested for the phenol oxidation reaction, as shown in Figure 19. The catalyst prepared using nitrate precursors showed similar performance in the phenol oxidation reaction to the catalyst prepared using chloride precursors. However, the catalyst prepared using chloride precursors did achieve a slightly higher phenol conversion of 77.8 % when compared to the 68.5 % achieved by the catalyst prepared by nitrate precursors. This

may have been related to greater dispersion of the metals when using the 'excess anion method'[25] to prepare the catalyst using chloride precursors. The excess HCl used when dissolving the $PdCl_2$ precursor may have aided the dispersion of the metal during catalyst preparation.

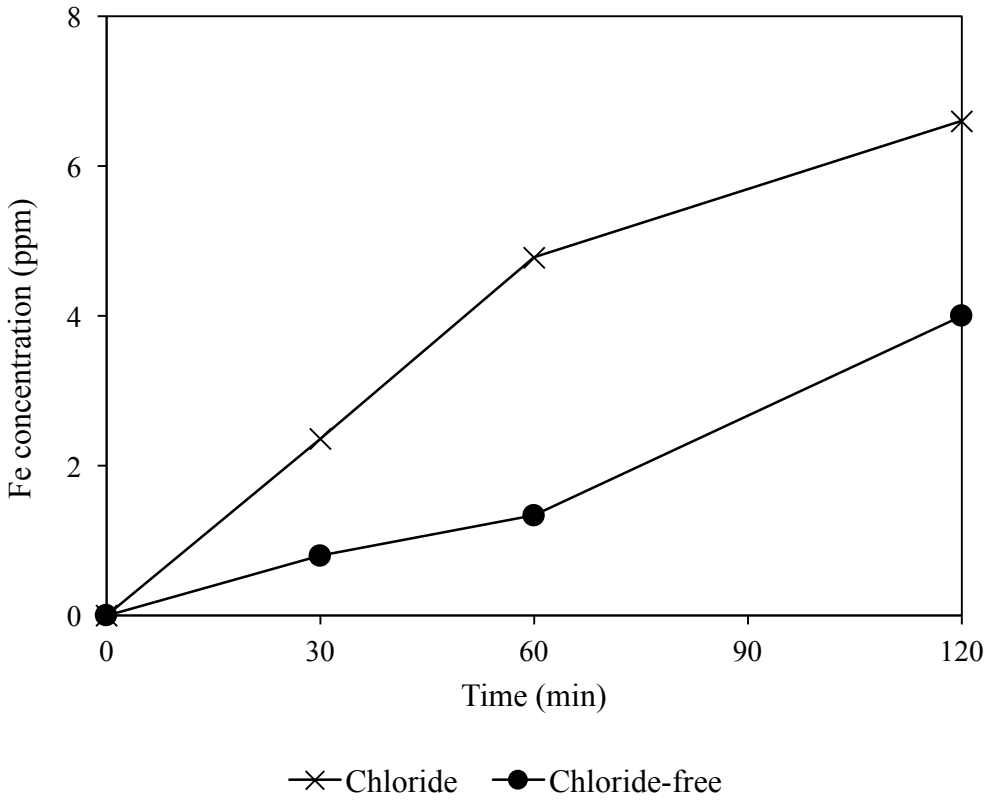

Figure 20: Leaching of Fe during reaction detected via MP-AES analysis. Conditions: 8.5 g 1000 ppm phenol solution, 420 psi 5%H_2/CO_2, 160 psi 25%O_2/CO_2, 10 mg 2.5%Pd-2.5%Fe/TiO_2, 1200 rpm stirring, 30 °C, reactions performed in Parr stainless steel autoclave. Legend: crosses = chloride, circles = chloride-free.

The analysis of metals leached during reaction by MP-AES is shown in Figure 20. Despite largely similar phenol oxidation activity achieved by the catalysts prepared by nitrate and chloride precursors, the catalyst prepared using nitrate precursors demonstrated increased stability when compared to the catalyst prepared using chloride precursors. After 2 h reaction, 6.6 ppm Fe was detected in the reaction solution when the catalyst from chloride precursors was used. This was in contrast with 4 ppm Fe detected in the reaction solution at the same point when the catalyst

from nitrate precursors was used. This result indicated that catalysts prepared using nitrate precursors were more stable against leaching than catalysts prepared using chloride precursors. However, it must be considered that there was slightly less conversion of phenol so this may be the cause behind the lower leaching. Therefore, further testing was performed to measure the catalyst stability in a way where the use of the two precursors could be more fairly compared.

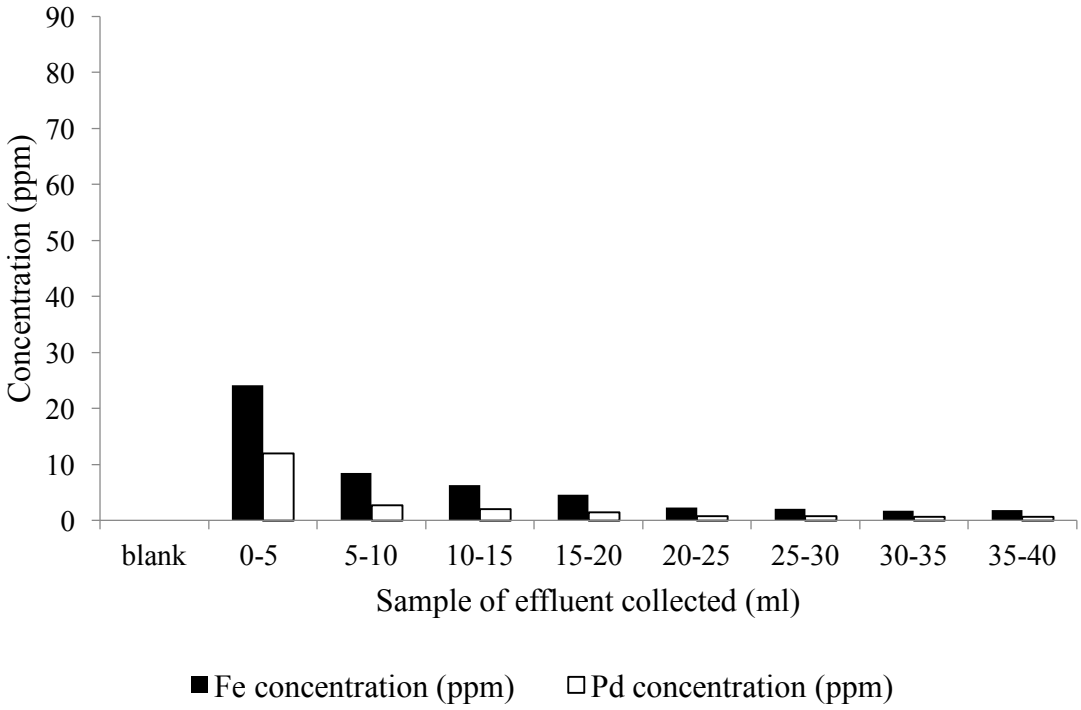

Figure 21: Effect of oxalic acid on the leaching of metals from catalyst. Conditions: 1000 ppm oxalic acid flowed over 50 mg of 0.5%Pd-0.5%Fe/TiO_2 (chloride-free) and metal leaching analysed using MP-AES. Legend: filled = Fe concentration (ppm), unfilled = Pd concentration (ppm).

To further investigate the effect of oxalic acid upon the leaching of metal from 2.5%Pd-2.5%Fe/TiO_2 (chloride-free), an experiment was performed whereby a solution of oxalic acid was flowed over the catalyst. The effluent was collected in aliquots of 5 ml and the Fe and Pd concentrations were measured using MP-AES as shown in Figure 21. The initial 5 ml aliquot of oxalic acid solution contained 24.14 ppm Fe and 11.99 ppm Pd after being passed over the catalyst at a rate of 1 ml/min.

Subsequent 5 ml aliquots collected contained decreasing concentrations of Fe and Pd suggesting that the rate of Fe and Pd leaching decreases with time. The results obtained for the chloride-free catalyst were then compared to the results obtained for the catalyst prepared using chloride precursors, as shown in Figure 13. The leaching in the initial 5 ml aliquot for the 2.5%Pd-2.5%Fe/TiO_2 prepared with chloride precursors was far higher than that observed for 2.5%Pd-2.5%Fe/TiO_2 (chloride-free). The 2.5%Pd-2.5%Fe/TiO_2 (chloride-free) leached 24.14 ppm Fe compared to 55.9 ppm Fe for the catalyst prepared by chloride precursors. Additionally, the 2.5%Pd-2.5%Fe/TiO_2 (chloride-free) leached 11.99 ppm Pd compared to 80.4 ppm Pd for the catalyst prepared by chloride precursors. Therefore, 2.5%Pd-2.5%Fe/TiO_2 (chloride-free) was more stable than the catalyst prepared from chloride precursors with respect to leaching by oxalic acid. While stability was enhanced for the Fe supported on the catalyst, the greatest stability enhancement was observed for the Pd supported on the catalyst. From previous experiments, a likely explanation for this stability enhancement could be due to the oxidation state of the Pd supported on the catalyst.

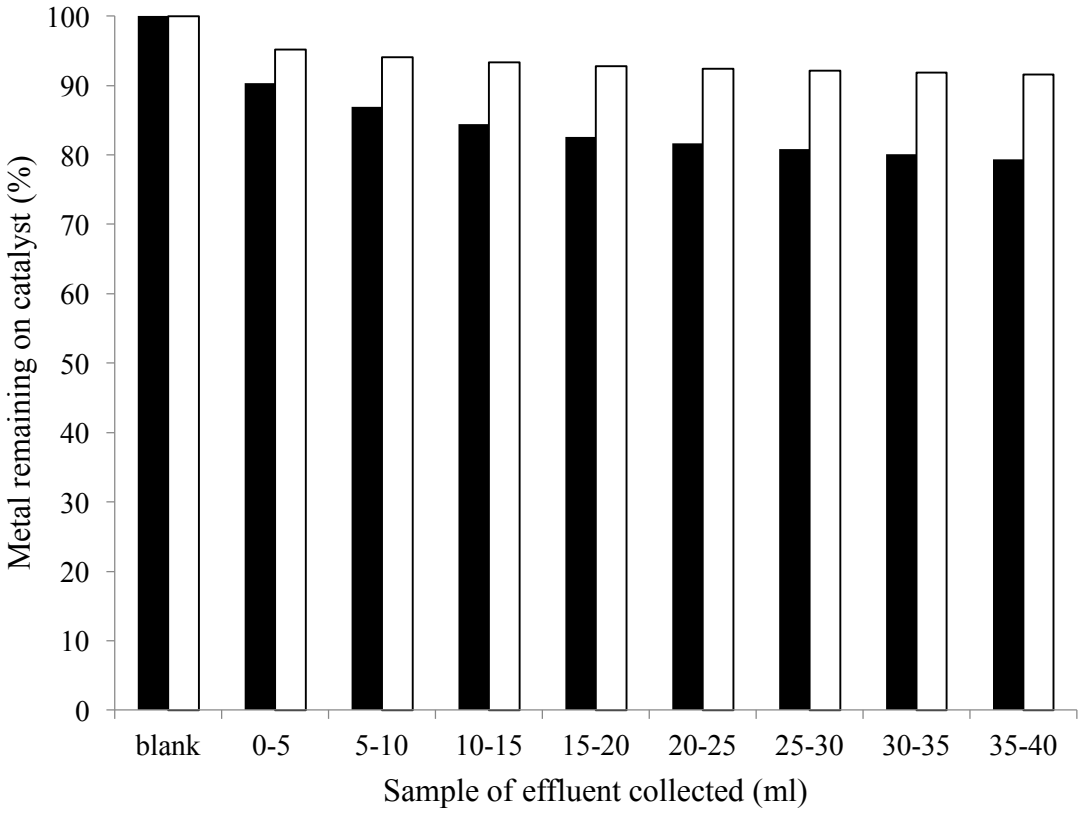

Figure 22: Effect of oxalic acid on the leaching of metals from catalyst. Conditions: 1000 ppm oxalic acid flowed over 50 mg of 0.5%Pd-0.5%Fe/TiO_2 (chloride-free) and metal leaching analysed using MP-AES. Legend: filled = Fe remaining (%), unfilled = Pd remaining (%)

The results were also analysed in terms of the percentage of metal lost from the catalyst. After flowing 40 ml 1000 ppm oxalic acid solution over the catalyst, a far lower percentage of the total amount of Pd and Fe supported on the catalyst was lost for the catalyst prepared from nitrate precursors when compared to the catalyst prepared from chloride precursors. This result further demonstrated the stability enhancement achieved when preparing the catalyst using nitrate precursors when compared to preparing the catalyst using chloride precursors. To determine whether this stability enhancement could be related to the oxidation state of the metals on the surface, the oxalic acid treated catalyst was collected and analysed using XPS.

Table 6: Surface concentrations of different elements on 2.5%Pd-2.5%Fe/TiO_2 (chloride-free) after treatment with flowing catechol or oxalic acid. Analysis performed using XPS.

Name	Fresh catalyst (At %)	Oxalic acid treated (At %)
O 1s	32.56	36.35
C 1s	51.48	48.4
Ti 2p	13.57	13.98
Fe 2p	1.8	1.04
Pd 3d	0.34	0.23
Cl 2p	0.25	-

The surface concentrations of expected elements were determined using XPS, as shown in Table 6. It was observed that for the oxalic acid treated catalyst there was a decrease from 1.8 At % to 1.04 At % in the surface concentration of Fe when compared to the fresh catalyst. This decrease was greater than the around 20 % decrease determined using MP-AES. However, this may have been related to leaching of the smaller nanoparticles which contribute more significantly to the surface concentration per amount of Fe. This could also have been attributed to error when calculating the surface concentrations. Additionally, for the oxalic acid treated catalyst the Pd surface concentration was observed to decrease from 0.34 At % to 0.23 At % when compared to the fresh catalyst. This decrease was again surprising because only a very low amount of Pd leaching was observed via the MP-AES analysis. This could again likely be attributed to greater loss of the smaller nanoparticles and error in the analysis. Interestingly, the fresh catalyst prepared using nitrate precursors had a surface Pd concentration of 0.34 At % whereas the fresh catalyst prepared using chloride precursors 0.82 At %. This result indicated that the dispersion of Pd over the surface of the catalyst was greater for the catalyst prepared using chloride precursors. This may have been part of the cause for the increased leaching observed when using

chloride precursors. This may also account for the lower catalyst activity observed for phenol oxidation when using the catalyst prepared with nitrate precursors. To further determine the cause of the enhanced Pd stability, the Pd $3d_{5/2}$ spectra was analysed to determine the oxidation state of the Pd lost after treatment with oxalic acid.

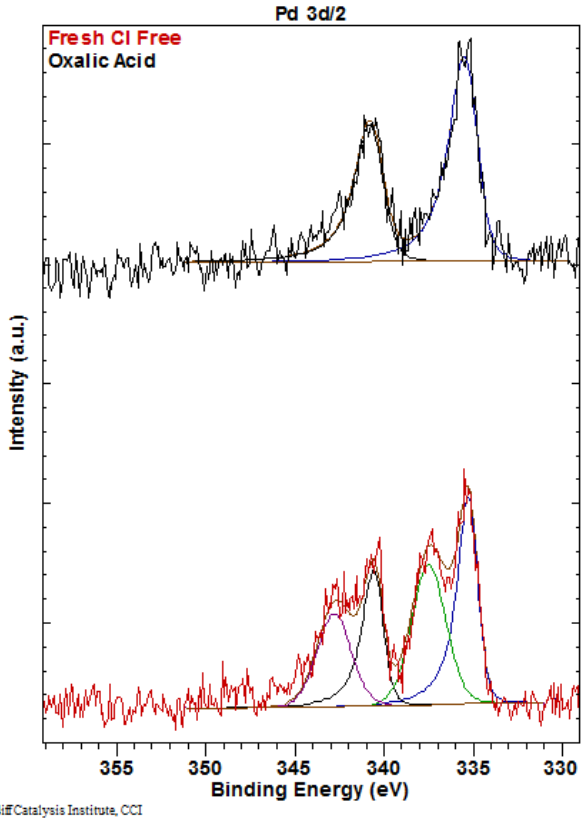

Figure 23: Pd $3d_{5/2}$ spectra of fresh and oxalic acid-treated 2.5%Pd-2.5%Fe/TiO_2 (chloride-free).

From the Pd $3d_{5/2}$ spectra, as shown in Figure 23, it was determined that Pd was present as both Pd^{2+} (at around 337 eV) and (Pd^{0} at around 335 eV) in the fresh catalyst. However, Pd^{0} appeared to be the dominant form of Pd in the fresh catalyst. This contrasted with the catalyst prepared using chloride precursors, where Pd^{2+} was the dominant form of Pd. After treatment with oxalic acid, there was a complete loss of Pd^{2+} whereas little/no leaching of Pd^{0} was observed. This result supported the previous observation that only Pd^{2+} was susceptible to leaching from the catalyst in the presence of oxalic acid. This evidence suggested that the cause for the enhanced

stability observed for the catalyst prepared with nitrate precursors was due to a change in the oxidation state of the Pd on the surface of the catalyst. Therefore, it appears that the obtainment of Pd^0 on the surface of the catalyst is essential when performing these types of oxidation reactions using *in situ* generated H_2O_2.

3.2.12 Potential of perovskite type materials for reducing Fe leaching

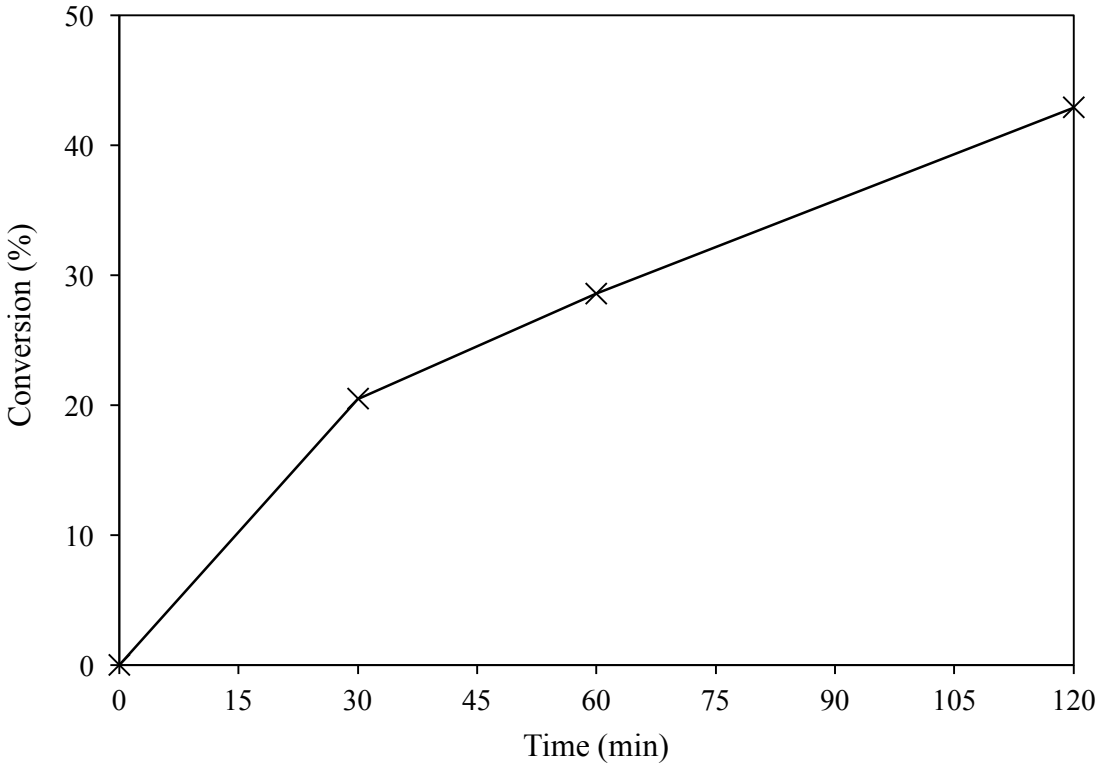

Figure 24: Phenol conversion observed using Pd supported on $LaFeO_3$ material. Conditions: 8.5 g 1000 ppm phenol solution, 420 psi 5%H_2/CO_2, 160 psi 25%O_2/CO_2, 10 mg 2.5%Pd/$LaFeO_3$, 1200 rpm stirring, 30 °C, reactions performed in Parr stainless steel autoclave.

While it remained possible to greatly enhance the stability of Pd on the surface of the catalyst, the stability of Fe on the surface of the catalyst was still problematic. One method considered to increase the stability of the Fe was to use an Fe containing perovskite structure. Therefore, $LaFeO_3$ was prepared by Evans *et al.*[26] and Pd was

supported on its surface using a simple impregnation procedure using nitrate precursors to give 2.5%Pd/$LaFeO_3$. 2.5%Pd/$LaFeO_3$ was then tested for the phenol oxidation reaction, as shown in Figure 24. After 2 h reaction, a phenol conversion of 42.9 % was achieved for 2.5%Pd/$LaFeO_3$ compared to 68.5 % achieved for 2.5%Pd-2.5%Fe/TiO_2. While the phenol conversion achieved for the perovskite supported catalyst was less, the result clearly demonstrated the potential of 2.5%Pd/$LaFeO_3$ for performing the phenol oxidation reaction with *in situ* generated H_2O_2. To determine whether the use of perovskite structures enhanced the stability of Fe under reaction conditions, the post-reaction effluent was collected and analysed using MP-AES.

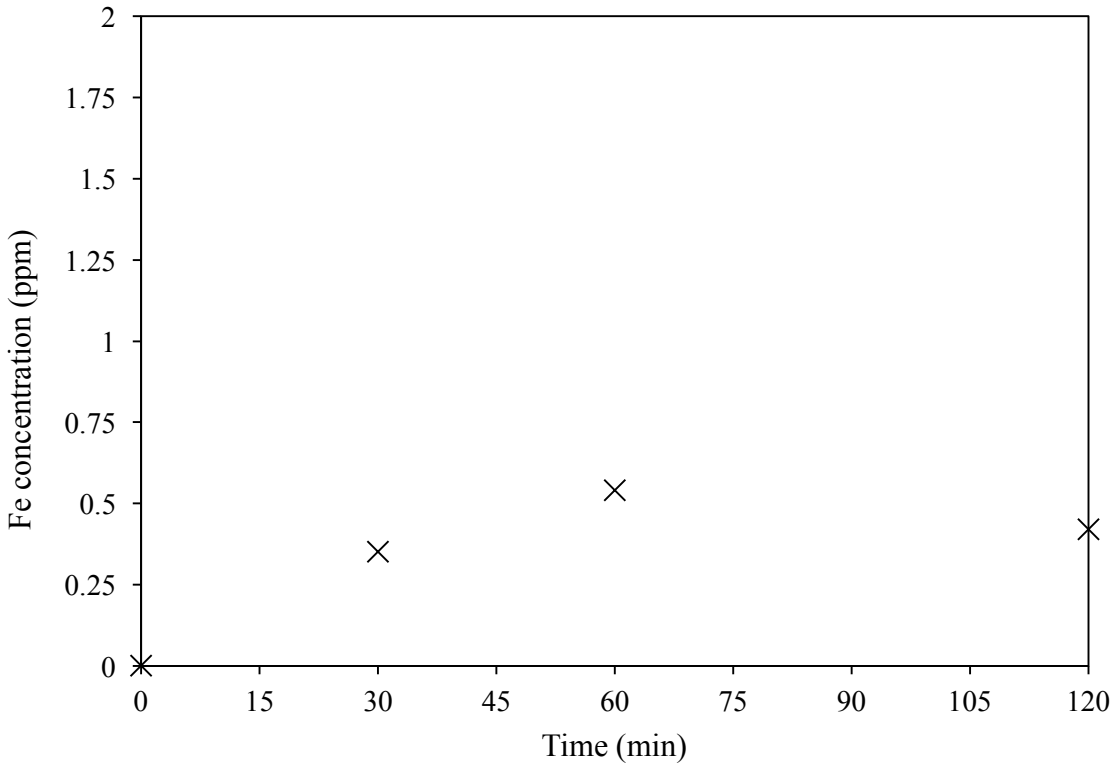

Figure 25: Leaching of Fe during reaction detected via MP-AES analysis. Conditions: 8.5 g 1000 ppm phenol solution, 420 psi 5%H_2/CO_2, 160 psi 25%O_2/CO_2, 10 mg 2.5%Pd/$LaFeO_3$, 1200 rpm stirring, 30 °C, reactions performed in Parr stainless steel autoclave.

Figure 25 displays the results from the MP-AES analysis of the post-reaction effluent. From the MP-AES analysis it was clear that there was still leaching of low concentrations of Fe during reaction. However, when using previous catalysts, the

concentration of Fe in solution was observed to increase as the reaction proceeded, whereas for 2.5%Pd-$LaFeO_3$ it remained mostly consistent over the course of the reaction. Therefore, in this case it appeared that the small amount of Fe leached very early in the reaction with no further leaching occurring later in the reaction. However, as the conversion of phenol observed was far lower, this may have been due to the generation of far lower concentrations of catechol/oxalic acid. Therefore, testing was performed whereby oxalic acid and catechol were flowed over the catalyst and leaching analysed using MP-AES. It was believed that this would give greater insight into any stability enhancements obtained by containing the Fe within a perovskite structure.

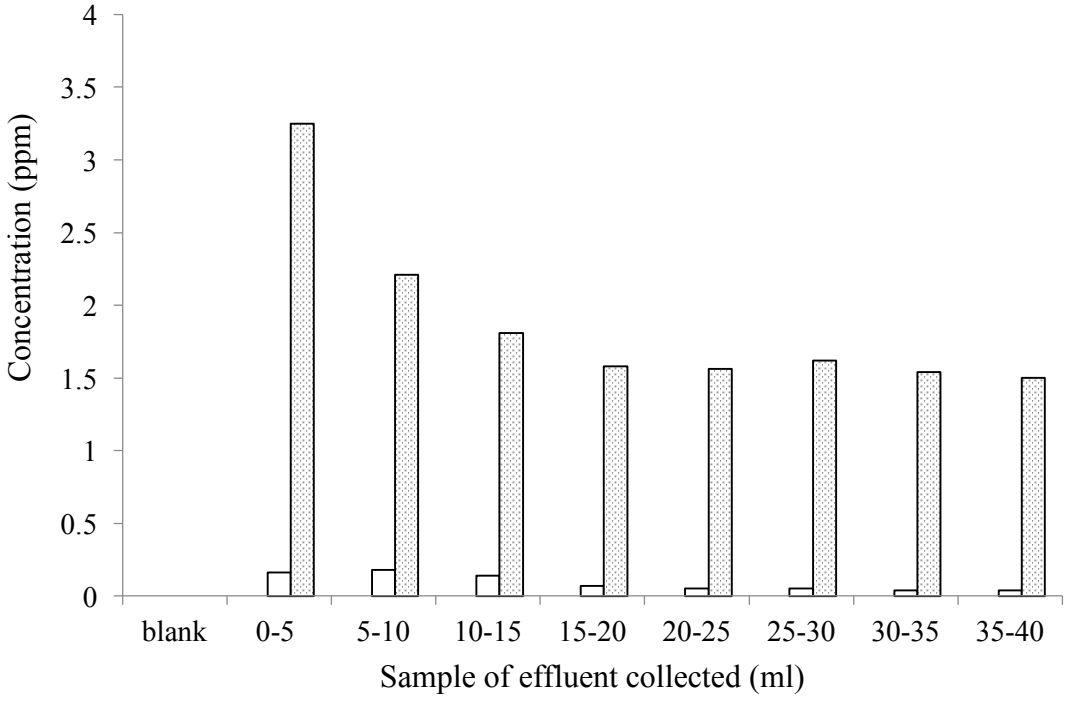

Figure 26: Effect of catechol on leaching of metals from the catalyst. Conditions: 1000 ppm catechol flowed over 50 mg of 2.5%Pd-$LaFeO_3$ and metal leaching analysed using MP-AES. Legend: filled = Fe concentration (ppm), unfilled = Pd concentration (ppm), dots = La concentration (ppm).

To further investigate the effect of catechol upon the leaching of metal from 2.5%Pd/$LaFeO_3$, an experiment was performed whereby a solution of catechol was flowed over the catalyst. The effluent was collected in aliquots of 5 ml and the Fe, Pd

and La concentrations were measured using MP-AES as shown in Figure 26. Interestingly, flowing 1000 ppm catechol over the catalyst resulted in no leaching of Fe from the surface of the catalyst. This result proved that containing the Fe within a perovskite structure is highly effective in preventing the loss of Fe from the catalyst via chelation with catechol during the phenol oxidation reaction. Additionally, only very low concentrations of Pd were leached under flowing catechol. Small amounts of La leaching were observed, this could have been related to excess La_2O_3 impurities.

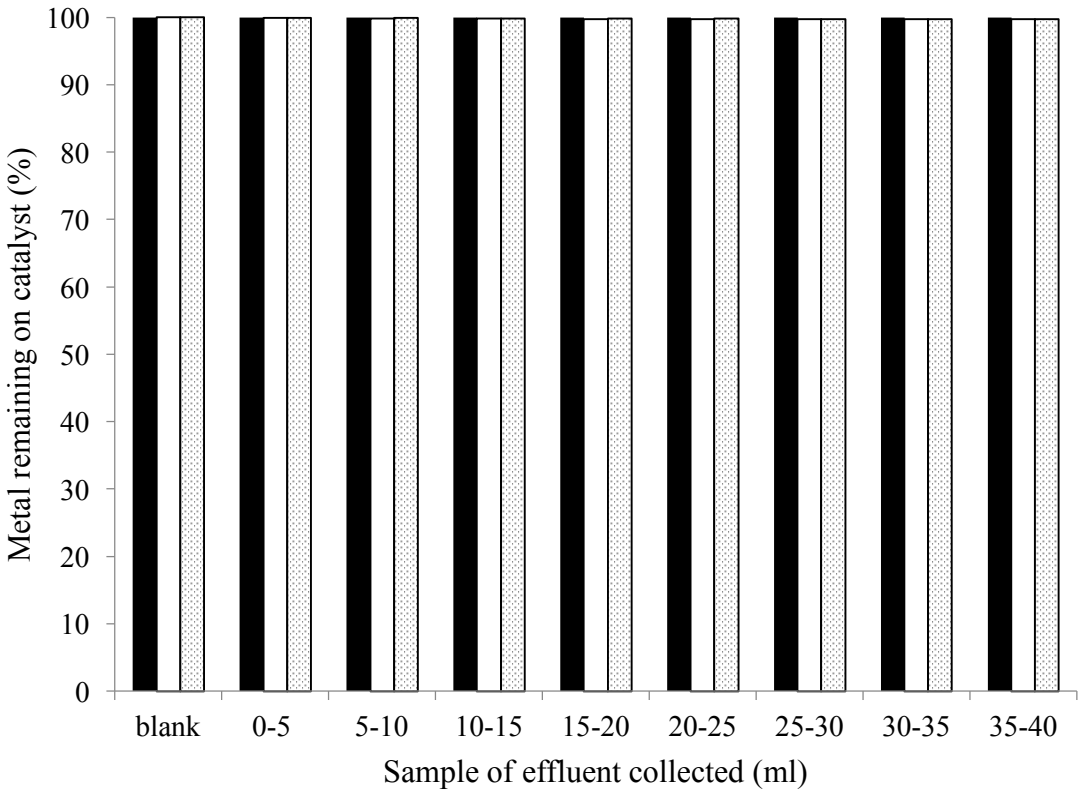

Figure 27: Effect of catechol on leaching of metals from the catalyst. Conditions: 1000 ppm catechol flowed over 50 mg of 2.5%Pd-$LaFeO_3$ and metal leaching analysed using MP-AES. Legend: filled = Fe remaining (%), unfilled = Pd remaining (%), dots = La remaining (%).

From Figure 27, it was observed that only an extremely small percentage of Fe, Pd and La were lost from the catalyst upon treatment with catechol. Therefore, the

catalyst was collected and tested for the phenol oxidation reaction to determine reusability.

Table 7: Re-usability of catalyst after treatment of catalyst with flowing catechol. Conditions: 8.5 g 1000 ppm phenol solution, 420 psi 5%H_2/CO_2, 160 psi 25%O_2/CO_2, 10 mg 2.5%Pd/$LaFeO_3$, 1200 rpm stirring, 30 °C, reactions performed in Parr stainless steel autoclave.

Catalyst	**Conversion (%)**	**Fe leaching (ppm)**
2.5%Pd-$LaFeO_3$ (before treatment)	43	0.42
2.5%Pd-$LaFeO_3$ (after treatment)	12	0.04

From the reusability testing, described in Table 7, it was observed that the phenol conversion achieved decreased from 43 % to 12 % after treatment with flowing catechol. This result was highly surprising as it was previously observed that little/no metal was lost during the treatment. It was considered that this large decrease in activity may be related to the poisoning of the catalyst surface by adsorbed catechol species. However, it remained clear that the Fe contained in $LaFeO_3$ is far more stable than the Fe supported on TiO_2.

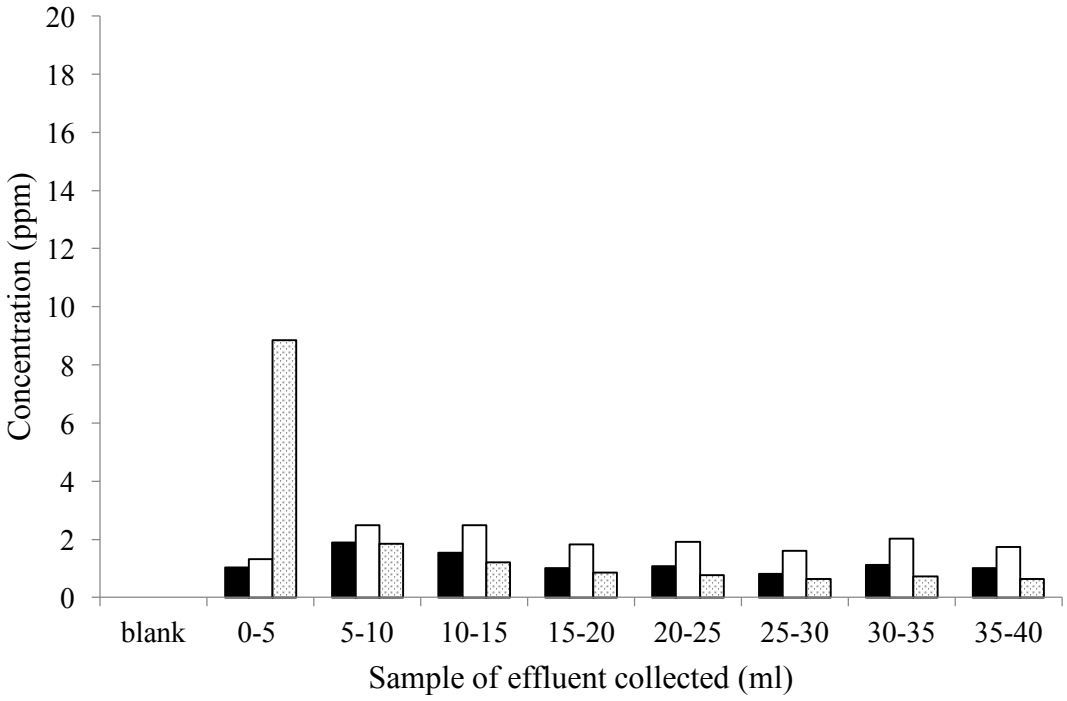

Figure 28: Effect of oxalic acid on metals leaching from the catalyst. Conditions: 1000 ppm oxalic acid flowed over 50 mg of 2.5%Pd-$LaFeO_3$ and metal leaching analysed using MP-AES. Legend: filled = Fe concentration (ppm), unfilled = Pd concentration (ppm), dots = La concentration (ppm).

To further investigate the effect of catechol upon the leaching of metal from 2.5%Pd/$LaFeO_3$, an experiment was performed whereby a solution of oxalic acid was flowed over the catalyst. The effluent was collected in aliquots of 5 ml and the Fe, Pd and La concentrations were measured using MP-AES as shown in Figure 28. Under flowing oxalic acid, Fe leaching was observed to occur. However, the concentrations of Fe leached for 2.5%Pd/Fe_2O_3 were still far lower than those observed for 2.5%Pd-2.5%Fe/TiO_2. Therefore, the use of $LaFeO_3$ represents a substantial enhancement to Fe stability against catechol and oxalic acid reaction products.

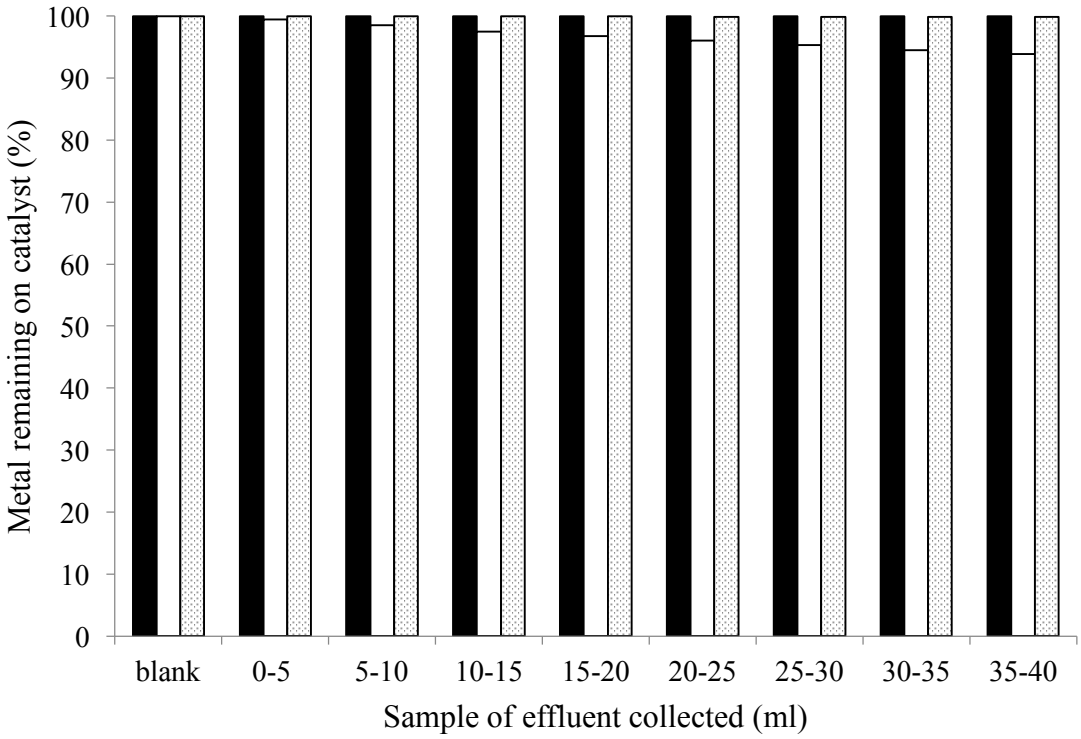

Figure 29: Effect of oxalic acid on metals leaching from the catalyst. Conditions: 1000 ppm oxalic acid flowed over 50 mg of 2.5%Pd-$LaFeO_3$ and metal leaching analysed using MP-AES. Legend: filled = Fe remaining (%), unfilled = Pd remaining (%), dots = La remaining (%).

When the percentage loss of total metal from the catalyst was considered, as shown in Figure 29, it was observed that extremely low percentages of Fe and La were lost from the catalyst. Around 4 % of the total Pd content was lost from the catalyst, similar to that observed for 2.5%Pd-2.5%Fe/TiO_2 which also used nitrate precursors during preparation. To determine the reusability of the catalyst after treatment with oxalic acid, the catalyst was collected and tested in the phenol oxidation reaction.

Table 8: Re-usability of catalyst after treatment of catalyst with flowing oxalic acid. Conditions: 8.5 g 1000 ppm phenol solution, 420 psi 5%H_2/CO_2, 160 psi 25%O_2/CO_2, 10 mg 2.5%Pd/$LaFeO_3$, 1200 rpm stirring, 30 °C, reactions performed in Parr stainless steel autoclave.

Catalyst	Conversion (%)	Fe leaching (ppm)
2.5%Pd-$LaFeO_3$ (before treatment)	43	0.42
2.5%Pd-$LaFeO_3$ (after treatment)	34	0.53

From the reusability testing, described in Table 8, the catalyst treated with oxalic acid was observed to achieve a phenol conversion of 34 % compared to the 43 % achieved by the fresh catalyst. This showed that the catalyst was capable of reuse after treatment with oxalic acid, with a minor decrease in activity. This contrasted with the catechol treated catalyst which demonstrated far less activity despite the lower loss of metal from the catalyst.

While $LaFeO_3$ was very stable towards oxalic acid and catechol intermediates, it was less effective in the phenol oxidation reaction than the supported Pd-Fe catalyst when phenol conversion was considered. One reason for this may have been due to the oxidation state of the Fe (Fe^{3+} in $LaFeO_3$). Therefore, further investigation was required to determine the most active oxidation state of Fe for the phenol oxidation reaction with *in situ* generated H_2O_2.

3.2.12 Identification of active forms of Fe

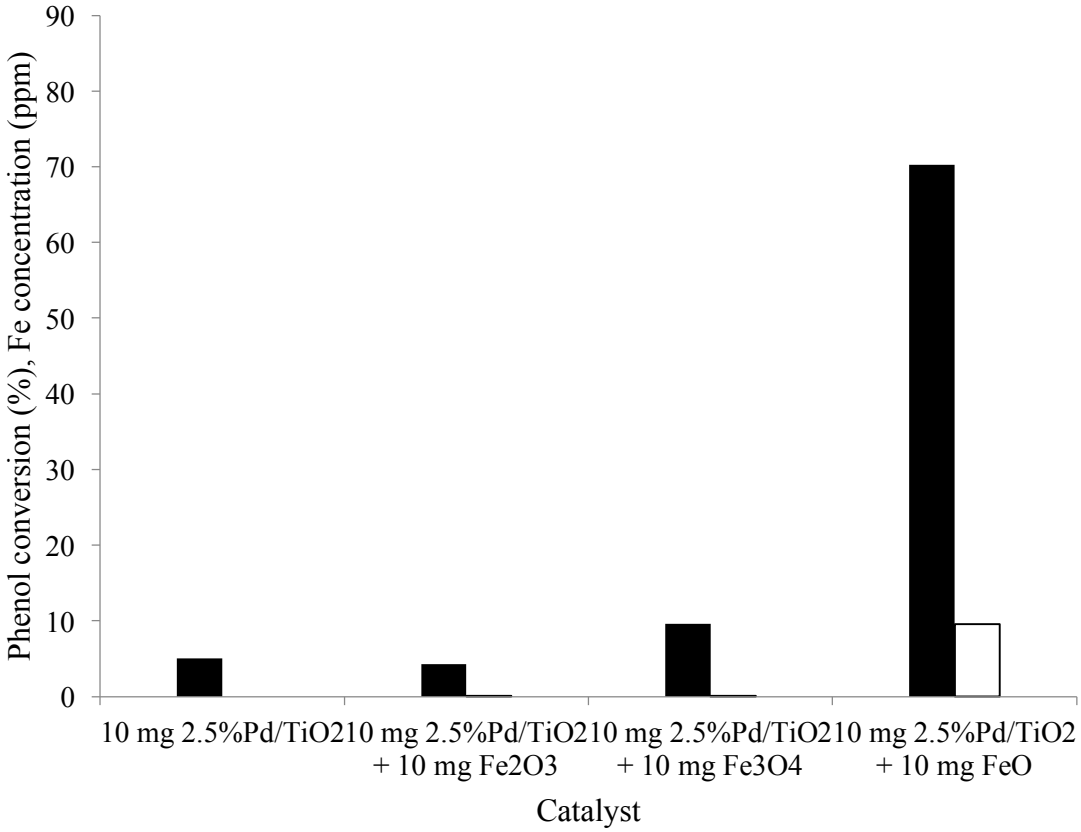

Figure 30: The effect on phenol conversion upon addition of various iron oxides. Conditions: 8.5 g 1000 ppm phenol solution, 420 psi 5%H_2/CO_2, 160 psi 25%O_2/CO_2, 2 h, 1200 rpm stirring, 30 °C, reactions performed in Parr stainless steel autoclave. Legend: filled = phenol conversion (%), unfilled = Fe concentration (ppm).

To determine the most active form of Fe for the phenol oxidation reaction with in situ generated H_2O_2, a variety of forms of Fe were tested for this reaction including Fe_2O_3, Fe_3O_4 and FeO. These were used alongside a monometallic Pd catalyst for the initial generation of H_2O_2. The results of these experiments were described in Figure 30. When a combination of Pd and Fe_2O_3 was utilised, a phenol conversion of 4.3 % was observed. The conversion achieved showed little difference to that achieved by the monometallic Pd catalyst alone. This result indicated that Fe_2O_3 was ineffective for

catalysing the phenol oxidation reaction with *in situ* generated H_2O_2. This could likely have been attributed to presence of Fe^{3+}. Therefore, Fe_3O_4 was tested, achieving a phenol conversion of 9.6 %. This moderate increase in conversion could be attributed to the presence of both Fe^{2+} and Fe^{3+} species. Interestingly, the utilisation of both forms of Fe resulted in only very low levels of Fe leaching. However, it is important to note that at these very low conversions, there will be only very low concentrations of the intermediates that we have previously established to contribute to the observed leaching. Due to the increase in phenol conversion achieved upon the introduction of Fe^{2+} into the reaction medium, FeO was also tested. Upon the introduction of FeO into the reaction medium, a phenol conversion of 70.3 % was achieved. This conversion was far greater than that observed when using either Fe_2O_3 and Fe_3O_4 and indicates that the presence of Fe^{2+} is essential to achieve high conversions of phenol using in situ generated H_2O_2. In addition to the higher conversions of phenol, the use of FeO resulted in far higher leaching of Fe into solution. However, this greater leaching of Fe is to be expected due to the increased presence of reaction intermediates which have been shown to cause this leaching. It is important to note that we cannot completely rule out some contribution to phenol conversion activity by some of these leached Fe species.

3.2.13 Effect of catalyst loading and support

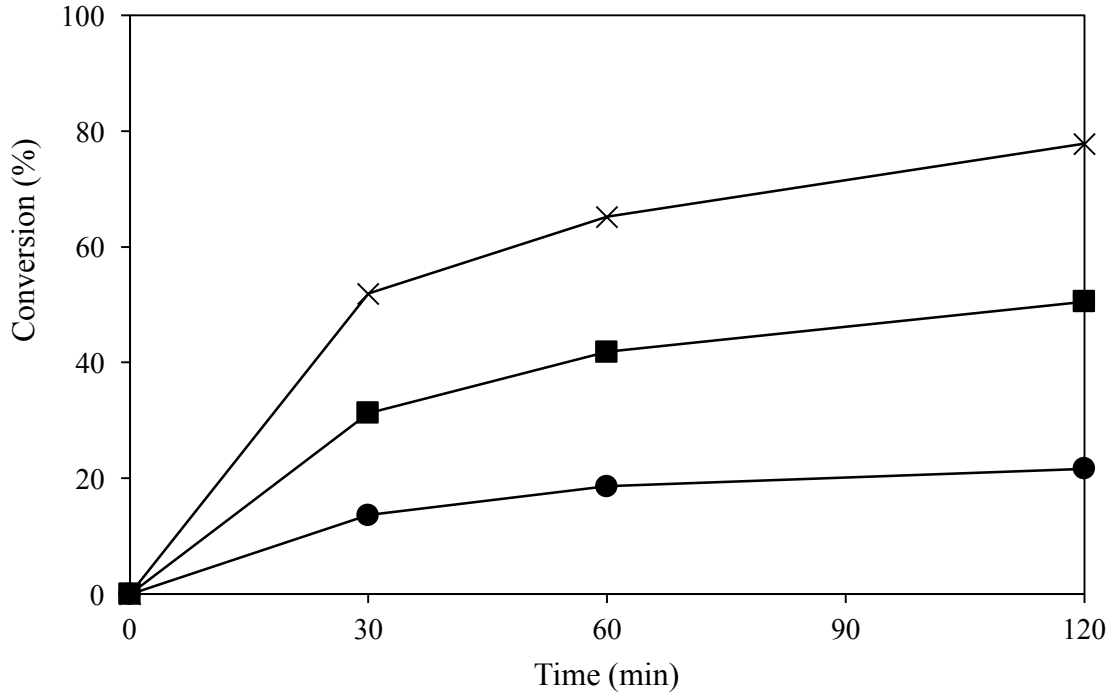

Figure 31: Effect of catalyst loading upon phenol conversion. Conditions: 8.5 g 1000 ppm phenol solution, 420 psi 5%H_2/CO_2, 160 psi 25%O_2/CO_2, X/TiO_2, 1200 rpm stirring, 30 °C, reactions performed in Parr stainless steel autoclave. Legend: crosses = 10 mg 2.5%Pd-2.5%Fe, circles = 10 mg 0.5%Pd-0.5%Fe, squares = 50 mg 0.5%Pd-0.5%Fe.

One method that was considered to help increase the phenol conversion obtained was to use lower loaded Pd-Fe catalysts while increasing the catalyst mass. It was considered that decreasing the catalyst loading could potentially result in greater dispersion of the metal over the catalyst surface and therefore lead to greater surface concentrations of active metal, thereby increasing catalyst activity. Therefore, a 0.5%Pd-0.5%Fe/TiO_2 catalyst was prepared. After 2 h reaction, as shown in Figure 31, the 0.5%Pd-0.5%Fe/TiO_2 catalyst achieved a phenol conversion of 21.7 % compared to 77.8 % for the 2.5%Pd-2.5%Fe/TiO_2 catalyst when using equal catalyst masses. This lower conversion was expected due to the 2.5%Pd-2.5%Fe/TiO_2 catalyst containing 5 times the concentration of active metal. However, to compare the catalysts with equal amounts of active metal, a test was performed using 50 mg 0.5%Pd-0.5%Fe/TiO_2 instead of 10 mg. When 50 mg of 0.5%Pd-0.5%Fe/TiO_2 was

used, a phenol conversion of 50.6 % was achieved after 2 h. This conversion was still lower than the 77.8 % phenol conversion obtained when using 10 mg of 2.5%Pd-2.5%Fe/TiO_2. This result was unexpected as it was thought that the lower loaded catalyst would lead to greater metal dispersion and higher activity. However, this lower activity could be related to mass transfer limitations.

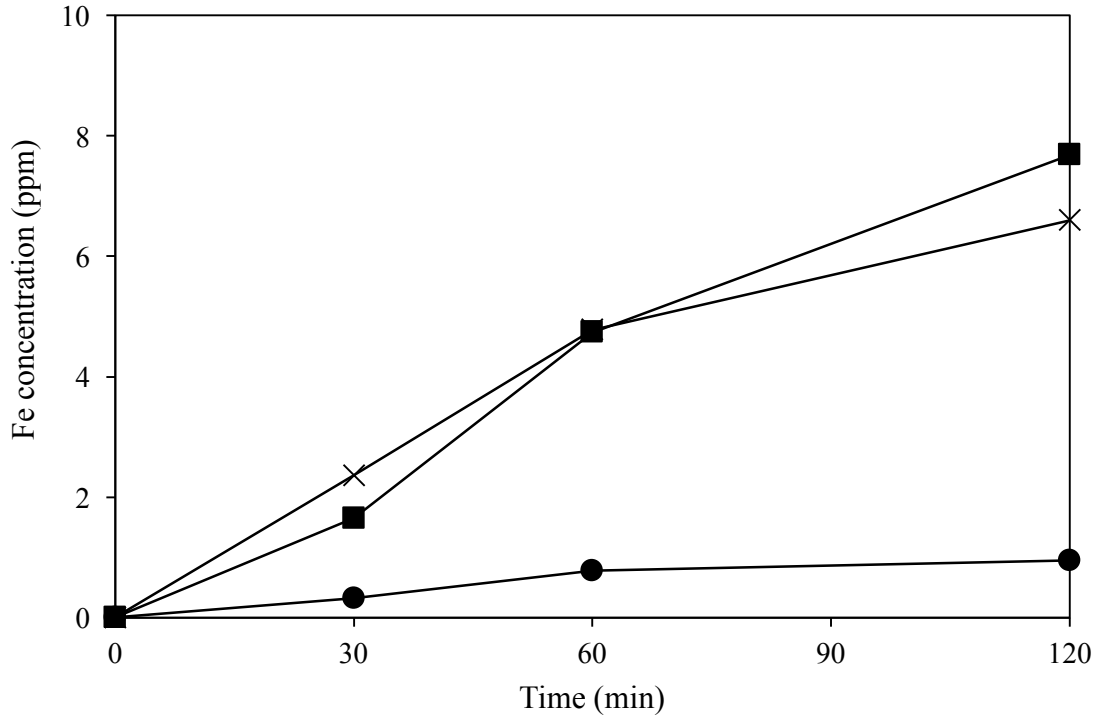

Figure 32: Fe leaching detected using MP-AES. Conditions: 8.5 g 1000 ppm phenol solution, 420 psi 5%H_2/CO_2, 160 psi 25%O_2/CO_2, X/TiO_2, 1200 rpm stirring, 30 °C, reactions performed in Parr stainless steel autoclave. Legend: crosses = 10 mg 2.5%Pd-2.5%Fe, circles = 10 mg 0.5%Pd-0.5%Fe, squares = 50 mg 0.5%Pd-0.5%Fe

When the leaching of metal during reaction was considered, as shown in Figure 32, it was observed that 10 mg 2.5%Pd-2.5%Fe/TiO_2 and 50 mg 0.5%Pd-0.5%Fe/TiO_2 leached very similar concentrations of Fe. This result ruled out that the discrepancy in activity when using 50 mg 0.5%Pd-0.5%Fe/TiO_2 could be due to lower levels of Fe species in solution assisting in the catalysis. An additional method that can be employed to increase the dispersion of metals over the support could be to use alternative supports with higher surface areas.

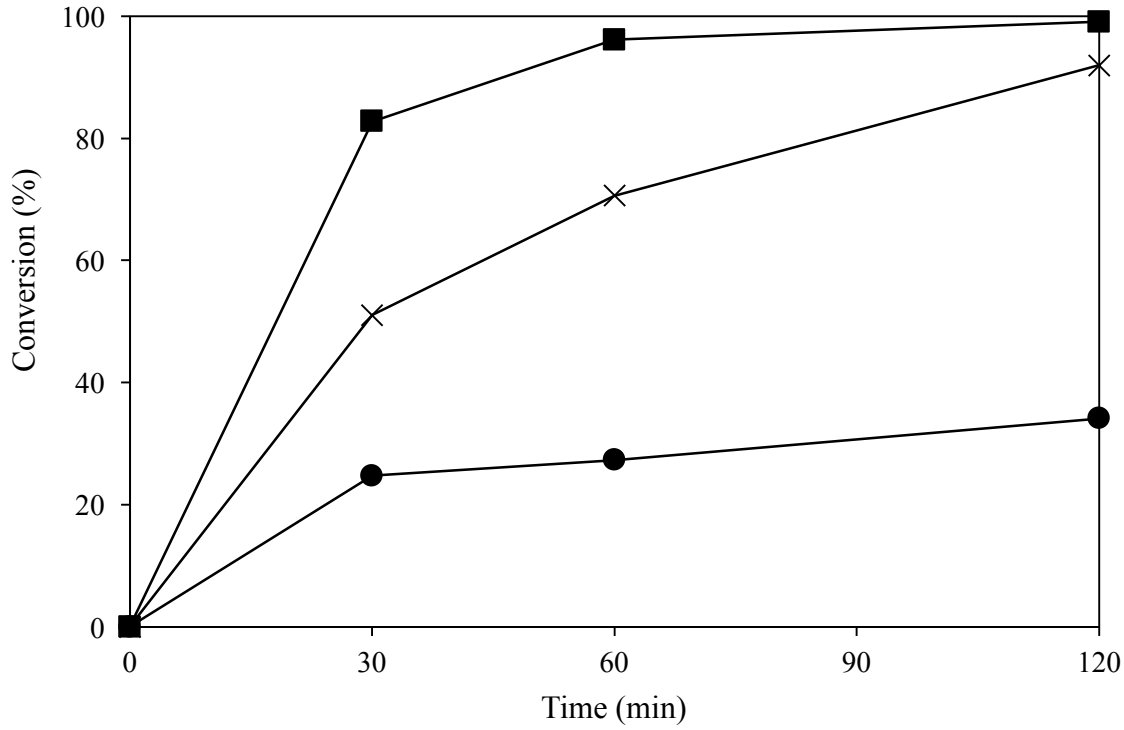

Figure 33: Effect of catalyst loading upon phenol conversion. Conditions: 8.5 g 1000 ppm phenol solution, 420 psi 5%H_2/CO_2, 160 psi 25%O_2/CO_2, X/SiO_2, 1200 rpm stirring, 30 °C, reactions performed in Parr stainless steel autoclave. Legend: crosses = 10 mg 2.5%Pd-2.5%Fe, circles = 10 mg 0.5%Pd-0.5%Fe, squares = 50 mg 0.5%Pd-0.5%Fe

To investigate the effect of using a support with a higher surface area, a 2.5%Pd-2.5%Fe/SiO_2 catalyst was prepared. The TiO_2 (P25, Degussa) used previously is reported to have a surface area of 35-65 m^2/g compared to the SiO_2 (60 A, 35-70 micron, Fisher Scientific) which is advertised to have a surface area of around 500 m^2/g. The 2.5%Pd-2.5%Fe/SiO_2 catalyst was tested for the oxidation of phenol with *in situ* generated H_2O_2, achieving a phenol conversion of 91.9 % after 2 h, as shown in Figure 33. This conversion was far higher than the 77.8 % achieved when using 2.5%Pd-2.5%Fe/TiO_2 and demonstrated the benefit of using supports with higher surface areas. Additionally, a 0.5%Pd-0.5%Fe/SiO_2 catalyst was prepared. Interestingly, when 50 mg 0.5%Pd-0.5%Fe/SiO_2 was tested it achieved a phenol conversion of 99.1 % compared to 91.9% when using 10 mg 2.5%Pd-2.5%Fe/SiO_2. Also, the initial rate of reaction was far higher when using 50 mg 0.5%Pd-

0.5%Fe/SiO_2. This demonstrated the positive effect of dispersing the same amount of active metal over a greater amount of support material, an effect that was not observed when using the TiO_2 support.

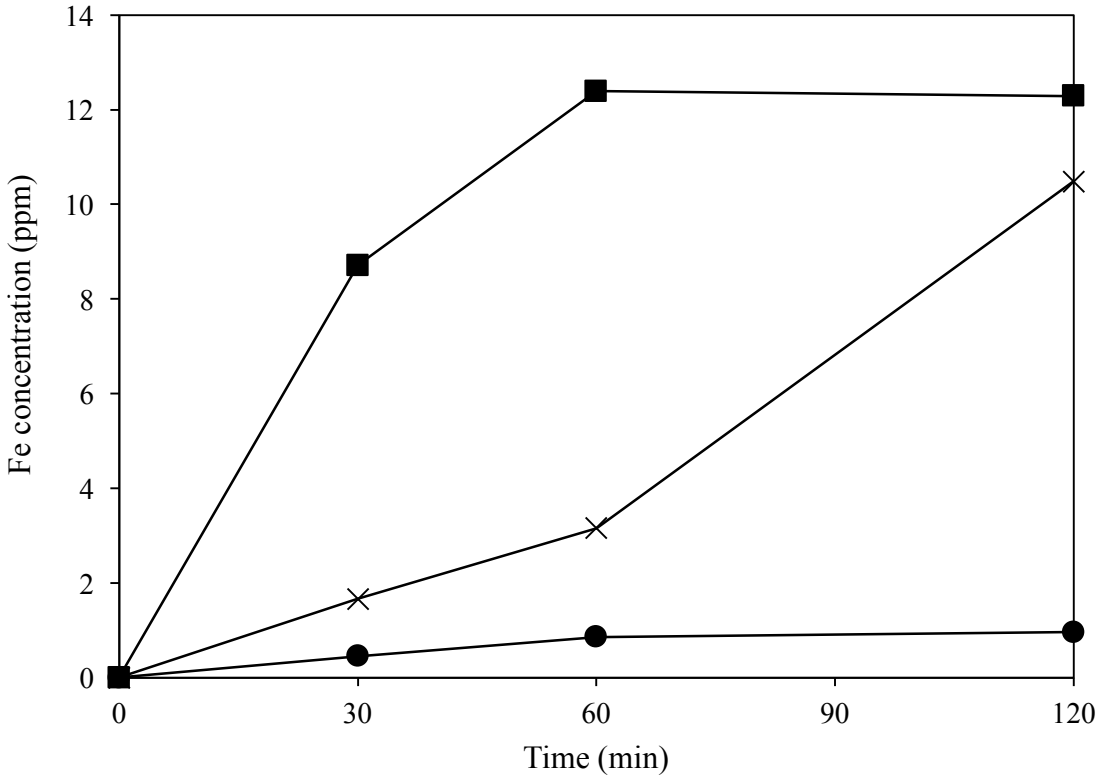

Figure 34: Fe leaching detected using MP-AES. Conditions: 8.5 g 1000 ppm phenol solution, 420 psi 5%H_2/CO_2, 160 psi 25%O_2/CO_2, X/SiO_2, 1200 rpm stirring, 30 °C, reactions performed in Parr stainless steel autoclave. Legend: crosses = 10 mg 2.5%Pd-2.5%Fe, circles = 10 mg 0.5%Pd-0.5%Fe, squares = 50 mg 0.5%Pd-0.5%Fe

The Fe concentrations in the post-reaction effluent was also considered, as shown in Figure 34. When 10 mg 2.5%Pd-2.5%Fe/SiO_2 was used, 10.48 ppm Fe was detected after 2 h. When 50 mg 0.5%Pd-0.5%Fe/SiO_2 was used, 12.29 ppm Fe was detected after 2 h. This difference can likely be attributed to the increased conversion achieved when using 50 mg 0.5%Pd-0.5%Fe/SiO_2. It is important to note that the Fe leaching was also greater for the SiO_2 supported catalysts compared to the TiO_2 supported catalysts. However, this is to be expected due to the greater conversions of phenol achieved, resulting in higher occurrence of the leaching-causing intermediates.

3.2.14 Activity and leaching of 0.5%Pd-0.5%Fe/SiO_2 over time

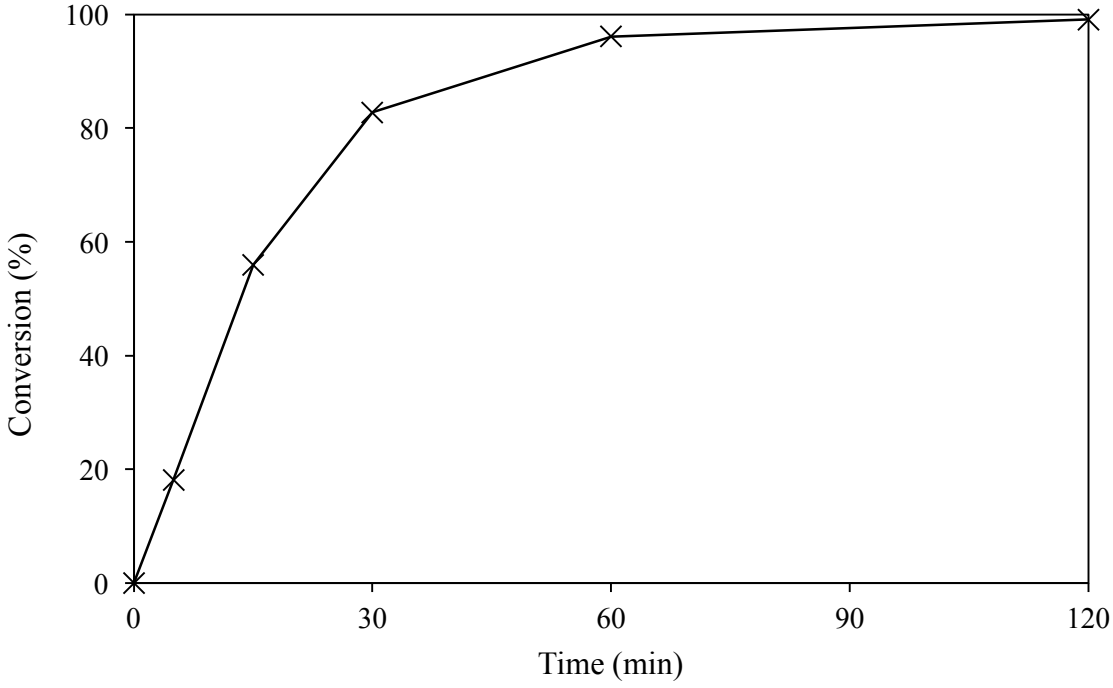

Figure 35: Time on line profile of phenol conversion. Conditions: 8.5 g 1000 ppm phenol solution, 420 psi 5%H_2/CO_2, 160 psi 25%O_2/CO_2, 50 mg 0.5%Pd-0.5%Fe/SiO_2, 1200 rpm stirring, 30 °C, reactions performed in Parr stainless steel autoclave.

The use of the 0.5%Pd-0.5%Fe/SiO_2 catalyst resulted in near total conversion of the phenol with *in situ* generated H_2O_2 after 2 h. This represented a large increase in catalyst activity as previous catalyst were incapable of achieving over 80 % phenol conversion over the same timescale. When using 0.5%Pd-0.5%Fe/SiO_2 it was also noted that the initial rate of phenol conversion was very high. Therefore, a series of experiments of even shorter duration were performed, as described in Figure 35. After only 5 minutes of reaction it was observed that 18.2 % of the phenol was converted. After 15 minutes of reaction it was observed that 56.0 % of the phenol was converted. Therefore, these results demonstrated that the catalyst can achieve high levels of phenol conversion over short timescales.

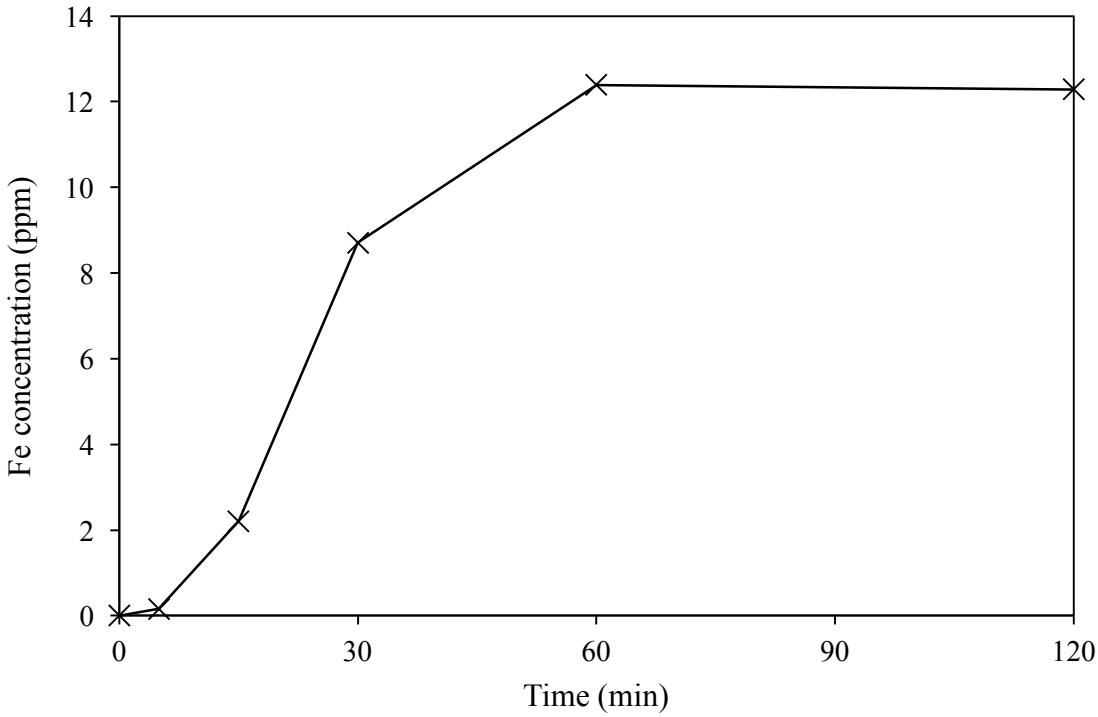

Figure 36: Fe leaching detected using MP-AES. Conditions: 8.5 g 1000 ppm phenol solution, 420 psi 5%H_2/CO_2, 160 psi 25%O_2/CO_2, 50 mg 0.5%Pd-0.5%Fe/SiO_2, 1200 rpm stirring, 30 °C, reactions performed in Parr stainless steel autoclave.

Over these timescales, the occurrence of Fe leaching was also monitored using MP-AES, as described in Figure 36. After 5 minutes and 15 minutes of reaction, Fe concentrations of 0.16 ppm and 2.21 ppm were detected respectively. These represented relatively low concentrations of Fe in solution. It was noted that at these times, the rate of phenol conversion was at its highest. Therefore, it seems unlikely that the leached Fe species are playing a large role in the achievement of high conversions of phenol. Indeed, when the concentration of Fe species in solution was highest, the lowest rates of phenol conversion were observed. However, at these timescales there was less phenol available to react, which may have resulted in the reduced rate. Additionally, the reaction between the reactive oxygen species generated and the intermediates created during the phenol oxidation may have also caused the reduced rate of phenol conversion.

3.2.15 Effect of varying phenol concentration

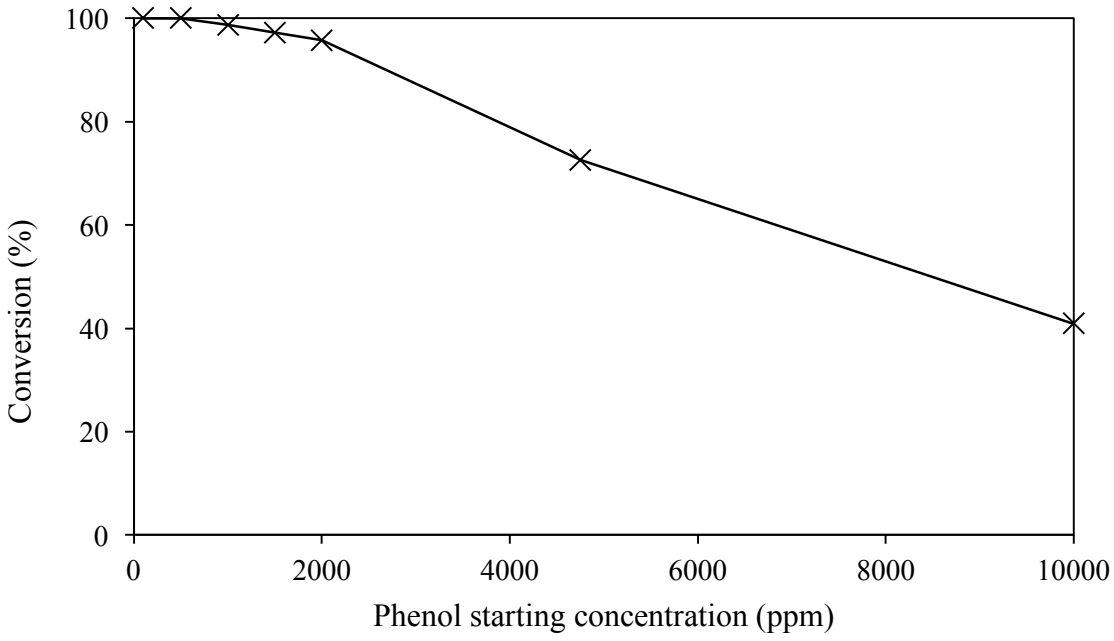

Figure 37: Effect on phenol conversion when varying the initial concentration of phenol. Conditions: 8.5 g phenol solution, 420 psi 5%H_2/CO_2, 160 psi 25%O_2/CO_2, 50 mg 0.5%Pd-0.5%Fe/SiO_2, 1200 rpm stirring, 30 °C, 2 h, reactions performed in Parr stainless steel autoclave.

Due to the near complete removal of 1000 ppm phenol from the reaction medium after 2 h. A series of experiments were performed with increasingly higher concentrations of phenol. It was considered that with higher starting concentrations of phenol, even greater amounts of phenol could be converted within the 2 h timescale. The results of these experiments are described in Figure 37. From these results, it was observed that even when starting with 2000 ppm phenol, 95.8 % conversion could be achieved. When 10000 ppm phenol was used, 40.9 % phenol conversion was achieved. While this conversion appeared lower, it represented the conversion of over 4 times the amount of phenol converted when compared to using a starting concentration of 1000 ppm phenol. The reason for this improved conversion of phenol is likely due to the increased chance of contact between reactive oxygen species formed at the catalyst support and the phenol in solution.

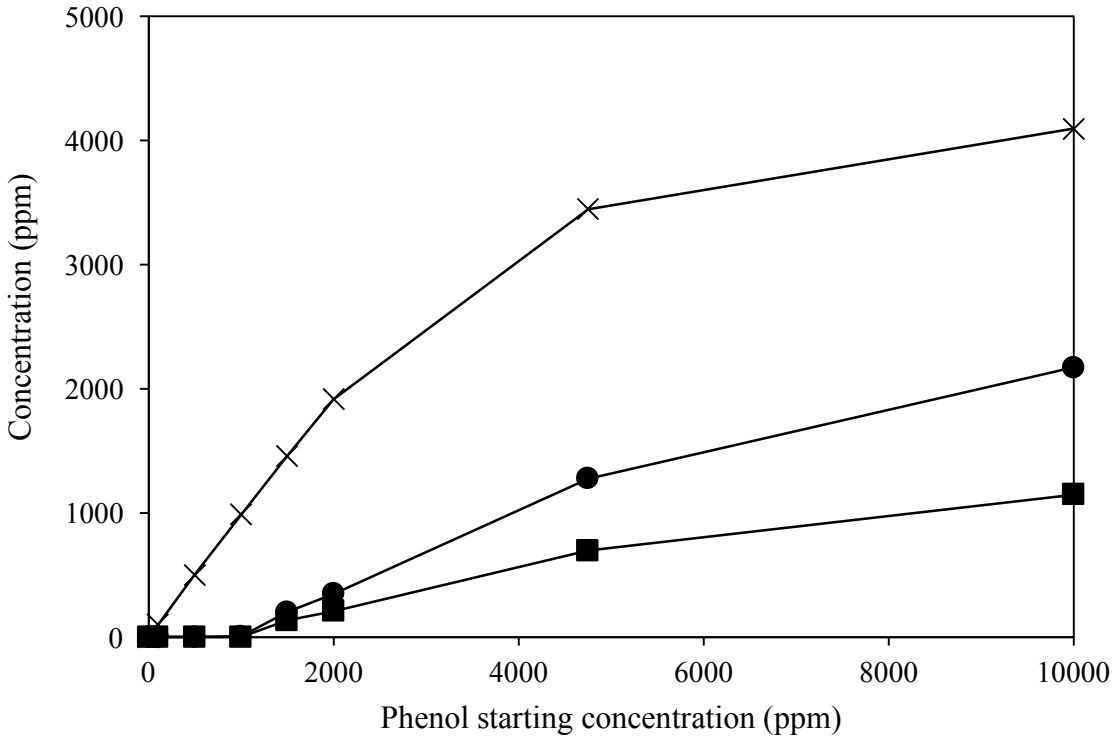

Figure 38: Conversion of phenol and evolution of intermediates when varying the initial concentration of phenol. Conditions: 8.5 g phenol solution, 420 psi 5%H_2/CO_2, 160 psi 25%O_2/CO_2, 50 mg 0.5%Pd-0.5%Fe/SiO_2, 1200 rpm stirring, 30 °C, reactions performed in Parr stainless steel autoclave. Legend: crosses = phenol concentration (ppm), circles = catechol concentration (ppm), squares = hydroquinone concentration (ppm).

The evolution of the initial aromatic intermediates (catechol and hydroquinone) during these reactions was also considered, as described in Figure 38. From this data it was clearly observed that extremely low levels of aromatic intermediates were observed when starting with phenol concentrations up to and including 1000 ppm. This indicated a large amount of further oxidation of phenol to subsequent short chain acid intermediates and potentially CO_2. However, when the phenol starting concentration was increased past 1000 ppm, increasingly higher amounts of initial aromatic intermediates were observed. This indicated that while increasing amounts of phenol were converted, there was less further oxidation past that point. When a phenol starting concentration of 10000 ppm was used, there was a very large amount of catechol and hydroquinone observed, indicating little/no further oxidation

occurring. Therefore, when using higher initial concentrations of phenol, while more phenol is ultimately converted, there was far less further oxidation occurring. This was likely caused by the reactive oxygen species formed reacting with the excess phenol instead of the initial aromatic intermediates.

3.2.16 Effect of leachate on phenol conversion

Due to the leaching of Fe species during reaction, it was important to gain further insight into the role played by these leached species upon the observed catalysis. To gain this greater understanding, a series of 'hot filtration' experiments were performed. To conduct these experiments, a reaction was run for 2 h to almost complete phenol conversion in the presence of 0.5%Pd-0.5%Fe/SiO_2. After this, the reaction effluent was filtered to remove the solid catalyst and spiked with additional phenol to provide a solution containing 1000 ppm phenol and the 'leachate' from the previous reaction.

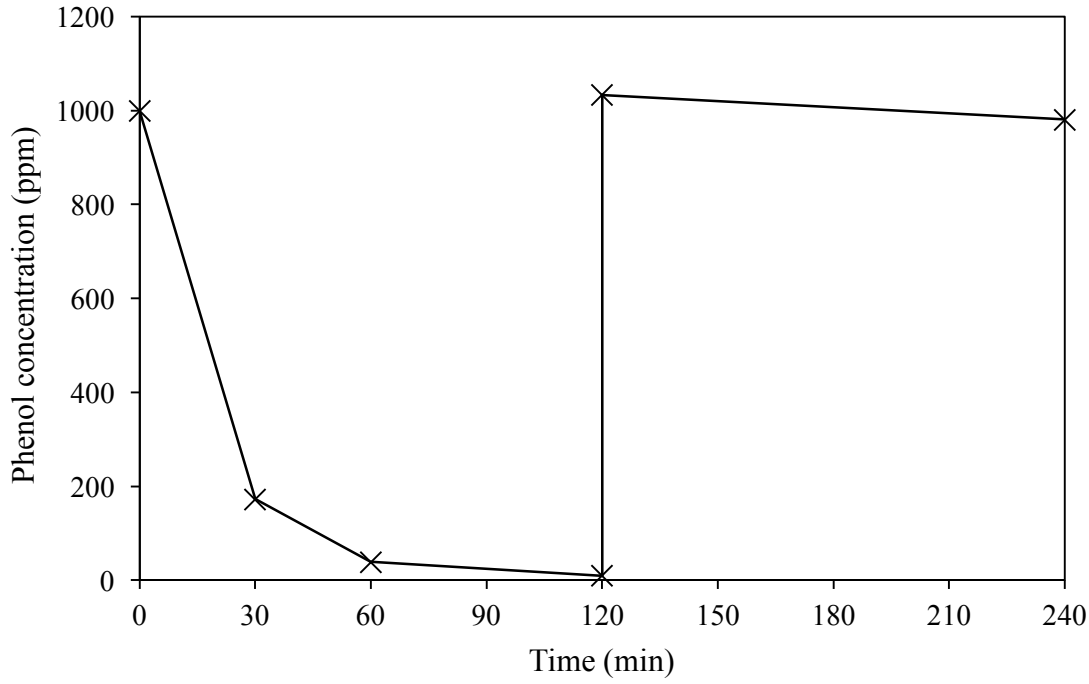

Figure 39: Experiment 1. Conditions for initial 2h: 8.5 g 1000 ppm phenol solution, 420 psi 5%H_2/CO_2, 160 psi 25%O_2/CO_2, 50 mg 0.5%Pd-0.5%Fe/SiO_2, 1200 rpm

stirring, 30 °C. After 2h catalyst was filtered and the reaction solution collected and spiked with more phenol to achieve a concentration of 1000 ppm. After 2h, the following conditions were employed: 8.5 g 1000 ppm phenol in leachate solution, 420 psi 5%H_2/CO_2, 160 psi 25%O_2/CO_2, 1200 rpm stirring, 30 °C, reactions performed in Parr stainless steel autoclave.

For the initial 'hot filtration' experiment, as described in Figure 39, this solution containing 1000 ppm and 'leachate' was reacted for a further 2 h in the presence of H_2 and O_2 but the absence of a heterogeneous catalyst. After this reaction was performed, very little phenol conversion was observed. This reaction demonstrated that in the absence of a heterogeneous catalyst, very little phenol conversion could be obtained. This result was unsurprising as we have previously shown that no Pd was present in the reaction medium. We have previously shown that the presence of Pd is essential for the *in situ* generation of H_2O_2. Therefore, further experiments were required to determine the effect of the leachate upon the reaction.

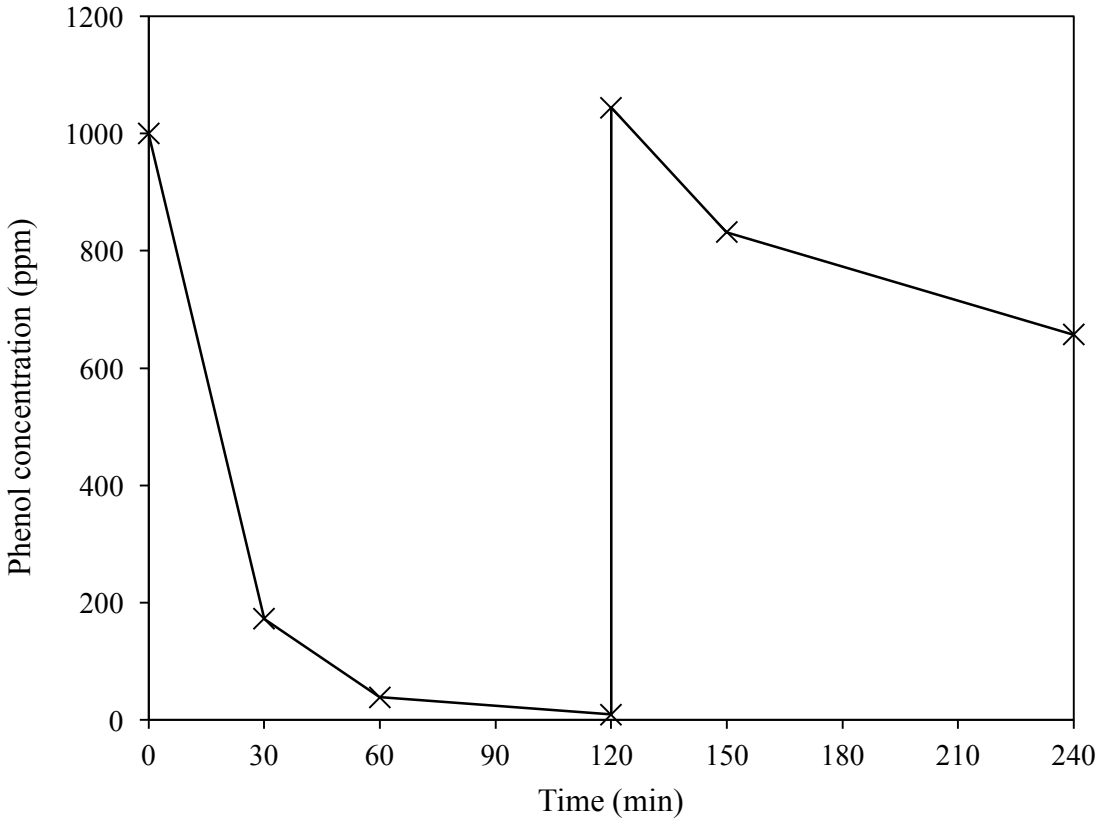

Figure 40: Experiment 2. Conditions for initial 2h: 8.5 g 1000 ppm phenol solution, 420 psi 5%H_2/CO_2, 160 psi 25%O_2/CO_2, 50 mg 0.5%Pd-0.5%Fe/SiO_2, 1200 rpm stirring, 30 °C. After 2h catalyst was filtered and the reaction solution collected and spiked with more phenol to achieve a concentration of 1000 ppm. After 2h, the following conditions were employed: 8.5 g 1000 ppm phenol in leachate solution, 420 psi 5%H_2/CO_2, 160 psi 25%O_2/CO_2, 50 mg 0.5%Pd/SiO_2, 1200 rpm stirring, 30 °C, reactions performed in Parr stainless steel autoclave.

For the next 'hot filtration' experiment, as described in Figure 40, the solution containing 1000 ppm and 'leachate' was reacted for a further 2 h in the presence of H_2 and O_2 alongside a monometallic 0.5%Pd/SiO_2 catalyst. With the combination of 'leachate' alongside a Pd catalyst, a phenol conversion of 33 % was observed. This result indicated that the leached Fe species alongside a Pd catalyst for H_2O_2 generation can catalyse the oxidation of phenol. However, the rate of phenol conversion observed was significantly lower than when the heterogeneous 0.5%Pd-0.5%Fe/SiO_2 catalyst was utilised. Although, this test did confirm that the presence of leached Fe in solution could have been assisting in the catalyst activity observed. To confirm that the effect

on phenol conversion from the monometallic catalyst alone, an additional experiment was performed using 0.5%Pd/SiO_2 in the absence of 'leachate', this resulted in an observed phenol conversion of 5 %. This confirmed that most of the catalyst activity could be attributed to a combination of heterogeneous Pd and leached Fe in this case.

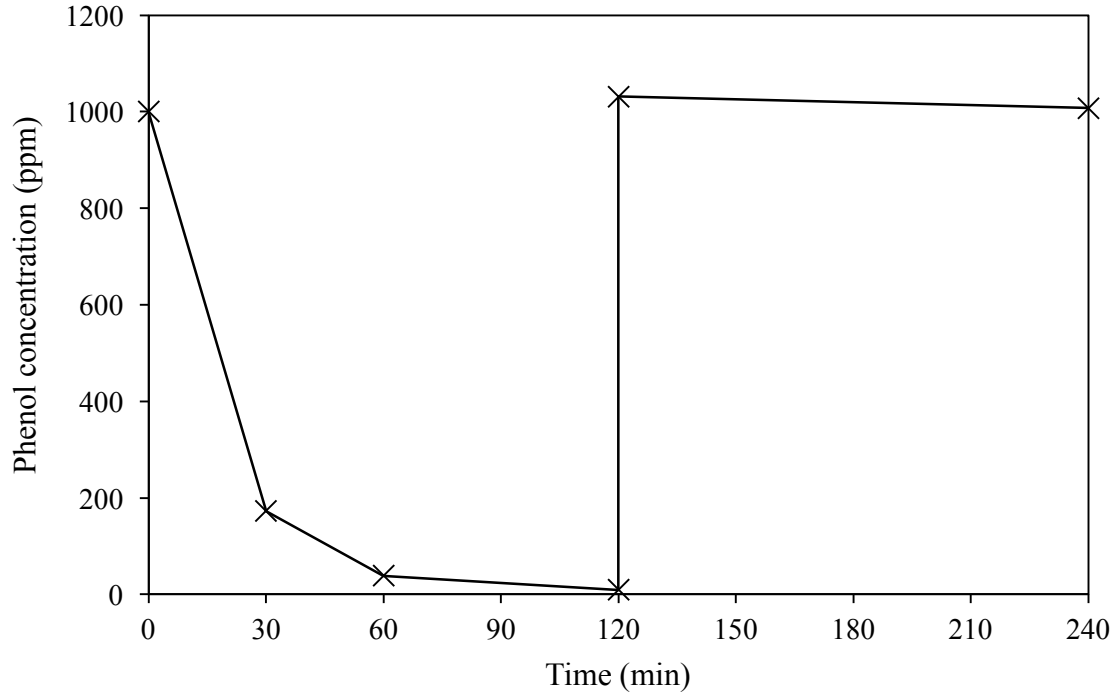

Figure 41: Experiment 4. Conditions for initial 2h: 8.5 g 1000 ppm phenol solution, 420 psi 5%H_2/CO_2, 160 psi 25%O_2/CO_2, 50 mg 0.5%Pd-0.5%Fe/SiO_2, 1200 rpm stirring, 30 °C. After 2h catalyst was filtered and the reaction solution collected and spiked with more phenol to achieve a concentration of 1000 ppm. After 2h, the following conditions were employed: 8.5 g 1000 ppm phenol in leachate solution, 0.5 wt.% H_2O_2, 580 psi 25%O_2/CO_2, 1200 rpm stirring, 30 °C, reactions performed in Parr stainless steel autoclave.

Due to the catalyst activity observed when using a combination of Pd alongside the 'leachate', it was considered whether it would be possible to achieve phenol conversion when using the leachate alongside bulk addition of 'pre-formed' commercially-available H_2O_2. Therefore, an experiment was performed using a combination of 'leachate' alongside bulk addition of 0.5 wt.% H_2O_2. Additionally, the

reactor was charged with 25%O_2/CO_2 to maintain the presence of carbonic acid in solution. After reaction, as described in Figure 41, a phenol conversion of 2 % was observed. It was determined that the leached Fe species was incapable of catalysing the phenol oxidation reaction alongside bulk addition of H_2O_2. It appeared that the presence of a heterogeneous Pd catalyst was required to observe any reasonable activity. One potential cause for the lack of activity observed was the absence of a reducing atmosphere due to the lack of H_2 in this system. Therefore, an additional experiment was performed whereby the 25%O_2/CO_2 mixture was replaced by a 5%H_2/CO_2 mixture, as described in Figure 41.

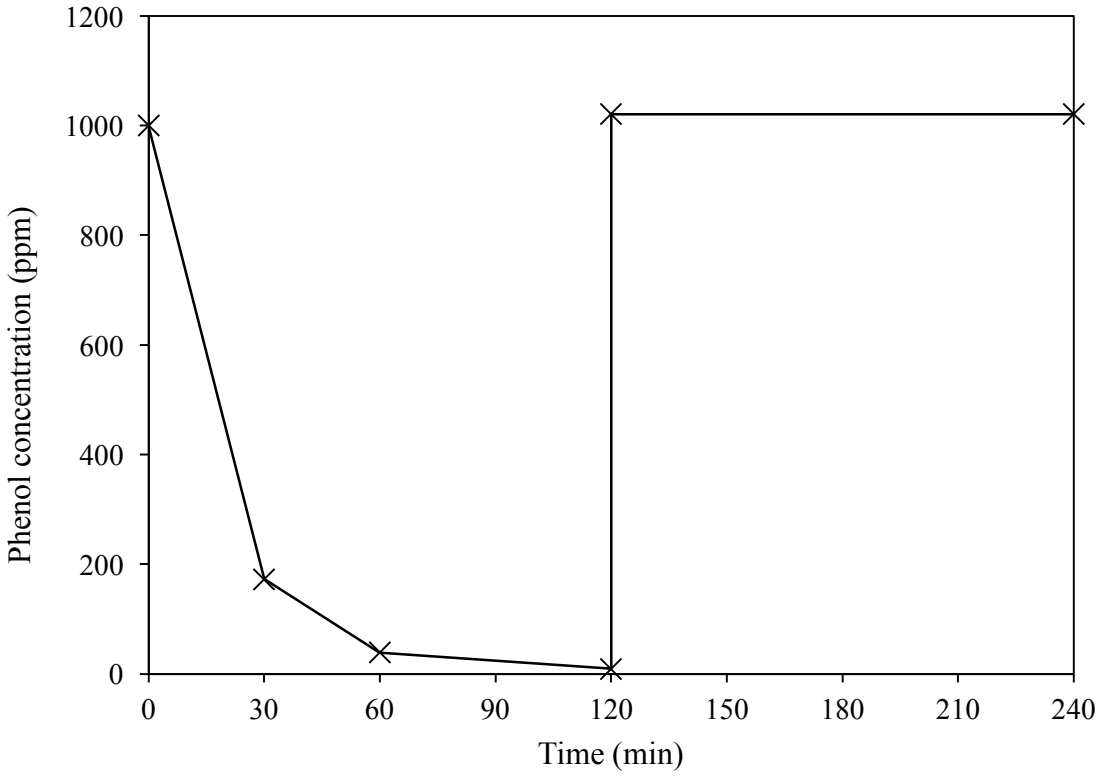

Figure 42: Experiment 5. Conditions for initial 2h: 8.5 g 1000 ppm phenol solution, 420 psi 5%H_2/CO_2, 160 psi 25%O_2/CO_2, 50 mg 0.5%Pd-0.5%Fe/SiO_2, 1200 rpm stirring, 30 °C. After 2h catalyst was filtered and the reaction solution collected and spiked with more phenol to achieve a concentration of 1000 ppm. After 2h, the following conditions were employed: 8.5 g 1000 ppm phenol in leachate solution, 0.5 wt.% H_2O_2, 420 psi 5%H_2/CO_2, 1200 rpm stirring, 30 °C, reactions performed in Parr stainless steel autoclave.

However, when 25%O_2/CO_2 was replaced by 5%H_2/CO_2, 0 % phenol conversion was observed. Therefore, it was confirmed that the lack of activity was not due to the absence of a reducing atmosphere.

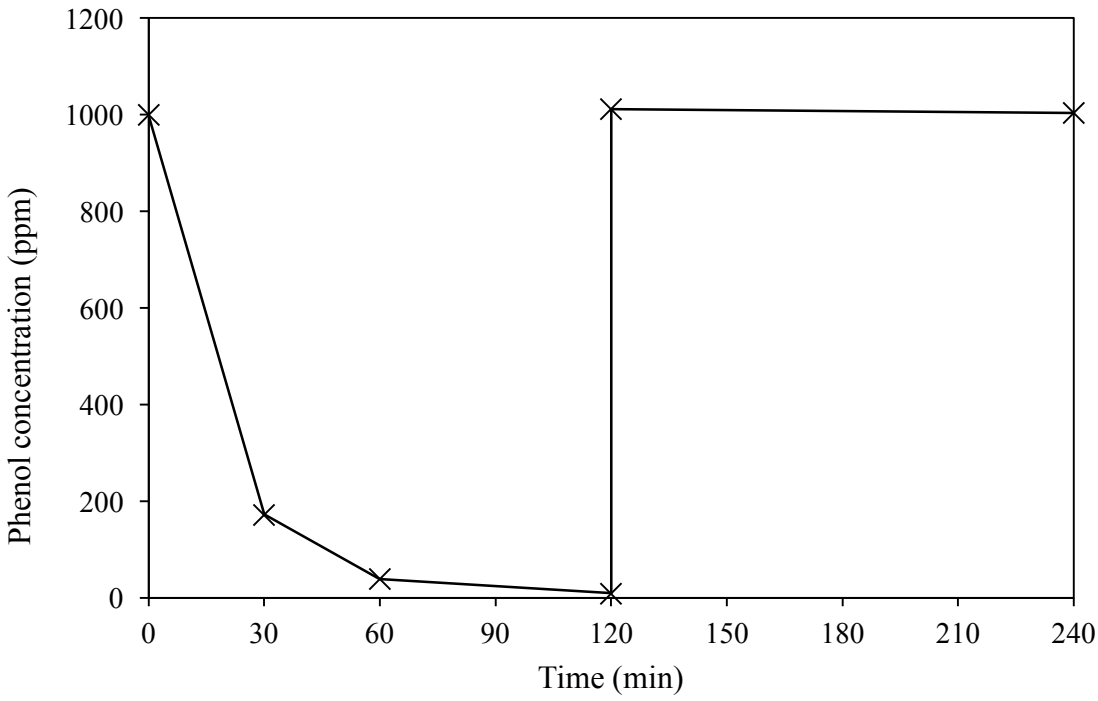

Figure 43: Experiment 6. Conditions for initial 2h: 8.5 g 1000 ppm phenol solution, 420 psi 5%H_2/CO_2, 160 psi 25%O_2/CO_2, 50 mg 0.5%Pd-0.5%Fe/SiO_2, 1200 rpm stirring, 30 °C. After 2h catalyst was filtered and the reaction solution collected and spiked with more phenol to achieve a concentration of 1000 ppm. After 2h, the following conditions were employed: 8.5 g 1000 ppm phenol in leachate solution, 0.5 wt.% H_2O_2, 580 psi 25%O_2/CO_2, 50 mg 0.5%Pd/SiO_2, 1200 rpm stirring, 30 °C, reactions performed in Parr stainless steel autoclave.

As it was previously established that the presence of Pd was required to achieve phenol conversion activity, it was considered whether a combination of Pd alongside bulk addition of H_2O_2 and 'leachate' would be effective. Therefore, a further experiment was performed using 0.5%Pd/SiO_2, 0.5 wt.% H_2O_2 and 'leachate'. The reactor was again charged with 25%O_2/CO_2 to maintain the presence of carbonic acid

in solution. The results are described in Figure 43, whereby a phenol conversion of 1 % was observed. To confirm whether the lack of activity was due to the absence of a reducing atmosphere, the experiment was re-run with the presence of 25%O_2/CO_2 replaced with 5%H_2/CO_2. The results of this experiment are described in Figure 43.

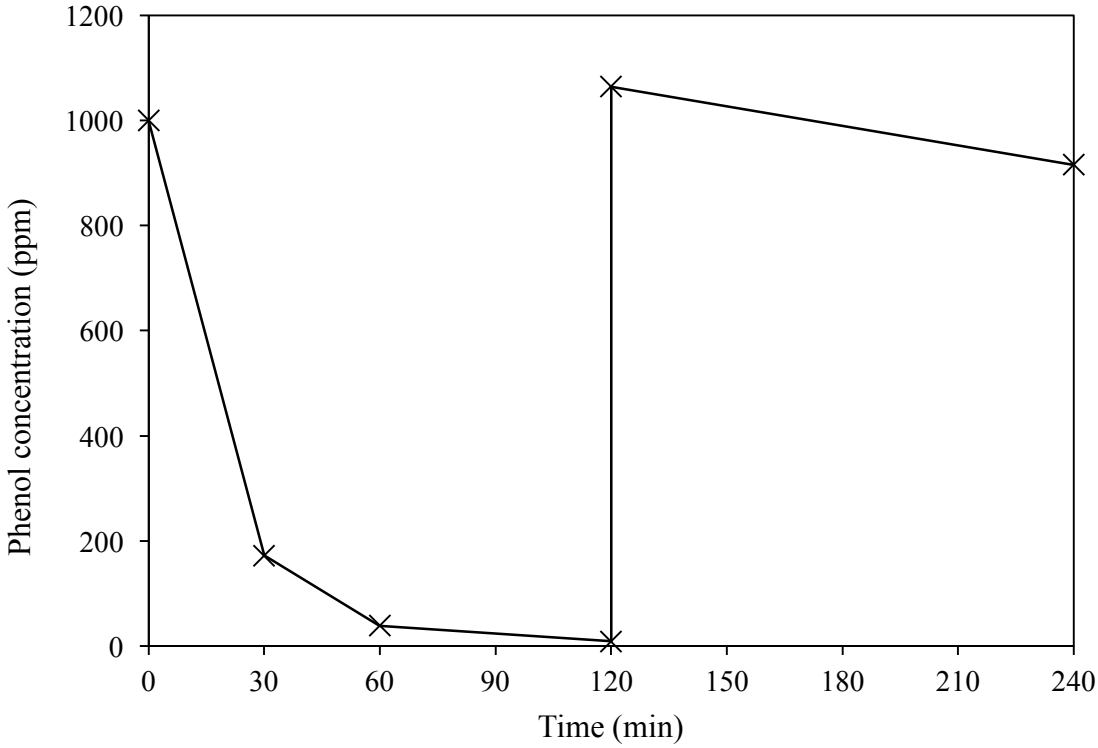

Figure 44: Experiment 7. Conditions for initial 2h: 8.5 g 1000 ppm phenol solution, 420 psi 5%H_2/CO_2, 160 psi 25%O_2/CO_2, 50 mg 2.5%Pd-2.5%Fe/SiO_2, 1200 rpm stirring, 30 °C. After 2h catalyst was filtered and the reaction solution collected and spiked with more phenol to achieve a concentration of 1000 ppm. After 2h, the following conditions were employed: 8.5 g 1000 ppm phenol in leachate solution, 0.5 wt.% H_2O_2, 420 psi 5%H_2/CO_2, 50 mg 0.5%Pd/SiO_2, 1200 rpm stirring, 30 °C, reactions performed in Parr stainless steel autoclave.

Interestingly, when 25%O_2/CO_2 was replaced with 5%H_2/CO_2, a phenol conversion of 15 % was observed. However, when this experiment was run in the absence of leachate and H_2O_2, a phenol conversion of 16 % was observed. This confirmed that the observed phenol conversion was likely due to a hydrogenation reaction catalysed

by the monometallic Pd catalyst. Hydrogenation of phenol by monometallic Pd catalysts under similar mild conditions has been previously reported in the literature.[14]

Table 9: The effect of Fe leachate upon the reaction

Expt.	Phenol	Pd	H_2	O_2	H_2O_2	Leachate	Conversion (%)
1	x		x	x		x	5
2	x	x	x	x		x	33
3	x	x	x	x			5
4	x			x	x	x	2
5	x		x		x	x	0
6	x	x		x	x	x	1
7	x	x	x		x	x	15
8	x	x	x				16

For ease of comparison, the previous results were collected and placed into a table, shown in Table 9. From these results, it appeared clear that the *in situ* generation of H_2O_2 was required to achieve any activity in the phenol oxidation reaction. From these results, it also appeared that the leachate can catalyse the reaction in the presence of a heterogeneous Pd containing catalyst. Although the catalyst activity was far less than when a fully heterogeneous Pd-Fe catalyst was employed for the reaction.

To determine whether part of this decreased activity could have been due to catalyst poisoning from residual intermediates from the initial part of the reaction to collect the 'leachate', a further experiment was performed whereby fresh 0.5%Pd-0.5%Fe was added to the leachate solution and the reaction run in the presence of H_2 and O_2. The results from this experiment are described in Figure 44.

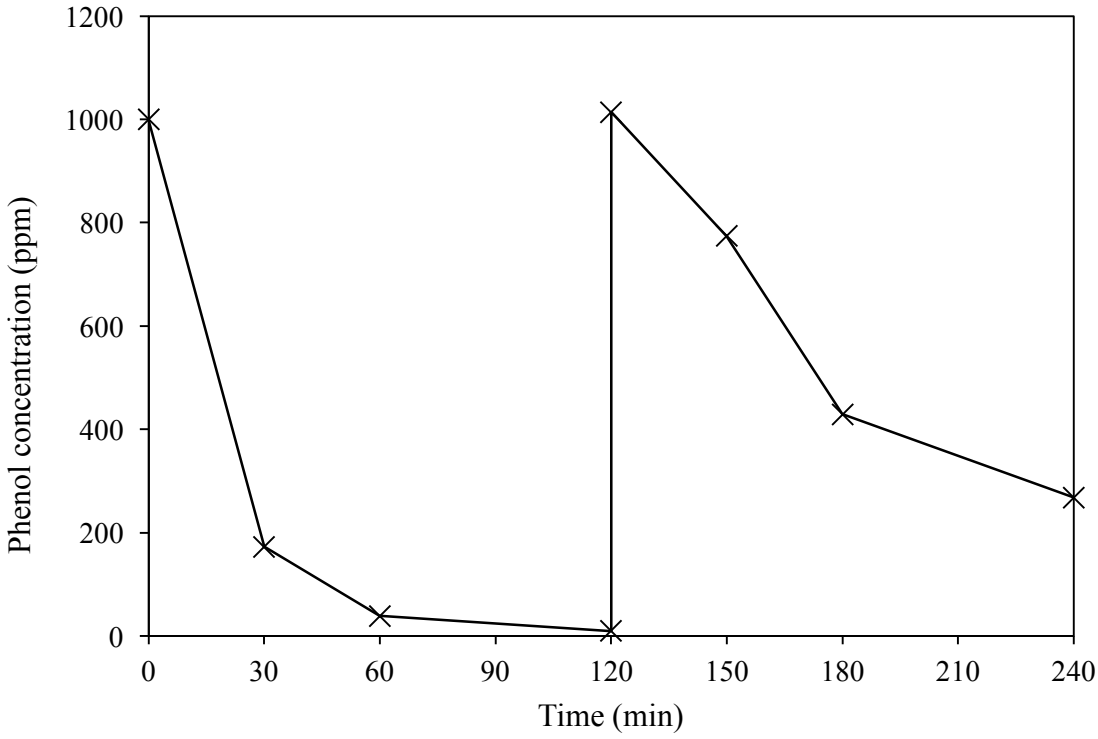

Figure 45: Effect of further addition of Pd-Fe catalyst. Conditions for initial 2h: 8.5 g 1000 ppm phenol solution, 420 psi 5%H_2/CO_2, 160 psi 25%O_2/CO_2, 50 mg 2.5%Pd-2.5%Fe/SiO_2, 1200 rpm stirring, 30 °C. After 2h catalyst was filtered and the reaction solution collected and spiked with more phenol to achieve a concentration of 1000 ppm. After 2h, the following conditions were employed: 8.5 g 1000 ppm phenol in leachate solution, 420 psi 5%H_2/CO_2, 160 psi 25%O_2/CO_2, 50 mg 2.5%Pd-2.5%Fe/SiO_2, 1200 rpm stirring, 30 °C, reactions performed in Parr stainless steel autoclave.

Upon addition of fresh 0.5%Pd-0.5%Fe/SiO_2, a further phenol conversion of 74 % was observed. This catalyst activity was less than that observed in the absence of the 'leachate solution. This result indicated that there was likely some deleterious effect from residual intermediates present in the 'leachate' solution. However, the use of a heterogeneous Pd-Fe catalyst still resulted in greater activity than the heterogeneous Pd catalyst when both were utilised in the presence of the leached Fe species.

3.2.17 Comparison of *in situ* generated H_2O_2 with commercial H_2O_2

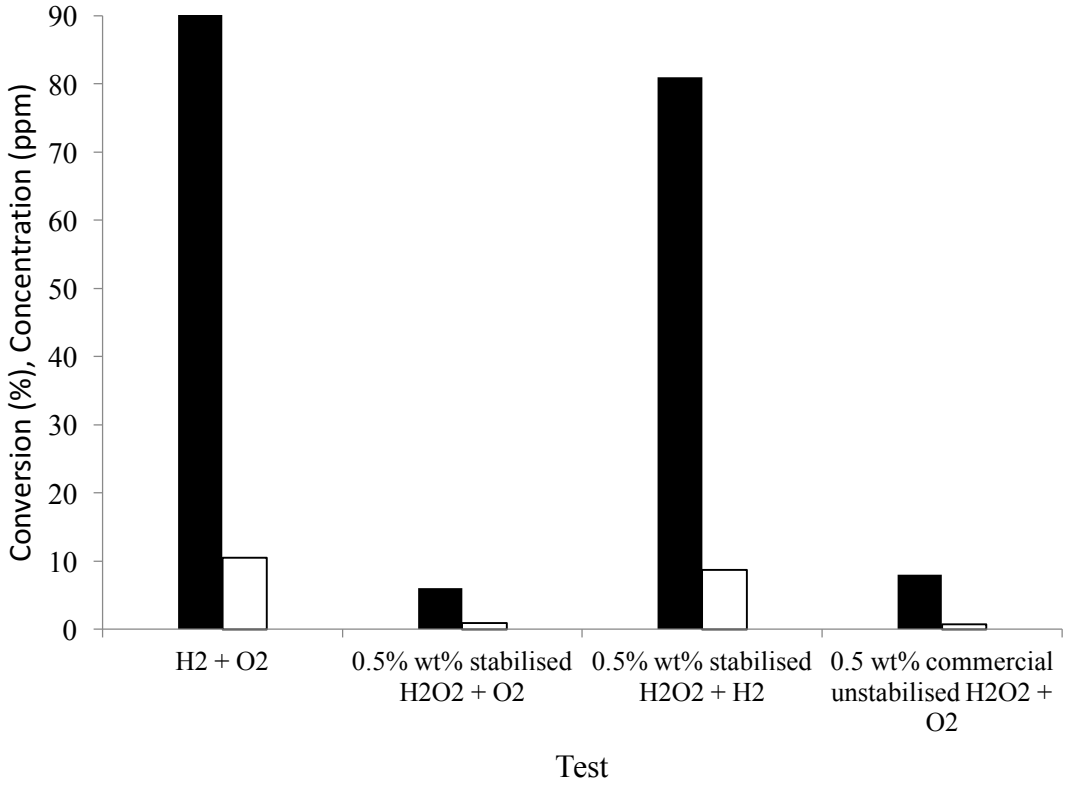

Figure 46: Comparison of *in situ* generated H_2O_2 with bulk addition of commercial H_2O_2. Conditions: 8.5 g 1000 ppm phenol solution, 420 psi 5%H_2/CO_2 (when used), 160 psi 25%O_2/CO_2 (580 psi in absence of H_2), 10 mg 2.5%Pd-2.5%Fe/SiO_2, 1200 rpm stirring, 30 °C, reactions performed in Parr stainless steel autoclave. Legend: filled = phenol conversion (%), unfilled = Fe concentration (ppm)

Due to the utilisation of *in situ* generated H_2O_2 with this reaction, it was important to benchmark the effectiveness of this *in situ* system with the bulk addition of H_2O_2 when employing a heterogeneous Pd-Fe catalyst. Therefore, a reaction was performed with the bulk addition of H_2O_2 instead of using both H_2 and O_2 reactant gases, as shown in Figure 46. The reactor was also charged with 25%O_2/CO_2 to maintain the presence of carbonic acid in solution. With the bulk addition of H_2O_2, a phenol conversion of 6 % was achieved. This phenol conversion was clearly far lower than the 92 % achieved when using *in situ* generated H_2O_2. This demonstrated the benefit of using *in situ* generated H_2O_2 for oxidation reactions. Interestingly, when the reactor was charged

with 5%H_2/CO_2 instead of 25%O_2/CO_2 alongside bulk addition of H_2O_2, a phenol conversion of 81 % was achieved. It was thought that some of this enhancement may have been achieved due to the reduction of Fe by Pd during the reaction. Reduction of Fe^{3+} to Fe^{2+} by Pd on Pd-Fe catalysts at low temperatures has previously been reported in the literature.[27] However, this activity may also be due to the *in situ* generation of H_2O_2 from H_2 and O_2 and not reaction with the bulk added H_2O_2. While the reactor was not initially charged with O_2, O_2 could have been added to the reaction medium via the decomposition of the bulk H_2O_2 over the Pd-Fe catalyst. One reason considered for the poor activity observed upon bulk addition of H_2O_2 was the presence of stabilisers in commercially available H_2O_2. Therefore, a test was conducted using commercially available unstabilised H_2O_2. However, only a modest increase in phenol conversion from 6 % to 8 % was observed. Therefore, these results clearly demonstrated the effectiveness of *in situ* generated H_2O_2 against bulk addition of H_2O_2.

3.2.18 Comparison of substrates

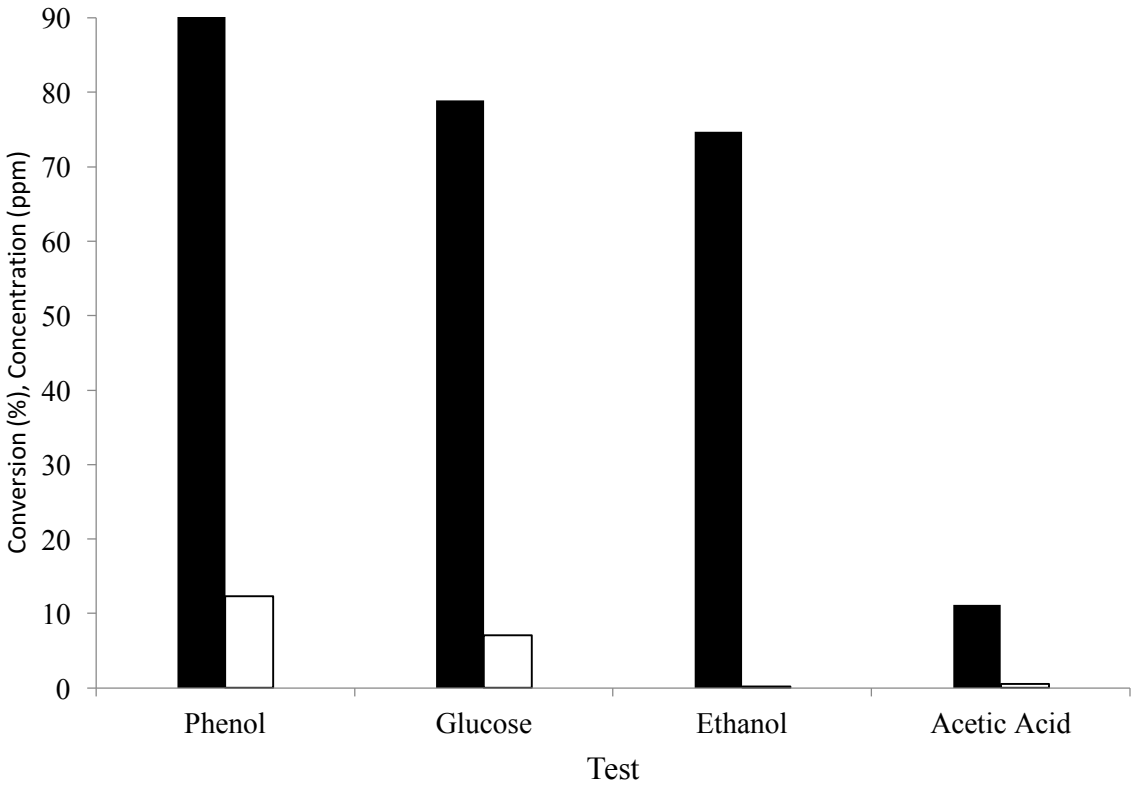

Figure 47: Investigating the effectiveness of the *in situ* generated H_2O_2 for conversion of other substrates. Conditions: 8.5 g 1000 ppm substrate solution, 420 psi 5%H_2/CO_2, 160 psi 25%O_2/CO_2, 50 mg 2.5%Pd-2.5%Fe/SiO_2, 1200 rpm stirring, 30 °C, reactions performed in Parr stainless steel autoclave. Legend: filled = conversion (%), unfilled = Fe concentration (ppm).

For destroying pollutants in wastewater effluent, it would be required for this system to be able to convert other substrates in addition to phenol. Therefore, this system was also tested for the conversion of glucose, ethanol and acetic acid. The results from these experiments are described in Figure 47. From this testing, it was confirmed that the catalyst can achieve high conversions of phenol, glucose and ethanol. Interestingly, very little Fe was leached from the catalyst during the conversion of ethanol. This was likely due to the absence of intermediates formed that would chelate with the Fe on the catalyst. This also showed the capability of the catalyst to perform the oxidation in the absence of leached Fe species. In the case of acetic acid, only

11.2 % conversion was achieved. This demonstrated the resilience of short chain organic acids towards oxidation using this system. However, it was clear from these experiments that the combination of the Pd-Fe catalyst with in situ generation of H_2O_2 is highly capable of converting a wide range of organic substrates that could be present in wastewater effluents.

3.3 Conclusions

In this chapter, it was demonstrated that bimetallic Pd-Fe catalysts were highly effective for the oxidation of phenol using H_2O_2 generated *in situ* from H_2 and O_2 under mild reaction conditions. The activity of the catalyst in oxidising phenol under such mild conditions represents an exciting new method for the treatment of wastewater. Through the development of the Pd-Fe catalyst it was found that high concentrations of phenol could be converted over impressively short timescales. It was also found that the presence of both Pd and Fe on the surface of the catalyst was essential for achieving appreciable rates of phenol conversion as highlighted in Figure 48.

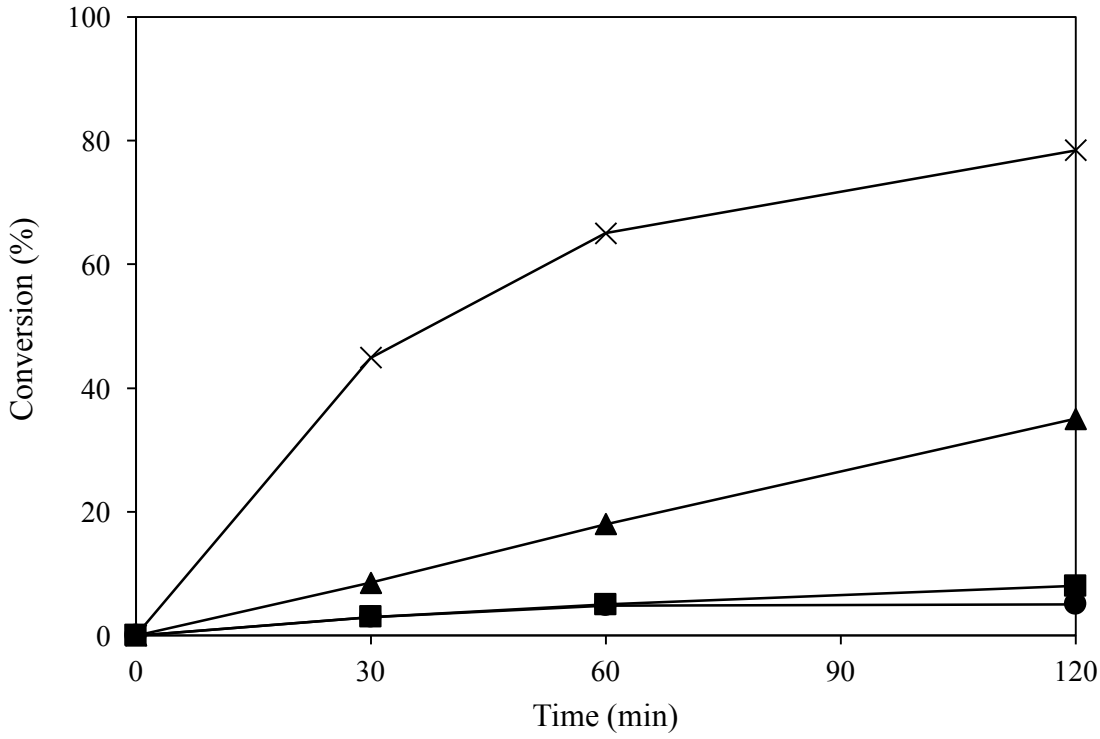

Figure 48: Comparison of bimetallic Pd-Fe catalyst with monometallic Pd and Fe catalysts. Conditions: 8.5 g 1000 ppm phenol solution, 420 psi 5%H_2/CO_2, 160 psi 25%O_2/CO_2, 10 mg 5%X/TiO_2 or 2.5%X/TiO_2 for monometallic catalysts (20 mg for

physical mixture), 1200 rpm stirring, 30 °C, reactions performed in Parr stainless steel autoclave. Legend: crosses = Pd-Fe, circles = Pd, squares = Fe, triangles = Pd + Fe.

From the evidence gathered, it appeared that the presence of Pd was essential to generate H_2O_2 whereas the presence of Fe was required to decompose the H_2O_2 into appropriate radical species (i.e •OH or •OOH). In addition to this, it was determined that Fe^{2+} was far more active than Fe^{3+} for catalysing phenol oxidation using in situ generated H_2O_2. This observation ties in with the evidence found that catalysts that had undergone a reductive heat-treatment step were far more active for the reaction than those that had undergone an oxidative heat-treatment step. While no direct evidence was found that H_2O_2 was present in the reaction medium, it was confirmed that a combination of catalyst, H_2 and O_2 was required to achieve the oxidation of phenol. This was considered powerful evidence for involvement of H_2O_2 (or a H_2O_2 related species such as surface bound peroxy or hydroxyl species) in the oxidation mechanism.

The *in situ* generated H_2O_2 was also found to be far superior than using bulk addition of commercially available H_2O_2 as highlighted in Figure 49.

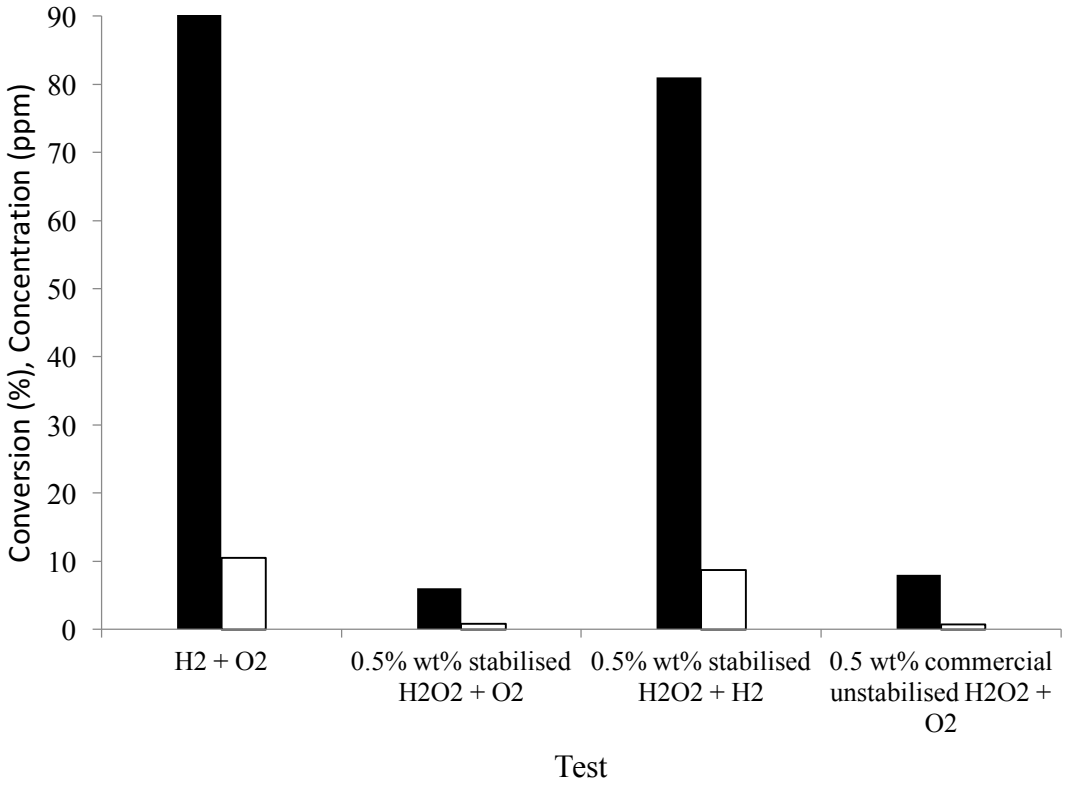

Figure 46: Comparison of *in situ* generated H_2O_2 with bulk addition of commercial H_2O_2. Conditions: 8.5 g 1000 ppm phenol solution, 420 psi 5%H_2/CO_2 (when used), 160 psi 25%O_2/CO_2 (580 psi in absence of H_2), 10 mg 2.5%Pd-2.5%Fe/SiO_2, 1200 rpm stirring, 30 °C, reactions performed in Parr stainless steel autoclave. Legend: filled = phenol conversion (%), unfilled = Fe concentration (ppm)

There were several reasons thought to be behind the superior performance of *in situ* generated H_2O_2 when compared with bulk addition of commercially available H_2O_2. One reason was thought to be due to the quenching of reactive oxygen species with the bulk addition of H_2O_2 (i.e H_2O_2 + •OH → •OOH + H_2O). Other reasons included the lack of stabilisers in the H_2O_2 generated *in situ* and the presence of H_2O_2 concentrated near the active site.

One issue with the usage of Pd-Fe catalysts in the phenol oxidation reaction was the occurrence of active metal leaching from the surface of the catalyst. Within this chapter, it was shown that the generation of phenol oxidation intermediates such as catechol and oxalic acid were responsible for the observed leaching. A variety of methods were employed to help reduce the occurrence of this leaching including adjustments to the heat treatment of the catalyst, varying the Fe loading and the use

of alternative metal salt precursors. Through a detailed XPS study, it was determined that Pd^{2+} was far more susceptible to leaching under the reaction conditions than Pd^{0}. It was also found that encasing the Fe within a perovskite structure lead to greater robustness towards leaching by oxalic acid and especially catechol. These represent promising new pathways for the development of stable catalysts for performing the oxidation of phenol using *in situ* generated H_2O_2.

Another aspect of this work that was thoroughly investigated was the contribution of leached Fe species towards the catalyst activity observed. A series of tests were performed using 'hot filtration' type experiments. While these experiments showed that some of the observed catalyst activity may be associated with leached homogeneous Fe species, it appeared clear that the majority of the activity could be attributed to the heterogeneous Pd-Fe species.

The work contained in this chapter represents an exciting method for the treatment of wastewater that is applicable across a wide range of organic wastewater substituents. Utilising *in situ* generated H_2O_2 for wastewater treatment satisfies many of the principles of green chemistry including waste prevention, atom economy, energy efficiency, less hazardous chemicals, safer solvents, reduction of derivatives, use of catalysis and design for degradation. Additionally, if the H_2 used in the system could be produced electrolytically using power derived from solar sources, it would represent the use of a renewable feedstock. In addition to the environmental benefits of the *in situ* system, it has been shown that the use of *in situ* generated H_2O_2 leads to far superior oxidation performance when compared to the use of commercially available H_2O_2 without the safety risks associated with transporting and storing large quantities of concentrated H_2O_2.

3.4 References

1 C. Samanta, *Appl. Catal. A Gen.*, 2008, **350**, 133–149.

2 J. M. Campos-Martin, G. Blanco-Brieva and J. L. G. Fierro, *Angew. Chemie - Int. Ed.*, 2006, **45**, 6962–6984.

3 Y. Yi, L. Wang, G. Li and H. Guo, *Catal. Sci. Technol.*, 2016, **6**, 1593–1610.

4 B. Puértolas, A. K. Hill, T. García, B. Solsona and L. Torrente-Murciano, *Catal. Today*, 2015, **248**, 115–127.

5 M. S. Yalfani, S. Contreras, F. Medina and J. Sueiras, *Appl. Catal. B Environ.*, 2009, **89**, 519–526.

6 M. S. Yalfani, S. Contreras, F. Medina and J. E. Sueiras, *J. Hazard. Mater.*, 2011, **192**, 340–346.

7 M. S. Yalfani, S. Contreras, J. Llorca, M. Dominguez, J. E. Sueiras and F. Medina, *Phys. Chem. Chem. Phys.*, 2010, **12**, 14673–14676.

8 S. Contreras, M. S. Yalfani, F. Medina and J. E. Sueiras, *Water Sci. Technol.*, 2011, 63, 2017–2024.

9 O. Osegueda, A. Dafinov, J. Llorca, F. Medina and J. Suerias, *Catal. Today*, 2012, **193**, 128–136.

10 S. Yuan, Y. Fan, Y. Zhang, M. Tong and P. Liao, *Environ. Sci. Technol.*, 2011, **45**, 8514–20.

11 P. Landon, P. J. Collier, A. J. Papworth, J. Kiely and J. Graham, *Chem. Commun.*, 2002, 2058–2059.

12 J. K. Edwards, B. E. Solsona, P. Landon, A. F. Carley, A. Herzing, C. J. Kiely and G. J. Hutchings, *J. Catal.*, 2005, **236**, 69–79.

13 J. A. Zazo, J. A. Casas, A. F. Mohedano, M. A. Gilarranz and J. J. Rodríguez, *Environ. Sci. Technol.*, 2005, **39**, 9295–9302.

14 C. J. Lin, S. H. Huang, N. C. Lai and C. M. Yang, *ACS Catal.*, 2015, **5**, 4121–4129.

15 J. K. Edwards, B. Solsona, E. N. N, A. F. Carley, A. a Herzing, C. J. Kiely and G. J. Hutchings, *Science (80-.).*, 2009, **323**, 1037–1041.

16 S. J. Freakley, Q. He, J. H. Harrhy, L. Lu, D. A. Crole, D. J. Morgan, E. N. Ntainjua, J. K. Edwards, A. F. Carley, A. Y. Borisevich, C. J. Kiely and G. J. Hutchings, 2015, **351**, 279–296.

17 J. K. Edwards, N. N. Edwin, A. F. Carley, A. A. Herzing, C. J. Kiely and G. J. Hutchings, *Angew. Chemie - Int. Ed.*, 2009, **48**, 8512–8515.

18 M. Armbrüster, K. Kovnir, M. Friedrich, D. Teschner, G. Wowsnick, M. Hahne, P. Gille, L. Szentmiklósi, M. Feuerbacher, M. Heggen, F. Girgsdies, D. Rosenthal, R. Schlögl and Y. Grin, *Nat. Mater.*, 2012, **11**, 690–693.

19 L. Piccolo, *Chem. Commun. (Camb).*, 2013, **49**, 9149–51.

20 A. A. Herzing, A. F. Carley, J. K. Edwards, G. J. Hutchings and C. J. Kiely, *Chem. Mater.*, 2008, **20**, 1492–1501.

21 J. K. Edwards, J. Pritchard, M. Piccinini, G. Shaw, Q. He, A. F. Carley, C. J. Kiely and G. J. Hutchings, *J. Catal.*, 2012, **292**, 227–238.

22 P. Sanchez, G. Natividad, E. Colacio, E. Minones and J. M. Dominguez-Vera, *Dalt. Trans.*, 2005, **4**, 811–813.

23 D. Panias, M. Taxiarchou, I. Paspaliaris and A. Kontopoulos, *Hydrometallurgy*, 1996, **42**, 257–265.

24 J. H. Walton and D. P. Graham, *J. Am. Chem. Soc.*, 1928, **50**, 1641–1648.

25 M. Sankar, Q. He, M. Morad, J. Pritchard, S. J. Freakley, J. K. Edwards, S. H. Taylor, D. J. Morgan, A. F. Carley, D. W. Knight, C. J. Kiely and G. J. Hutchings, *ACS Nano*, 2012, **6**, 6600–6613.

26 C. D. Evans, S. A. Kondrat, P. J. Smith, T. D. Manning, P. J. Miedziak, G. L. Brett, R. D. Armstrong, J. K. Bartley, S. H. Taylor, M. J. Rosseinsky and G. J. Hutchings, *Faraday Discuss.*, 2016, **0**, 1–24.

27 J. W. Niemantsverdriet, J. Van Grondelle and A. M. Van der Kraan, *Hyperfine Interact.*, 1988, **41**, 677–680.

4 Oxidation of glycerol utilising H_2O_2 generated *in situ* from H_2 and O_2

4.1 Introduction

In the previous chapter, it was determined that the Pd-Fe bimetallic materials prepared could catalyse the oxidation a wide variety of substrates including sugars. It was also observed that when using higher starting concentrations of the target substrates, a dramatic increase in product selectivity was observed.

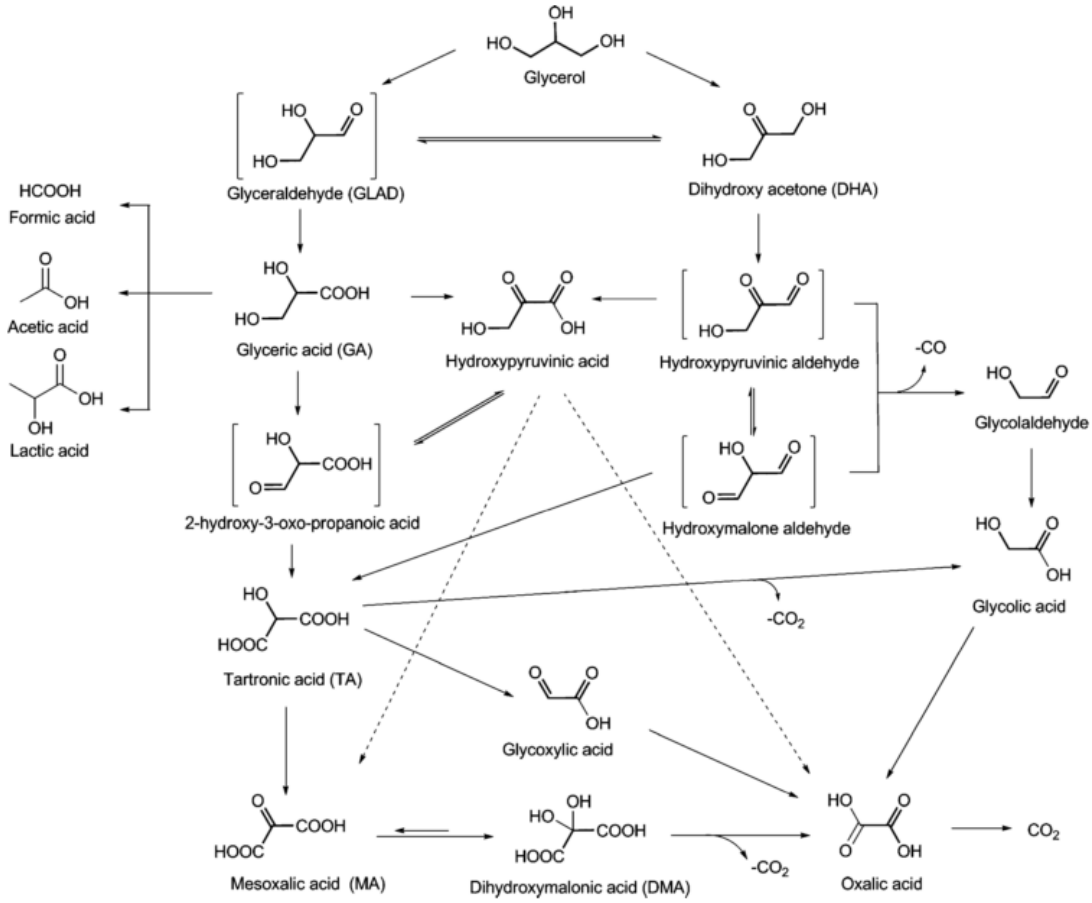

Scheme 1: Products obtained from the oxidation of glycerol.[1]

Glycerol is produced as a by-product of biodiesel production. Therefore, there is a great amount of interest into the conversion of glycerol into higher value products. A

review by Katryniok *et al.*[1] highlighted the amount of research that has been performed into developing the catalytic oxidation of glycerol to higher value products. The wide variety of products that can be obtained from the oxidation of glycerol are illustrated in Scheme 1.

To the best of this authors knowledge, there has been no previous literature investigating the oxidation of glycerol from H_2O_2 generated in situ from H_2 and O_2. Therefore, within this chapter, the 0.5%Pd-0.5%Fe/SiO_2 catalyst designed during the work presented in chapter 3 was tested for application in the oxidation of glycerol using *in situ* generated H_2O_2.

4.2 Results and discussion

4.2.1 Glycerol oxidation using *in situ* generated H_2O_2

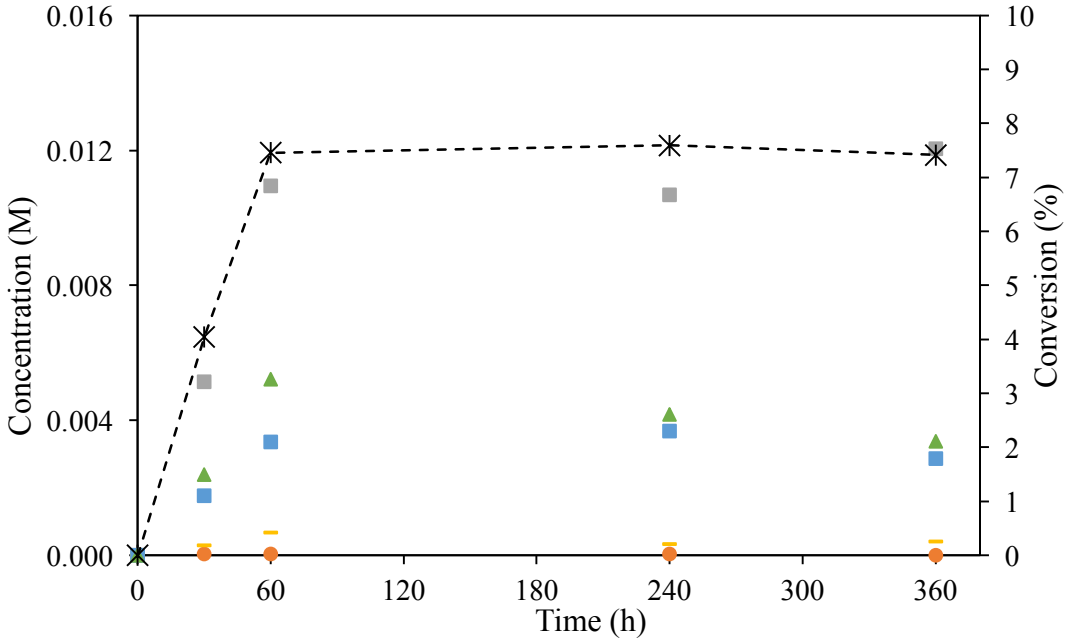

Figure 1: Glycerol oxidation using *in situ* generated H_2O_2. Conditions: 10 g 0.3 M glycerol solution, 420 psi 5%H_2 / CO_2, 160 psi 25%O_2 / CO_2, 50 mg 0.5%Pd-0.5%Fe / SiO_2, 1200 rpm stirring, 30 °C. Legend: grey square = glyceraldehyde, blue square = dihydroxyacetone, green triangle = formic acid, orange circle = oxalic acid, yellow dash = glycolic acid.

A 1%Pd-Fe/SiO_2 catalyst was tested for the oxidation of glycerol using H_2O_2 generated *in situ* from H_2 and O_2. The results of this testing are described in Figure 1. Over the first 1 h of reaction, the conversion of glycerol was observed to be linear over time. Interestingly, the selectivity profile over this time contained predominantly C_3 products, although the formation of formic acid was also observed which indicated the early occurrence of scission products. However, after 1 h, no further conversion of glycerol was observed. The concentration of C_3 oxidation products was also found

to remain largely unchanged over the remaining 5 h of reaction, ruling out competing oxidation reactions occurring. This was thought to be potentially due to several reasons. Firstly, for the oxidation of glycerol to proceed requires the generation of H_2O_2. The generation of H_2O_2 is dependent on the availability of H_2 in the system for the direct synthesis reaction to occur. Therefore, after 1 h, the reaction may have become H_2 limited. O_2 limitation was unlikely to be a factor as it was provided in a 2:1 ratio with respect to hydrogen and oxygen is evolved during the decomposition of H_2O_2. Another factor that could cause the cessation of glycerol conversion was catalyst deactivation either due to catalyst leaching or inhibition of the active sites by the products formed. However, there was a decrease in the concentration of formic acid over the remaining 5 h of reaction. The decomposition of formic acid to H_2 and CO_2 has previously been reported in the literature over Pd-Fe catalysts.[2] It was found that formic acid was readily decomposed by Pd-Fe catalysts to form H_2 and CO_2. It was considered that this reaction occurring during glycerol oxidation with *in situ* generated H_2O_2 might lead to an increase in H_2 concentration past the explosive limit. However, when the concentrations of formic acid produced were considered, this was found to not be the case.

4.2.2 Effect of recharging reaction with H_2 and O_2 throughout the reaction

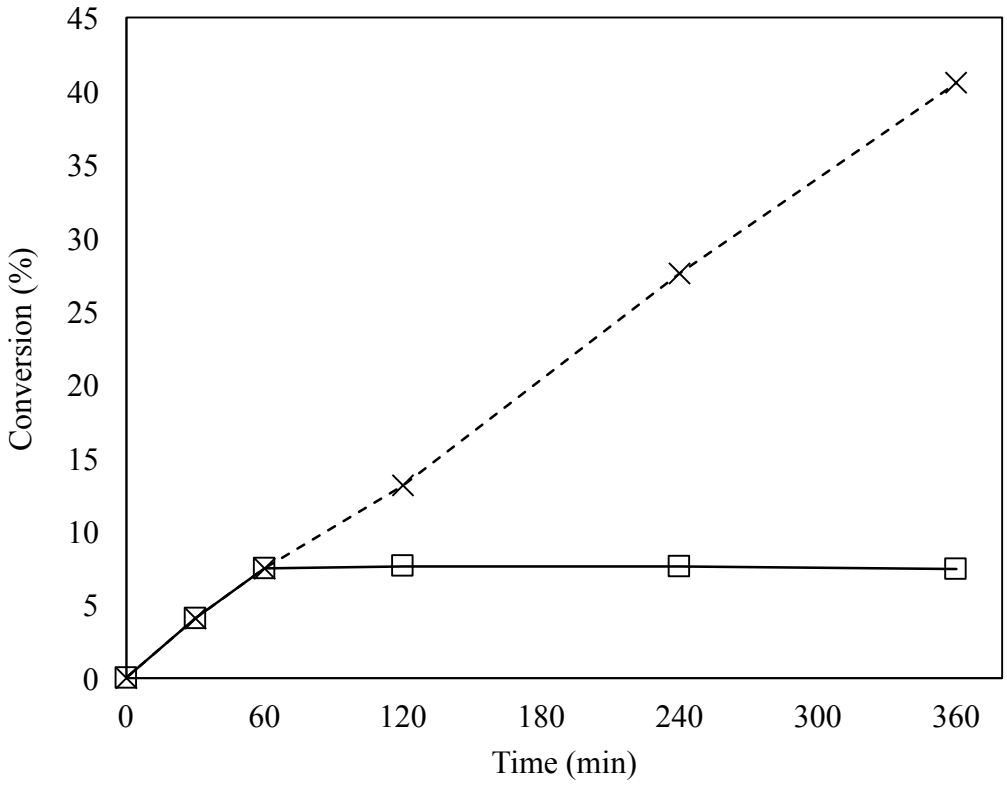

Figure 2: Effect of hydrogen limitation upon the reaction. Conditions: 10 g 0.3 M glycerol solution, 420 psi 5%H_2 / CO_2, 160 psi 25%O_2 / CO_2, 50 mg 0.5%Pd-0.5%Fe / SiO_2, 1200 rpm stirring, 30 °C. For recharge experiment, gases were vented and replenished every hour. Legend: crosses = with recharging of gases, square = no recharging of gases.

To investigate the loss of catalytic performance further, the reaction was performed with recharging of H_2 and O_2 every hour. The results are described in Figure 2. It was observed that when fresh H_2 was introduced every hour, conversion increased linearly with respect to time over 6 h. This showed that the reaction became H_2 limited after 1h. Therefore, recharging of gases was required every hour to achieve sustained glycerol conversion. The linear increase in conversion indicated that the observed loss of catalyst performance in the prior test was not due to catalyst deactivation.

Table 1: Hydrogen conversion per recharge. Conditions: 10 g 0.3 M glycerol solution, 420 psi 5%H_2 / CO_2, 160 psi 25%O_2 / CO_2, 50 mg 0.5%Pd-0.5%Fe / SiO_2, 1 h, 1200 rpm stirring, 30 °C. Gas collected and analysed using GC.

H_2 conversion (%)	**H_2 in (moles)**	**H_2 out (moles)**	**H_2 converted (moles)**
67.4	0.00364	0.00119	0.00245

GC analysis was performed on the effluent gas after each recharge to determine the concentration of hydrogen consumed per recharge. The results are described in Table 1. It was found that 67.4% of the available hydrogen was consumed after 1h. However, at this point there was no further conversion of glycerol observed. Therefore, not all the hydrogen input is available for the generation of H_2O_2. This is likely due to the poor solubility of H_2 in aqueous medium.

4.2.3 Glycerol oxidation profile with recharging of H_2 and O_2 reactant gases

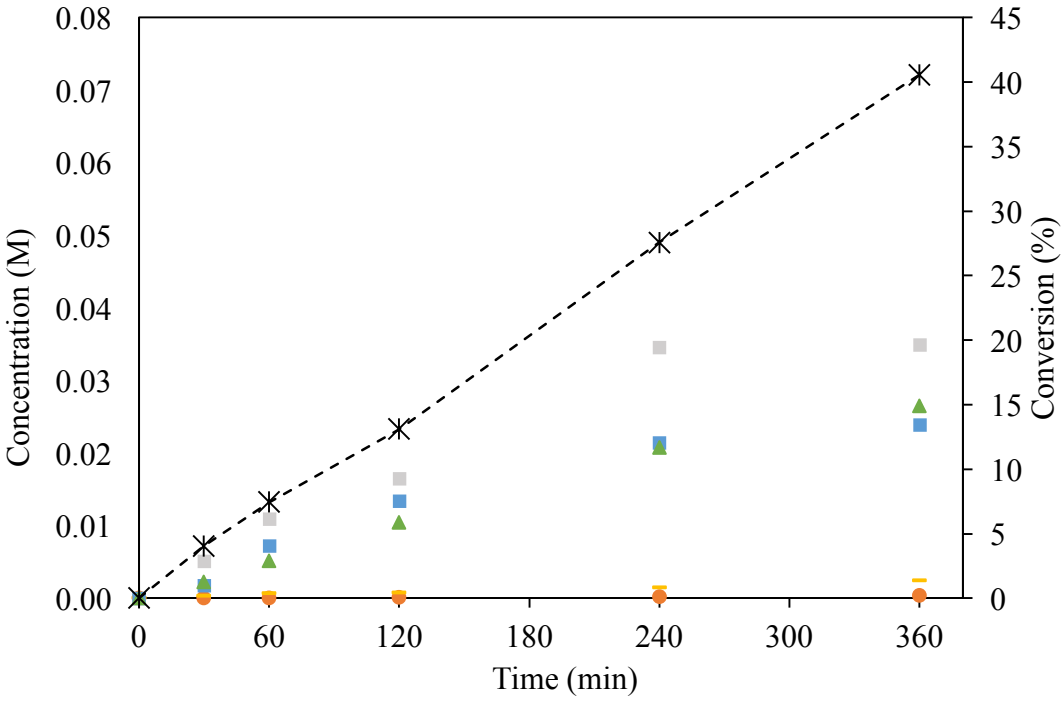

Figure 3: Product distribution over 6 h with recharging of gases every 1 h. Conditions: 10 g 0.3 M glycerol solution, 420 psi 5%H_2 / CO_2, 160 psi 25%O_2 / CO_2, 50 mg 0.5%Pd-0.5%Fe / SiO_2, 1200 rpm stirring, 30 °C. Gases were vented and replenished every hour. Legend: grey square = glyceraldehyde, blue square = dihydroxyacetone, green triangle = formic acid, orange circle = oxalic acid, yellow dash = glycolic acid.

The evolution of products over the 6 h reaction was also considered, as described in Figure 3. Over the 6 h reaction, increasing concentrations of dihydroxyacetone and glyceraldehyde were observed. However, formic acid was also observed in significant quantities, demonstrating the occurrence of c-c scission during the reaction. Between 4 h and 6h, the concentration of dihydroxyacetone and glyceraldehyde increased only slightly. This was likely due to the rate of scission product formation increasing during this time as the rate of glycerol conversion remained constant. Interestingly, the concentration of formic acid also only increased slightly between 4 h and 6h. This was unexpected because if the rate of c-c scission reactions increase, more formic acid

should be observed. A possible reason for this could be that the formic acid was being decomposed over the catalyst surface at a rate that was greater than its formation. Unfortunately, the formation of CO_2 could not be monitored during this reaction due to the presence of CO_2 as a diluent for the reactant gases.

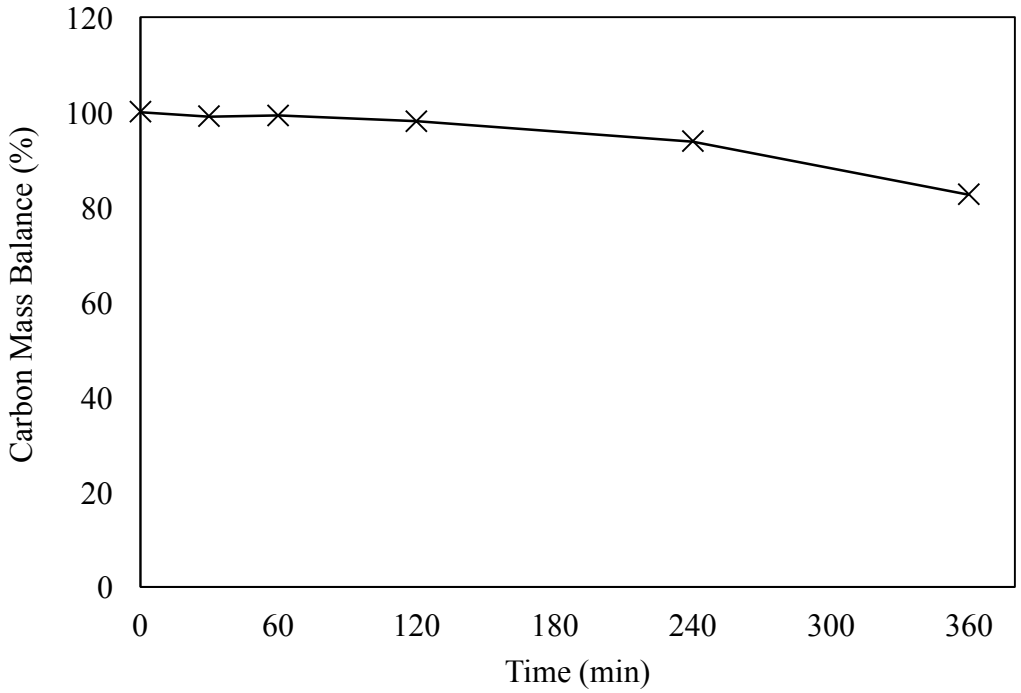

Figure 4: Carbon mass balance during reaction. Conditions: 10 g 0.3 M glycerol solution, 420 psi 5%H_2 / CO_2, 160 psi 25%O_2 / CO_2, 50 mg 0.5%Pd-0.5%Fe / SiO_2, 1200 rpm stirring, 30 °C. Gases were vented and replenished every hour.

Furthermore, when the carbon mass balance was considered in Figure 4, it was found that it began to decrease significantly between 4 h and 6 h. This indicated either the formation of unidentified products or the formation of gaseous products. It is important to note that there were two peaks present in the HPLC chromatogram that were unable to be identified, therefore these peaks may account for the discrepancy in carbon mass balance during the later stages of the reaction.

4.2.4 Effect of oxidation by molecular oxygen

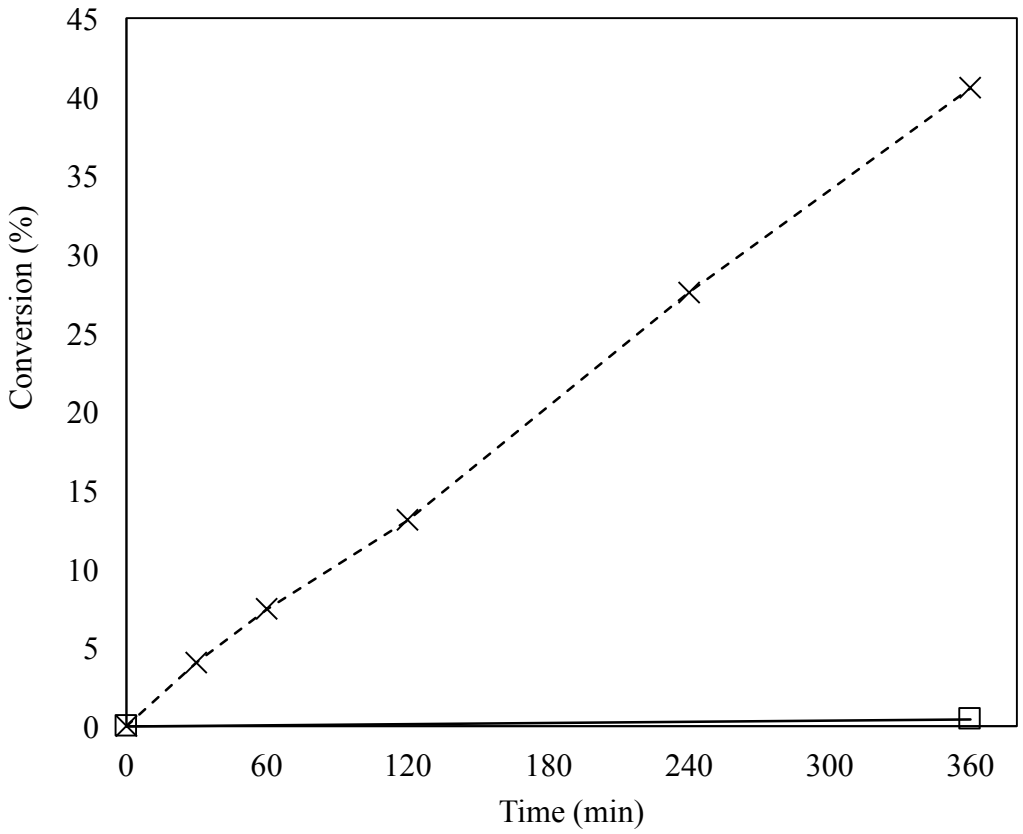

Figure 5: Contribution of O_2 in oxidation of glycerol. Conditions: Conditions: 10 g 0.3 M glycerol solution, 420 psi 5%H_2 / CO_2, 160 psi 25%O_2 / CO_2 (580 psi 25%O_2 / CO_2 for reaction in absence of H_2), 50 mg 0.5%Pd-0.5%Fe / SiO_2, 1200 rpm stirring, 30 °C. Gases were vented and replenished every hour. Legend: crosses = H_2 + O_2, squares = O_2.

Oxidation of glycerol with molecular oxygen has been widely reported using Pd-containing catalysts.[1] To investigate whether some of the observed glycerol conversion could be attributed to this reaction pathway, an experiment was performed in the absence of hydrogen. The results of this experiment are described in Figure 5. In the absence of hydrogen, little to no glycerol conversion was observed. This clearly demonstrated the requirement of hydrogen to attain oxidation of glycerol, indicating that all the observed conversion was due to the formation of hydrogen peroxide or reactive oxygen species and not oxidation with molecular oxygen.

4.2.5 Effect of monometallic counterparts of catalyst upon glycerol oxidation

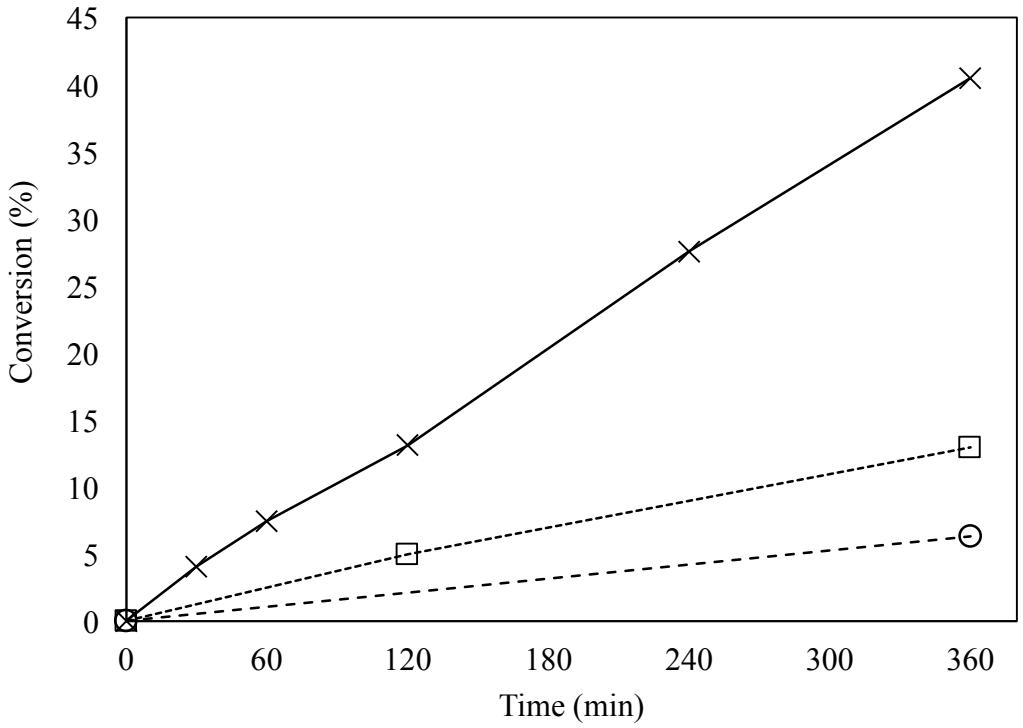

Figure 6: Effect of iron on glycerol oxidation. Conditions: 10 g 0.3 M glycerol solution, 420 psi 5%H_2 / CO_2, 160 psi 25%O_2 / CO_2, 50 mg 0.5%Pd-0.5%Fe / SiO_2 or 0.5%Pd / SiO_2, 1200 rpm stirring, 30 °C. Gases were vented and replenished every hour. Legend: crosses = 0.5%Pd-0.5%Fe/SiO_2, squares = 0.5%Pd/SiO_2, circles = 0.5%Fe/SiO_2.

It was important to consider the role that each active metal present on 0.5%Pd-0.5%Fe/SiO_2 played in the overall catalysis. Therefore, monometallic 0.5%Pd/SiO_2 and 0.5%Fe/SiO_2 catalysts were tested for the oxidation of glycerol, as described in Figure 6. For the Pd-only catalyst, a significantly lower rate of glycerol conversion was observed than for the bimetallic Pd-Fe catalyst. Iron containing catalysts have been reported to be very effective in catalysing oxidations with H_2O_2 as the oxidant through the Fenton reaction. Therefore, while Pd is a very effective catalyst for the direct synthesis of H_2O_2 form H_2 and O_2, a secondary metal is required to effectively utilise the generated H_2O_2. For the Fe-only catalyst, even less conversion of glycerol was observed. This was unsurprising as the presence of Pd is required for the

generation of H_2O_2 to perform the oxidation of glycerol. The low levels of conversion observed may have been due to low levels of Pd contamination in the reactor. To date, there has been no reports in the literature of Pd-free catalysts being active for the direct synthesis of H_2O_2 in significant quantities under these conditions.

4.2.6 Comparison of *in situ* generated H_2O_2 with bulk addition of H_2O_2

Table 2: Comparison of *in situ* generated H_2O_2 with *ex situ* addition of H_2O_2. Conditions: 10 g 0.3 M glycerol solution, 420 psi 5%H_2 / CO_2, 160 psi 25%O_2 / CO_2 (or 580 psi 25%O_2 / CO_2 for test with addition of H_2O_2), 50 mg 0.5%Pd-0.5%Fe / SiO_2, 1200 rpm stirring, 30 °C. Gases were vented and replenished every hour. GLD = glyceraldehyde, GA = glycolic acid, GCA = glyceric acid, DHA = dihydroxy acetone, FA = formic acid, OXA = oxalic acid, CMB = carbon mass balance.

Reactants	**Time (h)**	**Conv. (%)**	**Selectivity (%)**						**CMB (%)**
			GLD	**GA**	**GCA**	**DHA**	**FA**	**OXA**	
$H_2 + O_2$	6	40.56	50.3	2.3	<0.1	34.3	12.7	0.4	82.60
$H_2 + O_2$	1	7.46	53.8	2.2	<0.1	35.5	8.4	0.1	99.33
O_2 + 4%H_2O_2	6	7.82	27.8	8.6	4.1	5.9	53.4	0.2	101.05
H_2 + 4%H_2O_2	6	13.5	53.6	6	3.2	10.8	25.5	0.2	96.82

There have been reports in the literature for the oxidation of glycerol with bulk addition of H_2O_2 using Fe containing catalysts.[3,4] To compare the effectiveness of *in situ* generation of H_2O_2 compared with bulk addition of commercially available H_2O_2, 0.5%Pd-0.5%Fe/SiO_2 was tested for the oxidation of glycerol with bulk addition of H_2O_2. The results are shown in Table 2. Over a 6 h reaction the observed conversion of glycerol was far lower upon addition of bulk H_2O_2 when compared to the reaction utilising *in situ* generation of H_2O_2. This could have been due to several factors. With the addition of bulk H_2O_2, there was a very high initial concentration of H_2O_2. When

radicals are generated at the catalyst surface, these radicals can react with excess H_2O_2 in the reaction medium. This could limit the availability of radical species to perform the glycerol oxidation reaction. Additionally, commercially available H_2O_2 contains stabilisers which could act as radical scavengers, this could potentially have had a deleterious effect on the glycerol oxidation reaction. Interestingly, at similar conversions of glycerol, the *in situ* system was observed to be far more selective towards the generation of C_3 products when compared to bulk addition of H_2O_2. When the 1 h *in situ* reaction was compared with the 6 h bulk reaction it was observed that the concentration of dihydroxyacetone was far less than for bulk reaction. The reaction with bulk addition of H_2O_2 also resulted in far higher concentrations of scission products such as glycolic acid and formic acid. The activity observed when using *in situ* generated H_2O_2 when compared to addition of bulk H_2O_2 demonstrates the effectiveness of utilising the direct synthesis of H_2O_2 for reactions using H_2O_2 as the oxidant.

4.2.7 Investigation into leaching of Fe during glycerol oxidation reaction

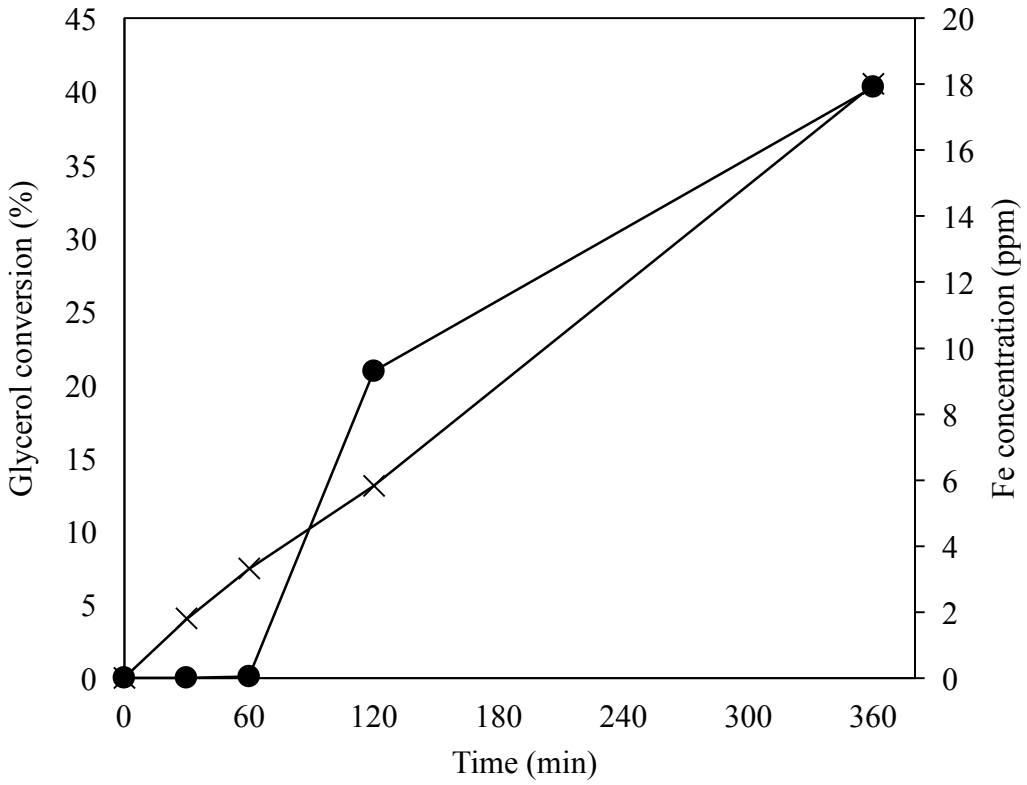

Figure 7: Fe leaching as reaction proceeds. Conditions: 10 g 0.3 M glycerol solution, 420 psi 5%H_2 / CO_2, 160 psi 25%O_2 / CO_2, 50 mg 0.5%Pd-0.5%Fe / SiO_2, 1200 rpm stirring, 30 °C. Gases were vented and replenished every hour. Reaction solutions were collected and analysed using MP-AES. Legend: crosses = glycerol conversion, circles = Fe leaching.

When employing heterogeneous catalysts in aqueous medium, leaching of metals from the catalyst surface can be a problem. To investigate the occurrence of leaching, the reaction solutions were collected and analysed using MP-AES. The results are described in Figure 7. No Pd was detected in the reaction medium, indicating that the Pd did not leach during the reaction. However, a significant concentration of Fe was detected in the reaction medium post reaction. Interestingly, despite the occurrence of Fe leaching from the catalyst, the rate of glycerol conversion was observed to remain consistent. This indicated that the leaching of iron had no effect on catalyst activity over the duration of the reaction. Homogeneous Fe species have been shown to be

effective for catalysing oxidations using H_2O_2 as the oxidant, such as in Fenton's oxidation. Therefore, the leached Fe may be performing some of the catalysis in the later part of the reaction with H_2O_2 generated on the surface of the catalyst. However, it could also be that the leached Fe has little effect upon the reaction, as evidenced by the lack of change in the rate of glycerol conversion. Interestingly, no leaching of Fe was observed during the initial 1 h of reaction despite high levels of glycerol conversion. So, the observed activity is clearly not dependent on the presence of homogeneous Fe species.

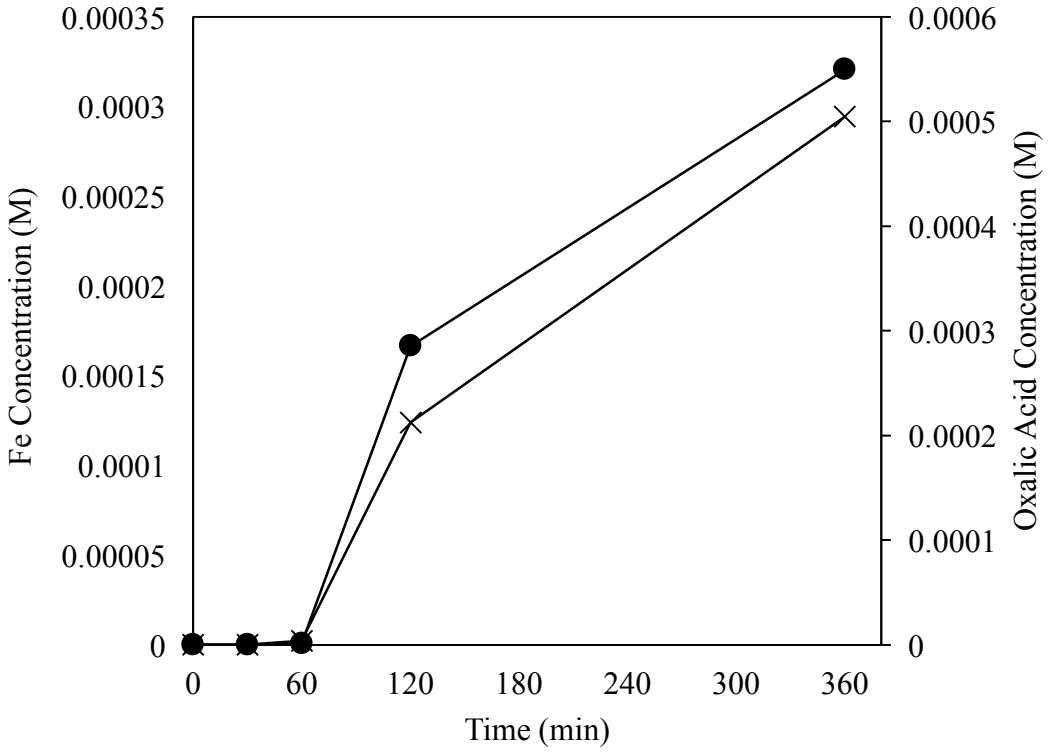

Figure 8: Comparison of Fe concentration in solution with oxalic acid concentration. Conditions: 10 g 0.3 M glycerol solution, 420 psi 5%H_2 / CO_2, 160 psi 25%O_2 / CO_2, 50 mg 0.5%Pd-0.5%Fe / SiO_2, 1200 rpm stirring, 30 °C. Gases were vented and replenished every hour. Reaction solutions were collected and analysed using MP-AES. Legend: circles = Fe concentration, crosses = oxalic acid concentration.

The lack of leaching during the initial 1 h of reaction indicated that the observed leaching could not be attributed to inherent instability of the metals on the surface of

the catalyst. Additionally, when the catalyst was stirred in water for 6 h, there was no Fe leached from the catalyst. Therefore, it was considered that the leaching of the metals could be due to reaction products generated during the glycerol oxidation reaction. This was observed previously during the oxidation of phenol using *in situ* generated H_2O_2. Therefore, the concentration of oxalic acid in solution was compared with the concentration of Fe in solution, as described in Figure 8. When the Fe concentration was compared to the concentration of oxalic acid formed during the reaction, a strong correlation was observed. Therefore, it appears that the generation of oxalic acid, which chelates to the heterogeneous Fe species during the reaction, is responsible for the observed leaching. Oxalic acid is widely known as a highly effective chelating agent which can produce both Fe^{2+} and Fe^{3+} oxalates when binding Fe species.

4.2.8 Evaluation of glycerol oxidation using homogeneous Fe catalysts

To determine whether the glycerol oxidation reaction could proceed using a homogeneous Fe source, a series of reactions were performed using a monometallic Pd catalyst alongside $FeCl_3$ as a homogeneous Fe source. The results from this testing were described in Figure 9.

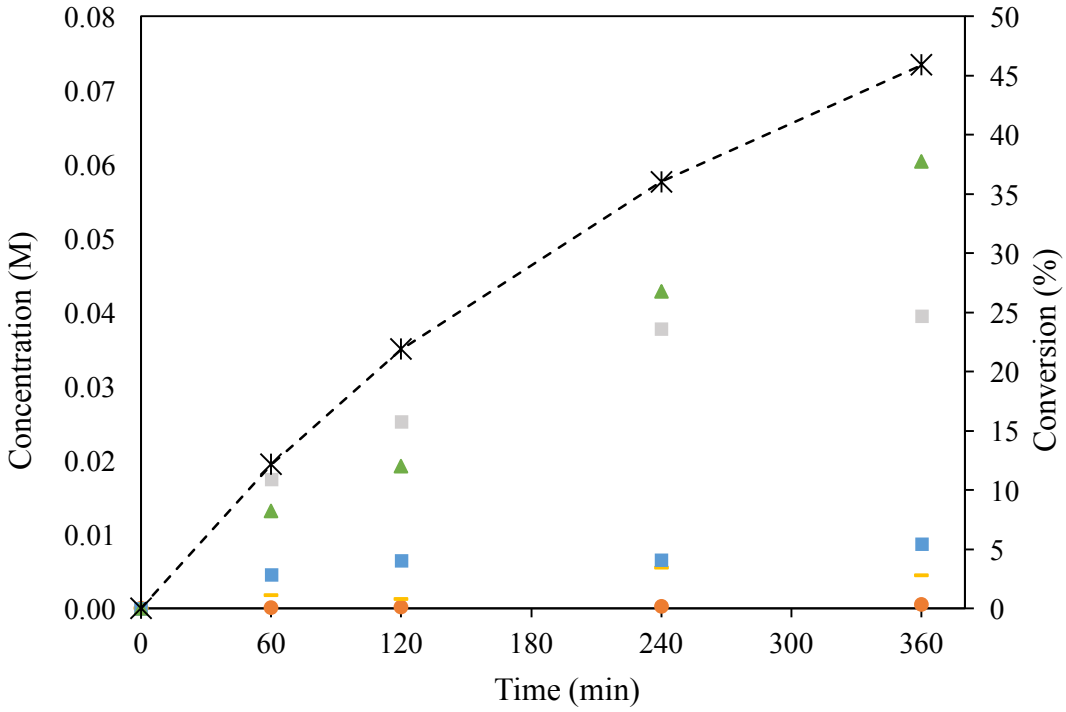

Figure 9: 10 g 0.3 M Glycerol solution, 420 psi 5%H_2/CO_2, 160 psi 25%O_2/CO_2, 50 mg 0.5%Pd/SiO_2, 0.25 mg Fe (as $FeCl_3$), 1200 rpm stirring, 30 °C, reactions performed in Parr stainless steel autoclave. Legend: grey square = glyceraldehyde, blue square = dihydroxyacetone, green triangle = formic acid, orange circle = oxalic acid, yellow dash = glycolic acid, conversion = cross with dotted lines.

With the use of a mono-metallic Pd catalyst alongside a homogeneous Fe source it was clearly observed that a high conversion of glycerol could be achieved. A glycerol conversion of 45.9 % was observed compared to 40.6 % observed when using the

bimetallic Pd-Fe catalyst. However, when homogenous Fe was utilised, far higher concentrations of the scission products formic acid and glycolic acid were observed. Therefore, it appeared that selectivity towards C_3 products decreased upon usage of a homogeneous Fe source. Additionally, the rate of glycerol conversion was observed to decrease over the course of the 6 h reaction. This contrasted with the heterogeneous Pd-Fe system where the rate of glycerol conversion was observed to be constant over the 6 h reaction. This decrease in the rate of glycerol conversion may be related to Fe catalyst inhibition due to chelation by oxalic acid. Oxalic acid has been previously shown to inhibit the Fenton reaction due to chelation of Fe species.[5] However, the high activities observed using a combination of heterogeneous Pd alongside homogeneous Fe demonstrates the potential of using homogeneous Fe catalysts with this system.

4.2.9 Addition of carbon to reaction medium to remove leached Fe species

To help determine the effect of homogeneous iron in solution during the reaction, experiments were performed with addition of carbon to help remove homogeneous iron from the reaction solution.

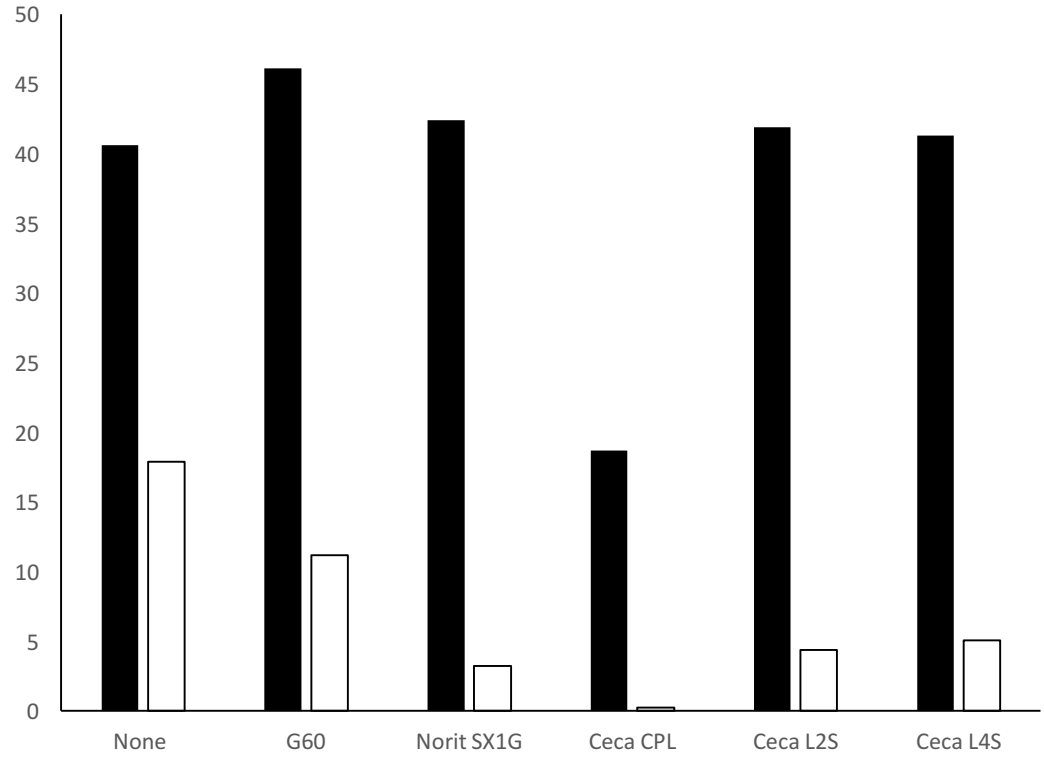

Figure 10: Addition of various carbon materials to remove Fe species from solution. Conditions: 10 g 0.3 M glycerol solution, 420 psi 5%H_2 / CO_2, 160 psi 25%O_2 / CO_2, 50 mg 0.5%Pd-0.5%Fe / SiO_2, 50 mg carbon, 6 h, 1200 rpm stirring, 30 °C. Gases were vented and replenished every hour. Reaction solutions were collected and analysed using MP-AES. Legend: filled = glycerol conversion (%), unfilled = Fe leaching (ppm).

A variety of carbon materials were added during the glycerol oxidation reaction to help determine the optimum type of carbon to remove leached Fe species from the reaction medium. The results of these experiments are described in Figure 10. Upon addition of G60, the conversion of glycerol was observed to increase from 40.6 % to 46.1 %. Interestingly, the concentration of Fe in solution post-reaction was also observed to decrease from 17.9 ppm to 11.2 ppm. Furthermore, upon addition of Norit SX1G carbon, glycerol conversion was observed to increase from 40.6 % to 42.4 % with a corresponding decrease of Fe in solution from 17.9 ppm to 3.2 ppm. The low concentration of Fe in solution coupled with the complete maintenance of glycerol conversion activity strongly indicated that the leached Fe played only a minor role in the observed catalysis. A similar effect was observed upon addition of Ceca L2S and

Ceca L4S. However, when Ceca CPL was added to the reaction medium, a large decrease in glycerol conversion was observed from 40.6 % to 18.7%. This was also accompanied by only 0.23 ppm Fe detected in the post-reaction effluent. From these results, it was unclear whether this loss in catalyst activity was due to the low concentration of Fe in solution. However, it was also likely that the lower concentration of Fe could be attributed to the lower conversion and therefore lower concentration of oxalic acid in solution. In addition to this, the Ceca CPL is phosphoric acid activated and retains some of the phosphorus in its pore structure. Phosphoric acid is typically added to commercial H_2O_2 to help stabilise it. Therefore, this could be part of the reason for the reduced glycerol conversion observed upon addition of Ceca CPL.

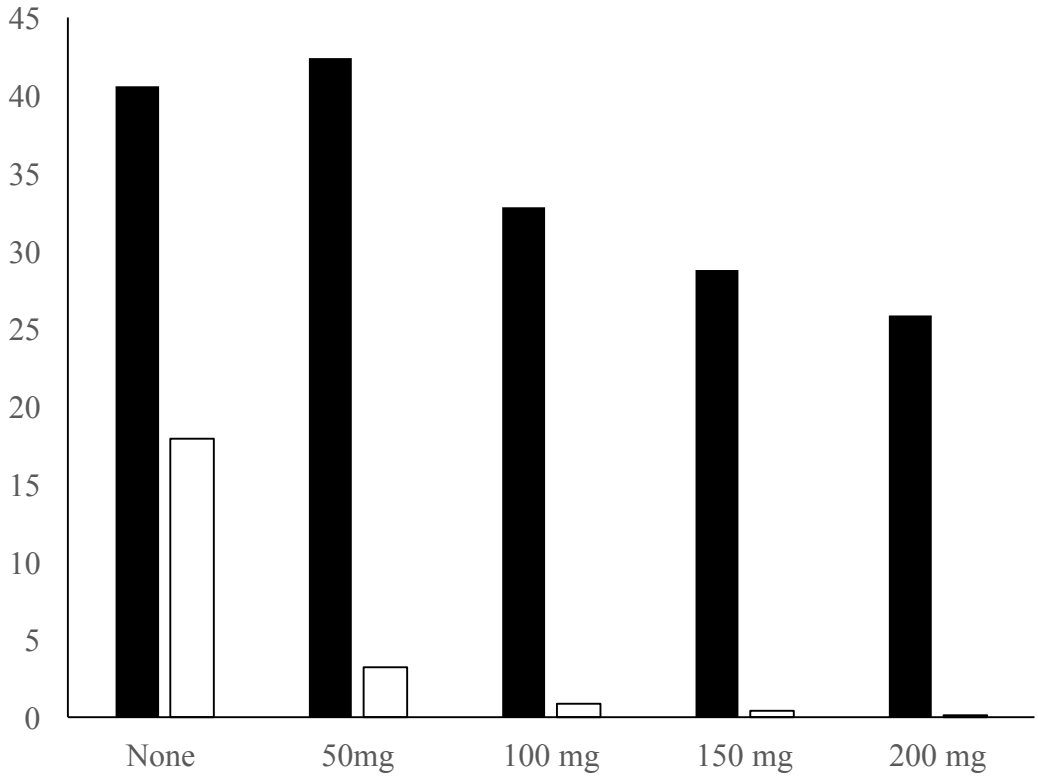

Figure 11: Addition of Norit SX1G carbon to remove Fe species from solution. Conditions: 10 g 0.3 M glycerol solution, 420 psi 5%H_2 / CO_2, 160 psi 25%O_2 / CO_2, 50 mg 0.5%Pd-0.5%Fe / SiO_2, X mg Norit SX1G, 6 h, 1200 rpm stirring, 30 °C. Gases were vented and replenished every hour. Reaction solutions were collected and analysed using MP-AES. Legend: filled = glycerol conversion (%), unfilled = Fe leaching (ppm).

Due to the excellent performance observed upon addition of Norit SX1G carbon to the reaction medium, increasing amounts of this carbon were added to lead

to an elimination of leached Fe species in solution. The results of these experiments are described in Figure 11. Upon addition of 50 mg of carbon in the reaction medium, the concentration of iron in solution was reduced substantially. However, no loss in the catalyst activity was observed, indicating that the concentration of Fe in solution plays little to no role in the conversion of glycerol. As the amount of carbon added was increased, there a was corresponding decrease in the conversion of glycerol along with almost complete elimination of the homogeneous iron from solution. However, this decrease in conversion may have been due to other factors such as mass transfer limitation due to the high amount of carbon present. Additionally, carbon could be acting as a scavenger for the radicals generated. Despite the decreased glycerol conversion, the experiment with addition of 200 mg carbon clearly demonstrates that substantial conversions of glycerol can be achieved in the near absence of homogeneous iron in solution.

4.2.10 Carbon supported Pd-Fe catalysts for the oxidation of glycerol

Due to the positive effect observed upon addition of Norit SX1G carbon in the reaction medium, a 0.5%Pd-0.5%Fe/C catalyst was prepared. Due to difficulties associated with preparing the catalyst using the modified impregnation procedure that has so far been employed[6], the catalyst was prepared using a sol immobilisation procedure which has been described previously in the literature.[7]

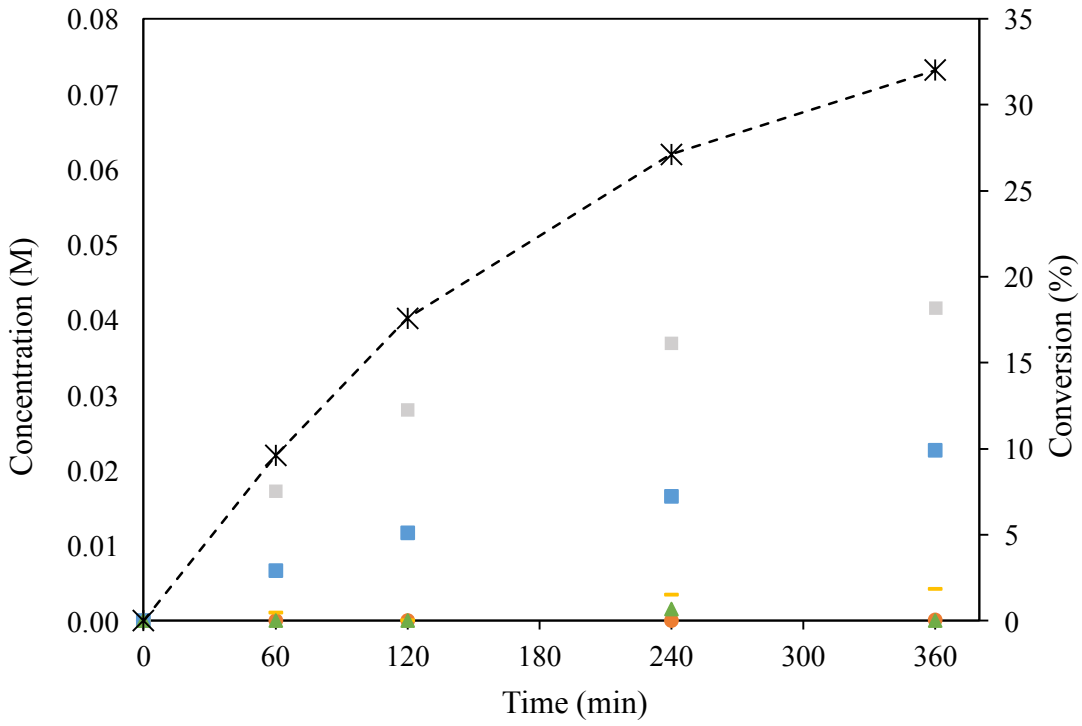

Figure 12: Glycerol oxidation using 0.5%Pd-0.5%Fe/C prepared by sol immobilisation. Conditions: 10 g 0.3 M glycerol solution, 420 psi 5%H_2 / CO_2, 160 psi 25%O_2 / CO_2, 50 mg 0.5%Pd-0.5%Fe / C (prepared with Norit SX1G), 1200 rpm stirring, 30 °C. Gases were vented and replenished every hour. Legend: grey square = glyceraldehyde, blue square = dihydroxyacetone, green triangle = formic acid, orange circle = oxalic acid, yellow dash = glycolic acid.

The testing of the 0.5%Pd-0.5%Fe/C catalyst prepared by sol immobilisation is described in Figure 12. After 6 h of reaction, a glycerol conversion of 32 % was observed. While this glycerol conversion was lower than the 40.6 % observed for the 0.5%Pd-0.5%Fe/SiO_2 catalyst, it was unclear whether this difference was due to the change in support or preparation method. Interestingly, very low concentrations of formic acid were observed in the reaction medium. However, it is possible that the formic acid peak was obscured by the dihydroxyacetone peak present in the HPLC chromatogram, due to them having very similar retention times. However, the principle reason for this test was to determine whether an enhancement in Fe stability

could be achieved. Therefore, the post-reaction effluents were collected and analysed using MP-AES.

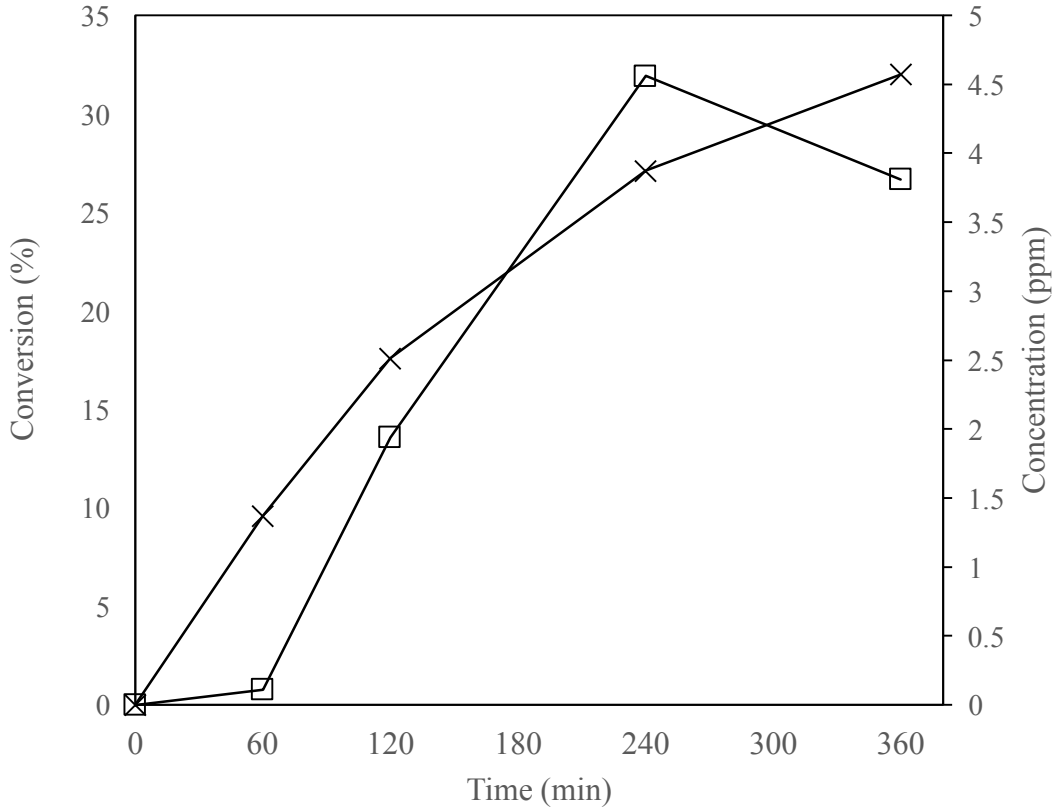

Figure 13: Glycerol oxidation using 0.5%Pd-0.5%Fe/C prepared by sol immobilisation. Conditions: 10 g 0.3 M glycerol solution, 420 psi 5%H_2 / CO_2, 160 psi 25%O_2 / CO_2, 50 mg 0.5%Pd-0.5%Fe / C (prepared with Norit SX1G), 1200 rpm stirring, 30 °C. Gases were vented and replenished every hour. Fe concentration analysis performed using MP-AES. Legend: crosses = glycerol conversion, squares = Fe concentration (ppm).

From the MP-AES analysis, as described in Figure 13, it was observed that after 360 minutes the post-reaction effluent contained an Fe concentration of 3.81 ppm Fe. This result was comparable to the 3.22 ppm detected in the post-reaction effluent when a combination of 50 mg 0.5%Pd-0.5%Fe/SiO_2 with 50 mg Norit SX1G was used. However, the Fe detected in the post-reaction effluent was still far lower for the catalyst supported on carbon when compared the catalyst supported on silica. It was

also observed that the post-reaction effluent Fe concentration decreased between 240 minutes and 360 minutes. This was likely due to the re-adsorption of the leached Fe species on the carbon support. Therefore, it appeared that the Fe was still leaching from the carbon support but was then re-adsorbing over the duration of the reaction. However, the carbon supported catalyst was still inferior to the silica supported catalyst in terms of glycerol conversion activity.

4.2.11 Reaction pathways from glyceraldehyde and dihydroxyacetone

The primary initial products from the oxidation of glycerol using *in situ* generated H_2O_2 were found to comprise of glycerol and dihydroxyacetone. Therefore, to gain further insight into the reaction pathways from these products, a series of reactions were performed using glyceraldehyde and dihydroxyacetone as the starting substrates.

Table 3: 10 g 0.23 M Glyceraldehyde solution, 420 psi 5%H_2/CO_2, 160 psi 25%O_2/CO_2 (580 psi for reactions in absence of H_2), 50 mg 0.5%Pd-0.5%Fe/SiO_2, 1200 rpm stirring, 30 C, reactions performed in Parr stainless steel autoclave. GLY OX = glyoxylic acid, GA = glycolic acid, GCA = glyceric acid, DHA = dihydroxyacetone, FA = formic acid, OXA = oxalic acid, CMB = carbon mass balance.

Reactant gases	**Time (h)**	**Conv. (%)**	**Selectivity (%)**						**CMB (%)**
			GLY OX	**GA**	**GCA**	**DHA**	**FA**	**OXA**	
H_2 + O_2	*6*	*40.8*	*7.6*	*15.2*	*31.4*	*0*	*43.6*	*2.2*	*91.24*
O_2	*6*	*0*	-	-	-	-	-	-	-

The initial test utilised glyceraldehyde as a starting substrate which was then reacted in the presence of H_2 and O_2 using 0.5%Pd-0.5%Fe/SiO_2 as a catalyst. The results from this experiment are described in Table 3. From this test, a glyceraldehyde conversion of 40.8 % was observed. A large variety of mostly scission products were

observed during this reaction including glyoxylic acid, glycolic acid, glyceric acid, formic acid and oxalic acid. It is important to note that there were a few minor peaks observed in the HPLC chromatogram that were unable to be identified during the analysis. However, most the products were accounted for as shown by the high carbon mass balance of 91.24 %. In addition to this test, an experiment was performed in the absence of H_2 to determine whether any of the glyceraldehyde conversion activity could be attributed to oxidation by O_2 alone. However, during the reaction in the absence of H_2, 0 % conversion of glyceraldehyde was observed. Therefore, it appeared that the *in situ* generation of H_2O_2 was required in order to achieve conversion of glyceraldehyde.

Table 4: 10 g 0.13 M Dihydroxyacetone solution, 420 psi 5%H_2/CO_2, 160 psi 25%O_2/CO_2 (580 psi for reactions in absence of H_2), 50 mg 0.5%Pd-0.5%Fe/SiO_2, 1200 rpm stirring, 30 C, reactions performed in Parr stainless steel autoclave. GLY OX = glyoxylic acid, GA = glycolic acid, GCA = glyceric acid, DHA = dihydroxyacetone, FA = formic acid, OXA = oxalic acid, CMB = carbon mass balance.

Gases	**Time (h)**	**Conv (%)**	**Selectivity (%)**						**CMB (%)**
			GLY OX	**GA**	**GCA**	**DHA**	**FA**	**OXA**	
H_2 + O_2	*6*	*31.8*	*9*	*85.1*		-		*5.9*	*76.81*
O_2	*6*	*0*	-	-	-	-	-	-	-

A further test utilised dihydroxyacetone as a starting substrate which was then reacted in the presence of H_2 and O_2 using 0.5%Pd-0.5%Fe/SiO_2 as a catalyst. The results from this experiment are described in Table 4. From this test, a dihydroxyacetone conversion of 31.8 % was observed. This conversion was lower than the 40.8 % observed for glyceraldehyde. This lower conversion of dihydroxyacetone was especially surprising given that the starting concentration of dihydroxyacetone was 0.13 M whereas the starting concentration of glyceraldehyde was 0.23 M. Therefore, it appeared that dihydroxyacetone was less susceptible to oxidation by *in situ* generated H_2O_2 than glyceraldehyde. Products identified during the oxidation of

dihydroxyacetone included glyoxylic acid, glycolic acid and oxalic acid. However, it is important to note that there were another 2 substantial peaks in the HPLC chromatogram that were unable to be identified. This was reflected in the low carbon mass balance of 76.81 % which was observed for the reaction. These two peaks were also present as minor peaks during the oxidation of glycerol using *in situ* generated H_2O_2. Therefore, further analysis using a method such as preparative HPLC to separate the compounds alongside NMR and MS would be highly useful. Interestingly, there was no evidence of formic acid present within the reaction mixture. Although minor concentrations of formic acid may have been masked by the large peak for dihydroxyacetone in the HPLC chromatogram. Therefore, it appeared that the high concentrations of formic acid observed during the oxidation of glycerol could be predominantly attributed to the further oxidation of glyceraldehyde. Additionally, a further experiment was performed in the absence of H_2 to rule out contribution to dihydroxyacetone conversion by O_2 alone. In the absence of H_2, 0 % conversion of dihydroxyacetone was observed.

4.2.12 EPR analysis to help elucidate the nature of the reactive oxygen species

In this work it has been determined that with the use of an appropriate catalyst alongside H_2 and O_2, substantial oxidation activity can be observed. However, the nature of the oxidising species is currently unclear. A likely explanation could be that the H_2O_2 is produced via the direct synthesis reaction from H_2 and O_2. This H_2O_2 can then be decomposed using the catalyst to produce hydroxyl (HO•) and hydroperoxy (HOO•) radicals in solution which can then react with the substrate. An alternative mechanism for oxidation could involve the oxidation of the substrate by surface bound hydroperoxy intermediates formed during the direct synthesis reaction. Using computational studies, Staykov *et al*.[8] proposed a mechanism of H_2O_2 formation involving the formation of a surface bound OOH species over Pd sites. Computational studies performed by Deguchi *et al*.[9] also supported the formation of these surface bound OOH species over Pd sites. However, this mechanism seemed unlikely owing to the lack of oxidation activity observed when using the monometallic Pd catalyst. The requirement of Fe on the catalyst to observe substantial activity indicates that the

presence of Fe plays an important role in the generation of the reactive oxygen species responsible for the oxidation reaction. To determine whether the observed glycerol conversion activity could be attributed to the presence of radicals in solution a series of experiments were performed using a radical spin trap. The use of these spin traps are required due to the short-lived nature of radicals such as HO• and HOO• which are likely responsible for the observed oxidation.

5,5-dimethyl-pyrroline N-oxide (DMPO) was chosen as the radical trap. DMPO can react with short-lived free radicals in solution such as HO• and HOO• to form an adduct with a substantially longer lifetime than the radicals, which can be detected using electron paramagnetic spectroscopy (EPR) techniques.

For the initial test, DMPO was reacted in the presence of H_2 and O_2, but in the absence of catalyst. The reaction solution was then analysed using EPR spectroscopy. The EPR spectra obtained during this analysis showed peaks corresponding to the formation of a DMPO-OH adduct. While there was no catalyst present in the reaction mixture, it is likely that radicals in solution were formed due to the low levels of Pd contamination present in the reactor catalysing the reaction between H_2 and O_2. In the absence of catalyst, no glycerol conversion is observed, therefore these radicals are not responsible for the oxidation of glycerol observed during reactions using 0.5%Pd-0.5%Fe/SiO_2.

A reaction was then performed in the presence of 0.5%Pd-0.5%Fe/SiO_2, H_2, O_2 and DMPO. However, in this case no EPR signal was observed. Upon addition of glycerol to the reaction mixture, no EPR signal was observed again. These results were highly surprising because a far higher concentration of radicals in solution were expected in the presence of the catalyst than in the absence of catalyst. It was thought that the reason for this lack of signal may have been due to the destruction/adsorption of DMPO by the catalyst. Therefore, the solutions were collected and analysed using quantitative nuclear magnetic resonance spectroscopy (NMR).

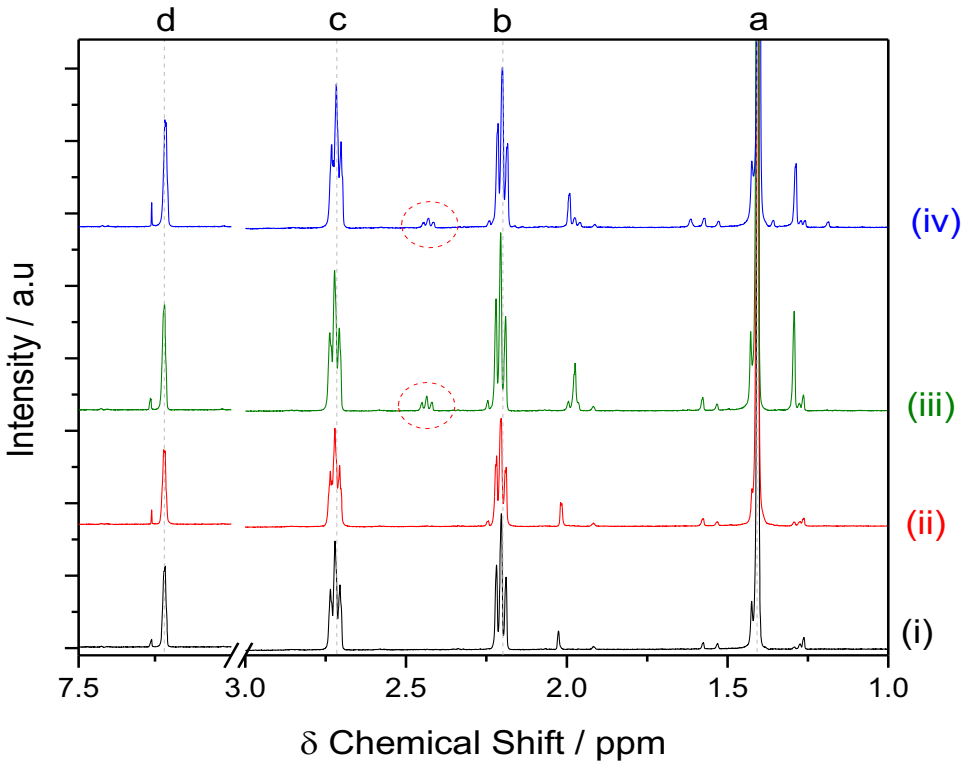

Figure 14: NMR analysis of the post-reaction solutions from spin trap experiments. (i) 10 μL DMPO in 10 ml H_2O, (ii) 10 μL DMPO in 10 ml H_2O after 5 minute reaction with H_2 and O_2, (iii) 10 μL DMPO in 10 ml H_2O after 5 minute reaction with H_2, O_2 and 0.5%Pd-0.5%Fe/SiO_2, (iv) 10 μL DMPO in 10 ml 0.3 M glycerol solution after 5 minute reaction with H_2, O_2 and 0.5%Pd-0.5%Fe/SiO_2.

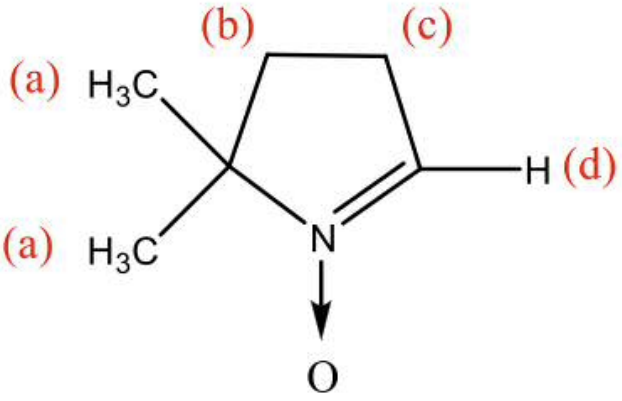

Figure 15: NMR assignment for DMPO.

Table 5: Resonances integrated using TopSpin 3.5 NMR software and areas normalised to proton H^d at 7.22 ppm. Note: resonance at δ 1.41 overlaps with ^1H resonance of contaminant water present within the $CDCl_3$/TMS insert, hence deviation from the predicted 6:2:2:1 ratio (a:b:c:d)

Sample	**δ 1.41 ppm (a)**	**δ 2.20 ppm (b)**	**δ 2.72 ppm (c)**	**δ 7.22 ppm (d)**
(i) 10 μL DMPO in 10 ml H_2O	7.5	2.2	2.2	1
(ii) 10 μL DMPO in 10 ml H_2O after 5 minute reaction with H_2 and O_2	7.3	2.2	2.2	1
(iii) 10 μL DMPO in 10 ml H_2O after 5 minute reaction with H_2, O_2 and 0.5%Pd-0.5%Fe/SiO_2	7.3	2.2	2.2	1
(iv) 10 μL DMPO in 10 ml 0.3 M glycerol solution after 5 minute reaction with H_2, O_2 and 0.5%Pd-0.5%Fe/SiO_2.	7.2	2.2	2.2	1

The results from the quantitative NMR experiments are described in Figure 14. The assignments of the various peaks are described in Figure 15. In addition to this the results from the integrations are described in Table 5. From this analysis, it was observed that almost all the DMPO remained intact during the experiments. The formation of a DMPO adduct would be expected to result in a shift of resonance (d) downfield and would lead to a change in the ratio of b,c,d: a. This was not observed. However, there was the presence of an unknown resonance at δ 2.43 ppm when catalyst was used. This may have been attributed to contamination introduced upon addition of the catalyst. However, from these results it was determined that the lack of a DMPO adduct detected during EPR analysis for (iii) and (iv) was not due to complete catalytic destruction/adsorption of the DMPO by the catalyst.

Therefore, the results from the spin trap experiments seemed to indicate that the production of radicals in solution was not responsible for the observed oxidation of glycerol. Indeed, in the presence of radicals in solution in the absence of catalyst, no glycerol conversion was observed. Therefore, it appears that the reaction between the reactive oxygen species and the glycerol occurs either on or in very proximity to the surface of the catalyst.

4.2.13 XPS analysis of catalyst

To gain more insight into the nature of the metals on the surface of the catalyst, a series of XPS experiments were performed to analyse 0.5%Pd-0.5%Fe/SiO_2 both before and after use in the glycerol oxidation reaction. In addition to this, both the 0.5%Pd/SiO_2 and 0.5%Fe/SiO_2 monometallic catalysts were analysed. The surface concentrations of the various elements are described in Table 6.

Table 6: Surface concentration of different elements on 0.5%Pd-0.5%Fe/SiO_2 (fresh), 0.5%Pd-0.5%Fe/SiO_2 (used), 0.5%Pd/SiO_2 and 0.5%Fe/SiO_2

Name	**Fresh 0.5%Pd-0.5%Fe/SiO_2 (At %)**	**Used 0.5%Pd-0.5%Fe/SiO_2 (At %)**	**Fresh 0.5%Pd/SiO_2 (At %)**	**Fresh 0.5%Fe/SiO_2 (At %)**
O 1s	66.29	66.70	67.92	64.14
C 1s	3.23	3.9	1.69	5.21
C 1s	1.09	2.14	0.61	0.89
C 1s	0.52	0.98	0.15	0.34
Si 2p	28.53	26.04	29.51	29.13
Fe 2p	0.25	0.15	0	0.29
Pd 3d	0.09	0.08	0.12	0

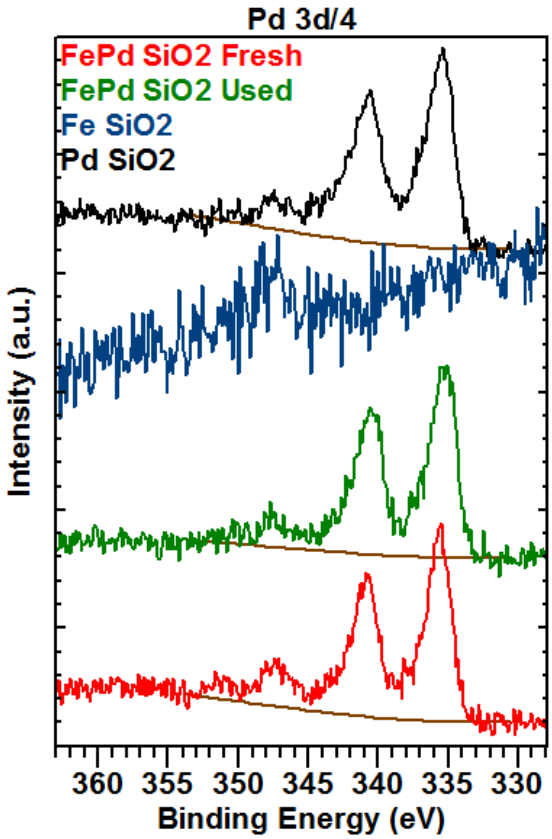

Figure 16: Pd $3d_{5/2}$ spectra of 0.5%Pd-0.5%Fe/SiO_2 (fresh), 0.5%Pd-0.5%Fe/SiO_2 (used), 0.5%Pd/SiO_2 and 0.5%Fe/SiO_2

From the Pd $3d_{5/2}$ spectra, as shown in Figure 16, a peak was observed at around 335.5 eV which corresponds to the presence of metallic Pd for all Pd containing catalysts. Interestingly, after 6 h of reaction during glycerol oxidation, no loss of Pd was observed from the Pd-Fe catalyst. This result confirmed the observation in the previous chapter that metallic Pd species are far more stable towards leaching in the presence of oxalic acid. Indeed, it is likely that the lack of Pd leaching is responsible for the sustained rate of glycerol conversion over the 6 h of reaction. Therefore, it is possible to design catalysts that do not leach Pd under these reaction conditions.

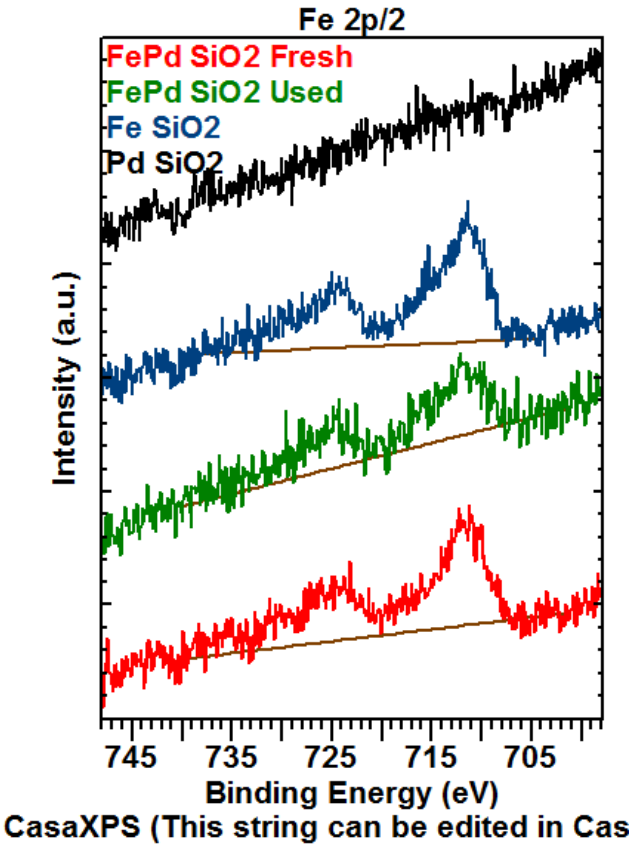

Figure 17: Fe $2p_{3/2}$ spectra of 0.5%Pd-0.5%Fe/SiO_2 (fresh), 0.5%Pd-0.5%Fe/SiO_2 (used), 0.5%Pd/SiO_2 and 0.5%Fe/SiO_2

From the Fe $2p_{3/2}$ spectra, as shown in Figure 17, a peak was observed at around 711.5 to 711.8 eV for all Fe containing catalysts which is typical for iron in the Fe^{3+} oxidation state (likely Fe_2O_3). A decrease in Fe concentration on the surface of the Pd-Fe catalyst after use was also observed. This was unsurprising as the leaching of Fe during reaction had been observed already during MP-AES analysis.

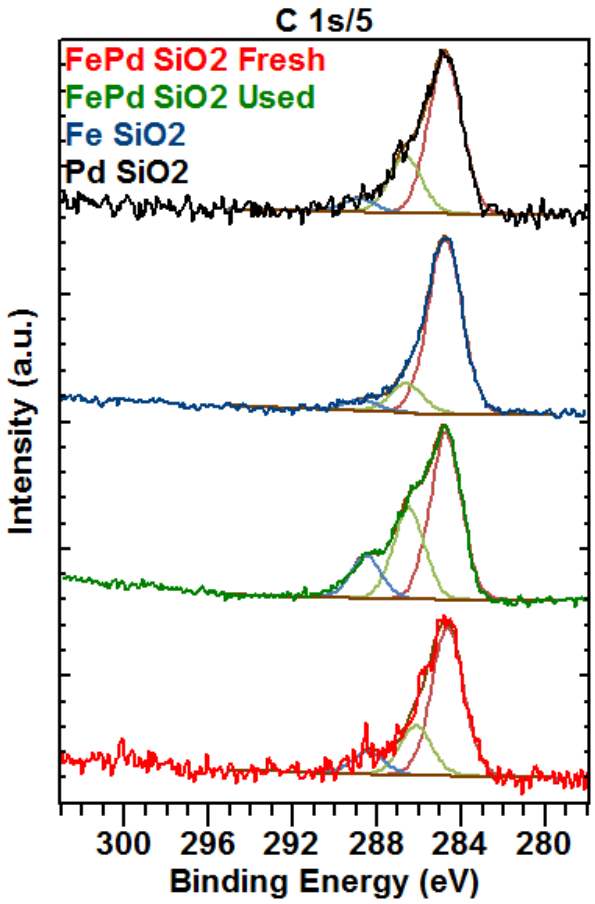

Figure 18: C 1s spectra of 0.5%Pd-0.5%Fe/SiO_2 (fresh), 0.5%Pd-0.5%Fe/SiO_2 (used), 0.5%Pd/SiO_2 and 0.5%Fe/SiO_2

Additionally, from the C 1s spectra, as shown in Figure 18, a lot of organic residue was detected at the surface of the catalyst. This could indicate that reaction intermediates were adsorbing to the surface of the catalyst during reaction. However, carbon contamination is clearly present on all the fresh and used catalysts.

4.2.14 Electron microscopy of Pd-Fe catalyst

To gain insight into the nature of the metals on the surface of the catalyst, a series of experiments were performed using HAADF-STEM (high angle annular dark field – scanning transmission electron microscopy) analysis of the catalyst coupled with elemental mapping using EDX (energy dispersive x-ray) analysis.

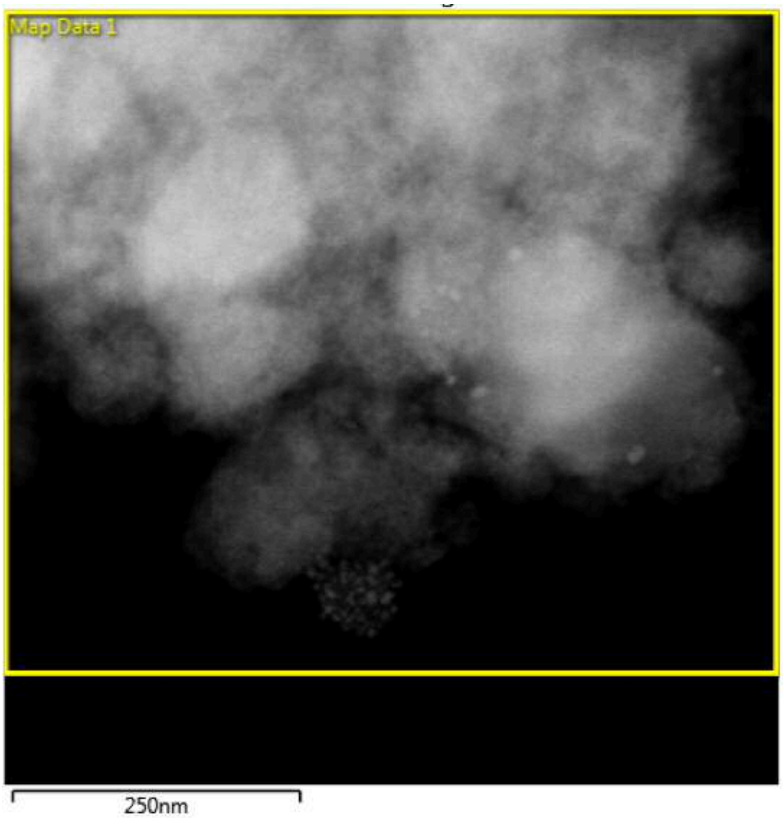

Figure 19: HAADF-STEM image of 0.5%Pd-0.5%Fe/SiO_2 (site 1)

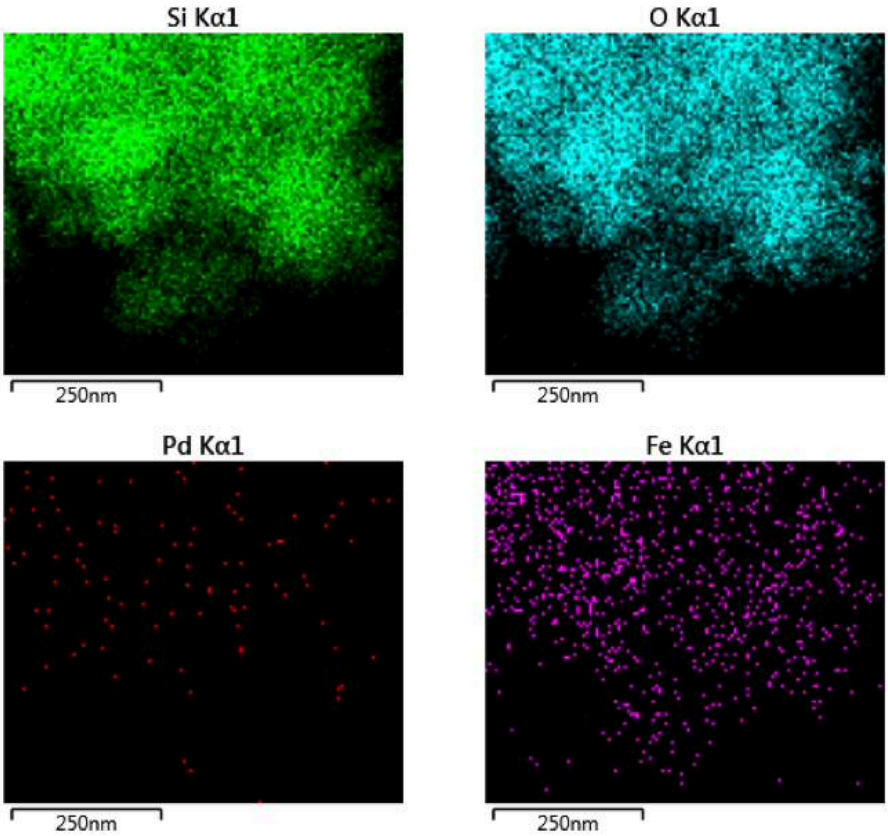

Figure 20: Elemental mapping of 0.5%Pd-0.5%Fe/SiO_2 (site 1)

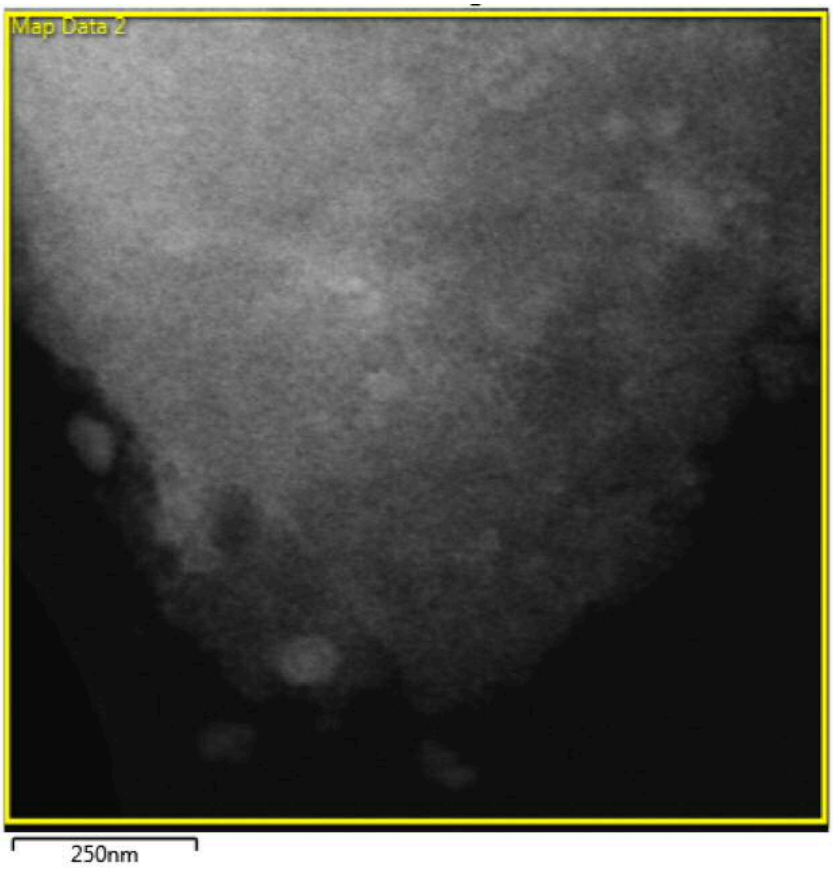

Figure 21: HAADF-STEM image of 0.5%Pd-0.5%Fe/SiO_2 (site 2)

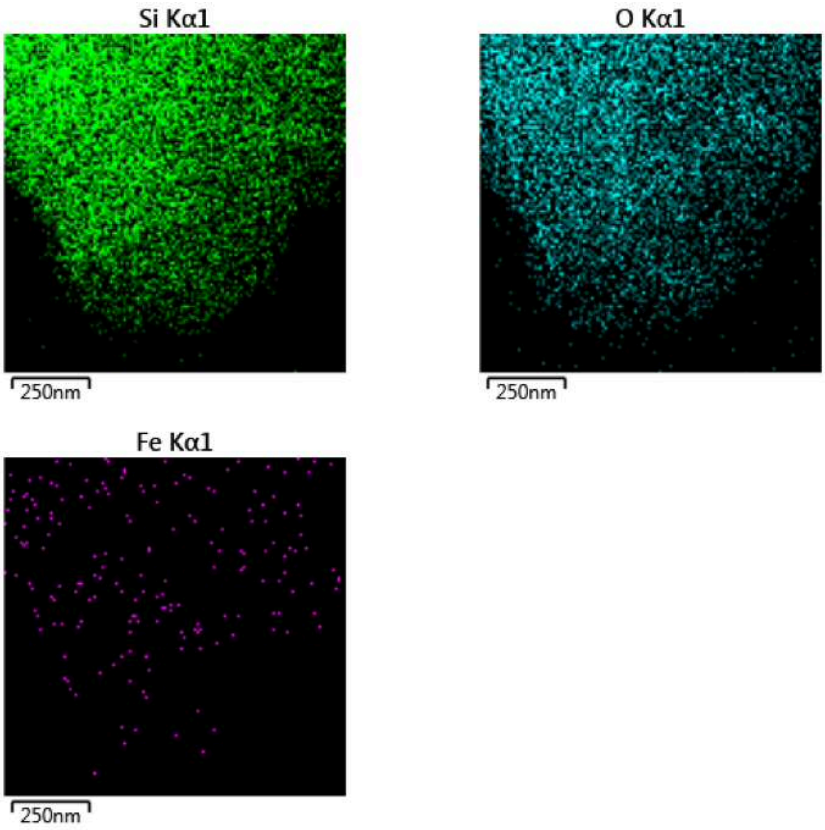

Figure 22: Elemental mapping of 0.5%Pd-0.5%Fe/SiO_2 (site 2)

The imaging and elemental mapping analysis for the first site is described in Figures 19 and 20. It was clearly observed that Pd and Fe nanoparticles are present on the catalyst surface. The Fe is well dispersed over the surface of the support. However, it appeared that the Pd seemed to aggregate into islands. Therefore, the dispersion of Pd was lesser than that of Fe over the surface of the catalyst. This could likely be attributed to the sintering of Pd nanoparticles during the catalyst heat treatment.

When another site was analysed, as shown in Figures 21 and 22, it was observed that there was no Pd in certain areas of the catalyst. However, even in these sites there was good dispersion of Fe over the surface of the catalyst.

Therefore, it appeared that on the catalyst there was a large dispersion of Fe over the surface of the catalyst with islands of Pd. It is likely that these islands of Pd are responsible for the generation of H_2O_2. Whether the generation of radicals occurs at the Fe sites near the Pd 'islands' or not remains unclear. Due to the lack of high resolution images obtained it was not possible to gain information on average particle size distributions and the potential occurrence of alloying.

4.3 Conclusions

Within this chapter, it has been demonstrated that supported Pd-Fe catalysts are highly effective for the oxidation of glycerol using H_2O_2 generated *in situ* from H_2 and O_2. It has been shown that a linear rate of glycerol conversion can be achieved with appropriate recharging of H_2 and O_2 reactant gases, as shown in Figure 23.

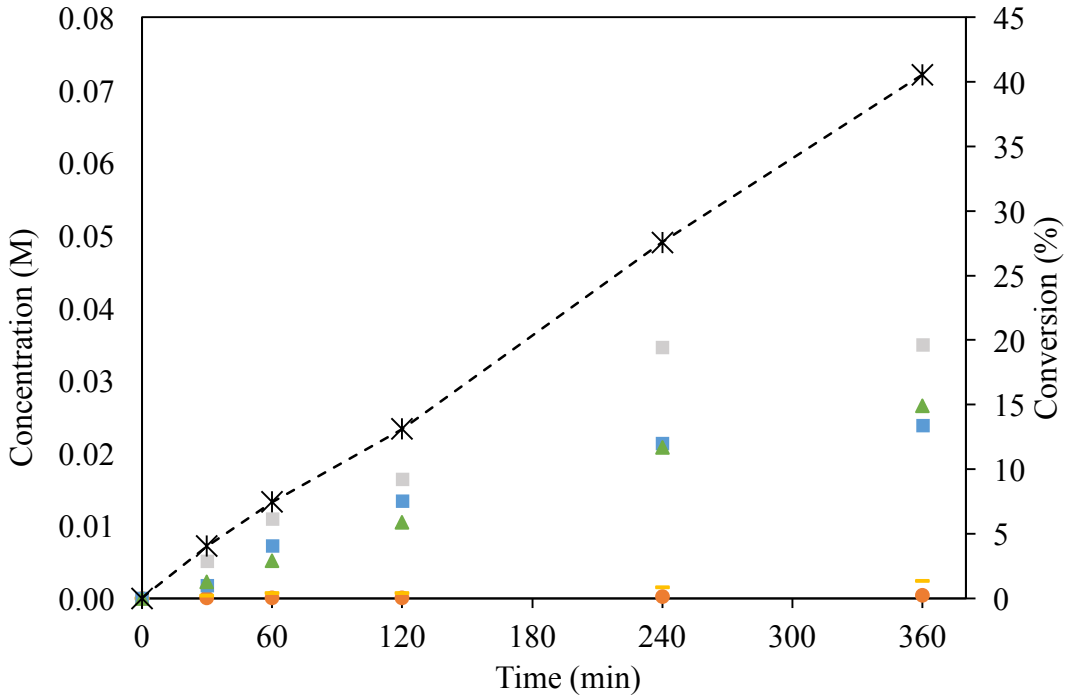

Figure 23: Product distribution over 6 h with recharging of gases every 1 h. Conditions: 10 g 0.3 M glycerol solution, 420 psi 5%H_2 / CO_2, 160 psi 25%O_2 / CO_2, 50 mg 0.5%Pd-0.5%Fe / SiO_2, 1200 rpm stirring, 30 °C. Gases were vented and replenished every hour. Legend: grey square = glyceraldehyde, blue square = dihydroxyacetone, green triangle = formic acid, orange circle = oxalic acid, yellow dash = glycolic acid.

There were high concentrations of formic acid formed showing high rates of C-C scission. There were also significant concentrations of dihydroxyacetone formed, a highly desired product owing to its current usefulness in the cosmetics industry.

However, as was the case with the phenol oxidation described in chapter 3, leaching of active metal remained an issue. In this case, the leaching of Fe was directly correlated with the formation of oxalic acid, as shown in Figure 24.

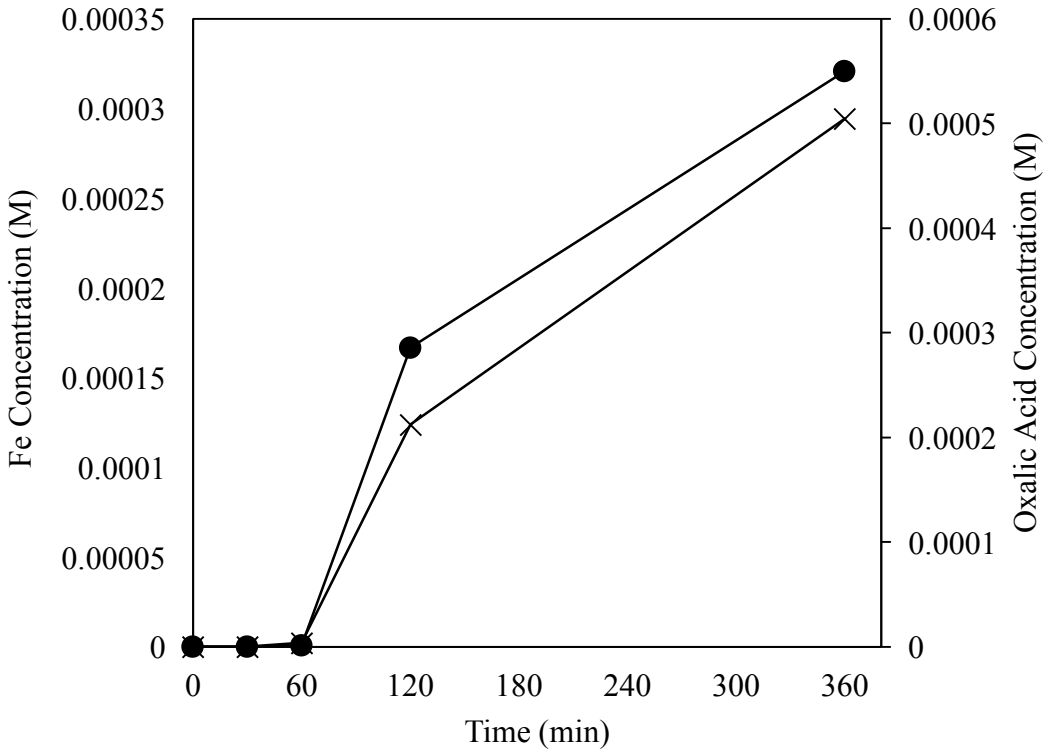

Figure 24: Comparison of Fe concentration in solution with oxalic acid concentration. Conditions: 10 g 0.3 M glycerol solution, 420 psi 5%H_2 / CO_2, 160 psi 25%O_2 / CO_2, 50 mg 0.5%Pd-0.5%Fe / SiO_2, 1200 rpm stirring, 30 °C. Gases were vented and replenished every hour. Reaction solutions were collected and analysed using MP-AES. Legend: circles = Fe concentration, crosses = oxalic acid concentration.

The link between oxalic acid concentration and Fe leaching helped to further confirm the observations and conclusions presented in chapter 3 whereby leaching of active metal was directly related to the formation of 'chelating' intermediates formed during the oxidation reactions. The leached species in this case was likely iron oxalate. XPS analysis of the catalyst before and after reaction also indicated little/no leaching of Pd during the reaction. The XPS data also showed that the Pd-Fe catalyst prepared was comprised almost completely of Pd^0, fitting with the observation in chapter 3 that it was Pd^{2+} species that were susceptible to leaching. A removal of Fe species from the

reaction medium was performed upon addition of activated carbon, although the research showed that the nature of the carbon was vital for optimum performance. Of the carbon materials tested, Norit SX1G was found to be the best.

When the *in situ* H_2O_2 system was benchmarked against the bulk addition of commercially available H_2O_2, the *in situ* H_2O_2 showed remarkably improved performance in the glycerol oxidation reaction. Interestingly, the *in situ* system showed greater selectivity towards C_3 products when compared to when bulk addition of H_2O_2 was used. This was indicative of a more selective oxidation reaction mechanism and the creation of a different oxidising species. To probe the nature of the oxidising species in the *in situ* H_2O_2 system, a series of EPR experiments were performed with the use of a spin trap (DMPO). Surprisingly, the results from this experiment indicated that there was no •OH or •OOH radicals present in the bulk of the reaction medium, as was initially expected. This indicated that the oxidative species that was responsible for the observed activity occurred at or very near to the surface of the catalyst.

The work contained in this chapter represents and exciting and novel new method for performing the oxidation of glycerol. This method can be conducted at near-ambient conditions and can achieve very high rates of glycerol conversion in the absence of any base to promote the reaction. As discussed in chapter 3, the *in situ* system satisfies the majority of the principles of green chemistry whilst achieving superior performance when compared to bulk addition of commercially available H_2O_2. This showed that the oxidation of glycerol using *in situ* generated H_2O_2 can provide a viable method for the valorisation of glycerol.

4.4 References

1 B. Katryniok, H. Kimura, E. Skrzyńska, J.-S. Girardon, P. Fongarland, M. Capron, R. Ducoulombier, N. Mimura, S. Paul and F. Dumeignil, *Green Chem.*, 2011, **13**, 1960.

2 M. S. Yalfani, S. Contreras, J. Llorca, M. Dominguez, J. E. Sueiras and F. Medina, *Phys. Chem. Chem. Phys.*, 2010, **12**, 14673–14676.

3 C. Crotti and E. Farnetti, *J. Mol. Catal. A Chem.*, 2015, **396**, 353–359.

4 P. Mcmorn, G. Roberts and G. J. Hutchings, *Catal. Letters*, 1999, **63**, 193–197.

5 N. Kishimoto, T. Kitamura, M. Kato and H. Otsu, *J. Water Environ. Technol.*, 2013, **11**, 21–32.

6 M. Sankar, Q. He, M. Morad, J. Pritchard, S. J. Freakley, J. K. Edwards, S. H. Taylor, D. J. Morgan, A. F. Carley, D. W. Knight, C. J. Kiely and G. J. Hutchings, *ACS Nano*, 2012, **6**, 6600–6613.

7 M. Sankar, E. Nowicka, R. Tiruvalam, Q. He, S. H. Taylor, C. J. Kiely, D. Bethell, D. W. Knight and G. J. Hutchings, *Chem. - A Eur. J.*, 2011, **17**, 6524–6532.

8 A. Staykov, T. Kamachi, T. Ishihara and K. Yoshizawa, *J. Phys. Chem. C*, 2008, **112**, 19501–19505.

9 T. Deguchi and M. Iwamoto, *J. Phys. Chem. C*, 2013, **117**, 18540–18548.

5 Conclusions and future work

5.1 Summary

As discussed in Chapter 1, the direct synthesis of H_2O_2 from H_2 and O_2 in aqueous systems represents a significant challenge due to limitations associated with H_2 solubility and the decomposition of synthesised H_2O_2 leading to decreased yields of H_2O_2 upon completion of the reaction. However, it was clear that with careful design of the catalyst, the decomposition reaction can be suppressed under laboratory scale conditions. The application of *in situ* generated H_2O_2 to perform oxidation reactions has also been discussed. The use of *in situ* generated H_2O_2 to perform oxidation reactions presents a significant opportunity to catalytic chemists as, unlike producing bulk concentrations of H_2O_2 using the direct synthesis method, the produced H_2O_2 can be utilised instantaneously. The use of this H_2O_2 immediately upon production can lead to decreased losses of H_2O_2 due to decomposition in contrast with attempting to produce larger concentrations of H_2O_2 for later use. Additionally, the continued production and utilisation of H_2O_2 can be preferable to bulk addition of H_2O_2 due to the quenching of produced radicals by excess H_2O_2 concentrations. Commercially produced H_2O_2 typically contains stabilisers which may be deleterious to the oxidation reactions performed. However, the *in situ* production of H_2O_2 in oxidation reactions removes the need to add these stabilisers. Thereby reducing the amount of waste materials in the reaction.

5.2 Oxidation of phenol utilising H_2O_2 generated *in situ* from H_2 and O_2

As discussed in Chapter 3, the oxidation of phenol (in 1000 ppm aqueous solutions) using *in situ* generated H_2O_2 has been investigated. Phenol was chosen as a model compound to represent an organic contaminant in wastewater effluent. The *in situ* production of H_2O_2 for wastewater remediation represents an area ripe for investigation due to the multiple benefits of H_2O_2 utilisation in wastewater treatment.

Firstly, H_2O_2 produces water as a by-product, which is far more environmentally desirable than by-products produced when using Cl based treatments. Upon catalytic activation, it is also capable of producing •OH species, which is one of the most powerful oxidising agents known. Additionally, the direct synthesis of H_2O_2 represents the most atom efficient means of producing H_2O_2 and if the H_2 can be produced from water electrolysis, with the integration of solar power, would represent the use of a renewable feedstock. The direct synthesis of H_2O_2 for use in wastewater treatment clearly satisfies most principles of green chemistry, as discussed in Chapter 1.

In Chapter 3, it was established that catalysts comprising supported Pd-Fe were highly effective for the oxidation of phenol using H_2O_2 generated *in situ* from H_2 and O_2. However, it was also found that substantial leaching of Fe species from the surface of the catalyst occurred during the reaction, which would limit the reusability of the catalyst. Through a study of catalyst synthesis conditions, it was found that improvements in catalyst stability could be achieved by adjusting the Pd:Fe ratios and employing increased temperatures for the reduction step. It was determined that metal leaching during reaction could be linked to the presence of phenol oxidation intermediates such as catechol and oxalic acid. Through a detailed XPS study, it was found that Pd^0 was far more stable on the surface of the catalyst than Pd^{2+}. To limit leaching of Fe during reaction, the use of a $LaFeO_3$ perovskite material was found to be far more stable against leaching due to oxalic acid and catechol than supported Fe species. Although, this increased stability did come at a cost to overall catalyst activity, potentially due to far lower surface areas. It was also found that using supports with higher surface areas, such as SiO_2 could lead to far greater conversions of phenol, capable of achieving substantial conversions of phenol even when concentration was increased from 1000 to 10000 ppm. Through a detailed experimental study into the effect of the Fe leachate upon the reaction, it was determined that leached Fe was not responsible for most the catalyst activity observed. A comparison of *in situ* generated H_2O_2 with bulk addition of H_2O_2 demonstrated the improved phenol oxidation activity that could be observed when using *in situ* generated H_2O_2. The *in situ* system was also shown to be effective against other types of organic compounds such as glucose and ethanol.

The observation that Pd-Fe catalysts are highly effective for the oxidation of organics in water using in situ generated H_2O_2 represents an exciting new method for wastewater treatment. However, further work must be conducted to improve the system. One area that needs improvement is the stability on the surface of the catalyst. We have shown that perovskite materials show promise for achieving greater Fe stability, although further work is required to improve the activity of these catalysts for more effective utilisation. Additionally, the work contained in this thesis was conducted under batch conditions, it would be desirable to conduct these experiments under a flow regime. It is possible that when employing a flow regime, the leaching of metal may be reduced due to decreased contact time between the catalyst and intermediates such as catechol and oxalic acid. The activity of catalysts in this thesis has been determined mostly by monitoring the conversion of phenol. It would be useful to perform chemical oxygen demand testing, as discussed in section 1.3.2, to determine the reduction in organic loading post-reaction. To gain greater insight into the real-world application of this system it would be useful to perform testing using actual wastewater effluents, monitored using chemical oxygen demand.

5.3 Oxidation of glycerol utilising H_2O_2 generated *in situ* from H_2 and O_2

In Chapter 4, the Pd-Fe catalyst was investigated for the oxidation of glycerol using *in situ* generated H_2O_2. For these experiments, a far greater substrate concentration was employed than in Chapter 3. It was demonstrated that, with appropriate recharging of H_2 and O_2 reactant gases, substantial conversions of glycerol could be achieved under base-free conditions using *in situ* generated H_2O_2. To the best of this authors knowledge, this represents the first example of glycerol oxidation using H_2O_2 generated *in situ* from H_2 and O_2 in the literature. It was found that the initial conversion of glycerol lead to C_3 products such as glyceraldehyde and dihydroxyacetone however, as the reaction proceeded further, increased concentrations of C-C scission products were observed. However, Fe leaching remained problematic. This leaching was directly linked to the presence of oxalic acid in the reaction medium. Although, it was found that upon addition of a suitable carbon material, the Fe in solution could be substantially reduced while maintaining glycerol

conversion activity. In addition to this, spin trap experiments were performed which indicated that the reactive oxygen species responsible for the observed glycerol oxidation activity were generated at/very near to the surface of the catalyst. XPS analysis of the catalyst before and after use indicated that no Pd leaching occurred at the surface of the catalyst, likely due to the presence of Pd^0 exclusively.

The oxidation of glycerol using *in situ* generated H_2O_2 represents a novel method for performing glycerol oxidation under base-free conditions. There are many future experiments that can be performed to gain greater insight into the reaction and improve its performance. During this work there were a number of unidentified products, this lead to unreliable carbon mass balance values and made it impossible to measure the amount of glycerol that may have been totally oxidised to CO_2. To remedy this, it would be useful to separate the unknown products using preparative HPLC and analyse them using NMR and mass spectrometry. Additionally, further experiments using radical scavengers could be performed to support the findings from the spin trap experiments. As with the work discussed in Chapter 3, the testing of the catalyst under a 'flow' regime would be highly desirable. Additionally, it would be worthwhile to test Fe containing perovskite materials in this reaction, due to their enhanced Fe stability when compared to supported Fe catalysts. It would also be useful to test alternative Fe species in conjunction with *in situ* generated H_2O_2 to lead to enhanced selectivity towards desired products such as dihydroxyacetone.

5.4 Final remarks

Within this thesis, it has been demonstrated that that bimetallic Pd-Fe catalysts are highly effective for the oxidation of both phenol and glycerol using H_2O_2 generated *in situ* from H_2 and O_2. It has been demonstrated that with further work, these systems could be an effective, novel and environmentally friendly process for the treatment of organically-loaded wastewaters and the conversion of glycerol into higher value products. The work presented in this thesis demonstrates the efficacy of *in situ* generated H_2O_2 when compared to widely employed bulk addition of commercially available H_2O_2.